EXCITABLE FIBROBLASTS!

Ion Channels, Gap Junctions, Action Potentials and Calcium Oscillations in Normal Rat Kidney Fibroblasts

Erik G.A. Harks

EXCITABLE FIBROBLASTS!

Ion Channels, Gap Junctions, Action Potentials

and Calcium Oscillations in Normal Rat Kidney Fibroblasts

EXCITABLE FIBROBLASTS!

Ion Channels, Gap Junctions, Action Potentials and Calcium Oscillations in Normal Rat Kidney Fibroblasts

Een wetenschappelijke proeve op het gebied van de
Natuurwetenschappen, Wiskunde en Informatica

PROEFSCHRIFT

ter verkrijging van de graad van doctor aan de
Katholieke Universiteit Nijmegen,
op gezag van de Rector Magnificus Prof. dr. C.W.P.M. Blom,
volgens besluit van het College van Decanen
in het openbaar te verdedigen op maandag 1 december 2003
des namiddags om 1.30 uur precies door

Erik Godefridus Antonius Harks

geboren op 16 maart 1976 te Veldhoven

Promotores:	Prof. Dr. E.J.J. van Zoelen
	Prof. Dr. D.L. Ypey
Co-promotor:	Dr. A.P.R. Theuvenet

Manuscriptcommissie:	Prof. Dr. H.J. Jongsma (UU)
	Dr. B.G. Jenks

Druk: Ponsen & Looijen BV, Wageningen
ISBN: 90-9017406-0

Printing of this thesis was financially supported by HEKA Elektronik, Lambrecht/Pfalz, Germany.

Abbreviations

2-APB	2-aminoethoxydiphenyl borate
AP	action potential
BAPTA-AM	1,2-bis(2-aminophenoxy)ethane-N,N,N’,N’-tetraacetic acid, tetra(acetoxymethyl) ester
BK	bradykinin
cADPR	cyclic adenosine diphosphate ribose
CICR	calcium-induced calcium release
Cm	membrane capacitance
COX	cyclooxygenase
Cx43	connexin 43
E_{Ca}	reversal potential for calcium
E_{Cl}	reversal potential for chloride
E_{K}	reversal potential for potassium
E_{leak}	reversal potential for the leak
EGF	epidermal growth factor
ER	endoplasmic reticulum
ESI-MS(/MS)	electrospray ionization (tandem) mass spectrometry
ET-1	endothelin-1
FFA	flufenamic acid
G01x	estimated gap junctional conductance between the patched cell and the surrounding cells
G_{CaL}	L-type calcium conductance
$G_{Cl(Ca)}$	calcium-activated chloride conductance
G_{gj}	gap junctional conductance
G_{Kir}	inwardly rectifying potassium conductance
G_{leak}	leak conductance
GJIC	gap junctional intercellular communication
HEK	human embryonic kidney
HPLC	high pressure liquid chromatography
I_{CaL}	L-type calcium current
$I_{Cl(Ca)}$	calcium-activated chloride current
I_{Kir}	inward rectifying potassium current
I_{leak}	leak current
IC_{50}	concentration causing half-maximal inhibition

IP_3	inositol-1,4,5 trisphosphate
LPA	lysophosphatidic acid
MFA	meclofenamic acid
NAADP	nicotinic acid adenine dinucleotide phosphate
NFA	niflumic acid
NRK	normal rat kidney
NSAID	non-steroidal anti-inflammatory drug
PGF2α	prostaglandin F2α
PKC	protein kinase C
PLC	phospholipase C
RA	retinoic acid
Rm	membrane resistance
SERCA	sarcoplasmic/endoplasmic reticulum Ca-ATPase
SOC	store-operated calcium
TGFβ	transforming growth factor β
TransX	active compound(s) in the medium conditioned by phenotypically transformed NRK fibroblasts
TRP	transient receptor potential
Vh	holding potential

Table of contents

CHAPTER 1

General Introduction

The development of a multicellular organism from a fertilized egg cell to an adult organism is based on a balanced interplay between growth and differentiation processes that finally results in a large diversity of cooperating tissues and organs. In the adult organism most cells are non-proliferating due to local control mechanisms, but proliferation of cells can still be initiated when necessary, for example for tissue regeneration and wound healing. During development and also in the adult organism cellular growth is strictly regulated by various control mechanisms that ensure cells to start and stop dividing at the proper time and place. Dysfunction of these intricate regulatory mechanisms may result in uncontrolled proliferation of cells and can be the basis for a large diversity of pathogenic conditions including cardiovascular diseases, autoimmune diseases and cancer. Therefore, understanding of the elementary mechanisms that control normal cell growth is crucial for understanding pathogenic abnormalities.

NRK fibroblasts as a model system to study density-dependent growth regulation and phenotypic transformation

Proliferation of normal cells is strictly dependent on the binding of small signaling molecules such as polypeptide growth factors to their specific receptors in the cellular plasma membrane. Upon *in vitro* culturing, non-tumorigenic cells grow until a critical cell density is reached after which they stop dividing by a mechanism known as density-dependent growth inhibition, also referred to as contact-inhibition. In contrast to normal cells, tumor cells are characterized by a reduced requirement of external growth factors for their proliferation and a loss of density-dependent growth inhibition, resulting in uncontrolled proliferation of these cells.

Normal rat kidney (NRK) fibroblasts form an attractive *in vitro* model system to study the mechanisms of density-dependent growth inhibition and cellular alterations upon phenotypic transformation (Van Zoelen, 1991), since these immortalized cells have a normal phenotype and are strictly dependent on externally added growth factors for their proliferation. Therefore, the proliferation of cultured NRK cells can very easily be manipulated by addition and removal of growth factors, as shown schematically in Fig. 1. When NRK cells are cultured in the presence of serum, a confluent monolayer is formed after 3-4 days and NRK cells in these exponentially growing monolayer cultures are unsynchronized, i.e. they are present in various stages of the cell cycle. Upon subsequent addition of serum-free medium, cell growth is stopped due to the absence of growth factors, and all cells become synchronized in the G_0-phase of the cell cycle. Most of the experiments

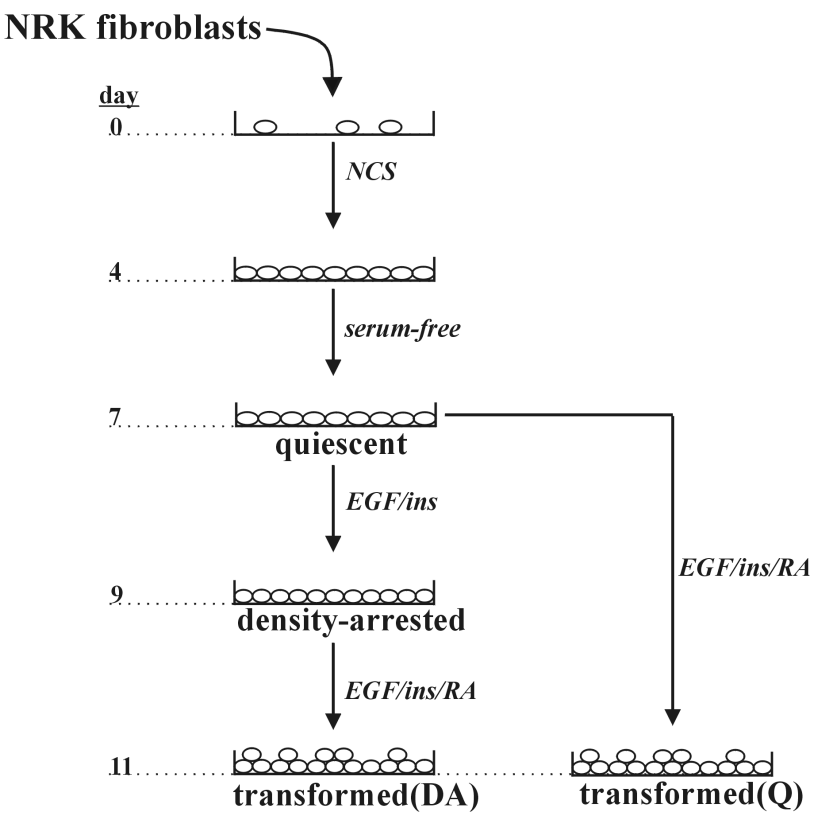

Figure 1 Schematic overview showing how NRK fibroblasts are cultured to different growth states. In the presence of serum-containing medium (NCS; newborn calf serum) NRK cells are grown to confluence (day 4), after which all growth factors are removed from the culture medium and NRK cells become quiescent. At day 7, approximately 40% of the NRK cells are triggered to enter the cell cycle upon EGF (5 ng/ml) treatment in the presence of insulin (5 μg/ml), but NRK cells are unable to proceed through additional cell cycles and become density-arrested (day 9). Finally, by addition of RA (50 ng/ml), EGF (5 ng/ml), and insulin (5 μg/ml) to density-arrested NRK monolayers, density-dependent growth inhibition is overcome and NRK cells become phenotypically transformed and proliferate in multilayers (day 11). NRK cells can also directly be transformed from quiescent monolayers by addition of RA (50 ng/ml), EGF (5 ng/ml), and insulin (5 μg/ml), such that density-dependent growth inhibition is prevented. Phenotypic transformation of NRK cells was also observed when TGFβ (2 ng/ml) was used instead of RA.

described in this thesis have been performed on such monolayers of quiescent NRK cells. Next, upon addition of epidermal growth factor (EGF) as the only growth stimulating hormone and insulin as an anti-apoptotic agent (Kim et al., 1995), some 40% of the cells reenter the cell cycle and undergo one additional cell cycle, but are unable to proceed through additional cell cycles, in spite of the maintained presence of EGF (Van Zoelen et al., 1988). Under these conditions NRK cells in culture have become arrested in their proliferation as a result of high cell density (*see* Fig. 2A). This ability to undergo density-arrested growth inhibition is one of the major differences that discriminates non-transformed NRK cells from their transformed counterparts. However, when cultured in the additional presence of a transforming agent, such as transforming growth factor β (TGFβ) or retinoic acid (RA), NRK cells lose their density dependence of proliferation, which results in the formation of cellular multilayers (Fig. 2B). So, by the addition of specific combinations of growth factors, density-dependent growth inhibition is lost or prevented, and NRK cells obtain a transformed phenotype. Phenotypically transformed NRK cells also exhibit the ability to grow under anchorage-independent conditions, which allows them to grow in soft agar. Anchorage-independent growth is considered to be the best *in vitro* correlate of tumorigenesis *in vivo* (Cifone and Fidler, 1980; Shin et al., 1975).

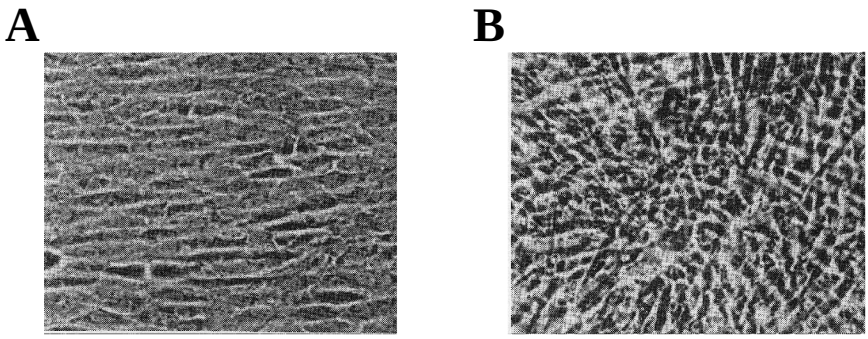

Figure 2 Phenotypic transformation of NRK cells induced by EGF and TGFβ. NRK fibroblasts in monolayer culture were grown to confluence in serum-containing medium and subsequently cultured in the above growth factor inactivated serum-containing medium supplemented with **A)** 5 μg/ml insulin and 2 ng/ml EGF such that density-arrested monolayers were obtained, or **B)** 5 μg/ml insulin, 2 ng/ml EGF, and 1 ng/ml TGFβ, which induces phenotypic transformation of NRK cells. Cultures were photographed after 72 h of incubation of these latter media. (adapted from Van Zoelen et al., 1991).

Mechanisms involved in growth control of NRK fibroblasts

A wide variety of pathological disorders, including numerous types of cancer, results from dysfunction of the EGF receptor signaling pathway (Yarden and Sliwkowski, 2001), and therefore this receptor forms an important target for antitumor therapies (Haluska and Adjei, 2001; Solbach et al., 2002; Voldborg et al., 1997). The EGF receptor also plays an important role in the growth control of NRK cells. At higher cell densities the expression of this receptor is decreased (Rizzino et al., 1990; Rizzino et al., 1988) and it has been postulated that as a consequence normal cells become unresponsive to the action of EGF as soon as a certain cell density is reached whereby EGF receptor levels have decreased below a critical threshold (Van Zoelen, 1991). This regulatory role for the EGF receptor in contact-inhibition has been confirmed by the observation that density-dependent growth inhibition of NRK cells was prevented in NRK cells in which the EGF receptor is overexpressed (Kizaka-Kondoh et al., 2000). Moreover, this could be mimicked by stimulation of quiescent NRK cells with transforming factors, such as TGFβ, RA, prostaglandin F2α (PGF2α) or bradykinin (BK), which all strongly increase EGF receptor binding levels (Lahaye et al., 1998). These agents have no growth stimulating activity on NRK cells by themselves, but induce phenotypic transformation in the additional presence of EGF, whereas the time course of phenotypic transformation correlates very well to the increase of EGF receptor binding levels. (Lahaye et al., 1998).

Transforming agents such as TGFβ and RA not only prevent density-dependent growth inhibition, but also make density-arrested NRK cells responsive again to EGF. This is paralleled by an increase in EGF receptor levels (Assoian, 1985; Roberts et al., 1984), such that growth stimulating signals induced by EGF are enhanced and density-dependent growth inhibition is overcome. Based on these observations, it has been postulated that all factors that increase the number of EGF receptors in the plasma membrane of density-arrested NRK cells reinitiate them to proliferate in an EGF-dependent manner, resulting in the loss of density-dependent growth inhibition and concomitant

phenotypic transformation (Rizzino et al., 1990; Van Zoelen et al., 1994). Alternatively, proliferation of density-arrested NRK cells by EGF can be restored upon the addition of parallel-acting growth factors such as platelet-derived growth factor (PDGF) and lysophosphatidic acid (LPA), also resulting in phenotypic transformation (Van Zoelen, 1991; Van Zoelen et al., 1988).

Recently, the ability of ligands of G-protein receptors to induce phenotypic transformation of NRK fibroblasts has been investigated in relation to the induction of second messengers by these ligands (Lahaye et al., 1999b). Endothelin-1 (ET-1) and LPA rapidly induced phenotypic transformation of NRK cells, while transformation by PGF2α and BK occurred with delayed kinetics. The fast induction of loss of density-arrest by LPA is explained by the fast enhancement of EGF receptor levels and the mitogenic activity of LPA itself. Although the enhancement of EGF receptor levels seems to be essential for the induction of transformation, the rate of upregulation of EGF receptor levels by ET-1, which has no mitogenic activity on NRK cells itself, was much slower and did not seem to correlate to the induction of phenotypic transformation of these cells. This discrepancy is explained in terms of different characteristics of second messenger induction by ET-1 compared to other G-protein ligands. Compared to BK, LPA and PGF2α, ET-1 is the most potent inducer of arachidonic acid release and phosphatidylinositol 4,5-bisphosphate hydrolysis and only the ET-1-induced transient enhancement of the intracellular calcium concentration was accompanied by both homologous and heterologous desensitization (Lahaye et al., 1999b).

Amongst the four ligands tested the nonapeptide BK seems to take a special place because only this ligand initially inhibited the loss of density-dependent growth inhibition and phenotypic transformation induced by TGFβ and RA, which was paralleled by a repression of EGF receptor levels (Afink et al., 1994; Lahaye et al., 1994; Van Zoelen et al., 1994). In contrast, upon prolonged exposure BK has growth stimulatory effects by itself and enhances the proliferative effects of TGFβ and RA. Bradykinin has previously been shown to induce the release of inositol-1,4,5 trisphosphate (IP_3) and to increase the intracellular calcium concentration of NRK cells (De Roos et al., 1997a; Lahaye et al., 1999b), but its inhibitory action on phenotypic transformation cannot be attributed to these effects since other IP_3 releasing agents such as PGF2α and LPA do not mimic the inhibitory effect by BK. Instead, the production of a prostaglandin derivative has been proposed to be involved in this process since a blocking of the cyclooxygenase pathway and thus the production of prostaglandins counteracted the inhibitory action of BK on the transformation process (Afink et al., 1994). Externally added PGJ2 could mimic the inhibitory action by bradykinin and therefore it has been proposed that this growth-inhibiting prostaglandin is specifically induced upon treatment of the cells with bradykinin (Lahaye et al., 1994).

Although the expression of EGF receptors seems to play a key role in growth regulation of NRK fibroblasts, several other factors have also been shown to play a role in density-dependent growth inhibition and phenotypic transformation, including PTPase activity (Rijksen et al., 1993), cyclins and

cyclin-dependent kinases (Zhu et al., 1996; Zhu et al., 2000b), inositol polyphosphate 5-phosphatase (Speed et al., 1996), connective tissue growth factor (Kothapalli et al., 1997), and extracellular matrix proteins such as fibronectin (Dalton et al., 1992; Ignotz and Massague, 1986). Protein phosphorylation and dephosphorylation processes are essential for many aspects of cellular signaling and the observation that inhibition of phosphatase activity by vanadate prevented the induction of density-dependent growth inhibition of NRK cells suggested a role for PTPase activity in growth control of NRK cells (Rijksen et al., 1993). In addition, normal adhesion requirement for expression of cyclin D1 is lost in NRK cells (Zhu et al., 1996) and it has been shown that this loss is causal for the induction of anchorage-independent growth by TGFβ (Zhu et al., 2000b). Also, underexpression of inositol polyphosphate 5-phosphatase in NRK cells, which hydrolyses the second messenger molecules inositol 1,4,5-trisphosphate (IP_3) and inositol 1,3,4,5-tetrakisphosphate (IP_4), was accompanied by cellular transformation (Speed et al., 1996). Since IP_3, IP_4 and intracellular calcium levels were elevated in these cells, these second messengers may be involved in growth control of NRK cells. It should be realized however that for all these parameters it is not always clear whether they really contribute to density-dependent growth inhibition and phenotypic transformation of NRK cells or that they are only regulated by these processes.

In addition to the growth-regulatory factors mentioned above, several findings have indicated that the biophysical properties of NRK cells may play a role in density-dependent growth inhibition and phenotypic transformation of these cells (De Roos et al., 1997c; Van Zoelen and Tertoolen, 1991). Therefore we have focused on the biophysical aspects of NRK cells including membrane potential, gap junctional intercellular communication (GJIC), and calcium signaling in relation to their growth regulation.

Membrane potential in cellular signaling

The membrane potential of cells, which generally ranges from -10 to -90 mV in eukaryotic cells (Binggeli and Weinstein, 1986), is determined by the concentration gradients for different ions and the relative permeabilities of the plasma membrane for these ions. This permeability depends primarily on the opening and closure of various ion channels present in the plasma membrane, which allow the passive flow of small ions down their electrochemical gradient. The selectivity filter in the pore of each ion channel ensures the selective permeability for a restricted class of ions.

One of the key events in cell cycle progression is the modulation of ion permeability, which is accompanied by alterations in the membrane potential (Boonstra et al., 1981; Sachs et al., 1974). Activation of a large diversity of K^+ and Cl^- channels at specific stages of the cell cycle is crucial to prevent cell cycle arrest in a variety of cell types (Chen et al., 2002; MacFarlane and Sontheimer, 2000). For example, activation of K^+ channels is required for many cell types to progress through the G_1 phase of the cell cycle (Wonderlin and Strobl, 1996), while Cl^- channels have been shown to play a role in both G_0/G_1 and G_1/S transition of NIH 3T3 fibroblasts (Zheng et al., 2003).

The modulation of the membrane potential may contribute to growth control of NRK cells. Whereas confluent monolayers of quiescent NRK fibroblasts have a stable hyperpolarized membrane potential around -70 mV (De Roos et al., 1997a), density-arrested monolayers spontaneously fire calcium action potentials that are characterized by a long duration plateau phase (~30s) and long-lasting interspike interval of 0.5-5 min (De Roos et al., 1997c). These action potentials are accompanied by transient rises in the intracellular calcium concentration and have never been measured in quiescent monolayers, although in these monolayers a propagating action potential can be evoked by local stimulation (De Roos et al., 1997d). In spite of this remarkable property of density-arrested monolayers, the role for the membrane potential and especially the action potential firing in growth control of NRK cells remained unclear and this finding was the incentive for the research presented in this thesis.

Since ion channels mediate the transport of electrical charges, they can be considered as electrical conductances. In contrast, the lipid bilayer of the plasma membrane itself is impermeable for ions and since this extremely thin insulating layer (~6 nm) separates internal and external conducting solutions, it naturally serves as an electrical capacitor which is charged or discharged upon changes in membrane current. Ion channels can be regarded as electrical units that are specifically responsive to a given stimulus such as a change in the membrane potential, the binding of a ligand and mechanic deformation. In excitable cells, the transient opening and closure of ion channels can induce pulse-like electrical signals called action potentials. These action potentials allow the rapid transmission of information over long distances, thereby mediating several processes including neurotransmitter release by nerve cells and contraction of muscle cells (Hille, 2001). In addition, electrical bursting activity has been shown to underlie pulsatory release of insulin by pancreatic beta cells (Santos et al., 1991). In all these processes cytoplasmic calcium ions play a prominent role, since calcium often serves as the ultimate trigger for the cellular responses. Internal calcium can also regulate the membrane potential by the gating of specific ion channels. For example, in NRK fibroblasts an increased intracellular calcium concentration results in a depolarization of the membrane by the opening of calcium-activated chloride channels (De Roos et al., 1997a).

In 1952, Hodgkin and Huxley introduced a mathematical model (HH-model) for dynamical changes of the membrane potential based on voltage-clamp measurements on the squid giant axon (Hodgkin and Huxley, 1952). The HH-model described the kinetics of selective (Na^+, K^+) ion conductance changes and predicted the major features of excitability such as action potential shape and conduction velocity. In addition, it suggested properties for the gating of ion channels. Typical for their model is that the conductance properties only depend on voltage and time, and that activation and inactivation are considered as entirely independent processes that both depend on the membrane potential. The HH-model contributed to the understanding of excitability of cells and formed the basis for much subsequent work in which membrane excitability was analyzed, including that of fibroblastic cells in the present study.

Besides for the generation of action potentials in excitable cells, ion channels also mediate several processes in non-excitable cells such as control of cell volume and regulation of ion flows across epithelial cells (Braun and Schulman, 1996; Hoenderop et al., 2002). Fibroblasts, which constitute the connective tissues of the body, are generally considered to be classical examples of non-excitable cells. Therefore it was very surprising that propagating action potentials have been measured in monolayers of NRK fibroblasts. They turned out to be the result of the activation of L-type calcium channels and the subsequent opening of calcium-dependent chloride channels (De Roos et al., 1997c; De Roos et al., 1997d). The underlying mechanisms of excitability in NRK fibroblasts have been part of the present study. It is however unclear if this action potential firing also occurs *in vivo* and what the possible role of this firing is. Previously, other fibroblasts have also been shown to express voltage-dependent calcium channels (Baumgarten et al., 1992; Chen et al., 1988; Lovisolo et al., 1988; Peres et al., 1988), while slow action potentials have been measured in Balb/c 3T3 fibroblasts (Lovisolo et al., 1988).

Gap junctional intercellular communication (GJIC)

For the coordinated behavior of cells in a multicellular organism, communication between individual cells is of paramount importance. Intercellular communication can either be achieved by direct cell-to-cell communication or indirectly by the secretion of hormones and growth factors. Gap junctions enable the direct exchange of small ions such as Ca^{2+} and low molecular weight (<1 kDa) metabolites such as IP_3 and cAMP (Bennett et al., 1991), thus mediating the transduction of signaling molecules between adjacent cells.

Gap junctions have been identified as tightly clustered particles, with each particle representing a gap junctional channel (Goodenough and Revel, 1970; McNutt and Weinstein, 1970). These intercellular channels are formed by the association of two hexameric hemichannels, or connexons, on the plasma membrane of opposite cells. Each connexon on its turn is composed of six protein subunits, called connexins, which are integral plasma membrane proteins. The expression of connexin genes is tissue and cell-type specific (Kumar and Gilula, 1996) and so far up to 20 connexin genes have been identified in the murine and human genomes, encoding for connexins with molecular weights ranging from 25 to 57 kDa (Willecke et al., 2002). From these connexin residues, connexin 43 (Cx43) is primarily expressed by fibroblasts (Goldberg and Lau, 1993), including NRK fibroblasts (Li et al., 1996). Gap junctional intercellular coupling is not restricted to two identical cells, but can also be achieved between different cell types as for example shown for fibroblasts and epithelial cells (De Roos, 1997).

GJIC is essential for the regulation of a variety of biological processes such as embryogenesis, cell proliferation, cardiac function, and propagation of calcium waves (Bruzzone et al., 1996; Chen et al., 1995; Kalimi and Lo, 1988; Kumar and Gilula, 1996). Gap junctions not only mediate the transfer of small signaling molecules and metabolites between neighboring cells (Goldberg et al., 1999; Saez et

al., 1989), but also establish electrical coupling between cells and can therefore be considered as electrical conductors. Due to electrical coupling, groups of cells can act as an electrical syncytium synchronizing their electrical activity. Electrical coupling is important for processes such as the contraction of smooth muscle (De Mello, 1994) and the propagation of action potentials, e.g. in the heart (Gros and Jongsma, 1996), but also *in vitro*, e.g. in NRK fibroblasts (De Roos et al., 1997d).

The permeability of gap junction channels can be regulated by a variety of stimuli that induce modification of these channels. Several growth factors have been described to reduce GJIC by the initiation of complex signaling pathways that eventually result in the activation of kinases and phosphatases, which modify the cytoplasmic C-terminal region of Cx43 (Hossain and Boynton, 2000) and induce closure of gap junctional channels by the so-called ball-and-chain model (Zhou et al., 1999). These include receptors for PDGF (Pelletier and Boynton, 1994) and EGF (Lau et al., 1992), whereas EGF has been shown to stimulate serine phosphorylation of Cx43, probably mediated by activated MAP kinases (Kanemitsu and Lau, 1993). However, EGF has also been reported to enhance GJIC (Vikhamar et al., 1998). In addition, activation of various types of G-protein coupled receptors, including those for LPA, thrombin, and ET-1, leads to gap junction closure through a signaling pathway involving the c-Src tyrosine kinase (Postma et al., 1998), which phosphorylates the C-terminal tail of Cx43 (Giepmans et al., 2001). GJIC can also be regulated by changes in intracellular pH (Hermans et al., 1995; Spray et al., 1981) and it has been proposed that the reduction of cardiac gap junctional conductance at decreased intracellular pH is achieved by the protonation of histidine residues in the cytoplasmic loop of Cx43 (Spray and Burt, 1990). In addition, transjunctional voltage differences and (non-physiological) increases in intracellular calcium concentrations may reduce gap junctional coupling. Besides the physiological regulation of GJIC, several chemicals can block gap junctions mostly by altering the lipid environment and cell membrane fluidity (Niggli et al., 1989; Takens-Kwak et al., 1992). However, this pharmacological inhibition is generally not very specific and accompanied by non-specific effects on ionic plasma membrane channels.

Several methods have been described to measure gap junctional intracellular communication. By monitoring the diffusion of fluorescent dyes (Loewenstein, 1979) or radioactively labeled metabolites (Goldberg et al., 1999), biochemical coupling of cells can be assessed. Moreover, electrical coupling of cells can be determined with the use of the patch-clamp technique (Hamill et al., 1981). A widely used method is to keep each of two coupled cells of a cell pair in voltage-clamp and step the voltage in one cell while keeping the voltage constant in the other cell (Neyton and Trautmann, 1985; Veenstra, 2001). Under favorable conditions the current flowing between the cells can be measured to determine the coupling conductance between the cells. Another method is simpler, because it uses only one patch pipette to apply voltage-clamp steps to a cell coupled to another cell or surrounded by coupled cells (Bigiani and Roper, 1995; De Roos et al., 1996). Analysis of the capacitive current transient allows one to infer changes in the coupling conductance between the measured cell and its neighbor cell or

the surrounding cells (Harks et al., 2001). Although the single electrode method is less direct, it allows *in situ* measurement of electrical coupling in intact cultures or tissues.

In general, tumorigenic transformation has been shown to result in a decreased GJIC (Binggeli and Weinstein, 1986; Holder et al., 1993; Loewenstein, 1979). It has been postulated that uncoupling of cells contributes to the transformation process by a reduction of the diffusion of putative growth inhibiting factors. In contrast with this general observation, dye-coupling experiments showed that upon phenotypic transformation of NRK fibroblasts GJIC was significantly increased (Van Zoelen and Tertoolen, 1991). On the other hand, other studies have shown that NRK cultures are electrically well-coupled (De Roos et al., 1996; Maldonado et al., 1988). Therefore, the role of GJIC in growth control of NRK cell remains elusive.

Calcium signaling

Cytoplasmic calcium is a ubiquitous second messenger that plays a crucial role in the regulation of many physiological processes such as smooth muscle contraction, cell proliferation and differentiation, apoptosis and neurotransmitter secretion. The coordination of such a diversity of complex events by a "simple" ion arises from the spatiotemporal aspects of calcium signaling (reviewed by Berridge et al., 1998). Spatial aspects of calcium signaling vary from elementary calcium puffs to intra- and intercellular calcium waves. In addition, the frequency and amplitude of calcium oscillations have been shown to control molecular mechanisms such as gene transcription and enzyme activation (De Koninck and Schulman, 1998; Dolmetsch et al., 1998).

At the cellular level, calcium can either be derived from the extracellular space by influx through plasma membrane channels or from release from internal calcium stores. In many non-excitable cells calcium signaling is initiated by external factors that activate plasma membrane receptors linked to inositol-lipid specific phospholipase C (PLC), which generates IP_3 from membrane phospholipids (Berridge, 1993). The second messenger IP_3 triggers calcium release from the endoplasmic reticulum (ER) upon binding to IP_3 receptors, which are located in the membrane of the ER. The IP_3 receptor is constituted of four subunits and opening of this calcium release channel requires the binding of both IP_3 and calcium (Marchant and Taylor, 1997). Calcium release is impeded by a slow auto-inhibitory process that involves the binding of calcium to another site at the IP_3 receptor (Parker and Ivorra, 1990).

The release of calcium from internal stores is closely followed by entry of extracellular calcium into the cytosol by a mechanism known as capacitative calcium entry or store-operated calcium (SOC) influx (Putney, 1986). Capacitative calcium entry may contribute to the rapid refilling of internal calcium stores and provides prolonged elevated intracellular calcium concentrations. Although capacitative calcium entry has been reported in many different cell types, the mechanism that links store emptying to the activation of store-operated calcium channels in the plasma membrane is still elusive. Several hypotheses about this signaling mechanism have been proposed. The first one

involves the release of a putative diffusible calcium influx factor (CIF) from the endoplasmic reticulum (Randriamampita and Tsien, 1993), such as 5,6-eopoxyeicosatrienoic acid (5,6-EET) (Graier et al., 1995; Rzigalinski et al., 1999). This compound is metabolized from arachidonic acid by cytochrome P-450 epoxygenase, which is activated upon store depletion, while inhibition of this enzyme has been shown to block capacitative calcium entry (Graier et al., 1995). In addition, it has been proposed that 14,15-EET participates in the CIF-mediated regulation of cytosolic calcium by blocking the 5,6-EET-induced elevation of the intracellular calcium concentration (Rzigalinski et al., 1999). The second mechanism proposed involves the direct interaction of IP_3 receptors in the ER with store-operated calcium channels in the plasma membrane by a mechanism known as conformational coupling (Berridge, 1995b; Irvine, 1990). According to this model, the release of calcium from internal stores leads to a conformational change in the IP_3 receptor, which can then bind to plasma-membrane calcium channels. In addition, a secretion-like coupling model has been suggested that implies a role for the reorganization of the cortical actin cytoskeleton in the modulation of capactitative calcium entry (Patterson et al., 1999). The pathway that eventually regulates capacitative calcium entry may be cell type specific or can involve a combination of the proposed mechanisms (Xie et al., 2002).

Besides IP_3, two other second messengers are known to stimulate the mobilization of calcium from internal stores. First, cyclic adenosine diphosphate ribose (cADPR) has been described to trigger calcium release in several cell types (Allen et al., 1995; Lee et al., 1989; Petersen and Cancela, 1999). cADPR is synthesized from β-NAD^+ by an ADP-ribosyl cyclase enzyme (Wilson and Galione, 1998) and activates ryanodine receptors by sensitizing them to calcium-induced calcium release (CICR) (Guo and Becker, 1997; Lee, 1993). By this action, cADPR has been shown to potentiate calcium release from ryanodine-sensitive calcium stores after calcium entry through L-type calcium channels, thus enhancing coupling between these voltage-activated channels and intracellular calcium release (Empson and Galione, 1997; Hashii et al., 2000). So, calcium and cADPR act as coagonists of the ryanodine receptor, such that the sensitization of this calcium release channel by cADPR is dependent on the presence of calmodulin (Lee et al., 1994), probably in combination with other accessory proteins (Lee, 1997). More recently, nicotinic acid adenine dinucleotide phosphate (NAADP) has emerged as a potent mobilizer of calcium (Bak et al., 1999; Cancela et al., 1999), e.g. in pancreatic β cells where it mediates glucose-induced calcium signaling (Masgrau et al., 2003). NAADP is synthesized from β-$NADP^-$ by an ADP-ribosyl cyclase enzyme (Wilson and Galione, 1998) and upon binding to its receptor, which has recently been characterized in sea urchin eggs (Berridge et al., 2002), NAADP initiates calcium release from a store with unique properties compared to the IP_3- and cADPR-sensitive calcium stores (Lee and Aarhus, 1995). First, NAADP-sensitive calcium release has distinct regulatory mechanisms compared to calcium release induced by IP_3 and cADPR. In contrast to IP_3 and cADPR, calcium release by NAADP does not exhibit positive feedback by calcium via CICR (Chini and Dousa, 1996). Moreover, subthreshold concentrations of NAADP fully inactivate

subsequent calcium release indicating that NAADP irreversibly binds to its receptor (Aarhus et al., 1996; Patel et al., 2000), although more recent studies have shown that NAADP self-inactivation in intact sea urchin eggs is reversible with resensitization occurring in approximately 20 min (Churchill and Galione, 2001). In addition, NAADP-sensitive calcium stores possess a Ca-ATPase which is insensitive to thapsigargin, whereas calcium uptake in IP_3- and cADPR-sensitive stores is blocked by this compound (Genazzani and Galione, 1996). Finally, the NAADP-sensitive calcium release can be blocked by L-type calcium channel blockers, which suggests the NAADP-sensitive release channel exhibits similarities with this voltage-activated calcium channel (Genazzani et al., 1997). So, cells generally possess multiple calcium stores and calcium signaling may thus result from an intricate interplay between different stores, as described for sea urchin eggs, pancreatic acinar cells and Jurkat T lymphocytes (reviewed by da Silva and Guse, 2000). In pancreatic acinar cells it has been shown that calcium released by NAADP merely serves as a trigger, which is amplified by CICR mediated by both cADPR- and IP_3-dependent mechanisms (Cancela et al., 1999).

Prostaglandins

Arachidonic acid is released from membrane phospholipids by phospholipase A2 (PLA2) in response to various stimuli, and this polyunsaturated fatty acid can subsequently be converted to a large diversity of bioactive lipids (Fig. 3). It can be converted to biologically active epoxides via the epoxygenase pathway, whereas conversion by lipoxygenase activity results in the production of leukotriens, lipoxins and hydroxy-fatty acids. In addition, prostanoids which include prostaglandins (PG) and thromboxanes (Tx) such as PGI2, PGD2, PGE2, PGF2α, and TxA2, are produced by the cycolooxygenase enzyme system (COX) and it is believed that these lipids act locally in the vicinity of their production in a paracrine or autocrine fashion. Especially PGI2 and TxA2 are chemically unstable with a half-life of 30 s to a few minutes (Narumiya et al., 1999).

Two isoforms of COX enzymes have been reported that differ in many respects. COX-1 is constitutively expressed in most tissues and is involved in physiological functions such as regulation of renal blood flow and maintenance of gastric mucosa (DeWitt and Smith, 1995; Smith et al., 2000). On the other hand, COX-2 is inducible by growth factors, cytokines and tumor promoters (Bradbury et al., 2002; Ershov and Bazan, 1999; Sato et al., 1997). Overexpression of COX-2 has been found to be play a key role in various stages of tumorigenesis (Singh and Lucci, 2002), and this observation has stimulated research to elucidate the role of prostaglandin synthesis in relation to cancer (Bishop-Bailey et al., 2002; Prescott and Fitzpatrick, 2000; Singh-Ranger and Mokbel, 2002). In fact, inhibiting COX-activity with aspirin, which is a classical nonsteroidal antiinflammatory drug (NSAID), has promising characteristics for tumor prevention (Bishop-Bailey et al., 2002). However, general inhibition of COX-activity with NSAIDs is accompanied by gastrointestinal side effects, which may result from impaired angiogenesis (Jones et al., 1999).

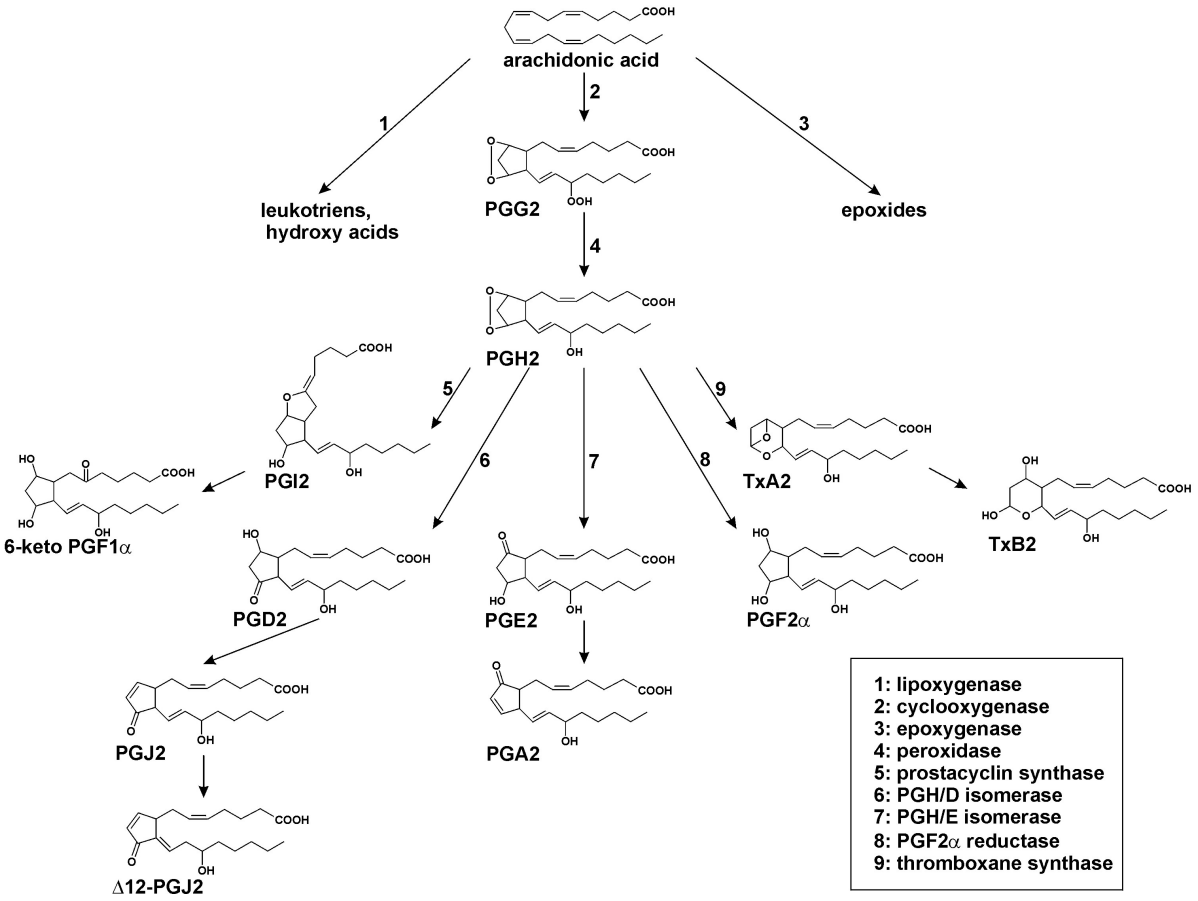

Figure 3 Schematic overview showing the enzymatic (indicated by the numbers) and non-enzymatic steps in the formation of prostaglandins (PG) and thromboxanes (Tx) from arachidonic acid.

It has been established that biological effects exerted by prostanoids are mediated by membrane-bound receptors, which mostly belong to the superfamily of G-protein coupled receptors (Narumiya, 1994). So far, eight isoforms of prostanoid receptors have been characterized and their nomenclature is based on the binding selectivity for the natural prostanoids (Coleman et al., 1994). DP receptors are activated by PGD2, EP receptors (with subtypes EP_1, EP_2, EP_3 and EP_4) by PGE2, FP receptors by PGF2α, IP receptors by PGI2, and TP receptors by TxA2. However, prostaglandins may also bind with lower affinity to one of the other receptors. Based on their signal transduction, prostanoid receptors can be divided into three categories. First, relaxant receptors mediate the increase in cAMP levels and include the DP, EP_2, EP_4 and IP receptor. Second, the EP_3 receptor belongs to the class of inhibitory receptors and mediates decreases in cAMP levels. Third, the EP_1, FP and TP receptor are contractile receptors and induce phosphatidyl-inositol phosphate hydrolysis by activation of PLC, which is accompanied by calcium mobilization from internal stores (reviewed by Narumiya et al., 1999). In addition to their binding on plasma membrane receptors, some prostaglandins may also act intracellularly by the activation of nuclear hormone receptors. For example, the PGJ2 derivative 15-deoxy PGJ2 is the natural ligand for peroxisome proliferator-activated receptor γ (PPARγ), which regulates the

transcription of numerous genes involved in intracellular lipid and lipoprotein metabolism (Willson and Wahli, 1997). Interestingly, PPARγ has been described as a therapeutical target in the treatment of cardiovascular pathologies (Bocher et al., 2002).

Outline thesis

In the present study we investigated excitability and calcium signaling in NRK fibroblasts. We show that confluent monolayers of quiescent NRK cells exhibit extensive electrical coupling, which is reversibly blocked by fenamates (*Chapter 2*). By performing voltage- and current-clamp experiments on single NRK cells and small clusters we show that an L-type calcium, calcium-dependent chloride and inward rectifier potassium conductance constitute the ionic basis for excitability of NRK fibroblasts (*Chapter 3*). Based on these membrane conductances we constructed a mathematical model for the excitability in NRK cells and could thus reconstruct voltage- and current-clamp behavior and action potential propagation (*Chapter 4*). This model also showed that slow periodic action potential firing could not be achieved solely by the present membrane conductances, suggesting the involvement of cytosolic calcium in determining periodicity. When using 2-APB to study calcium signaling in NRK cells, we found that it not only blocks agonist-induced calcium oscillations in these cells, but also reversibly inhibits gap junctional coupling. Since 2-APB did not inhibit the membrane conductances in NRK cells we could use it as a tool to measure membrane conductances in intact confluent monolayers (*Chapter 5*). We investigated the role of calcium influx and intracellular calcium stores in intracellular calcium oscillations that were measured upon stimulation of NRK cells with prostaglandin F2α, and showed that the initial peak results from release from IP_3-sensitive stores while subsequent calcium transients are mediated by an interplay between both IP_3-sensitive stores and calcium influx. Remarkably, the oscillations measured in confluent monolayers were not synchronized in spite of the fact that NRK cells were coupled by gap junctions (*Chapter 6*). Finally, we show that phenotypic transformation of NRK cells is accompanied by a depolarization of the membrane and the secretion of a calcium-mobilizing agent, which was identified with mass-spectrometry as PGF2α (*Chapter 7*). Results are discussed in terms of the putative role of the membrane potential, intracellular calcium and gap junctional communication in growth regulation of NRK fibroblasts. In addition, the mechanism of cell excitability, as well as that of the intracellular calcium oscillations that form the basis for periodicity in these cells, are reviewed (*Chapter 8*).

CHAPTER 2

Fenamates: a novel class of reversible gap junction blockers

E.G.A. Harks, A.D.G. de Roos, P.H.J. Peters, L.H. de Haan, A. Brouwer, D.L. Ypey, E.J.J. van Zoelen and A.P.R. Theuvenet

Abstract. The effect of fenamates on gap junctional intercellular communication was investigated in monolayers of NRK fibroblasts and of SKHep1 cells overexpressing the gap junction protein connexin 43 (Cx43). Using two different methods to study gap junctional intercellular communication, single electrode voltage-clamp step response measurements and dye microinjection, we show that fenamates are reversible blockers of Cx43-mediated intercellular communication. After adding fenamates to a confluent monolayer of electrically coupled NRK fibroblasts, the voltage-step induced capacitive current transient changed from a transient characteristic for charging multiple coupled cell capacitances, to one characteristic for a single cell in isolation. The capacitance of completely uncoupled cells was 19.7 ± 1.0 pF (mean ± S.E.M.; n=11). Junctional conductance between the patched cell and the surrounding cells in the monolayer changed from >140.7 ± 9.6 nS (mean ± S.E.M.; n=14) to <1.4 ± 0.4 nS (mean ± S.E.M.; n=11) after uncoupling. Electrical coupling could be restored to >51.8 ± 4.2 nS (mean ± S.E.M.; n=11) by wash-out of the fenamates. Voltage-clamp step response measurements showed that the potency of fenamates in inhibiting electrical coupling decreases in the order meclofenamic acid > niflumic acid > flufenamic acid. The half-maximal concentration determined by dye-coupling experiments was 25 μM and 40 μM for meclofenamic acid and flufenamic acid, respectively. Inhibition of gap junctional communication by fenamates did not involve changes in intracellular calcium or pH, and was unrelated to protein kinase C activity or an inhibition of cyclooxygenase activity. Voltage-clamp step response measurements in confluent monolayers of SKHep1 cells that had been stably transfected with Cx43, revealed that fenamates are potent blockers of Cx43-mediated intercellular communication. In conclusion, fenamates represent a novel class of reversible gap junction blockers that can be used to study the role of Cx43-mediated gap junctional intercellular communication in biological processes.

Introduction

Fenamates belong to the class of *N*-phenylanthranilic acids and are widely used as nonsteroidal anti-inflammatory drugs (NSAIDs) by their ability to inhibit cyclooxygenases (Brogden, 1986). In addition, fenamates modulate a diversity of ion channels. They have been identified as inhibitors of voltage-gated and ATP-sensitive potassium channels (Grover et al., 1994; Lee and Wang, 1999), voltage-gated calcium channels (Li et al., 1998a), calcium-activated chloride channels (White and Aylwin, 1990) and non-selective cation channels (Gogelein et al., 1990). On the other hand, fenamates have been shown to activate calcium-activated and voltage-dependent potassium channels (Farrugia et al., 1993; Ottolia and Toro, 1994). Since we had found that flufenamic and niflumic acid inhibited the propagation of calcium action potentials in monolayers of NRK fibroblasts (De Roos et al., 1997c), we investigated whether fenamates could also block gap junctional channels.

Gap junctional intercellular communication (GJIC) is of paramount importance in the regulation of a variety of biological processes. Gap junctional channels allow intercellular diffusion of small (<1kDa) hydrophilic molecules and ions. This intercellular diffusion of signal molecules regulates a variety of biological processes including embryogenesis, cell proliferation, cardiac function, and propagation of calcium waves (Bruzzone et al., 1996; Kumar and Gilula, 1996). Besides diffusion of small molecules, gap junctions also mediate electrical coupling between cells and allow clusters of cells to behave as an electrical syncytium. Electrical coupling underlies synchronous electrical activity between excitable cells and has been shown to be essential in the propagation of the cardiac action potential (Gros and Jongsma, 1996), the contraction of smooth muscle (De Mello, 1994) and the coordination of hormone secretion (Stauffer et al., 1993).

Gap junctions are present in the plasma membrane of cells as clusters of tightly packed particles each of which represents a single channel (Bukauskas et al., 2000). Each channel is formed by the docking of two hemi-channels (connexons) located in apposing cell membranes of neighboring cells. Each hemi-channel consists of six polypeptides called connexins. Connexin43 (Cx43) is the major gap junctional protein identified in fibroblasts (Goldberg and Lau, 1993). GJIC can be regulated by intracellular calcium and pH (Loewenstein, 1981; Spray and Bennett, 1985). In addition, several processes that induce modifications of Cx43, including phosphorylation on serine and threonine residues following activation of PKC (Lampe et al., 2000) and on tyrosine residues upon growth factor receptor activation (Lau et al., 1996) have been shown to modulate GJIC. The contribution of each of these processes to the modulation of GJIC is dependent on the cell type.

We (De Roos et al., 1996) and others (Maldonado et al., 1988) have shown that confluent NRK fibroblasts are electrically well coupled and here we show that fenamates can completely block intercellular communication of not only NRK cells but also of SKHep1 cells overexpressing Cx43. The observed inhibition is reversible and not mediated by changes of intracellular calcium or pH, and was unrelated to PKC activity or an inhibition of cyclooxygenase activity.

Results

Previously we showed that capacitance measurements can be used to study changes in GJIC in small clusters of NRK cells (De Roos et al., 1996). Here we added meclofenamic acid, flufenamic acid, niflumic acid and tolfenamic acid to a confluent monolayer of NRK cells and investigated their effect on the membrane potential and capacitive current transient at different time points after their addition. Meclofenamic acid (100 μM) depolarized the membrane of monolayer NRK fibroblasts (Fig. 1A) and the average depolarization was 25.7 ± 2.8 mV (n=33). The depolarization could be restored to the resting membrane potential by wash-out of the fenamate. Flufenamic acid, niflumic acid and tolfenamic acid induced comparable reversible depolarizations in monolayers of NRK fibroblasts of 23.2 ± 4.6 mV, 25.9 ± 2.6 mV and 24.8 ± 3.7 mV (all n=10), respectively.

Application of a voltage-clamp step to a single NRK fibroblast evokes a characteristic current transient that is determined by the series resistance (Rser) and the membrane capacitance and conductance of the individual cell (De Roos et al., 1996). In confluent monolayers of NRK fibroblasts, however, membrane capacitance and conductance of the surrounding cells also contribute to this current transient, since these cells are electrically well coupled. This is reflected by a slow and multi-exponential initial decay of the induced current and a subsequent large prolonged steady-state current (*see a*, Fig. 1B). Application of 100 μM meclofenamic acid to a monolayer of NRK fibroblasts caused an acceleration of the decay of the induced current and reduced the level of the prolonged steady-state current. This effect of meclofenamic acid was already observed under conditions that the membrane potential was still unchanged (*see b*, Fig. 1B). In this typical example, after 4 min the steady-state current reached a minimal value. The evoked current transient could be fitted by a single exponential, indicating a complete block of intercellular communication, since more than one exponential is needed to fit the transient during a partial block of intercellular communication (De Roos et al., 1996). The capacitance calculated from this transient was 23.7 pF (*see e*, Fig. 1B). The capacitance of cells completely uncoupled by meclofenamic acid was 19.7 ± 1.0 pF (n=11), which is of the same order of magnitude as previously measured in single isolated NRK cells (De Roos et al., 1996). Electrical coupling could be largely restored by wash-out of the fenamate (*see f-h*, Fig.1B). These results demonstrate that fenamates can reversibly block electrical coupling in NRK fibroblasts and that blocking is not mediated by changes in the membrane potential.

The time course of the uncoupling could be followed by calculating the estimated gap junctional conductance between the patched cell and the surrounding cell ring (G01x) from each capacitive current transient (Fig. 1C). G01x in the coupled monolayer was 140.7 ± 9.6 nS (n=14) and was reduced after addition of 100 μM meclofenamic acid to 1.4 ± 0.4 nS (n=11) within 6.0 ± 0.4 min (n=11). Since the single cell conductance is close to 1 nS (De Roos et al., 1996), this indicates that the patched cell is completely uncoupled from the surrounding cells. Although G01x could not completely be restored, partial recovery to 51.8 ± 4.2 nS (n=11) was reached within 7.2 ± 1.4 min (n=11).

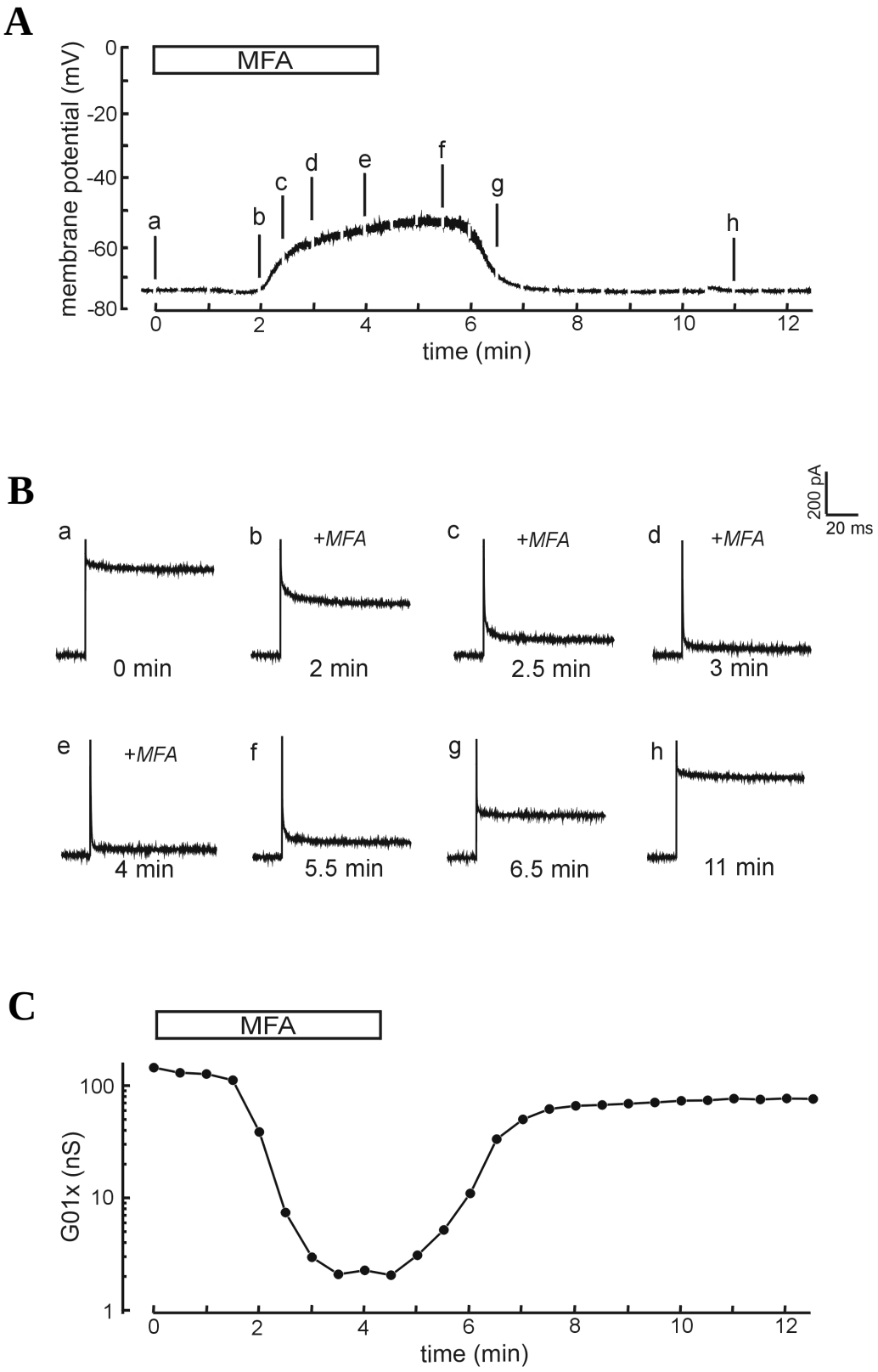

Figure 1 A) Membrane potential of a confluent monolayer of NRK cells was measured and addition of 100 µM meclofenamic acid (MFA) is indicated by the bar. The membrane potential recording shows short interruptions to the voltage-clamp mode. **B)** Capacitive current transients, evoked by application of a short voltage-clamp step (10 mV), at the in A) indicated time points a-h. **C)** Corresponding calculated gap junctional conductance (G01x) as a function of time. Addition of 100 µM meclofenamic acid (MFA) is indicated by the bar.

In order to compare the potency of different fenamates, the concentration dependence of their effects on electrical coupling has been determined. To obtain dose-response curves, G01x was calculated 15 to 20 min after addition of the fenamates when the capacitive current transient had reached a steady-state (Fig. 2). Although G01x reflects only an estimation of the gap junctional coupling, the dose-response curves clearly show that the potency of the fenamates in blocking electrical coupling decreases in the order meclofenamic acid > niflumic acid > flufenamic acid.

Fluorescent dye transfer of Lucifer Yellow was used to investigate whether fenamates, in addition to electrical coupling, can also affect dye-coupling. Lucifer Yellow was injected into a single cell of a confluent monolayer of NRK fibroblasts and intercellular diffusion of the dye showed that these cells were extensively dye-coupled (*upper panel*, Fig. 3). Pretreatment for 5 min with 100 µM meclofenamic acid completely prevented this diffusion of the injected dye to the neighboring cells (*lower panel*, Fig. 3). Dye-transfer was also completely inhibited when flufenamic acid was used at a concentration of 250 µM. These results demonstrate that fenamates can also completely block dye-coupling in NRK cells.

To quantify the reduction of intercellular communication by fenamates, the number of cells to which Lucifer Yellow could be transferred was determined 10 min after injection into a monolayer NRK cell. For meclofenamic acid, complete block of dye-coupling was achieved at a concentration of 100 µM, while block was half-maximal at 25 µM (*MFA*, Fig. 4). Flufenamic acid completely blocked dye-coupling at 250 µM. The inhibition of dye-coupling by flufenamic acid was half-maximal at 40 µM (*FFA*, Fig. 4). In agreement with their effects on electrical coupling, dye-coupling experiments show that meclofenamic acid is a more potent blocker of GJIC than flufenamic acid.

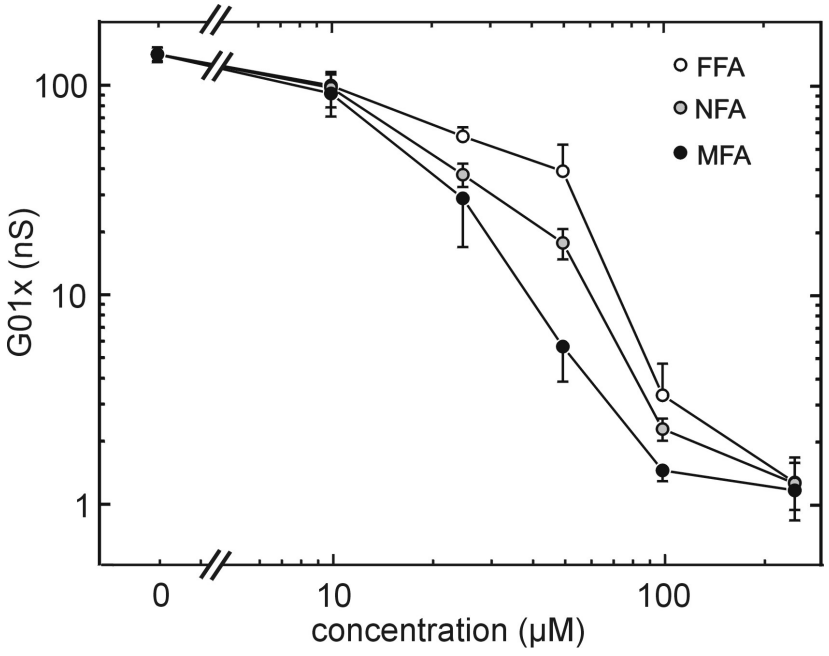

Figure 2 Dose-response curve of the inhibition of electrical coupling by fenamates. The calculated gap junctional conductance (G01x) as a function of the concentration flufenamic acid (FFA), niflumic acid (NFA) and meclofenamic acid (MFA) is shown. G01x was determined 15 to 20 min after addition of fenamates when the capacitive current transient had reached a steady-state (mean ± S.E.M.; n=4, control n=14).

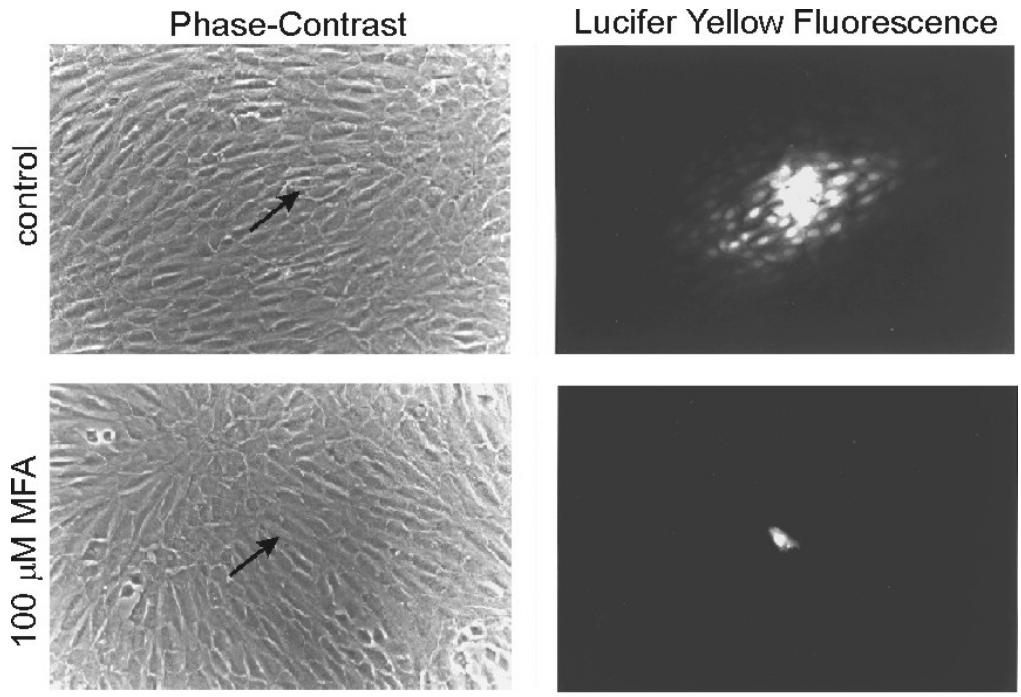

Figure 3 Dye-coupling in NRK fibroblasts. Lucifer Yellow was injected into one single cell of the monolayer and intercellular diffusion of the dye was monitored 10 to 15 min after injection. Phase-contrast and Lucifer Yellow fluorescence in control cells *(upper panel)* and after pretreatment with 100 μM meclofenamic acid (MFA) for 5 min *(lower panel)*. Arrows indicate the injected cell.

Next, we investigated whether the block of intercellular communication by fenamates could result from changes in the levels of the intracellular calcium concentration or pH, which are physiological modulators of gap junctions (Spray and Bennett, 1985). However, exposure of the cells to 250 μM meclofenamic acid for 10 min did not change the intracellular calcium concentration significantly. Fluorescence (340nm/380nm) values of intracellular fura-2 before and after exposure were 0.44 ± 0.01 and 0.43 ± 0.01 (n=10), respectively. Furthermore, the intracellular pH was unaffected under these conditions. The basal intracellular pH was 7.06 ± 0.04 and after adding meclofenamic acid the pH was 7.01 ± 0.05 (n=8). These data demonstrate that inhibition of GJIC by fenamates is neither mediated by changes in intracellular calcium nor pH.

PKC has been described as a regulator of GJIC (Lampe et al., 2000) and therefore we investigated whether block of GJIC by fenamates is mediated by activation of PKC. In a previous study, we investigated modulation of gap junctions by activation of PKC using the phorbol ester TPA (De Roos et al., 1996) and found that TPA caused a partial block of GJIC. In the present study we have found that after prolonged (24 h) pretreatment of NRK fibroblasts with TPA, which causes the complete down-regulation of PKC activity in these cells, electrical coupling was completely restored and could not be blocked anymore by 100 ng/ml TPA. However, in these PKC down-regulated NRK fibroblasts electrical coupling could still be blocked by fenamates. After addition of meclofenamic acid and niflumic acid (250 μM) to these cells for 10 min, the voltage step-induced current transients could be

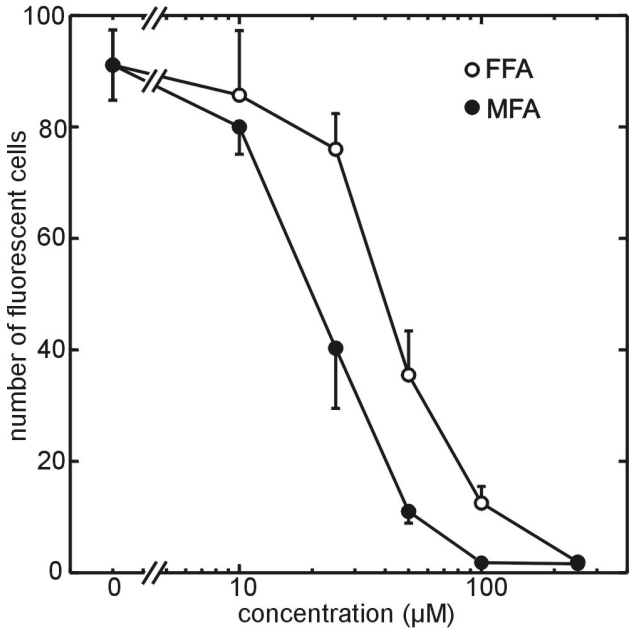

Figure 4 Dose-response curve of the inhibition of intercellular communication by fenamates. Number of dye-coupled cells as a function of the concentration meclofenamic acid (MFA) and flufenamic acid (FFA). Number of dye-coupled cells was determined 10 to 15 min after dye injection into a single cell (mean ± S.E.M.; n=4, control n=10).

fitted by single exponentials and the calculated capacitance of the cells was 20.1 ± 1.2 pF and 18.7 ± 2.6 pF (n=7), respectively. This excludes a role for PKC in the inhibition of GJIC by fenamates.

Whether the impairment of GJIC by fenamates could be directly related to an inhibition of cyclooxygenase activity in the NRK cells, was investigated by application of two other potent cyclooxygenase inhibitors, indomethacin and flurbiprofen. Pretreatment of NRK fibroblasts for 3 h with 1 μM of either of these inhibitors has been shown to cause a complete inhibition of cellular cyclooxygenase activity (Lahaye et al., 1994). We have found in the present study, however, that pretreatment of the cells for 3 h with either indomethacin or flurbiprofen did not affect their electrical coupling at all. G01x before and after the pretreatment with these inhibitors was 155.3 ± 12.8 nS (n=8) and 153.9 ± 16.4 nS (n=8), respectively. These results indicate that the impairment of GJIC by fenamates is unrelated to an inhibition of cyclooxygenase activity.

Since GJIC in NRK fibroblasts is mainly mediated by Cx43 (Li et al., 1996) we investigated whether impairment of intercellular communication can be attributed to a direct effect of fenamates on Cx43 function. To address that issue we added meclofenamic acid, flufenamic acid and niflumic acid to SKHep1 cells and SKHep1 cells that had been stably transfected with Cx43 (SKHep1-Cx43 cells). Monolayers of SKHep1 as well as SKHep1-Cx43 cells showed a membrane potential around -35 mV and application of 250 μM meclofenamic acid reversibly depolarized the membrane with 10.3 ± 2.5 mV (n=7) in SKHep1 cells and 11.4 ± 2.4 mV (n=7) in SKHep1-Cx43 cells. Voltage-clamp step response experiments showed that monolayers of wild-type SKHep1 cells, which do not express Cx43 and endogenously express only low levels of Cx45 (Moreno et al., 1995), were less well coupled than NRK fibroblasts (*control*, Fig. 5A). The capacitance derived from the initial fast current transient was 16.9 ± 0.3 pF (n=7), which is in the range of that of single cells in isolation. Thus, this capacitance is

that of the patched cell in the monolayer. The corresponding G01x was 10.3 ± 0.3 nS (n=7) and was reduced to 2.9 ± 0.2 nS (n=7) after application of 250 µM meclofenamic acid to these cells (*8 min*, Fig. 5A). The capacitance of the patched cell was 17.1 ± 0.4 pF (n=7). G01x could partially be recovered to 8.2 ± 0.3 nS (n=7) by wash-out of meclofenamic acid, whereas the initial fast capacitive transient remained unchanged (*wash-out,* Fig. 5A). Thus, 250 µM meclofenamic acid at least partly blocked intercellular coupling mediated by Cx45. SKHep1-Cx43 cells showed larger capacitive current transients indicating that these cells were better electrically coupled (*control*, Fig. 5B). G01x was 60.6 ± 4.3 nS (n=7) for the coupled monolayer and was reduced to 2.7 ± 0.2 nS (n=7) after adding 250 µM meclofenamic acid (*6 min*, Fig. 5B). The capacitance calculated from the initial fast transient was 17.5 ± 0.4 pF (n=7), also indicating that the cells were largely uncoupled under these conditions. Electrical coupling could be restored by wash-out of meclofenamic acid and G01x was partially recovered to 23.0 ± 1.9 nS (n=7) (*wash-out*, Fig. 5B). Flufenamic acid and niflumic acid were also able to block electrical coupling in these cells when added at a concentration of 250 µM. After uncoupling with flufenamic acid G01x was 2.7 ± 0.4 nS (n=3) and the calculated capacitance was 19.0 ± 0.8 pF (n=3). Niflumic acid reduced G01x to 2.9 ± 0.2 nS (n=3) and the capacitance to 17.9 ± 1.1 pF (n=3). These results demonstrate that fenamates are reversible blockers of Cx43-mediated intercellular communication.

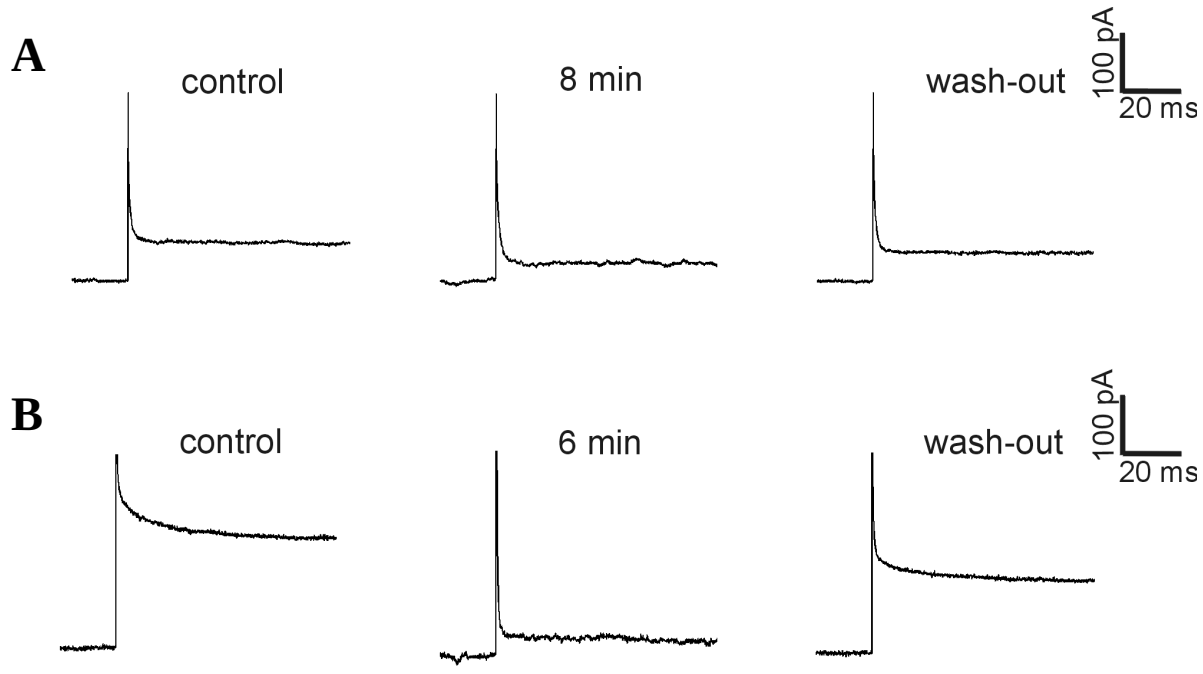

Figure 5 The effect of 250 µM meclofenamic acid (MFA) on the capacitive current transient, evoked by a short voltage-clamp step (10 mV), in confluent monolayers of **A)** SKHep1 cells and **B)** SKHep1-Cx43 cells. Data shown are representative traces of at least 4 experiments.

Discussion

In the present study we show that fenamates represent a novel class of reversible blockers of Cx43-mediated GJIC. The effects of fenamates on GJIC were assessed by using an analysis of single-electrode voltage-clamp step responses, which is based on a simplified electric circuit of the patched cell with the surrounding monolayer.

Gap junctions have been shown to be essential for the direct diffusion of for example calcium and small signal molecules such as IP_3 between neighboring cells (Giaume and Venance, 1998) and for their electrical coupling. A variety of biological processes including cellular growth, propagation of calcium waves, and cardiac function is regulated by GJIC (Kumar and Gilula, 1996; Yamasaki and Naus, 1996). Impaired GJIC has been reported in several diseases including cardiovascular diseases (Jongsma and Wilders, 2000) and tumorigenesis (Laird et al., 1999; Yamasaki et al., 1999; Zhang et al., 1998). Although in some cells a decrease in GJIC correlates with tumor growth (Hotz-Wagenblatt and Shalloway, 1993), phenotypic transformation of NRK cells is accompanied by an increase in intercellular communication (Van Zoelen and Tertoolen, 1991).

GJIC can be inhibited by physiological agents that initiate complex signaling pathways resulting in activation of kinases, phosphatases and interacting proteins (Hossain and Boynton, 2000) or changes in levels of intracellular calcium and pH (Bruzzone et al., 1996). Furthermore, different classes of chemicals have been shown to block GJIC. Some of them affect the conformation of the connexins by disturbing the bulk membrane fluidity or the membrane protein interface. Examples of chemicals that block GJIC by changing the lipid structure around connexins include alcohols such as heptanol and octanol (Johnston et al., 1980), halothane (Burt and Spray, 1989), and fatty acids like oleamides (Lerner, 1997), arachidonamide (Boger et al., 1999) and anandamide (Venance et al., 1995). Phorbol esters block GJIC by phosphorylation of connexin residues (Lampe, 1994), whereas glycyrrhetinic acid derivatives block by dephosphorylation of connexin43 (Guan et al., 1996). For selective inhibition of gap junctions, synthetic oligopeptides that interact with the external loop of connexins have been developed (Kwak and Jongsma, 1999).

Fenamates are widely used as inhibitors of cyclooxygenase activity (Brogden, 1986). Their inhibitory effect on gap junctions, however, is not related to their ability to inhibit cyclooxygenase activity, since indomethacin and flurbiprofen, two potent cyclooxygenase inhibitors, did not affect the electrical coupling of the cells at all.

Previously, we found that blocking GJIC with the phorbol ester TPA resulted in a depolarized membrane (De Roos et al., 1996). Furthermore, halothane, another gap junction blocker, has been reported to have effects on the resting membrane potential in skeletal muscle cells (Sauviat et al., 2000). Complete uncoupling by fenamates was also accompanied by depolarizations of the membrane of variable magnitude. Uncoupling of the NRK cells by fenamates, however, already started when the membrane potential was still unchanged (*see b*, Fig. 1). Moreover, complete uncoupling was

sometimes observed under conditions that the membrane potential was unaffected. These results exclude that membrane depolarization caused the uncoupling by fenamates.

Complete block of GJIC by fenamates was sometimes accompanied with increased fluctuations of the membrane potential (*see e*, Fig. 1). Most likely, electrical coupling of the monolayer cells caused fluctuations in the membrane potential to be averaged by a mechanism of channel-sharing (Atwater et al., 1983; Sherman et al., 1988) resulting in a stable membrane potential. So, the increased fluctuations of the membrane potential after application of fenamates may reflect the loss of channel-sharing by blocking GJIC. However, since fenamates have been reported to block anionic as well as cationic channels at various concentrations from 10-100 μM (Gogelein et al., 1990; Grover et al., 1994; Lee and Wang, 1999, Li, 1998 #77; White and Aylwin, 1990), additional effects of fenamates on plasma membrane ion channels may also have contributed to the increased membrane potential fluctuations and the depolarization of the uncoupled cell.

Fenamates did not affect intracellular calcium and pH, two physiological modulators of gap junctions. In addition, fenamates could still block GJIC in PKC downregulated cells, excluding a role for PKC. Although a role for other second messenger pathways cannot be excluded, it is more likely that the reversible block of GJIC by fenamates results from either a direct interaction with connexins or an indirect action through perturbations in the bulk membrane fluidity or the membrane protein interface that would affect the conformation of the connexins.

Anti-inflammatory therapy is often accompanied by unwanted side effects including gastrointestinal toxicity. However, nonsteroidal anti-inflammatory drugs have also been described to prevent colon cancer and Alzheimer's disease (Rich et al., 1995; Sheng et al., 1997). Whether there is a link between these unwanted and/or beneficial effects of nonsteroidal anti-inflammatory drugs and the (partial) block of gap junctions by fenamates requires further investigation. It should however be mentioned that the concentration needed to inhibit cyclooxygenase is much lower than that required to block GJIC. For example, the IC_{50} of meclofenamic acid is about 0.05 μM in inhibiting cyclooxygenase (Kalgutkar et al., 2000) and about 25 μM in blocking GJIC (*see* Fig. 4). Nevertheless, the present finding that fenamates are able to block GJIC not only in NRK fibroblasts, but also in Cx43-overexpressing SKHep-1 cells, strongly indicates that fenamates can be used as a pharmacological tool to reversibly block Cx43-mediated intercellular communication. Whether fenamates can also be used as blockers of intercellular communication mediated by other connexins remains to be investigated.

Acknowledgements.
We thank Dr. M. Rook (University of Utrecht) for kindly providing us the SKHep1 and SKHep1-Cx43 cells.

Materials and Methods

Cell culturing: Normal rat kidney fibroblasts (NRK clone 49F), SKHep1 human hepatoma cells and SKHep1 stably transfected with rCx43, designated SKHep1-Cx43 cells (Hermans et al., 1995), were grown in bicarbonate-buffered Dulbecco's modified Eagle's medium (DMEM; Gibco Life Technologies, Paisly, UK) supplemented with 10% newborn calf serum (HyClone Laboratories, Logan, UT, US) under 7.5% CO_2 at 37°C. Confluent cultures were first made quiescent by subsequent incubation for one to three days in serum-free medium consisting of a 1:1 mixture of DMEM and Ham's F12 (Gibco, Life Technologies) supplemented with 30 nM Na_2SeO_3 and 10 μg/ml human transferrin.

Electrophysiology: For patch-clamp experiments cells were perfused with serum-free medium consisting of a 1:1 mixture of bicarbonate-buffered DMEM and Ham's F12, equilibrated with 7.5% CO_2 to a pH of 7.4. Whole-cell patch-clamp experiments and voltage-clamp step response measurements were carried out as previously described (De Roos et al., 1996) using an EPC-7 patch-clamp amplifier (List Electronic, Darmstadt, Germany). Current and voltage-clamp protocols and data acquisition were performed using CED software in conjunction with a CED 1401 interface (Cambridge Electronic Design, Cambridge, UK). Data were filtered at 10 kHz, and stored on hard disk for subsequent analysis. Briefly, recording of the membrane potential was shortly interrupted by switching to the voltage-clamp mode and the subsequent application of a voltage pulse of +10 mV (duration 180 ms) from a holding potential of -70 mV. The resulting capacitive current transient was analyzed (Bio-Patch software, BioLogic, Claix, France) to obtain the initial peak current Ipk, the final steady-state current Iss and the time constant τ of the initial component of the capacitive transient, representing the charging of the patched cell. This component was in particular recognizable in the later stages of uncoupling. Pipettes were made from borosilicate glass capillaries (GC150-15, Harvard Apparatus LTD, Edenbridge, UK) using a two-stage pipette puller (L/M-3P-A, List Electronic, Darmstadt, Germany). Intracellular pipette solution contained (in mM) 25 NaCl, 120 KCl, 1 $CaCl_2$, 1 $MgCl_2$, 10 HEPES, 3.5 EGTA (pH 7.4) and pipettes had a resistance of 4-6 MΩ.

Determining electrical coupling: We have used two simple equations allowing an estimation of the gap junctional conductance G01 between the patched cell (#0) and the cells in the surrounding cell ring (#1) (*see* Appendix). G01 was assessed by measuring parameters from the overshooting current response to voltage-clamp steps of 10 mV (Fig. 1B) and then filling in these parameters in one of the two equations of the Appendix. The first equation, which may only be used for G01<Gser (R01>Rser), is:

$$G01 = Ish \cdot Gser / (Ipk-Ish) \qquad (1)$$

with Gser, the series conductance (Ipk/10 mV) between the patch pipette and the interior of cell #0; Ipk, the peak of the current transient after cancellation of the fast capacitive current charging the pipette capacitance or obtained by back extrapolation to t=0 from the current transient after the fast transient; Ish, the peak of the current component charging cell ring #1 and visible as a shoulder in the foot of the Cm0 charging current. The second equation is more general and practical and has the same shape:

$$G01x = Iss \cdot Gser / (Ipk-Iss) \qquad (2)$$

with G01x, the (under)estimated value of G01 and Iss, the final steady-state current of the current transient, i.e. after completion of charging all the membrane capacitances of the successive cell rings around cell #0 (set at 180 ms in our recordings). Equation (2) is used in all cases, i.e. for measuring uncoupling and recoupling kinetics and for dose-response curves, while equation (1) is only used for checking G01x values under conditions that R01>Rser.

Fluorescence measurements: Dye-coupling of cells was determined by microinjection of a 10% Lucifer Yellow (Molecular Probes, Eugene, OR) solution in 0.33 M LiCl into a single monolayer cell by means of a glass capillary tip using a vertical microinjection system (Olympus IMT-2, Tokyo, Japan) as previously described (De Haan et al., 1994). About 20 different

monolayer cells per dish were injected (1 per 5 s) and the number of fluorescent cells was counted 10 min after injection. Only the 5 injections per dish that caused most substantial dye-transfer were used for further analysis.

For ratio fluorimetric measurements of intracellular calcium concentrations, cells grown to confluence on glass coverslips were made quiescent and subsequently loaded with 2 μM fura-2/AM (Molecular Probes, Eugene, OR) for 30 min, after which they were washed for 20 min in serum-free medium, as previously described (De Roos et al., 1997c). Fluorescence measurements were performed on a SPF-500 spectrofluorimeter (Aminco, Silver Spring, MD) at 37°C. Excitation wavelengths were 340 and 380 nm, and emission was detected at 492 nm. Background fluorescence was determined after addition of 2 μM ionomycin and 2 mM $MnCl_2$, which caused complete quenching of fura-2 fluorescence. Ratio values of the background-corrected fluorescence intensities at 340 and 380 nm excitation were used as a measure for the cytoplasmic calcium concentration.

Fluorimetric intracellular pH measurements were carried out as previously described (Van Zoelen and Tertoolen, 1991). Briefly, cells grown to confluence on glass coverslips were made quiescent and subsequently loaded with 10 μM BCECF-AM (Molecular Probes, Eugene, OR) for 45 min at 37°C, after which they were washed with a 1:1 mixture of DMEM and Ham's F12 supplemented with 5 mM BTP. Excitation was performed at 506 nm and emission was detected at 532 nm. Calibration of fluorescence intensity to intracellular pH was done in the presence of 5 μM nigericin.

Chemicals: Meclofenamic acid, niflumic acid, flufenamic acid, tolfenamic acid, indomethacin, flurbiprofen and nigericin were from Sigma (St. Louis, Mo., US).

Numerical data are represented as mean ± S.E.M. throughout this paper.

Appendix

Assessment of fenamate-induced electrical uncoupling of NRK cells in a monolayer with the use of an electrical equivalent circuit

In the whole-cell voltage-clamp configuration we consider the patched cell in the middle of an NRK-cell monolayer as a central cell (#0), surrounded by concentric rings (#1, 2, 3, etc.) of cells (*see* Fig. 6A). Cell #0 is coupled to the voltage source E by Gser (or Rser), the series conductance (or resistance) associated with the pipette-cell connection. Each ring is considered as one isopotential compartment with the summed membrane conductance (Gm1, Gm2, etc.) and capacitance (Cm1, Cm2, etc.) of all its cells. Furthermore, each ring is electrically coupled to its inner and outer neighbor ring. Thus, cell #0 is coupled to ring #1 by G01 (or R01), ring #1 is coupled to ring #2 by G12 (or R12), etc. With increasing ring diameter, ring conductance and capacitance increase with the number of cells in the rings, e.g. Gm1~6Gm0 and Cm1~6Cm0 for 6 NRK-cells in ring #1 (as often found). Coupling conductance between the rings also increases with ring diameter. Membrane and coupling conductance are assumed to be voltage independent for the voltage steps applied (+10 mV from -70 mV).

In such an electrical equivalent circuit, which is essentially the same as described by others (Siegenbeek van Heukelom et al., 1970), the current response upon a voltage-clamp step may be viewed as the successive charging of cell #0 through Rser, ring #1 through Rser+R01, ring #2 through Rser+R01+R12, etc. This monolayer circuit allowed us to derive a simple equation to calculate whole-cell gap junctional conductance of cell #0 to ring #1 (G01) under conditions that $\tau1(=[Rser+R01]\cdot Cm1) >> \tau0(=Rser\cdot Cm0)$. Under these conditions, which exist during the development of uncoupling (R01>Rser, Cm1~6Cm0), Cm0 and subsequent Cm1 charging are more or less independent (cf. Ypey and DeFelice, 2000). Therefore, the beginning of the charging current of ring #1 can be seen as a shoulder current (Ish, i.e. the peak of the Cm1 charging current) in the foot of the charging current of cell #0. According to Ohm's law we can write for the peak of the current transient (Ipk) upon voltage steps dE the equation Ipk=dE/Rser and for the shoulder current Ish=dE/(Rser+R01). Combining both equations results in:

$$G01 = Ish \cdot Gser / (Ipk-Ish) \qquad (1)$$

For R01<Rser, G01 calculation from eq. (1) may become less reliable because the charging components of cell #0 and ring #1 become much less independent and Ish less recognizable. Furthermore, under favourable conditions (R01>Rser) back extrapolation of the current transient to t=0 may cause errors, because this transient is not single-exponential due to the subsequent slower charging of the more peripheral rings.

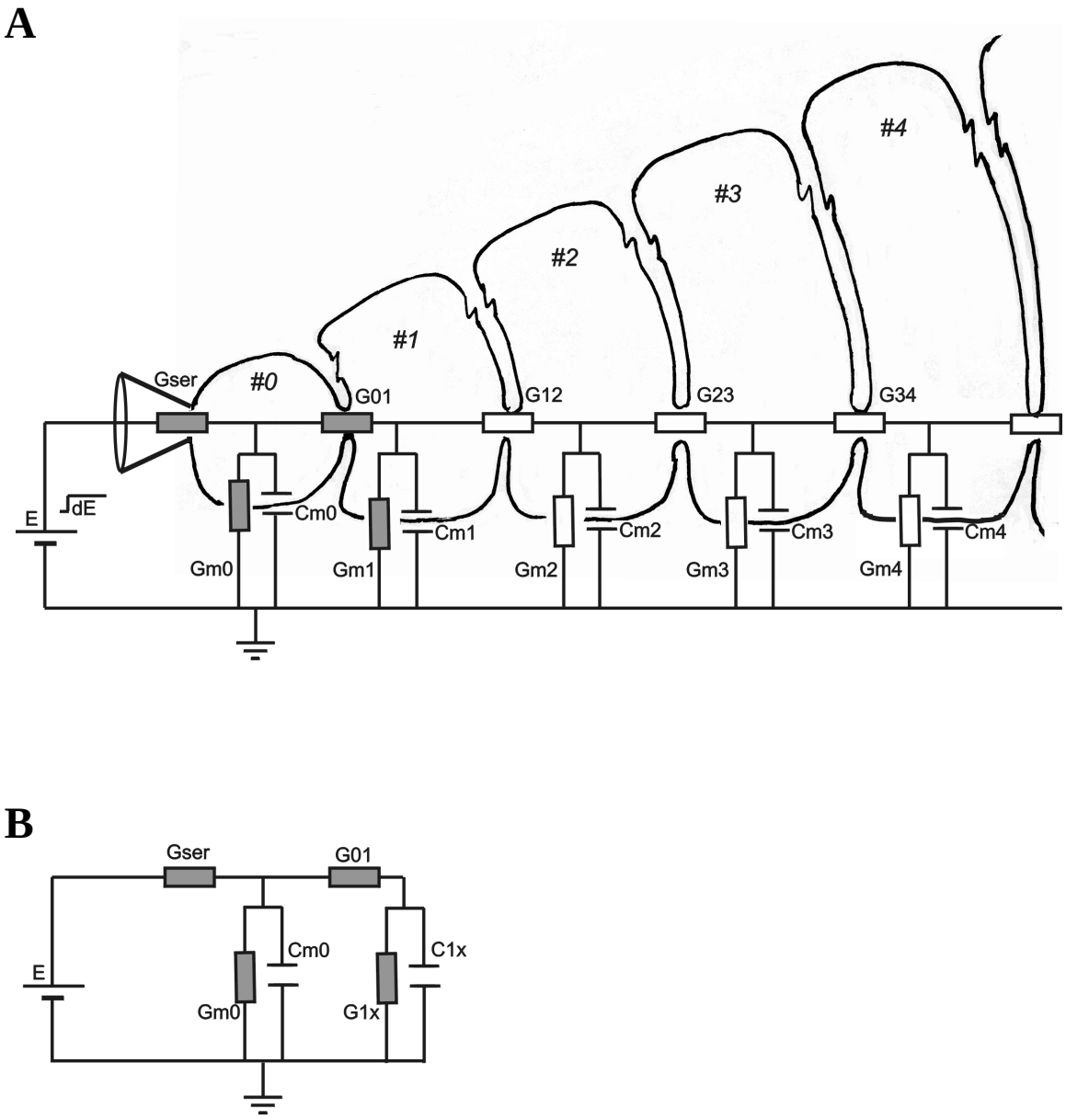

Figure 6 Electrical equivalent circuit of a voltage-clamp step response measurement on a patched whole-cell in a confluent monolayer of NRK cells. The voltage-clamp is represented by the voltage source E, which provides voltage steps dE through the patch pipette (at the left). **A)** The circuit, drawn in a (compressed) concentric ring representation of the monolayer around the patched cell (#0). This reduces the 2-dimensional monolayer to a 1-dimensionsal cable-like circuit. Pipette capacitance charging components are omitted in the circuit. For further explanation *see Appendix*. **B)** Simplified monolayer circuit, in which G1x represents the inverse of the total exit resistance (R1x) for current leaving the interior of cell ring #1 through whatever path (junctional or membrane resistance). The equivalent monolayer resistance R1x from ring #1 is paired with an equivalent monolayer capacitance C1x.

Because of the limitations mentioned we derived another simple, but more robust and general though less precise, steady-state equation for the estimation of G01. It is based on a simplification of the electrical equivalent circuit of the monolayer to a 2-compartment circuit (Fig. 6B), in which ring #1 represents the whole monolayer around cell #0 with an equivalent membrane resistance R1x (or G1x), the exit DC-resistance from ring #1 to ground for the entire current entering ring #1 through R01. Circuit analysis shows that Rm1//R12 (the equivalent resistance of Rm1 and Rm2 in parallel)<R1x<Rm1. Parallel to R1x one may imagine an equivalent membrane capacitance C1x giving a best possible (though not perfect) fit to the time course of the current transient upon the voltage step, but the precise C1x value is not of importance for the estimation of G01. Ohm's law allows us to write for the peak of the current transient (Ipk) Ipk=dE/Rser and for the steady-state current (Iss), reached after completion of the charging process of all capacitances of the monolayer involved, Iss=dE/(Rser+R01+R1x), assuming that Rm0>>R01 (as is the case under control conditions and during uncoupling until coupling becomes weak). Combining both equations results in:

$$G01x = Iss \cdot Gser / (Ipk-Iss) \qquad (2)$$

with G01x=1/(R01+R1x). This equation implies that G01x, called here the estimated coupling conductance between cell #0 and ring #1, is always smaller than the real coupling conductance (G01). Using eq. (1) we found for not strongly uncoupled cells with a clear Ish (*see a,b,c,f,g,h*, Fig. 1B) that the (G01/G01x) ratio was 1.8 ± 0.3 (n=6) meaning that G1x~G01. Under conditions of complete uncoupling (R01>>Rm0), eq. (2) has become the expression for Gm0. Thus, when eq. (2) provides single-cell conductance values ~Gm0 for the apparent G01x, as in the present study, one may conclude that G01x<Gm0. In conclusion, though eq. (2) does not provide exact G01 values, it is useful for G01 estimations of the right order of magnitude, for monitoring drug induced uncoupling and for comparing relative potencies of uncoupling drugs.

CHAPTER 3

Ionic Basis for Excitability of NRK Fibroblasts

E.G.A. Harks, J.J. Torres, L.N. Cornelisse, D.L. Ypey and A.P.R. Theuvenet

Abstract. Ionic membrane conductances of NRK fibroblasts were characterized by whole-cell voltage-clamp experiments on single cells and small cell clusters and their role in action potential firing in these cells and in monolayers was studied in current-clamp experiments. Activation of an L-type calcium conductance (G_{CaL}) is responsible for the initiation of an action potential, a calcium-activated chloride conductance ($G_{Cl(Ca)}$) determines the plateau phase of the action potential, and an inwardly rectifying potassium conductance (G_{Kir}) is important for the generation of a resting potential of ~-70 mV and contributes to action potential de- and repolarization. The unique property of the excitability mechanism is that it not only includes voltage-activated conductances (G_{CaL}, G_{Kir}) but that the intracellular calcium dynamics is also an essential part of it (via $G_{Cl(Ca)}$). Excitability was found to be an intrinsic property of a fraction (~25%) of the individual cells, and not necessarily dependent on gap junctional coupling of the cells in a monolayer. Electrical coupling of a patched cell to neighbor cells in a small cluster improved the excitability because all small clusters were excitable. Furthermore, cells coupled in a confluent monolayer produced broader action potentials. Thus, electrical coupling in NRK cells does not merely serve passive conduction of stereotyped action potentials, but also seems to play a role in shaping the action potential.

Introduction

Fibroblasts constitute the connective tissues of the body and are generally considered to be classical examples of non-excitable cells. For maintaining the integrity of the organ and tissue structure, fibroblasts are in continuous chemical communication with other surrounding cells via the intercellular space, while they are in direct contact with each other through intercellular channels organized in specialized contact structures called gap junctions. In a large number of studies we have used normal rat kidney (NRK) fibroblasts as an *in vitro* model system to study the mechanism(s) of growth regulation of cells by polypeptide growth factors (Lahaye et al., 1999b; Van Zoelen, 1991).

Previous studies have shown that confluent monolayers of NRK cells that have been made quiescent in their proliferation by removal of growth factors from their culture medium (further referred to as quiescent cells) have a stable resting membrane potential around -70 mV (De Roos et al., 1997a). Under these conditions the cells in the monolayer are electrically well coupled by gap junctions (De Roos et al., 1996; Harks et al., 2001). Remarkably, because these cells are usually considered as non-excitable cells, a propagating action potential can be induced in these monolayers by depolarizing cells in a small area in the monolayer. This depolarization can be achieved by either a local application of increased extracellular [K^+] or of an intracellular calcium mobilizing agent (e.g. bradykinin). In this way a single action potential is evoked characterized by a fast depolarizing spike to positive membrane potentials followed by a plateau phase around -20 mV that lasts about 30 s. These action potentials have been shown to propagate through the entire monolayer with a velocity of approximately 1 cm/s and are accompanied by an almost synchronized transient increase in the cytoplasmic Ca^{2+} concentration in all the cells in the monolayer (De Roos et al., 1997d). Apparently, like excitable cells such as cardiomyocytes and neuronal cells, NRK fibroblasts are able to communicate over a long distance by electrical signaling. The *in vivo* function of this excitability, however, is still unknown.

In the present study we performed whole-cell voltage-clamp experiments to identify and characterize the membrane conductances of major importance for NRK cell excitability. We show for the first time, that in addition to an L-type calcium conductance and a calcium-activated chloride conductance (De Roos et al., 1997c; De Roos et al., 1997a), NRK cells possess a prominent inwardly rectifying potassium conductance, and that the action potential evoked in cells and monolayers results from a sequential activation of each of these three conductances. We also show that excitability is not restricted to electrically coupled cells in monolayer culture, because a significant percentage of single isolated cells was already able to generate action potentials.

Results

Voltage-clamp measurements on single isolated NRK cells and small cell clusters were performed to identify and characterize the ionic membrane conductances exhibited by these cells. In addition, excitability of NRK cells was studied by applying current-injections in single cells and cell clusters and by evoking propagating action potentials in monolayers.

Voltage-clamp measurements on single NRK cells

For the characterization of the membrane conductances in NRK cells we first performed voltage-clamp experiments on isolated NRK cells that had been dissociated from quiescent confluent monolayers.

Under our standard conditions of voltage-clamp measurements (DF-ECS in the bath and S-ICS in the pipette), two types of voltage-dependent conductances were recognized as main conductances in single NRK cells, dissociated from quiescent monolayers (Fig. 1A): an inwardly rectifying potassium conductance (G_{Kir}) and an L-type calcium conductance (G_{CaL}). Consistent with its known properties (Hille, 2001), the inward rectifier was activated (actually unblocked from intracellular cations) upon hyperpolarization of the membrane to around and below its reversal potential and this reversal potential changed as expected for the equilibrium potential for K^+ ions when extracellular [K^+] was changed (n=11). The inward rectifier was completely blocked by 1-5 mM external Ba^{2+} ions (n=12) and the L-type calcium current was increased if Ba^{2+} instead of Ca^{2+} ions were used as charge carriers (Fig. 1B). The inward rectifier could also be blocked by 5-10 mM external Cs^+ ions (n=4). The presence of L-type currents in NRK fibroblasts had already been shown before in experiments on single NRK fibroblasts but in those experiments Ba^{2+} ions were used as charge carriers in order to increase the current for better resolution (De Roos et al., 1997c). Here we confirm the presence of this current for the more physiological condition that Ca^{2+} ions serve as charge carriers at approximately normal extracellular [Ca^{2+}] (2 mM). Under these conditions the currents are smaller and have faster inactivation kinetics (Hille, 2001) (cf. Fig. 1A and B).

Besides G_{Kir} and G_{CaL} we measured a calcium-activated chloride conductance $G_{Cl(Ca)}$ (further evidence is given below), which was very small using our standard strongly calcium buffering pipette solutions (Fig. 1A), but much larger using weakly buffering pipette solutions (Fig. 1C). Furthermore, it should be noted that I_{Kir}, and I_{CaL} and $I_{Cl(Ca)}$ were usually superimposed on a leak current I_{leak}, conducted by a leak conductance (G_{leak}) which is the sum of the basal membrane leak conductance and the seal conductance.

Fig. 1D shows the I-V curves corresponding to voltage-clamp measurements in panels A (solid lines) and B (dotted lines) for both total membrane currents at t=500 ms and inward L-type current which was maximal at ~50 ms. These curves clearly demonstrate activation of G_{Kir} at hyperpolarized potentials (-120 and -100 mV) and inhibition of this conductance by Ba^{2+}. In addition, G_{CaL} was

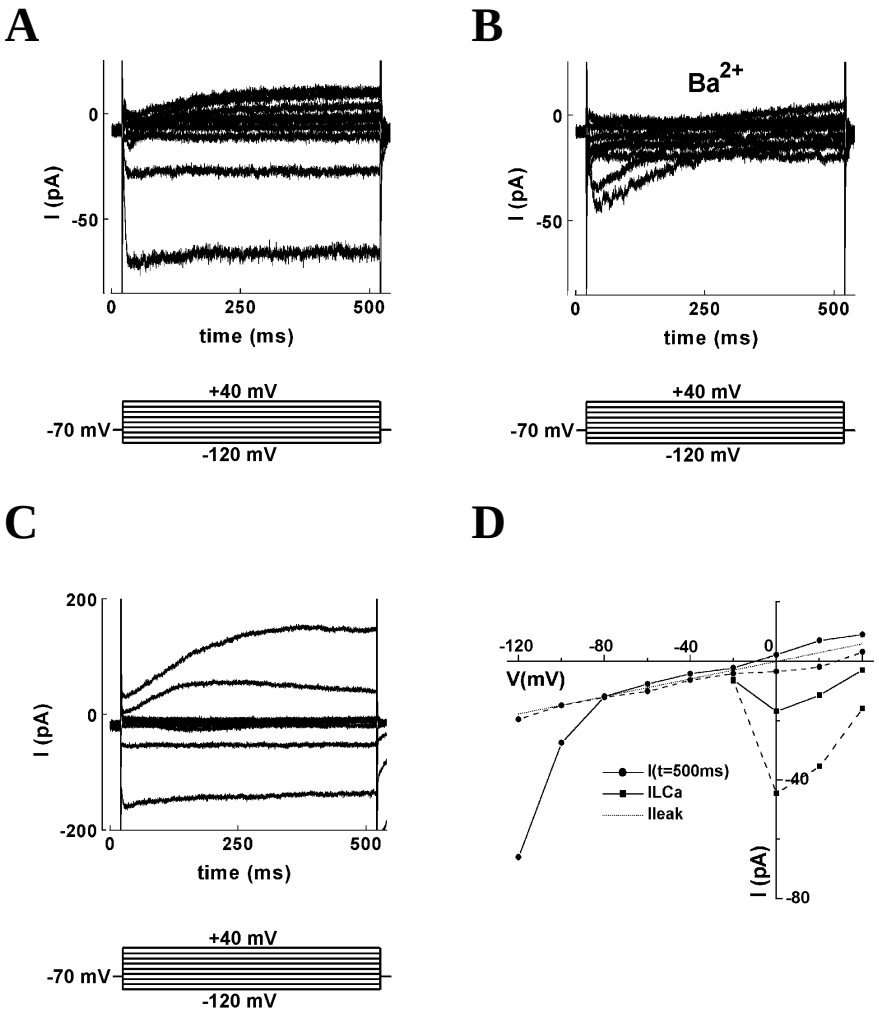

Figure 1 Whole-cell current records and I-V curves in single cells. **A)** Single cell (21.0 pF) with an inwardly rectifying potassium conductance ($\overline{G}_{Kir}$ =1.34 nS), an L-type calcium conductance ($\overline{G}_{CaL}$ =0.68 nS) and a calcium-activated chloride conductance ($\overline{G}_{Cl(Ca)}$ =0.08 nS). **B)** Same cell in the presence of 5 mM external Ba^{2+}. **C)** Single cell (20.8 pF) measured with weakly buffering pipette solution containing 100 µM EGTA and 0 mM $CaCl_2$, $\overline{G}_{Kir}$ =3.44 nS, $\overline{G}_{CaL}$ =0.52 nS and $\overline{G}_{Cl(Ca)}$ =4.35 nS. In all experiments voltage-clamp steps were applied from a holding potential (V_h) of -70 mV to test potentials of -120 mV and higher with increments of +20 mV and step intervals of 2 s. **D)** I-V curve corresponding to panels A (solid line) and B (dotted line).

increased when calcium ions were replaced by barium ions. Based on the I-V curves maximal conductances ($\overline{G}_i$) of G_{CaL}, $G_{Cl(Ca)}$, G_{Kir} and G_{leak} were calculated as described in the methods section. Table 1 shows that $\overline{G}_{Cl(Ca)}$ is the smallest conductance (~0.14 nS) at strong intracellular calcium buffering, but the largest (~9.18 nS) at weak buffering. Furthermore, $\overline{G}_{Kir}$ (~2.14 nS) > $\overline{G}_{CaL}$ (~0.67 nS) > G_{leak} (~0.29 nS). In conclusion, voltage-clamp experiments on isolated NRK cells showed the presence of G_{CaL}, $G_{Cl(Ca)}$ and G_{Kir} as the main conductances in NRK cells.

Voltage-clamp measurements on clusters of NRK cells

In order to increase current amplitudes and to average for differences in conductances between individual cells, we explored the voltage-clamp properties of small clusters of NRK cells (2-10 cells), which are known to be electrically well coupled (De Roos et al., 1996).

The current amplitudes measured in clusters were increased compared to those in single cells (compare current scales in Figs. 1 and 2) but were similar to those in single cells when normalized for the number of cells in the cluster (*see* Table 1). For example, $\overline{G}_{CaL}$ of single cells was not significantly different from that of cluster cells. This is consistent with acceptable voltage-clamp conditions for measuring these small calcium currents in cell clusters. By substitution of extracellular Ca^{2+} with Sr^{2+} ions the L-type current showed an increased amplitude and decelerated inactivation (Fig. 2B). The difference between $\overline{G}_{Kir}$ for single cells and cluster cells may be due to non-ideal voltage-clamp conditions in clusters for the larger Kir currents (*see* Methods), although differences in cytoplasmic conditions between single cells and clusters may be another reason. Whereas the basal membrane conductance is proportional to the number of cells, the seal conductance is only determined by the leak between the patch pipette and the patched cell. Therefore, the leak conductance per cluster cell (G_{leak}) decreased with an increasing cluster size, becoming closer to the real membrane leak conductance per cell (~0.10 nS, *see* Table 1).

Table 1: Calculated maximal conductances per cell in single NRK cells and small clusters

	condition	single cells	cell clusters
$\overline{G}_{CaL}$	$[Ca^{2+}]_e$ = 2 mM	0.67 ± 0.14 nS (n=13)*	0.48 ± 0.08 nS (n=23) [a]*
	$[Sr^{2+}]_e$ = 2 mM	N.D. [c]	0.98 ± 0.10 nS (n=7) [b]
$\overline{G}_{Cl(Ca)}$	$[EGTA]_i$ = 3.5 mM	0.14 ± 0.09 nS (n=13)	0.47 ± 0.08 nS (n=23) [a]
	$[EGTA]_i$ = 100 μM	9.18 ± 1.61 nS, (n=17)	N.D. [c]
$\overline{G}_{Kir}$		2.14 ± 0.46 nS (n=13)	1.04 ± 0.13 nS (n=23) [a]
G_{leak}		0.29 ± 0.06 nS (n=13)	0.10 ± 0.02 nS (n=23) [a]

[a] *mean cluster size 5.6 ± 0.5 cells (n=23).*

[b] *mean cluster size 4.7 ± 0.6 cells (n=7).*

[c] *Not Determined.*

** not significantly different*

The maximal L-type calcium conductance ($\overline{G}_{CaL}$) was calculated at its reversal potential (+50 mV), maximal calcium-activated chloride conductance ($\overline{G}_{Cl(Ca)}$) at +40 mV and maximal inwardly rectifying potassium conductance ($\overline{G}_{Kir}$) at -120 mV. The leak conductance (G_{leak}) was calculated from the current at -80 mV, where I_{Kir}=0 and assuming that E_{leak}=0 mV. These four conductances were measured in the presence of extracellular calcium ($[Ca^{2+}]_e$=2 mM) using standard intracellular calcium buffering (3.5 mM EGTA). In addition, $\overline{G}_{CaL}$ was calculated under conditions that extracellular calcium was substituted by strontium ($[Sr^{2+}]_e$=2 mM and $\overline{G}_{Cl(Ca)}$ under conditions that weak intracellular calcium buffering pipette solutions (100 μM EGTA) were used. Conductance values of the clusters were normalized by dividing by the number of cells in the cluster.

The delayed outward current through $G_{Cl(Ca)}$ was more easily studied in clusters (Fig. 2C), although the larger currents must have caused non-ideal voltage-clamp. $G_{Cl(Ca)}$ could be blocked by 50 µM BAPTA-AM (n=3), which is a membrane permeable intracellular calcium buffer (Fig. 2D). In addition, this outward current disappeared after blocking G_{CaL} with 1 µM nifedipine (n=3) and was reversed to an inward current in the presence of a low (7.6 mM) external chloride concentration (n=3). Apparently, Ca^{2+} ions that had entered the cells through L-type channels subsequently activated calcium-dependent chloride channels. Evidence for the existence of $G_{Cl(Ca)}$ in NRK fibroblasts has been shown before in current-clamp experiments on monolayers (De Roos et al., 1997a). Fig. 2B shows that $G_{Cl(Ca)}$ could also be activated under conditions that external Ca^{2+} ions were substituted by Sr^{2+} ions. As a matter of fact, activation of $G_{Cl(Ca)}$ by Sr^{2+} ions has also already been shown before in

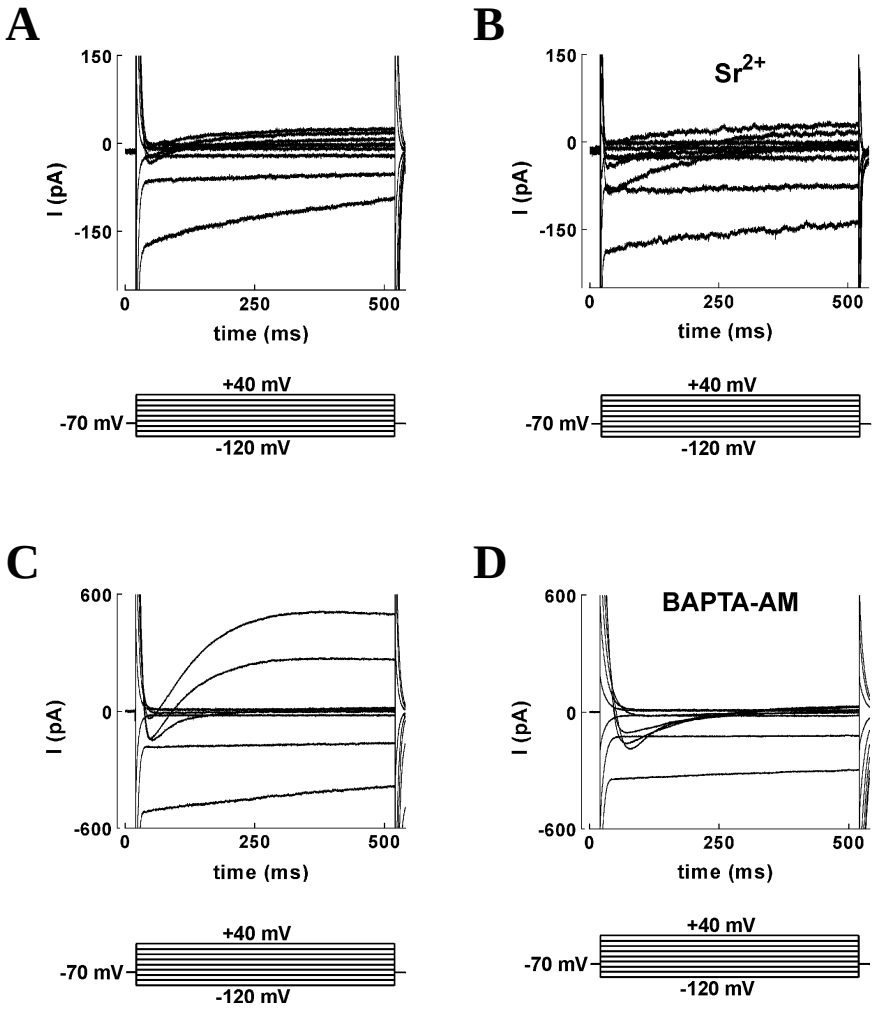

Figure 2 Whole-cell current records in cell clusters. **A)** Cluster (4 cells) with $\overline{G}_{Kir}$ =0.88 nS, $\overline{G}_{CaL}$ =0.33 nS and $\overline{G}_{Cl(Ca)}$ =0.09 nS per cell, in the presence of 2 mM external Ca^{2+}. **B)** Same cluster (4 cells) in the presence of 2 mM external Sr^{2+}. **C)** Cluster (10 cells) with $\overline{G}_{Kir}$ =1.19 nS, $\overline{G}_{CaL}$ =0.61 nS and $\overline{G}_{Cl(Ca)}$ =1.19 nS per cell. **D)** Same cluster (10 cells) after 4 min perfusion with 50 µM BAPTA-AM. In all experiments voltage-clamp steps were applied from a holding potential (V_h) of -70 mV to test potentials of -120 mV and higher with increments of +20 mV and step intervals of 2 s.

voltage-clamp experiments on neurones (Akasu et al., 1990).

These results show that voltage-clamp experiments on small clusters of electrically coupled NRK cells allow the characterization of membrane conductances with better resolution (I_{CaL}) and under more physiological conditions ($I_{Cl(Ca)}$) than in single cells, due to increased current amplitudes and a reduced washout of cluster cells with pipette solution. Apparently, the coupling between the cells in a cluster is good enough (<10 MΩ, *see* Harks et al., 2001) to monitor voltage-clamp currents <50 pA. Larger currents may only give a qualitative impression of the properties of the measured conductances.

Characterization of the L-type current

In order to obtain more information about the kinetic properties of L-type calcium channels in NRK cells, we performed voltage-clamp experiments under conditions that $G_{Cl(Ca)}$ and G_{Kir} were absent. $G_{Cl(Ca)}$ was blocked by 50 μM NPPB and G_{Kir} and any other possible K^+ current was blocked by substituting K^+ for Cs^+ in the intracellular and for TEA^+ in the extracellular solution.

First, we tried to measure L-type currents in single NRK cells using the same voltage protocols as in Fig. 1 and 2. However, the size of these currents (with Sr-ECS and Cs-ICS) was too small to do a reliable analysis, consistent with a current reducing effect of NPPB on I_{CaL} (Doughty et al., 1998). To improve the current resolution we continued with experiments on small clusters of 5-7 cells thereby using Sr^{2+} as the charge carrier to increase the current amplitude (cf. Fig. 2A and B). Fig. 3A shows an example, in which the activation properties of G_{CaL} were determined in a cluster of 6 cells by applying increasing stepwise depolarizations of 750 ms duration from a holding potential of -80 mV (Fig. 3A). Inward currents were evoked by steps to >-40 mV and were maximal at ~0 mV. All inward currents inactivated with a time constant of ~200 ms towards leak current levels. In the same cluster, inactivation properties could be determined by measuring the leak-corrected maximal inward current at 0 mV, following a pre-potential of 1 s duration and variable height (Fig. 3B). I_{CaL} was clearly reduced after pre-pulses of -50 mV and higher, indicating that this current inactivated at these potentials. Finally, deinactivation of G_{CaL} (at -100 mV) was measured by applying two consecutive voltage-steps to 0 mV from a holding potential of -100 mV, whereby the interpulse interval was increasing (Fig. 3C). I_{CaL} gradually recovered upon increasing pulse-intervals.

Based on the currents measured in 7 clusters of NRK cells we could plot mean activation, inactivation and deinactivation curves for G_{CaL}. Fig. 3D shows that activation of G_{CaL} starts between -40 and -30 mV and is maximal at 0 mV. Mean half maximal activation was determined from the individual activation curves and occurs at $E_{1/2a}$=-14.3 ± 0.8 mV (n=7). Inactivation starts at ~-50 mV and is complete at 0 mV, while mean half maximal inactivation was at $E_{1/2i}$=-36.6 ± 1.5 mV (n=7). Between -40 and -10 mV the activation and inactivation curves of G_{CaL} overlap, which could give rise to a small stationary calcium current around -20 mV. Fig. 3E shows that 50% deinactivation of G_{CaL} is achieved within ~124.6 ± 11.4 ms, while complete deinactivation is reached after ~2 s.

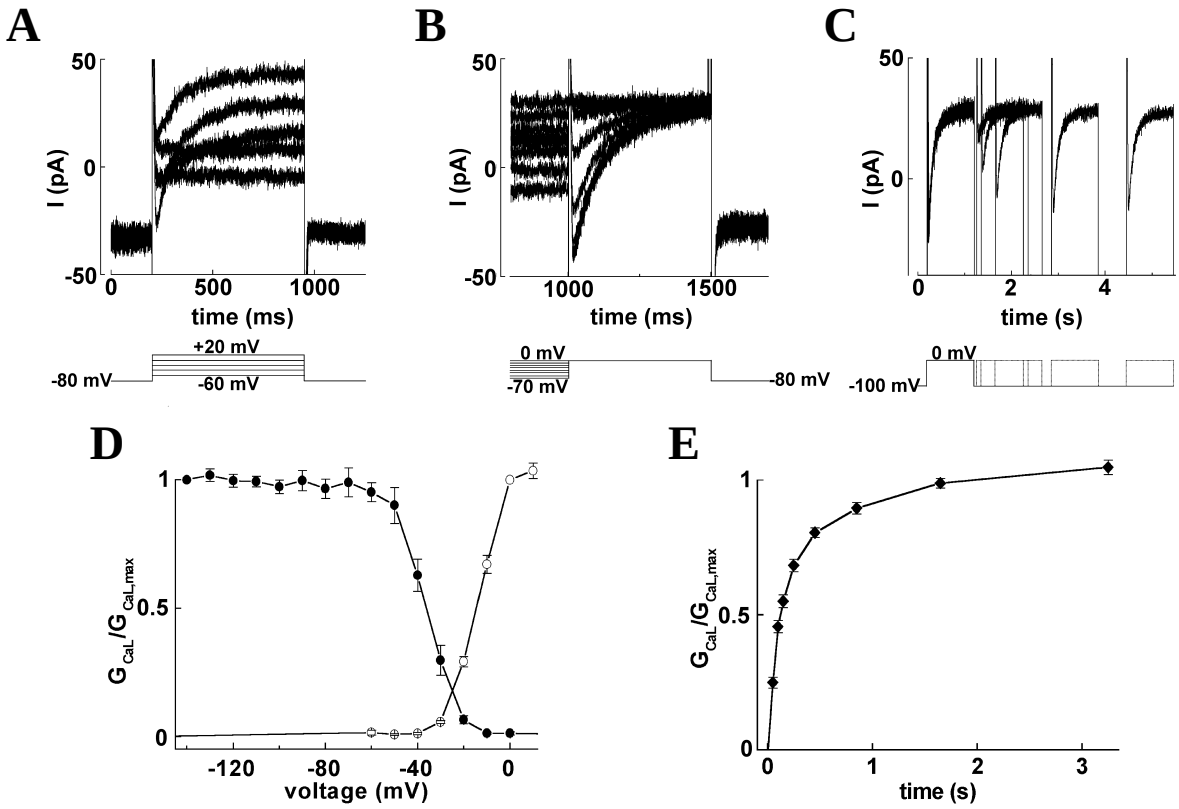

Figure 3 Kinetic properties of the L-type current. **A)** Activation: in a cluster of 6 cells voltage-clamp steps were applied from a holding potential of -80 mV to test potentials of -60 mV and higher with increments of +10 mV and sweep intervals of 2 s. Voltage-steps of 750 ms to -60, -40, -20, 0 and +20 mV are shown. **B)** Inactivation: voltage-clamp steps were applied to the same cluster as in (A) from a holding potential of -80 mV to (pre)potentials of -140 mV and higher with increments of +10 mV (prepulse duration 1 s). Voltage-steps of 500 ms from prepulses of -70 mV and higher are shown. Each prepulse was followed by a test voltage-step to 0 mV and a step interval of 2 s was used. **C)** Deinactivation: two consecutive voltage pulses were applied from a holding potential of -100 mV to 0 mV (duration 1 s) with increasing interpulse intervals (50, 100, 150, 250, 450, 850, 1650 and 3250 ms), while the sweep interval was 2 s. Currents corresponding to interpulse intervals of 50, 150, 450, 1650 and 3250 ms are shown. **D)** Activation (-o-), inactivation (-•-) and **E)** inactivation recovery (deinactivation) curve of the L-type current based on the currents measured in small clusters (mean ± S.E.M; n=7) using voltage protocols as in panels A-C. 100% activation in the activation and inactivation curve of G_{CaL} corresponded to respectively 0.30 ± 0.02 nS and 0.33 ± 0.03 nS (n=7). In all experiments 2 mM Sr^{2+} was used as charge carrier and $G_{Cl(Ca)}$ and G_{Kir} were blocked.

Excitability of single NRK cells

We studied the electrophysiological properties of NRK cells by inducing action potentials in single cells in the presence of 2 mM external Sr^{2+}. In addition, the contribution of the membrane conductances characterized in voltage-clamp experiments in the action potential evoked in monolayers was explored. Because of the variability of the resting membrane potential in these cells (De Roos, 1997), the excitability conditions of the cells were standardized by setting the membrane potential by a holding current at a standard value of -80 mV.

First we tried to evoke an action potential in a single isolated NRK cell. Subthreshold depolarizations had time constants RmCm of the order of 60 ms, consistent with Cm~20 pF and Rm~3 GΩ (G_{leak}~0.3 nS, *see* Table 1). Time constants increased with larger depolarizations because of closure of inward rectifier channels and decreased with hyperpolarization because of opening of these channels (*see* an illustration of this effect in Fig. 5 for cluster stimulation, described below). By applying sufficiently strong positive current pulses in single cells, the membrane potential was depolarized beyond a certain threshold resulting in an action potential in 7 of 25 cells tested. When the action potential was evoked using a strong intracellular calcium buffering solution, hardly any plateau phase of the action potential was measured (Fig. 4A). The contribution of $G_{Cl(Ca)}$ in the plateau phase became visible by reducing the calcium buffering capacity of the pipette solution (n=4; Fig. 4B). The plateau phase of the action potential was markedly prolonged when intracellular calcium was weakly buffered, which confirms the calcium dependence of this conductance.

These results clearly demonstrate that electrical coupling is not required for excitability in a fraction of cells (~25%) since those single isolated NRK cells could fire action potentials. The inability of the non-responding cells could be due to a too small $\overline{G}_{CaL}$ or due to a large G_{leak} and/or seal resistance.

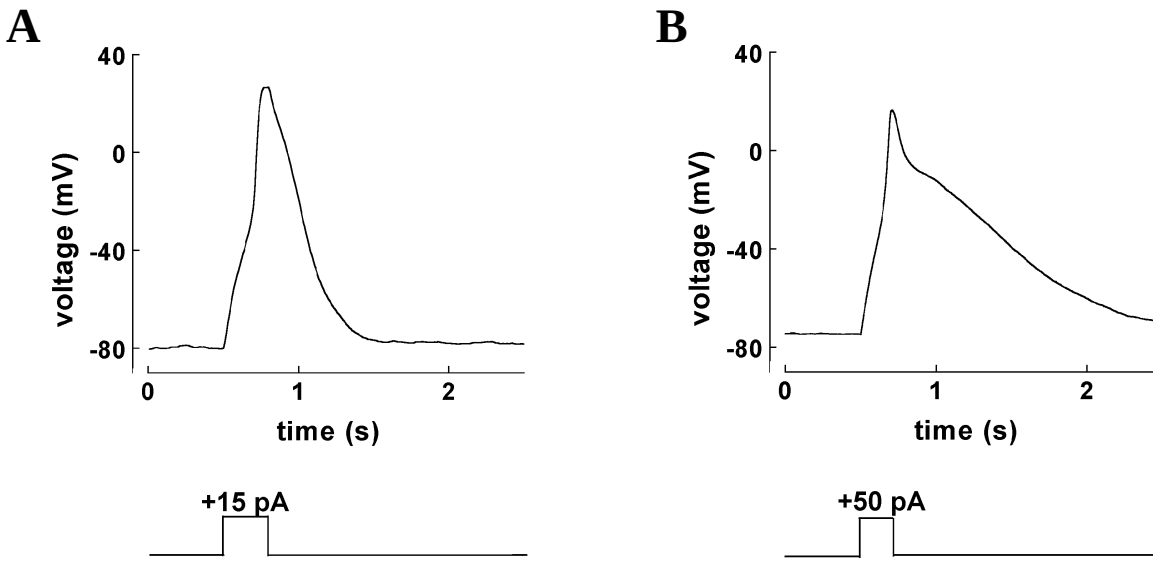

Figure 4 Action potentials evoked in single NRK cells, in which the membrane potential was hold at a standard resting membrane potential of -80 mV by applying a negative holding current. **A)** Action potential evoked in a single cell ($\overline{G}_{Kir}$ =0.93 nS, $\overline{G}_{CaL}$ =0.64 nS and $\overline{G}_{Cl(Ca)}$ =0.98 nS) with standard calcium buffering conditions by a current pulse of +15 pA. **B)** Action potential evoked in a single cell ($\overline{G}_{Kir}$ =2.18 nS, $\overline{G}_{CaL}$ =5.19 nS and $\overline{G}_{Cl(Ca)}$ =11.13 nS) with low calcium buffering capacity ([EGTA]=100 μM) by a current pulse of +50 pA. All experiments were performed with 2 mM external Sr^{2+}.

Excitability of clusters of NRK cells

In order to establish the involvement of electrical coupling in excitability of NRK cells, we performed current injections on small cell clusters of these cells, again in the presence of 2 mM external Sr^{2+}. The current pulses were applied to the patched cell, but due to the electrical coupling, the membrane potential response of the entire cluster (≤10 cells) was measured (n=23). A negative holding current was used to establish a standard resting membrane potential of -80 mV. Some of the clusters (n=8) had resting membrane potentials ~-70 mV and were also excitable at that physiological membrane potential (i.e. without holding current).

All tested clusters were able to fire action potentials upon current stimulation. Typical membrane potential responses after current injections in a cluster of 6 cells are shown in Fig. 5. In panel A the role of activation of G_{Kir} in the membrane potential response is clearly observed when a negative current pulse is applied. Under these conditions the membrane hyperpolarizes, resulting in an activation of G_{Kir} and influx of K^+ ions into the cells, thereby counteracting the hyperpolarization. This panel also demonstrates the upstroke of the action potential upon activation of G_{CaL} around -35 mV, the approximate threshold potential for activation of G_{CaL}. Fig. 5B shows the response of the same cluster upon two consecutive current pulses with increasing interpulse intervals. After repolarization of the first action potential, the cells are capable of firing a second action potential within 1 s, consistent with the time course of the deinactivation of G_{CaL} shown in Fig. 3E. Fig. 5C shows typical action potentials evoked in a cluster of 6 cells, which had a more than 5 times smaller $\overline{G}_{Kir} : \overline{G}_{Cl(Ca)}$ ratio, while G_{CaL} was similar. In this cluster, action potentials could already be evoked by application

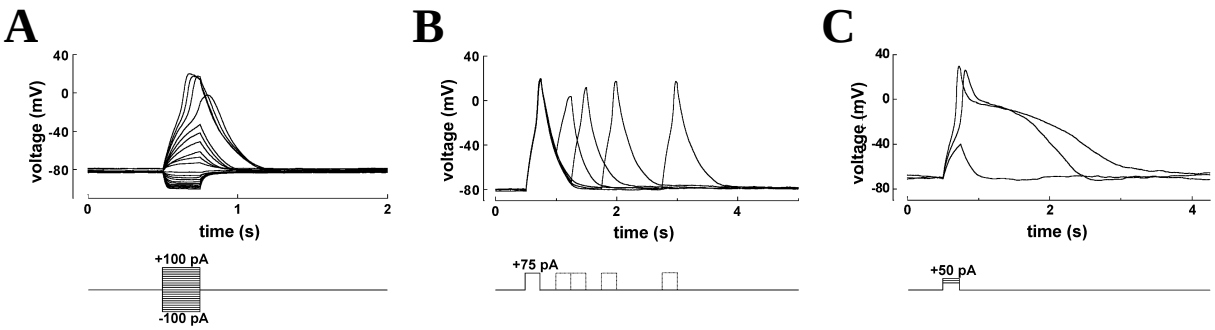

Figure 5 Action potentials evoked in small clusters of NRK cells. The resting membrane potential was kept at -80 mV by a negative holding current. **A)** Membrane potential response of a cluster of 6 cells ($\overline{G}_{Kir}$ =1.59 nS, $\overline{G}_{CaL}$ =0.94 nS and $\overline{G}_{Cl(Ca)}$ =3.00 nS per cell) upon application of current pulses with an amplitude ranging from –100 pA to +100 pA with step intervals of +10 pA. **B)** Action potentials evoked in the same cluster. In each sweep two consecutive action potentials were evoked by current pulses of +75 pA and the interpulse interval was doubled in every following sweep (250, 500, 1000 and 2000 ms). The time between two succesive double-pulse sweeps was 2 s. **C)** Membrane potential of current pulses of +30, +40 and +50 pA. All experiments were performed response of another cluster of 6 cells ($\overline{G}_{Kir}$ =0.17 nS, $\overline{G}_{CaL}$ =0.85 nS and $\overline{G}_{Cl(Ca)}$ =1.80 nS per cell) upon application with 2 mM external Sr^{2+}.

of a smaller current pulse (+40 pA compared to +60 pA in panel A), while the duration of the plateau phase was much longer. In general, the duration of the plateau phase seemed to correlate with the relative size of the conductances present in clusters of 5-8 cells, such that the time required for 50% repolarization of the action potential was significantly longer in clusters with smaller $\overline{G}_{Kir} : \overline{G}_{Cl(Ca)}$ ratios ($0.025>p>0.01$; n=13). The correlation with both conductances alone also exists, but is less significant ($0.1<p<0.05$; n=13).

Excitability of confluent NRK monolayers

Previously we have shown that it is possible to evoke propagating action potentials in confluent monolayers of NRK cells (De Roos et al., 1997d), and here we further explored the contribution of the membrane conductances identified in this study to the shape of this action potential by specifically blocking one of the conductances.

With the equipment available it was not possible to inject sufficient current into one cell of the monolayer to evoke an action potential due to the low input resistance of the monolayer because of gap junctional coupling between the cells. However, monolayers can be excited by a depolarization of cells in a small area by either a local elevation of extracellular $[K^+]$ or by the local application of an intracellular calcium mobilizing agent (e.g. bradykinin) (De Roos et al., 1997d). These action potentials were measured in only about 10% of the monolayer cultures using normal Ca^{2+} containing media, but the incidence was increased to almost 100% when Ca^{2+} was replaced by Sr^{2+}. Therefore, we also substituted external Ca^{2+} by Sr^{2+} ions. A typical example of an action potential evoked by a high extracellular $[K^+]$ stimulus under these conditions is shown in Fig. 6A. The duration of the action potential evoked in monolayers is much more prolonged (~30 s) compared to that evoked in single cells (~2 s; Fig. 4B) and small cell clusters (~3 s; Fig. 5C).

When G_{CaL} was completely blocked by nifedipine (1 μM), it was not possible to evoke an action potential (Fig. 6B, n=4), which is in accordance with earlier results (De Roos et al., 1997d). Activation of $G_{Cl(Ca)}$ could be prevented by buffering intracellular calcium upon application of BAPTA-AM (50 μM). Under these conditions, a propagating action potential could still be evoked but the plateau phase of the action potential was completely abolished (Fig. 6C, n=4), indicating that a rise in the intracellular calcium concentration is required for activation of the chloride conductance that accounts for the prolonged plateau phase of the action potential. The remaining shortened action potential is wider than the initial spike of the normal action potential. This implies that $G_{Cl(Ca)}$ normally contributes to the repolarization of the initial Ca^{2+} or Sr^{2+} driven spike of the action potential. The role of G_{Kir} in the electrical behavior of the cells was assessed by blocking G_{Kir} with Cs^+ ions (10 mM). After addition of Cs^+ the membrane immediately started to depolarize to about -50 mV (n=5), which indicates that G_{Kir} is important for setting the resting membrane potential around -70 mV. When a

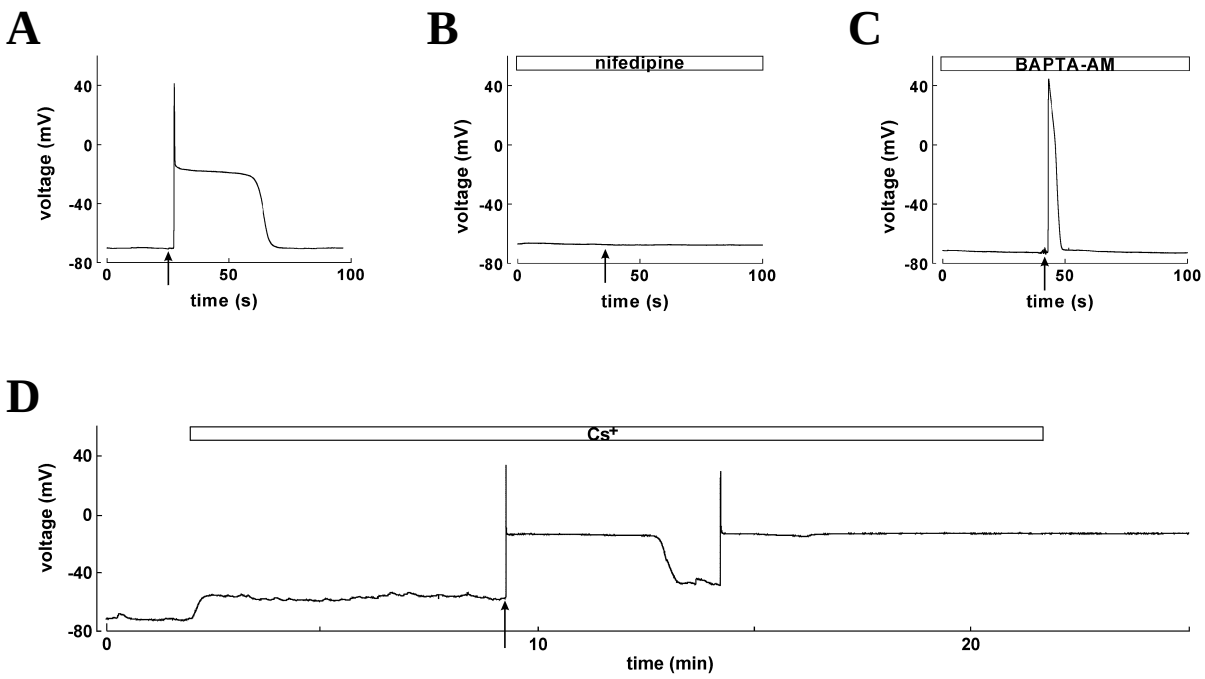

Figure 6 Contribution of membrane conductances to action potentials evoked in an NRK monolayer. Action potentials were evoked in a confluent monolayer by one distant stimulation (indicated by the arrow) of a few cells with a small volume (10 µl) of 124 mM KCl under conditions that: **A)** control **B)** G_{CaL} was blocked by 1 µM nifedipine, **C)** $G_{Cl(Ca)}$ was blocked by preincubation (10 min) with 50 µM BAPTA-AM and **D)** G_{Kir} was blocked by 10 mM Cs^+. All experiments were performed with 2 mM external Sr^{2+}.

propagating action potential was evoked under conditions that G_{Kir} was blocked, the action potential exhibited a prolonged plateau phase (n=5) or did not repolarize at all (n=2). Fig. 6D shows the effect of blocking G_{Kir} on the membrane potential of a monolayer of NRK cells and the prolonged plateau phase of the evoked action potential. In this particular example, after 4 min the action potential only partially repolarized to -40 mV. As a consequence the cells became competent to spontaneously fire a second action potential that did not repolarize within the time of observation (>20 min).

In conclusion, the action potential evoked in NRK monolayers clearly results from a sequential opening of G_{CaL}, $G_{Cl(Ca)}$ and G_{Kir}, respectively.

Discussion

In the present study we have characterized three principal membrane conductances in NRK fibroblasts by whole-cell voltage-clamp experiments and we have shown how excitability of the cell results from an interplay between these conductances via the membrane potential and intracellular calcium. These conductances are an inwardly rectifying potassium conductance (G_{Kir}), an L-type calcium conductance (G_{CaL}) and a calcium-activated chloride conductance ($G_{Cl(Ca)}$). Unique for this action potential is that the intracellular calcium dynamics is an essential part of the excitability mechanism. Thus, both

voltage-dependent (G_{CaL}, G_{Kir}) and calcium-dependent ($G_{Cl(Ca)}$) properties of the conductances involved essentially contribute to excitability.

Although fibroblasts are often considered as non-excitable cells, we have previously shown that in quiescent monolayers of NRK cells, which have a stable resting potential around -70 mV, a propagating action potential can be triggered that propagates throughout the entire monolayer (De Roos et al., 1997d). Such an action potential is induced by a depolarization of the membrane beyond the threshold for activation of G_{CaL} and the incidence of action potentials was increased from only about 10% in Ca^{2+} containing medium to almost 100% when external Ca^{2+} was replaced by Sr^{2+} ions. Voltage-clamp experiments now show that under these conditions $\overline{G}_{CaL}$ was about twofold increased whereas inactivation of this conductance was also slower.

The action potentials evoked in monolayers of NRK cells are characterized by a typical long-duration (~30 s) plateau phase. This plateau results from activation of $G_{Cl(Ca)}$ after Ca^{2+} or Sr^{2+} entry through L-type calcium channels and disappeared when these divalent ions were buffered using BAPTA-AM. The dependence of activation of this chloride conductance on calcium entry through L-type calcium channels was confirmed by voltage-clamp experiments. Membrane current recordings of cell clusters showed that BAPTA-AM did not block the inward calcium current, whereas the outward calcium-activated chloride current was completely abolished. In addition, voltage-clamp experiments on single cells showed that under our standard (strong) calcium buffering conditions (i.e. 3.5 mM EGTA in internal pipette solution) hardly any outward chloride current was measured, and that the action potential evoked by a current pulse did not have a plateau phase. However, when measured with weak calcium buffering pipette solutions (100 μM EGTA) this current was largely increased and the action potential showed a prominent plateau phase. These results clearly demonstrate that $G_{Cl(Ca)}$ generates the plateau phase of the action potential. In addition, activation of the $G_{Cl(Ca)}$ by the rise in cytoplasmic [Ca^{2+}] following the inflow of calcium or strontium through the G_{CaL} channels and probably supported by release of calcium from internal stores contributes to the repolarization of the initial spike of the action potential. This initial repolarization occurs at voltages of 0 to +40 mV, where the G_{Kir} channels are expected to be fully inactive. However, outward rectification of $G_{Cl(Ca)}$ may also contribute to that initial repolarization mechanism.

So far, only the presence of G_{CaL} and $G_{Cl(Ca)}$ has been reported for NRK fibroblasts (De Roos et al., 1997c; De Roos et al., 1997a). Here we show for the first time, that NRK fibroblasts also express a G_{Kir}. Expression of inwardly rectifying potassium channels has been shown before in fibroblasts such as human dermal fibroblasts (Estacion, 1991), but their function has remained elusive. In NRK fibroblasts G_{Kir} appears to be essential for the generation of the resting membrane potential as blocking this conductance with Cs^{+} ions depolarized the cells from around -70 to -50 mV. Under these conditions an action potential could still be evoked but the repolarization of the action potential was impaired. Previously it has been shown that the action potentials in NRK cells are accompanied by

intracellular calcium transients, and it was suggested that repolarization of the action potential occurred concomitant to the return of intracellular calcium concentrations to basal levels (De Roos et al., 1997c; De Roos et al., 1997d). Although this decrease in intracellular calcium levels indeed would shut off $G_{Cl(Ca)}$, we now know that it is insufficient to completely repolarize the cells to resting values of the membrane potential around -70 mV. The closure of the chloride channels, namely, will make the membrane subject to the repolarizing effect of I_{Kir}, which is required for the complete repolarization of the cells. This is in agreement with the results in Fig. 5C where a significantly prolonged plateau phase of the action potential was measured in a cluster with a relatively small $\overline{G}_{Kir} : \overline{G}_{Cl(Ca)}$ ratio. Moreover, blocking the activation of G_{Kir} with Cs^+ prevented a complete repolarization of the action potential. These results demonstrate that activation of G_{Kir} is essential for the complete repolarization of the action potential to the resting value of the membrane potential around -70 mV. This finding is in agreement with recently published data, showing that G_{Kir} is activated around -20 mV and constitutes one of the major components for the repolarization of the cardiac action potential from -20 to -60 mV (Ishihara et al., 2002).

We have never found evidence for another repolarizing conductance with a reversal potential Erev rather more negative than -20 mV. Any chloride conductance G_{Cl} will have an Erev~-20 mV, thus will be unable to contribute to the final repolarization. Any leak detected reverses around 0 mV (cf. Fig. 1D) and we never detected a delayed rectifier type of K^+ conductance. So, the only repolarizing conductance seems to be G_{Kir}. The fact that the leakage conductance G_{leak} (per cell) of gap junctionally coupled cells in cell clusters is relatively small (<~0.1 nS, *see* Table 1) implies that the repolarizing conductance needs to be very small, since $G_{Cl(Ca)}$ is declining to very low values due to calcium sequestering during the AP plateau. Thus, an extra G_{leak} or background conductance is probably not required for AP repolarization. Nevertheless, a very small background potassium conductance other than G_{Kir} cannot be excluded and a role for electrogenic ion transporters such as the Na/K-pump also remains a possibility. However, because we have been able to generate NRK-cell resting membrane potentials and action potentials with a mathematical model that only includes G_{Kir}, G_{CaL}, $G_{Cl(Ca)}$ and a small aselective G_{leak} (Torres et al., 2003), we have reasons not to invoke other repolarizing conductances. The role of G_{Kir} in the repolarization results from reactivation of G_{Kir} after deactivation during the upstroke of the action potential. Thus, G_{kir} also plays a role in action potential depolarization and in maintaining the plateau phase, as in heart cells, because deactivation accelerates the initial depolarization and in the deactivated state G_{Kir} allows $G_{Cl(Ca)}$ to dominate the membrane potential in the plateau phase.

The present study also provided an initial characterization of the activation and inactivation properties of the NRK-cell L-type calcium conductance (Fig. 3), when it conducts Sr^{2+} ions. Although these properties should be checked for conditions where G_{CaL} is not reduced (here by NPPB, consistent with Doughty et al., 1998), they allow a first comparison with current-clamp properties of NRK-cells.

The voltage-clamp experiments showed that the threshold for I_{CaL} activation is around -40 mV (*see* Fig. 3D) where inactivation is not far advanced (~50%). This explains that monolayer cells could spontaneously fire a second action potential after partial repolarization of the membrane to around -40 mV under conditions that G_{Kir} was blocked by Cs^+ (Fig. 6D). This finding suggests that any means that would depolarize the cells towards this potential should render them competent to fire an action potential. Indeed, previously we measured that cells fired an action potential if they became progressively depolarized by slow superfusion with medium containing an increasing K^+ concentration (De Roos et al., 1997b).

Excitability of NRK fibroblasts has so far only been measured in confluent monolayers (De Roos et al., 1997c; De Roos et al., 1997d). Under those conditions the cells are electrically well coupled by gap junctions and share each other's membrane conductances (Harks et al., 2001). However, electrical coupling appears not to be required for action potential firing since action potentials could be evoked in a significant percentage (~25%) of the single isolated NRK cells. The duration of the plateau phase of the action potential was, however, much shorter in single cells and clusters of cells compared to those evoked in monolayers. One reason of this difference may be that the whole-cell conditions established by the measuring patch pipette disturb the intracellular calcium dynamics in single cells and small cell clusters even with weak calcium buffering pipette solutions. In that case the activation of $G_{Cl(Ca)}$ channels would become mainly dependent on inflow of calcium through G_{CaL} channels and would no longer be supported by calcium release from intracellular stores.

The resting membrane potential of dissociated NRK cells varied enormously between cells, with values ranging from -10 to -75 mV. This large variability is most likely caused by the variation in the seal resistances (1-10 GΩ). Although the estimated maximal values of G_{Kir} are relatively high at -120 mV, G_{Kir} at -70 mV (resting membrane potential in monolayers) is often smaller (cf. the slope of the I-V-curve around -70 mV in Fig. 1D) than the single cell leak conductance (~0.3 nS). Therefore, the resting membrane potential in single cells is very sensitive to changes in the seal resistance. This variability in seal resistance may also explain why only a fraction of the single cells (~25%) was excitable. However, variability in expression of G_{Kir} (for the resting membrane potential) and G_{CaL} channels (for excitability) may also underlie the differences in excitability of single cells. In cell clusters and monolayers the leak conductance becomes much less effective in depolarizing the resting membrane potential, because the surrounding cells provide a relatively larger (summed) G_{Kir}. Moreover, the variability in the expression of G_{CaL} channels is sum-averaged over the whole cluster and the channels in the surrounding cells may be less subjected to run-down, because the intracellular milieu of those cells is screened off from the pipette-perfused cell by gap junctional channels. These effects together may explain why in contrast to single cells, all cell clusters were excitable.

The characterization of ionic membrane conductances was performed in cells derived from monolayers of quiescent NRK cells. When these monolayers are treated with epidermal growth factor (EGF) as the only growth stimulating polypeptide, the cells are induced to enter the cell division cycle

and become arrested in their growth when they have reached a critical cell density (Van Zoelen, 1991). In contrast to their quiescent counterparts, which exhibit a stable resting membrane potential around -70 mV, the growth-arrested cells (also called density-arrested) have been shown to spontaneously fire calcium action potentials with an interspike interval of approximately 150 s. The shape of these periodic action potentials is identical to that of the single action potential induced in quiescent monolayers and is also accompanied by transient increases in cytoplasmic calcium concentration (De Roos et al., 1997c). Preliminary voltage-clamp experiments on NRK cells derived from growth-arrested monolayers have shown that these cells express the same three prominent membrane conductances as their quiescent counterparts. Thus, spontaneous firing of density-arrested cells does not seem to result from the expression of extra ion channel types in the plasma membrane. Therefore, the mechanism providing the periodicity of the calcium spiking in density-arrested cells still remains unknown.

We now show by current injections in cell clusters that NRK cells are capable to fire a subsequent action potential within 1 s after repolarization of a preceding action potential. This is in agreement with voltage-clamp data, which showed that G_{CaL} was largely (~85%) deinactivated within 1 s (Fig. 3E). Obviously, the interspike interval in repetitively firing growth-arrested NRK monolayers (~150 s) is not determined by a refractory period of the action potential due to inactivation of the calcium channels. In accordance with that notion, it was found that an additional action potential could be evoked between two spontaneously fired consecutive action potentials by local stimulation with a high external $[K^+]$ pulse (De Roos et al., unpublished observation).

Possibly, the periodicity of spontaneous action potential firing by density-arrested NRK cells is determined by oscillatory changes in their intracellular calcium concentration. In recent years three different types of intracellular calcium stores have been identified, which are the IP_3-sensitive, cADPR-sensitive and NAADP-sensitive calcium stores (*see* e.g. Cancela et al., 2000). It has also been shown that a periodic release and uptake of calcium in one or more of these stores can result in intracellular calcium oscillations (*see* for review e.g. Patel et al., 2001). We hypothesize that in density-arrested NRK monolayers such oscillatory intracellular calcium rises transiently activate $G_{Cl(Ca)}$ by which the cells depolarize beyond the threshold for activation of G_{CaL}, and thereby fire action potentials periodically. Our current research is aimed at resolving the role and interplay of the different calcium stores in the oscillatory behaviour of NRK cells and to address the question why spontaneous oscillatory behaviour is exhibited by density-arrested NRK fibroblasts and not by their quiescent counterparts.

In the present study we have elucidated the ionic basis for excitability of cultured NRK fibroblasts, but we can still only speculate on the *in vivo* function of this excitability. As fibroblasts form cellular communicating networks *in vivo* (Hashizume et al., 1992; Komuro, 1989; Komuro, 1990) which expand throughout entire organs, their excitability in combination with electrical coupling might provide them with an efficient tool for fast and long-distance intercellular signaling. In

this way, agonist-induced depolarizations evoked in a few cells may be transduced to unstimulated neighboring cells, thereby recruiting a greater population of cells to respond in unison to local stimuli. As a matter of fact, we have found that action potentials induced in NRK fibroblasts can be transduced via heterocellular gap junctions to epithelial NRK cells, when both cell types are co-cultured (De Roos, 1997). This suggests that *in vivo* fibroblasts may couple to different cell types in a tissue and may act as an excitable and conductive pathway by which electrical signals generated at one side of a tissue or organ can be transduced to the other side. Also in other cells, the membrane potential has been shown to be involved in the coordination of cellular processes. For instance, calcium oscillations in pancreatic islets are synchronized by associated membrane potential changes (Santos et al., 1991). In addition, it has been shown that electrical coupling between endothelial cells and smooth muscle cells is implicated in the transmission of a hyperpolarization (Beny and Pacicca, 1994), presumably involved in vasoconstriction.

In conclusion, the results of the present study clearly demonstrate that a collection of only three types of ion channels besides leak channels, namely G_{Kir}, G_{CaL} and $G_{Cl(Ca)}$ channels, may be sufficient to provide single NRK cells with a mechanism for slow action potential generation. G_{Kir} and G_{CaL} are sufficient to produce conventional fast action potentials. Peculiar in the NRK cell excitability mechanism is the essential role of the intracellular calcium dynamics, coupling the activity of $G_{Cl(Ca)}$ channels to the activity of the depolarization activated G_{CaL} channels. Gap junctional coupling of cells does not only allow long-distance intercellular propagation of these action potentials, but also improves the excitability of neighboring cells with differences in channel expression by channel sharing.

Acknowledgements.

We thank Peter Peters for technical assistance in culturing NRK cells and Dr. W.P.M. Van Meerwijk for statistical advice. J.J.T. acknowledges support from MCyT and FEDER ("Ramón y Cajal" contract); contract grant number BFM2001-2841, and partial support from University of Granada ("Plan Propio de Investigación") and Dutch Technology Foundation. D.L.Y. is supported by the Foundation Nijmegen University Fund (SNUF).

Materials and Methods

Cell culturing. Normal rat kidney fibroblasts (NRK clone 49F) were cultured in bicarbonate buffered Dulbecco's modified Eagle's medium (DMEM; Life Technologies, Paisly, UK) supplemented with 10% newborn calf serum (HyClone Laboratories, Logan, UT, US) and confluent cultures were made quiescent by a subsequent one to three days incubation in serum-free DF medium (DMEM/Ham's F12, 1:1; Gibco, Life Technologies, Paisly UK) supplemented with 30 nM Na_2SeO_3 and 10 μg/ml human transferrin. For the experiments on single cells and cell clusters, cells were dissociated from quiescent monolayers by addition of a 0.25% trypsin solution for 5 min, after which cells were seeded in serum-free DF medium. The experiments on the dissociated cell cultures were performed 2-4 hours after trypsinization when NRK cells had been sufficiently attached to the culture dish.

Electrophysiology. Patch-clamp experiments were performed at room temperature on single cells, small cell clusters (≤10 cells) and monolayers. The cells were perfused with a standard extracellular solution, DF-ECS, which was the DF medium (DMEM/Ham's F12, 1:1; Gibco, Life Technologies, Paisly UK) containing (in mM) 120 NaCl, 4.2 KCl, 2 $CaCl_2$, 0.3 $MgCl_2$, 0.4 $MgSO_4$, 44 $NaHCO_3$ and 1.0 NaH_2PO_4, pH 7.4. Data were obtained using an EPC-7 patch-clamp amplifier (List Electronic, Darmstadt, Germany) in conjunction with Pulse/Pulsefit software (HEKA Elektronik, Lambrecht, Germany). The electrode was inserted in a side pool filled with the pipette solution and connected to the bath solution via a salt bridge with bath solution. For whole-cell voltage-clamp measurements on cells and clusters of 2-10 cells data were sampled at 10 kHz and the fast capacitive current transients were cancelled at the beginning of each experiment. In the current-clamp experiments on single cells and cell clusters the resting membrane potential was preset to -80 mV by a holding current. The standard intracellular pipette solution (S-ICS) contained (in mM) 25 NaCl, 120 KCl, 1 $CaCl_2$, 1 $MgCl_2$, 3.5 EGTA, 10 HEPES/KOH (pH 7.4), which corresponds to a free calcium concentration of ~55 nM (Schoenmakers et al., 1992). Pipettes with a resistance of 4-6 MΩ were used for optimal whole-cell stability. Series resistances were <~15 MΩ, causing acceptable voltage errors <3 mV at small currents (<200 pA) in the single cell whole-cell voltage-clamp experiments. For the characterization of the L-type current, clusters of 5-7 cells that had been dissociated from quiescent monolayers were used. In these experiments the extracellular solution (Sr-ECS) consisted of (in mM) 130 TEACl, 2 $SrCl_2$, 1 $MgCl_2$, 10 glucose and 10 HEPES, pH 7.4 supplemented with 50 μM NPPB, while pipettes were filled with Cs-ICS, composed of 145 CsCl, 1 $MgCl_2$,4 MgATP, 3.5 EGTA and 10 HEPES, pH 7.4.

Estimation of maximal conductances. Ionic membrane conductances in <u>single cells</u> were calculated from current-voltage relationships (I-V curves). The leak conductance (G_{leak}) was calculated by dividing the total current at -80 mV by the driving force for the leak current (-80 mV), assuming E_{leak}=0 mV. At a potential of -80 mV, which is the approximate equilibrium potential for potassium, only the leak contributes to the total current. In the voltage range measured the inwardly rectifying potassium conductance (G_{Kir}) was maximal at -120 mV. Therefore, the maximal conductance was calculated at that potential by dividing the maximal total current after leak correction, by the driving force for potassium (-40 mV). The inward calcium current was maximal at 0 mV, but because the L-type calcium conductance (G_{CaL}) was larger around its reversal potential (+46.8 ± 1.8 mV, n=36), it was calculated by determining the slope of the I-V curve at that potential. Finally, the calcium-activated chloride conductance ($G_{Cl(Ca)}$) was estimated by dividing the leak-corrected maximal outward current at +40 mV by the driving force for chloride at this potential in cells in which the calcium-activated chloride current was maximized by minimal intracellular calcium buffering. Current-clamp experiments on NRK monolayers have shown before that the equilibrium potential for chloride in monolayers is about -20 mV for these cells (De Roos et al., 1997a), but in our single-cell and cell cluster whole-cells we expect E_{Cl}~0 mV because of the applied symmetrical chloride concentration. Therefore, the driving force for chloride at +40 mV was assumed to be 40 mV. Membrane conductances in <u>cell clusters</u> were determined in the same way and were normalized as conductances per cluster cell by dividing the total membrane conductance by the number of cells. The calculated maximal conductances in cell clusters are underestimates. The error in the conductance estimation first depends on the size of the current and the value of the total series resistance to the surrounding cells. Series resistance to the membrane of the patched cell was <15 MΩ and the gap junctional resistance from the patched cell to the

surrounding cells <10 MΩ (Harks et al., 2001), thus total series resistance was <25 MΩ. For currents <200 pA this results in a <5 mV voltage error, which is <~12.5% error in an applied driving force of 40 mV (for G_{Kir} and $G_{Cl(Ca)}$). The underestimation of the conductance is of course larger, because of the voltage-activated properties of G_{Kir} and $G_{Cl(Ca)}$. For G_{Kir} we estimated a rough conductance error of ~20% based on non-linear I-V's for small total currents as in Fig. 1D. However, these values are approximations, merely serving to make sure that the better estimations are obtained from the smaller currents, e.g. the L-type calcium currents, which can better be resolved in the clusters. These currents were <50 pA, when measured in clusters in the presence of NPPB, thus the calculated voltage-clamp error in these experiments was <1.25 mV, which may be considered as acceptable. Maximal conductances in single cells and clusters were compared with a Mann-Whitney U test and the correlation between the duration of the action potential and the (relative) size of the maximal conductances was determined with a Spearman's Rho test. Data are represented as mean ± S.E.M. for n cells throughout this article.

CHAPTER 4

Modeling Action Potential Generation and Propagation in NRK Fibroblasts

J.J. Torres, L.N. Cornelisse, E.G.A. Harks, A.P.R. Theuvenet and D.L. Ypey

Abstract. Normal rat kidney (NRK) fibroblasts change their excitability properties through the various stages of cell proliferation. The present mathematical model was developed to explain excitability of quiescent (serum deprived) NRK cells. It includes as cell membrane components, based on patch-clamp experiments, an inwardly rectifying potassium conductance (G_{Kir}), an L-type calcium conductance (G_{CaL}), a leak conductance (G_{leak}), an intracellular calcium-activated chloride conductance ($G_{Cl(Ca)}$) and a gap junctional conductance (G_{gj}), coupling neighboring cells in a hexagonal pattern. This membrane model was extended with intracellular calcium dynamics resulting from calcium entry via G_{CaL} channels, intracellular buffering and calcium extrusion. It reproduces excitability of single NRK-cells and cell clusters and intercellular action potential (AP) propagation in NRK-cell monolayers. Excitation can be evoked by electrical stimulation, external potassium induced depolarization or hormone-induced intracellular calcium release. Analysis showed the roles of the various ion channels in the ultra-long (~30 sec) NRK-cell AP and revealed the particular role of intracellular calcium dynamics in this AP. We suggest that AP generation and propagation act as an intercellular mechanism for the propagation of intracellular calcium waves, thus contributing to fast intercellular calcium signaling. The present model serves as a starting point to further analyze excitability changes during contact inhibition and cell transformation.

Introduction

Normal Rat Kidney (NRK) cells are derived from a fibroblastic cell line (clone 49F) that has often been used for the *in vitro* study of fibroblast functions (De Roos et al., 1997c; Jinno et al., 2001; Van Zoelen and Tertoolen, 1991; Van Zoelen et al., 1988). In previous studies we have shown that these fibroblasts have excitable properties under certain growth conditions and are able to generate spontaneous or evoked action potentials (APs) with a long-duration plateau (30-60 s), which are propagated by electrical conduction through gap junctional channels between the cells in a confluent monolayer (De Roos et al., 1997c; De Roos et al., 1997d).

So far, channels of an L-type calcium conductance (G_{CaL}) have been shown to be responsible for the upstroke of the AP and channels of a calcium-activated Cl^- conductance ($G_{Cl(Ca)}$) for the long-duration plateau. However, ion channels responsible for the generation of the resting membrane potential had not yet been identified, which precluded exploration of the mechanisms of NRK cell excitability by modeling. Recently, we have demonstrated in voltage-clamp experiments the existence of an inwardly rectifying potassium conductance (G_{Kir}) in NRK fibroblasts (Harks et al., 2003c), consistent with previous experimental work showing the importance of the transmembrane K^+ concentration gradient in the generation of the resting membrane potential of these cells (De Roos et al., 1997d). This allowed us to start an analysis of NRK cell excitability by modeling the various conductances, including the G_{Kir}, to explore whether these conductances suffice to produce excitability and to see how the intracellular calcium dynamics affects AP-generation and AP-propagation between cells in a monolayer. We have chosen to study and analyze excitability in quiescent NRK cells rather than in density-arrested NRK cells, because the latter cells exhibit an extra electrophysiological feature, namely spontaneous AP firing (pacemaking) (De Roos et al., 1997c). This extra feature may result from extra complexity of the excitability mechanism. Starting with the simplest possible model system seemed a logical approach and would also allow us to answer the question whether simple adjustment of the parameters of the model components could in principle result in spontaneous firing. This would also help to make predictions for experimental testing of the membrane electrophysiological properties of density-arrested cells. Because the properties of the three active conductances involved (G_{Kir}, G_{CaL}, $G_{Cl(Ca)}$) were not yet fully quantified from voltage-clamp experiments on quiescent NRK cells, we used common or simplified descriptions for these conductances from the literature, as far as available. G_{Kir} was defined as in (Wallinga et al., 1999) for skeletal muscle fibers and G_{CaL} as in (Rasmusson et al., 1990) for bullfrog cardiac pacemaker cells. $G_{Cl(Ca)}$ was defined by assuming simple saturating binding kinetics of intracellular calcium ions to the calcium-sensitive chloride channels. Maximal conductance values, reversal potentials and stationary voltage-dependent properties of G_{Kir} and G_{CaL} were derived from our voltage-clamp experiments (Harks et al., 2003c). Intracellular calcium dynamics was simply modeled as a balance between the in of calcium ions through G_{CaL} and the efflux by active pumping. A simple calcium buffering

mechanism was also included. Before applying the model to the excitability behavior of single and coupled cells, we first checked the validity of the assumed component properties by reconstructing the experimental voltage-clamp records. The geometry of electrical intercellular coupling by gap junctional conductances was, as a first approximation, made as in a honey-comb structure (for hexagonal cells), because NRK cells in a monolayer were usually surrounded by six cells. The values of the coupling conductances were derived from coupling conductance estimations in NRK cells (Harks et al., 2001).

The resulting model reproduced the shapes of action potentials, which could be evoked in quiescent NRK single cells, cell clusters and monolayers, and propagation of APs across the monolayer. It also allowed us to analyze the ionic mechanism of AP-generation and to estimate the role of intracellular calcium dynamics in this mechanism. Future versions of the model will be extended with more complex intracellular dynamics (cf. Torres et al., 2001). This may help us to gain more insight in the mechanism of spontaneous AP firing in density-arrested cells.

Mathematical model

Single-cell model

Using standard Hodgkin-Huxley (HH) type equations, we consider the cell membrane as a single isopotential compartment whose basic equation is given by the membrane voltage equation:

$$C_m \frac{dVm}{dt} = -(I_{CaL} + I_{Kir} + I_{Cl(Ca)} + I_{leak}) \quad (1)$$

where C_m and V_m represent, respectively, the membrane capacitance and the membrane potential of the cell. The left-hand term of Eq. 1 represents a capacitive current, while the terms appearing at the right-hand side represent three active ionic currents and a small passive leak current which we consider (Harks et al., 2003c) involved in the membrane potential dynamics of real NRK fibroblasts. Physiological activation of $I_{Cl(Ca)}$ requires, besides calcium entry through calcium channels, intracellular calcium regulation by buffering and removal processes upon calcium entry. For this purpose we used a simple calcium dynamics assuming a simple calcium extrusion and buffering mechanism. The conceptual model is represented in Fig. 1A. Current-clamp simulations with the model cell were carried out by adding an extra constant term I_{CC} to the right-hand term (in parentheses) of Eq. 1, representing the applied current-clamp stimulus current. Voltage-clamp stimulation was simulated by adding (in stead of I_{CC}) an extra term $I_{VC}=G_{ser}\cdot (V_{clamp}-V_m)$ to Eq. 1 with V_{clamp} the applied (constant) voltage and G_{ser} the series conductance between the voltage clamp and the

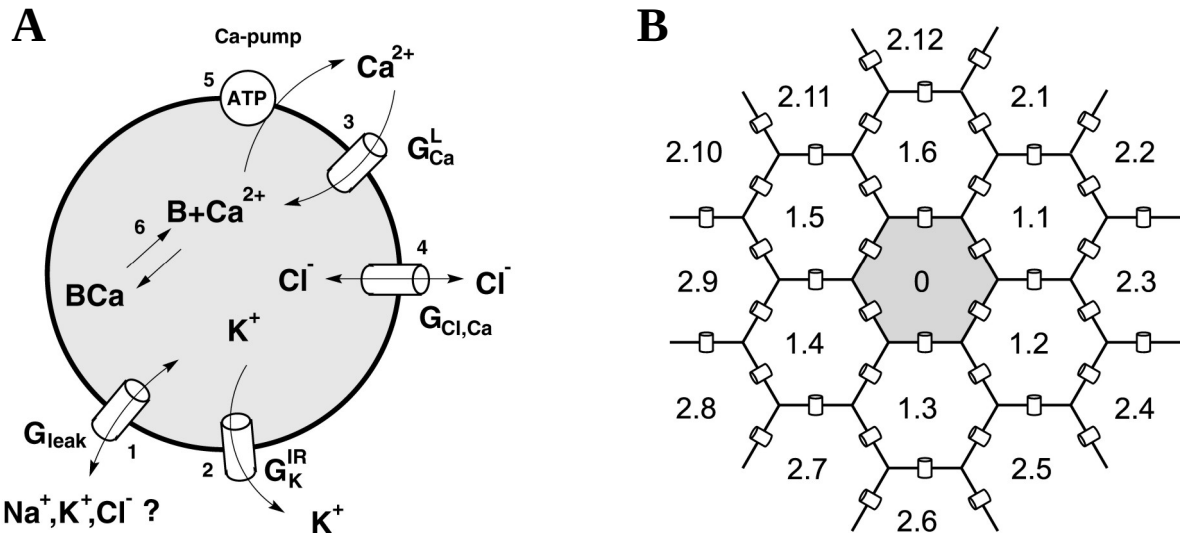

Figure 1 A) Conceptual model of a single NRK cell with components 1-6 (see text for explanation). **B)** Diagram illustrating hexagonal coupling of NRK cells in cell clusters and monolayers. Gap junctional coupling between a cell and its 6 nearest neighbors is symbolized. Intercellular spaces and membrane channels are not represented.

cell membrane (cf. Fig. 2). G_{ser} values were derived from experiments (Harks et al., 2003c). The description of each of the six basic components of the cell model is as follows:

1. Leak current, I_{leak}. We included this current since it was usually observed in patch-clamp experiments on single cells. The corresponding conductance, G_{leak}, was at least as large as the seal conductance (< 1nS). Then, we consider

$$I_{leak} = G_{leak} \cdot (V_m - V_{leak}) \tag{2}$$

   where, G_{leak} is the (linear) leak conductance. Voltage-clamp experiments reported in Harks et al. (2003c) suggest to set V_{leak} to ~0 mV.

2. Inward-rectifier potassium current, I_{Kir}. The presence of this current has been shown in voltage-clamp experiments on isolated NRK fibroblasts (Harks et al., 2003c). An adequate description of this current can be found in (Wallinga et al., 1999) for skeletal muscle fibers and is here used too:

$$I_{Kir} = \overline{G}_{Kir} \cdot \Im(Vm) \cdot (V_m - V_K) \tag{3}$$

   $\overline{G}_{Kir}$ is the maximal inward-rectifier potassium conductance. I_{Kir} activates at hyperpolarization around and below V_K=-80 mV. It contributes both to depolarization and repolarization of the action potential and is significant in the maintenance of the resting membrane potential. The

sigmoidal function $\Im(V_m)$ is defined in the Appendix as a simplified version of this function in (Wallinga et al., 1999) for a constant external potassium concentration. The parameters appearing in $\Im(V_m)$ were obtained from current-voltage curves derived from voltage-clamp records from real NRK fibroblasts (Harks et al., 2003c).

3. L-type voltage-gated calcium current, I_{CaL}. It is responsible for the fast depolarization of the membrane at the initiation of an action potential. It is expressed in terms of a voltage-dependent conductance with one activation (*m*) and one inactivation variable (*h*) multiplied by the HH driving force for calcium ions (V_m-V_{Ca}), which is:

$$I_{CaL} = \overline{G}_{CaL} \cdot m \cdot h \cdot (V_m - V_{Ca}) \quad (4)$$

where $\overline{G}_{CaL}$ is the maximal calcium conductance expressed in nS. The kinetics of the dynamic variables appearing in the definition of I_{CaL} has been taken from a model of the bullfrog cardiac pacemaker cell (Rasmusson et al., 1990). The main difference between Eq. 4 and the corresponding equation in (Rasmusson et al., 1990) is that we are using a HH driven force instead of a Goldman-Hodgkin-Katz formalism. We have also lowered the time constant for *m* and *h* with a factor of 100 to speed up the bullfrog heart I_{CaL} kinetics to that of rat fibroblasts. The dynamics of each of the gating variables (here *x*=*m*,*h*), in general, can be described by a regular Markov process,

$$\frac{dx}{dt} = \alpha_x (1 - x) - \beta_x x \quad (5)$$

where α_x and β_x are functions of V_m and represent the rates for transition from closed to open and from open to closed states, respectively. Here, we used the equivalent equation:

$$\frac{dx}{dt} = \frac{1}{\tau_x} \cdot (x_\infty - x) \quad (6)$$

where $x_\infty=\alpha_x/(\alpha_x+\beta_x)$ and $\tau_x=1/(\alpha_x+\beta_x)$ represent the steady-state and time constant, respectively, for each one of the channel gates. The dependence of τ_x and x_∞ on V_m is further defined in the Appendix. To simulate a *U*-shaped inactivation curve (Rasmusson et al., 1990), the inactivation variable *h* also includes a second term representing calcium-induced inactivation (*see* Table 2) as in (Rasmusson et al., 1990). The existence of I_{CaL} has been proven in voltage-clamp experiments on real NRK fibroblasts (De Roos et al., 1997c; Harks et al., 2003c).

4. Ca^{2+} -dependent chloride current, $I_{Cl(Ca)}$. The existence of the three above defined currents is not sufficient to qualitatively reproduce the observed behavior of real NRK fibroblasts. Experiments on monolayers of NRK fibroblasts suggested the presence of a cytosolic calcium-dependent chloride current ($I_{Cl(Ca)}$) in NRK fibroblasts responsible for the maintenance of a long-duration action potential plateau near -20 mV (De Roos et al., 1997a). In recent voltage-clamp experiments on single quiescent NRK cells and small cell clusters we have further defined $I_{Cl(Ca)}$ (Harks et al., 2003c). To take into account all these experimental findings, we have completed the model by including $I_{Cl(Ca)}$ as follows:

$$I_{Cl(Ca)} = \overline{G}_{Cl(Ca)} \cdot \left[\frac{[Ca^{2+}]}{[Ca^{2+}] + K_{Cl(Ca)}} \right] \cdot (V_m - V_{Cl}) \tag{7}$$

Here, $[Ca^{2+}]$ represents the cytosolic calcium concentration, $\overline{G}_{Cl(Ca)}$ the maximal chloride conductance, $K_{Cl(Ca)}$ the half-maximal activation concentration, and V_{Cl} the chloride equilibrium potential. The dependency of $I_{Cl(Ca)}$ on $[Ca^{2+}]$ implies that, for relatively large values of cytosolic calcium concentration, this current acts like a leak current that drives the membrane voltage towards V_{Cl}. For low levels of $[Ca^{2+}]$, the effect of $I_{Cl(Ca)}$ is significantly reduced.

5. Calcium extrusion. Above, we assumed that calcium ions enter the cell through L-type calcium channels. To maintain physiological cytosolic calcium concentrations, these ions should be pumped out to the extracellular medium via calcium pumps. Therefore, we also included calcium dynamics that represents this calcium extrusion mechanism without the presence of intracellular buffer mechanisms:

$$\frac{d[Ca^{2+}]}{dt} = -\frac{1}{z_{Ca} V_{cell} F} I_{CaL} - V_{pump}^{\max} \cdot \left(\frac{[Ca^{2+}]}{[Ca^{2+}] + K_d} \right) \tag{8}$$

The negative sign for the I_{CaL} term arises from the fact that inward calcium current has a negative sign. The factor $1/z_{Ca}V_{cell}F$ is a conversion factor that gives the increase of $[Ca^{2+}]$ produced by calcium influx into the cell via L-type calcium channels. Here F is the Faraday constant, z_{Ca} is the valence of the calcium ions and V_{cell} is the cell volume. In Eq. 8 we have considered a calcium pump system that requires energy in the form of one ATP molecule for each calcium ion pumped out with an affinity of K_d and maximal pump rate $V_{pump}^{\max}$ (Koch, 1999). Although the dynamics in Eq. 8 is rather simple, it is still an important component of the model, for example, for the termination of the long duration plateau of the action potential.

6. Calcium buffering. In many of the voltage and current-clamp experiments with real NRK fibroblasts, we have used non-natural calcium buffers like EGTA and BAPTA (Harks et al., 2003c). The buffer molecules bind to free calcium ions with a rate k_{on} forming a buffer-calcium complex (BCa), which can dissociate also with the rate k_{off} according to the reaction equation:

$$B + Ca^{2+} \underset{koff}{\overset{kon}{\rightleftharpoons}} BCa \tag{9}$$

Then, to include the dynamics of this reaction in the cytosolic calcium dynamics, we extended Eq. 8 as follows:

$$\begin{aligned} \frac{d[Ca^{2+}]}{dt} &= k_{off}[BCa] - k_{on}(T_B - [BCa])[Ca^{2+}] - \frac{1}{z_{Ca}V_{cell}F} I_{CaL} - V_{pump}^{\max} \cdot \left(\frac{[Ca^{2+}]}{[Ca^{2+}] + K_d} \right) ; \\ \frac{d[BCa]}{dt} &= k_{on}(T_B - [BCa])[Ca^{2+}] - k_{off}[BCa] \end{aligned} \tag{10}$$

where [B], and [BCa] denote the concentrations of the buffer and the buffer-calcium complex, respectively, and T_B denotes the total fixed concentration of buffer molecules, that is T_B=[B]+[BCa]. The same set of equations can also be used for natural intracellular buffering.

Coupled-cell model

It is known that many fibroblastic cell types in culture, including NRK cells, are electrically well coupled by gap junctional channels (De Roos et al., 1996; Harks et al., 2001; Postma et al., 1998). These intercellular aselective ion channels allow the passage of current between neighboring cells when these cells develop a difference in membrane potential. Thus, NRK cells in a monolayer form an electrical syncytium over which action potentials can propagate from cell to cell, as shown by De Roos et al. (1997d). We have modeled this action potential propagation in a monolayer by electrically coupling individual cells with surrounding cells in a hexagonal pattern of a model monolayer of definable size (cf. Fig. 1B). This network geometry approximates the packing of a monolayer of real NRK fibroblasts. Thus, the effect of the coupling can be simulated by adding an extra term at the right-hand side of Eq. 1, which is:

$$I_{gj}^{i} = \sum_{j\,nn\,i} G_{gj}^{i\,j} (V_m^i - V_m^j) \tag{11}$$

Here, $G_{gj}^{i\,j}$ is the gap junctional electrical conductance between two neighboring cells and the sum extends over the 6 nearest neighbors (nn) of cell *i*.

The single-cell and coupled-cell model introduced above is schematized in Fig. 1. It is a model of minimal complexity ("minimal model"), constructed to explore whether its basic properties were sufficient to qualitatively reproduce single and coupled NRK cell excitability. Below we show that this is the case. The values of maximal ionic conductances and reversal potentials for all the ionic currents (*see* the Appendix) have been taken in accordance with experiments (Harks et al., 2003c). Stationary activation and inactivation parameters (V_m of half-maximal (in)activation and steepness factors) were in the range of values found in real NRK fibroblasts (Harks et al., 2003c). All information about model details like transition rates and other functions or parameters of the model are summarized in the Appendix.

Results

Single-cell voltage-clamp properties

The model described by Eqs. 1-10 for a single NRK cell is able to reproduce the main features of voltage and current-clamp experiments on real NRK fibroblasts. Fig. 2 shows a set of illustrative voltage-clamp experiments on the cell model including buffering of cytosolic calcium for different values of the total amount of buffer. The numerical experiment simulates the effect of the EGTA buffer in the pipette solution in real voltage-clamp experiments. The figure illustrates the characteristic properties of the total current when clamping the membrane voltage with increasing voltage steps from -120 to +20 mV. For large, negative voltage steps the total current is mainly carried by an inward-rectifier potassium current (constant negative current records), because this current is hyperpolarization activated. For voltage steps above -40 mV, I_{CaL} becomes activated while I_{Kir} becomes deactivated. The total current then shows the main features of I_{CaL}, which is, an initial rapid increase in negative current (activation) followed by a slower decrease (inactivation). This is best visible in the bottom-right current-record panel where I_{CaL} is the only time-dependent current around 0 mV.

An important consequence of I_{CaL} is an increase of the cytosolic calcium concentration. For voltage steps higher than 0, this is reflected as the appearance of an outward increasing current, $I_{Cl(Ca)}$. This current is large if $[Ca^{2+}]$ is high and small for low $[Ca^{2+}]$, as can be shown by varying the total amount of buffer T_B. Thus, for relatively small T_B (~4 μM) the cytosolic calcium was hardly buffered and therefore $I_{Cl(Ca)}$ was high (top left panel of Fig. 2). For relatively high T_B (for example, T_B=100 μM) the cytosolic calcium was almost fully buffered and then $I_{Cl(Ca)}$ was zero (bottom-right current-record panel). For this situation, not any time-dependent outward current is observed and only I_{CaL} appears for large positive voltage steps. After comparison with experimental recordings presented in Harks et al. (2003c), one may conclude that the model behavior is quite similar to that observed in

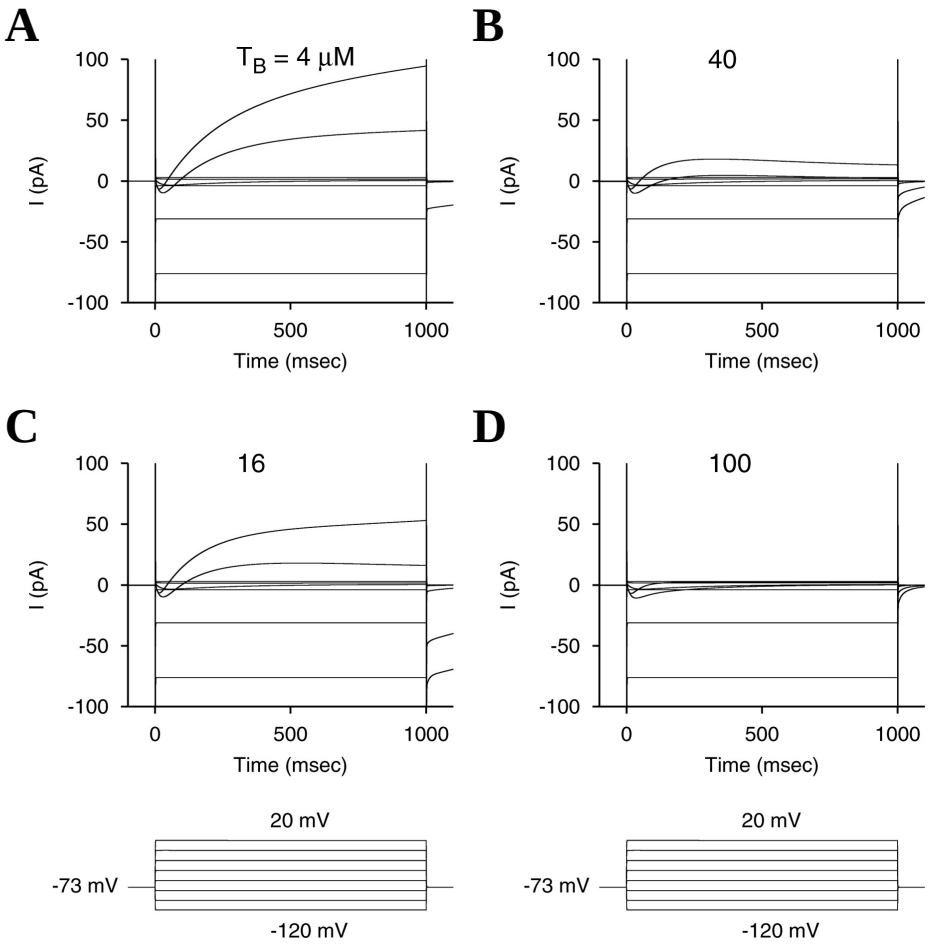

Figure 2 Voltage-clamp experiments on a NRK fibroblast single-cell model including buffering for different values of the total buffer amount T_B=4, 16, 40, and 100 μM respectively, and k_{on}=320 (mMsec)$^{-1}$ and k_{off}=0.06 sec^{-1}. Other parameter values as defined in the Appendix. Applied voltage step protocols shown in the bottom panels. The holding potential -73 mV has been taken equal to resting membrane potential of the cell. The initial sharp spike in the records is the capacitive current transient due to the presence of the series conductance G_{ser}=50 nS. The lowest current-records in the panels belong to -120 mV and the highest to +20 mV. Voltage increments between the records were +20 mV.

voltage-clamp experiments on real NRK fibroblasts. Those experiments were performed with EGTA in the pipette solution which is widely used as a calcium buffer. Due to the effect of EGTA, most of the current records do not show a high outward $I_{Cl(Ca)}$. By lowering the EGTA concentration in the pipette solution, calcium buffering was decreased and a large outward $I_{Cl(Ca)}$ was measured in single cells. In voltage-clamp experiments on clusters of cells, the small $I_{Cl(Ca)}$ currents of the individuals cells add up (*see* below) giving rise to larger outward currents. When, however, a strong intracellular calcium buffer was added (BAPTA), these outward currents disappeared, demonstrating that the outward current is a result of an intracellular calcium transient as in the model. Thus, all these changes in intracellular buffering by EGTA and BAPTA can be described, at least qualitatively, by choosing sets of buffer parameters in Eq. 10.

Voltage-clamp properties of small cell clusters

Patch-clamp experiments on small cell-clusters of NRK cells show similar current responses to voltage-clamp steps as in single cell experiments (Harks et al., 2003c). The main difference seems to be that the amplitude of the recorded currents is higher for the cell-cluster than for the single-cell, because currents are also being recorded from the cells coupled to the patched cell. Since the currents from single NRK cells are very small, we have used in our experimental studies voltage-clamp records from cell clusters to improve resolution. However, slower capacitive transients due to the overall coupling with the neighboring cells are visible in the records. This could imply worsened voltage-clamp conditions because of the gap junctional resistance serving as an access resistance to the cells surrounding the patched cell. We have used the present model to evaluate the voltage-clamp conditions in patch-clamp experiments on small cell clusters. We considered a cluster of a single cell coupled to 6 neighbor cells in a hexagonal geometry with different gap junctional conductances G_{gj} and included the effect of medium-strong buffering of calcium by EGTA (T_B=20 μM) in all cells.

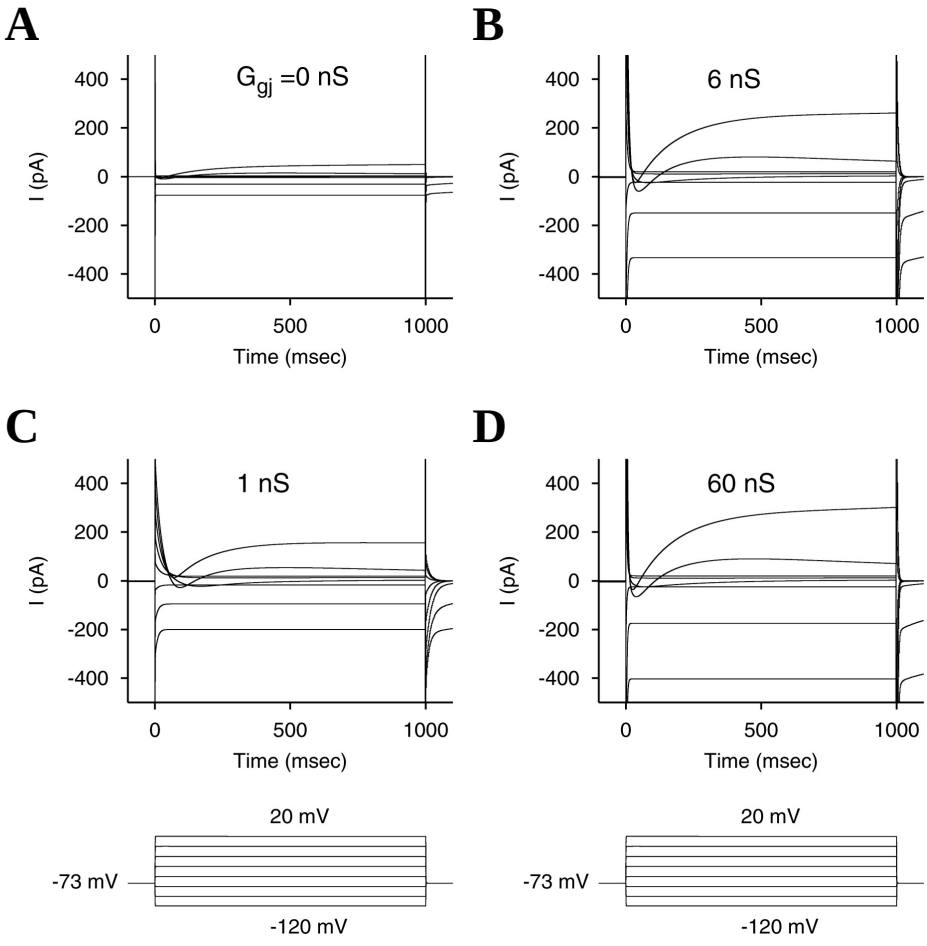

Figure 3 Voltage-clamp experiments in a cluster of 7 NRK model cells for different degrees of gap junctional coupling: G_{gj}=0, 1, 6, 60 nS as indicated. Buffer parameters were T_B=20 μM; k_{on}=320 (mMsec)$^{-1}$ and k_{off}=0.06 sec^{-1}. Series conductance G_{ser}=50 nS (R_{ser}=20 MΩ). Other parameter values as defined in the Appendix. Applied voltage step protocols are shown in the bottom panels.

Fig. 3 shows the main results. For G_{gj}=0 nS the records look like those from a single NRK cell experiment. The sharp needles at the up-and down-steps of the test voltage are the capacitive transients with peaks and time constants determined by the series resistance (R_{ser}) and the R_{ser} x C_m values, respectively (R_{ser}=20 MΩ as a worst case, C_m=20 pF). The voltage-clamp conditions are good for the small currents measured, because the voltage drop over R_{ser} is < 2 mV (20 MΩ x 100 pA). For increasing G_{gj}, the currents increase because of the contributions from the surrounding cells, but the capacitive current transients have become wider, indicating the delayed charging of the coupled cells to the applied voltage. The worst coupling (G_{gj}=1 nS) has the slowest capacitive current transient and the best coupling (G_{gj}=60 nS) the fastest. For ideal voltage-clamp, one would expect 7x as large currents on a 7-cell cluster compared to the current in a single cell. With G_{gj}=60 nS, this turned out to be the case for I_{CaL} (2% error in the estimation of I_{CaL} at -20 mV). G_{gj}=60 nS corresponds to a total coupling conductance to the surrounding cell ring G_{tgj}=360 nS (R_{tgj}~3 MΩ). In that case, R_{ser}=20 MΩ has become limiting in recording current from the surrounding ring, giving an underestimation of the inward rectifier current at -120 mV of 24%. Thus, although the reliable measurability of small currents (e.g. I_{CaL}) in a small (7-cell) NRK cell cluster may be much improved, the measurement of maximal values of the larger currents (I_{Kir} and sometimes $I_{Cl(Ca)}$) is less reliable than in single cells, depending on the sum of R_{ser} and R_{tgj}.

Excitability of single cells

The model cell is able to generate action potentials (APs) similar to those appearing in real NRK fibroblasts. Most of these experiments were performed with high EGTA concentrations (3.5 mM) in the pipette solution. We will take this into account by introducing the following buffer parameters in Eq. 10, T_B=20 μM, k_{on}=320 (mM sec)$^{-1}$ and k_{off}=0.06 sec^{-1}. As in real cells, Fig. 4 shows that upon stimulation with positive current pulses of sufficient strength the membrane potential quickly changes from its resting value towards more positive values. This depolarization is produced in the model mainly by a combination of an increasing inward I_{CaL} and a decreasing outward I_{Kir}, as illustrated in Fig. 4B where the individual currents have been plotted during an action potential. After activation, inactivation of I_{CaL} contributes to repolarization of the initial spike. I_{CaL} generates a significant influx of calcium ions that transiently increases the calcium concentration in the cytosol. The elevation of [Ca^{2+}] in the cytosol (*see* Fig. 4C) activates $I_{Cl(Ca)}$ which contributes to the initial repolarization by pulling the membrane voltage towards V_{Cl}=-20 mV. The end of the calcium transient produces a decreasing $I_{Cl(Ca)}$, such that the membrane becomes subject to the repolarizing effect of I_{Kir}. As a consequence, the membrane falls down from the voltage plateau at -20 mV to the resting potential near -70 mV (cf. Fig. 4B and C). At this voltage I_{Kir} remains active and I_{CaL} recovers from inactivation for repeated generation of an AP. The effect of I_{Kir} is to maintain the voltage near the resting

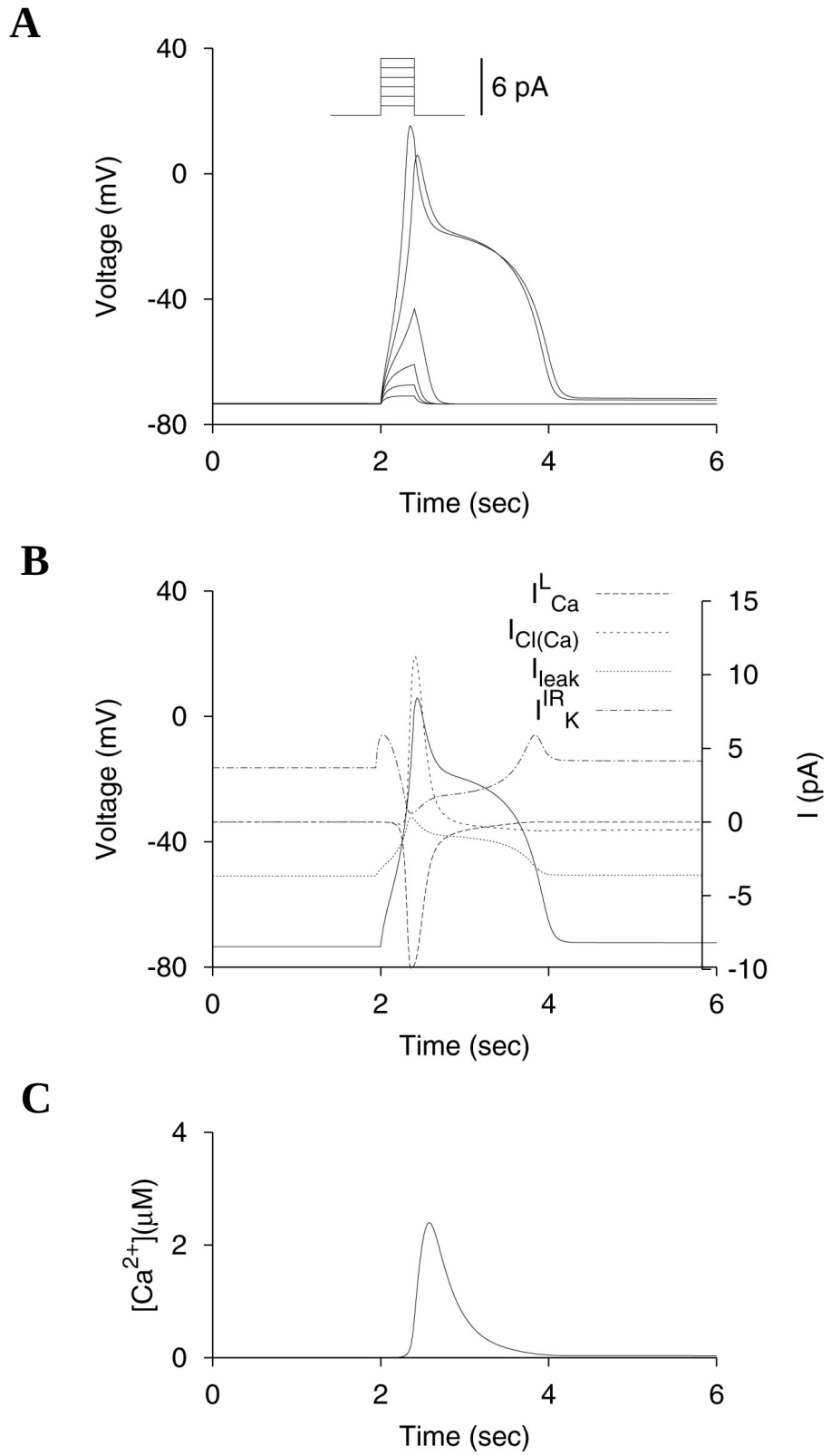

Figure 4 Current-clamp experiments in an isolated NRK fibroblast model cell. **A)** Subthreshold responses and action potentials generated upon different current steps of 1 to 6 pA. **B)** The time courses of the currents involved (dotted and dashed lines) in the NRK fibroblast cell-model to illustrate the relative importance of them during action potential generation by a 5 pA pulse (solid line). **C)** The intracellular calcium transient during the action potential. Buffer parameters were T_B=20 μM; k_{on}=320 $(mMsec)^{-1}$ and k_{off}=0.06 sec^{-1}. Other parameter values as defined in Appendix.

membrane potential by opposing the depolarizing effect of I_{leak} at low voltages. This is shown in Fig. 4B where I_{leak} and I_{Kir} are the most important currents under resting conditions. In the absence of intracellular calcium buffering the single-cell model AP is much larger because of an extended intracellular calcium transient (cf. Fig. 11 top left frame). This is further illustrated below.

Potassium pulse induced single-cell action potentials

We have also studied the ability of the NRK single-cell model to generate APs upon short-time exposure to a high concentration of external potassium. In this way a propagating action potential with a long-duration plateau could be evoked in NRK monolayers under conditions that external calcium ions were replaced by strontium ions (De Roos et al., 1997d; Harks et al., 2003c). We simulated the effect of K^+ pulses on the membrane by changing V_K from -80 to 0 mV for the duration of the pulse (~400 msec). Fig. 5 shows our main results for two different calcium buffering conditions. First, we observe that the NRK single-cell model can generate APs with the same properties upon current injections and potassium pulses (cf. Fig. 5A1 with previous figures). Second, removal of intracellular

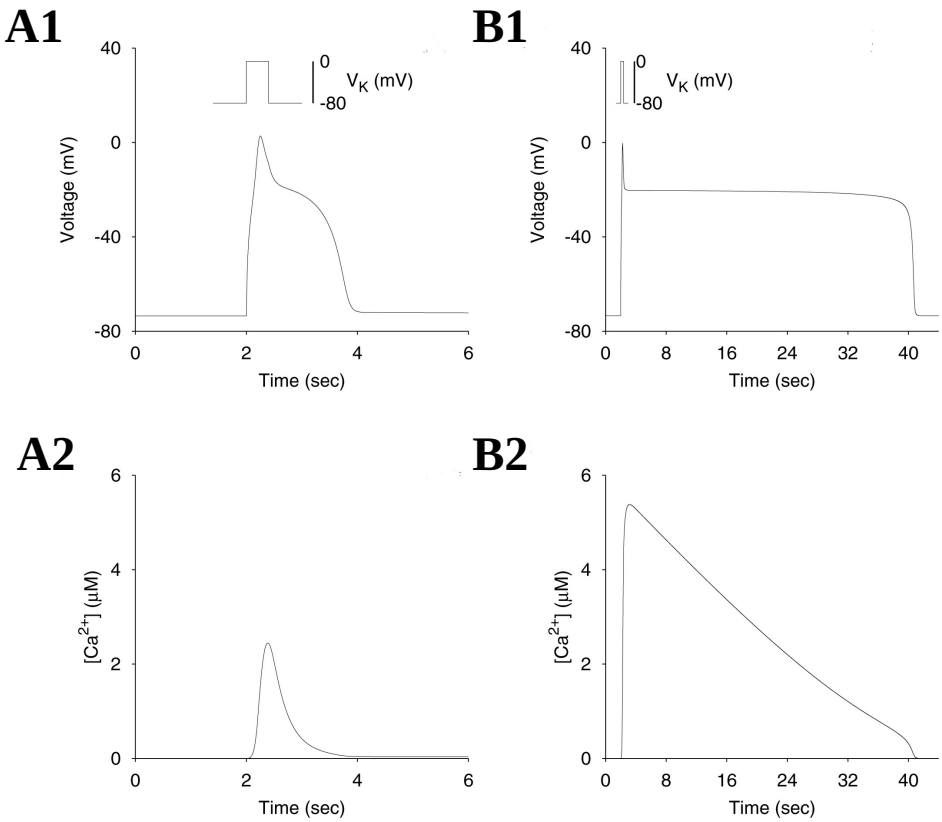

Figure 5 Excitation of the NRK fibroblast single-cell model by a short external potassium pulse (top panels) and the corresponding variation produced on the intracellular $[Ca^{2+}]$ (bottom panels) for two buffering conditions (A and B). This is simulated by changing the potassium equilibrium potential from -80 mV to 0 mV during 400 msec at two different buffer conditions. Buffer parameters were: Left panels (A1,2) T_B=20 µM; k_{on}=320 $(mMsec)^{-1}$ and k_{off}=0.06 sec^{-1} and right panels (B1,2) T_B=0 µM.

buffering from the model cell causes a tremendous (~20x) increase in the duration of the AP (Fig. 5B1). The figure also illustrates one of the predictions of our model, that is the correlation between duration of the action potential plateau and that of the intracellular calcium transient (Fig. 5A2, B2)[1].

Cytosolic calcium pulse induced single-cell action potentials

Excitation of NRK-cell monolayers by certain hormones (e.g. bradykinin) is the consequence of calcium release from intracellular stores evoked by those hormones (De Roos et al., 1997d). The presumed mechanism of this excitation was membrane depolarization via the calcium-activated chloride channels. We were, therefore, interested to know whether such a depolarization by a rise in the internal [Ca^{2+}] could also cause excitation of our NRK-cell model. An increasing [Ca^{2+}] will activate $I_{Cl(Ca)}$, thereby depolarizing the membrane beyond the threshold for I_{CaL} and causing the generation of an AP. To investigate this we applied intracellular calcium pulses to the cell. The NRK single-cell model was indeed able to produce APs upon applying calcium pulses to the cytosol. We increased the [Ca^{2+}] in the cytosol by adding a positive constant term of 0.01 mM sec^{-1} in the right-hand side of the first equation of Eqs.10. Fig. 6 shows the AP generated in a NRK single-cell model under two different calcium buffering conditions (Fig. 6A and 6B). The results are similar to those with potassium pulses except that there is no significant initial overshooting spike in the AP. One reason for this difference must be that the effect of I_{CaL} on V_m now acts against a background of $I_{Cl(Ca)}$, which is not the case during electrical stimulation.

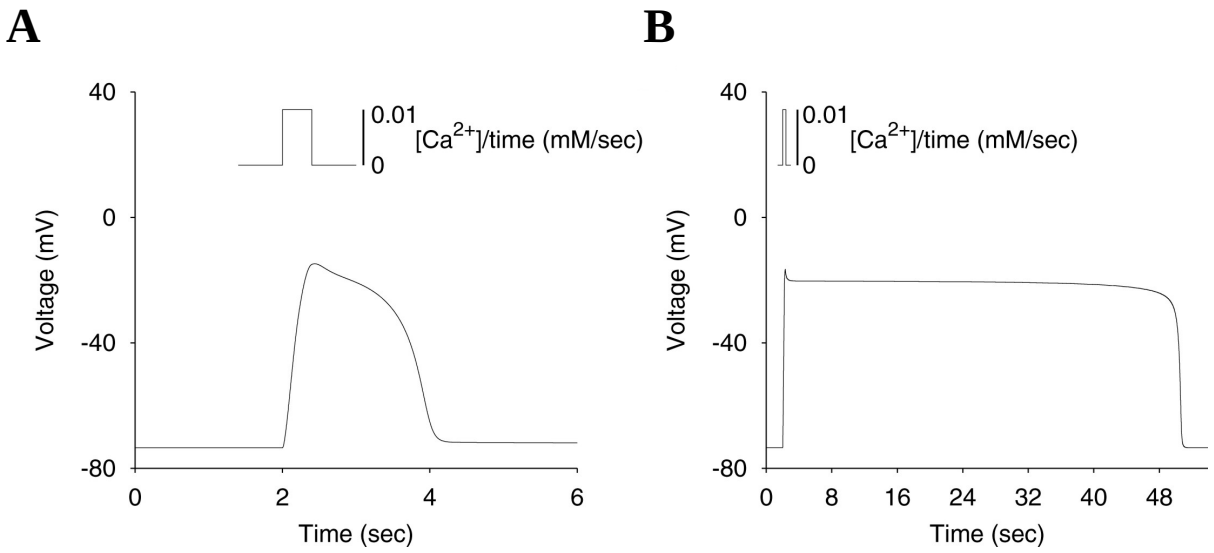

Figure 6 Excitation of the NRK fibroblast single-cell model by an intracellular calcium pulse for two buffering conditions (A,B). This is simulated by increasing the intracellular calcium concentration with 0.01 $mMsec^{-1}$ during 400 msec at two different buffer conditions. Buffer parameters were: Left panel **A)** T_B=20 μM; k_{on}=320 $(mMsec)^{-1}$ and k_{off}=0.06 sec^{-1} and right panel **B)** T_B=0 μM.

[1] The shape of the calcium transient in absence of calcium buffering may not be realistic due to the simple calcium dynamics we are considering

Single-cell excitability with strontium

Patch-clamp experiments on AP generation in NRK monolayers have been performed by substituting the calcium ions in the extracellular medium by strontium ions to improve excitability (Harks et al., 2003c). By this procedure, I_{CaL} in our voltage-clamp experiments on living single cells was increased by a factor 2, and moreover, strontium decelerated inactivation of L-type calcium channels. To take into account these two effects of strontium on I_{CaL} and to be able to generate APs in the NRK single-cell model in the presence of strontium, we changed in the model G_{CaL}=0.5 nS to G_{SrL}=1 nS. Furthermore, we changed the second term in the equation for *h* (steady state inactivation, *see* Table 2) to 0 (no calcium-induced inactivation of the channel by strontium) and shifted the half inactivation voltage from -45 mV to -49,3 mV, so that only voltage-induced inactivation remained. Fig. 7A,B and 8A,B show AP generation in an NRK single-cell model by, respectively, [K^+] and [Ca^{2+}] pulses in the presence of 2 mM external strontium, for two different buffering conditions. The results are essentially the same as with calcium, except that the initial action potential spikes are more pronounced now because of a stronger inward current by Sr^{2+}. For simplicity, we assumed here that the calcium channel properties were determined by the conducted Sr^{2+} ions and not by the intracellularly released calcium ions and that the intracellular buffer buffers Sr^{2+} ions in the same way as Ca^{2+} ions.

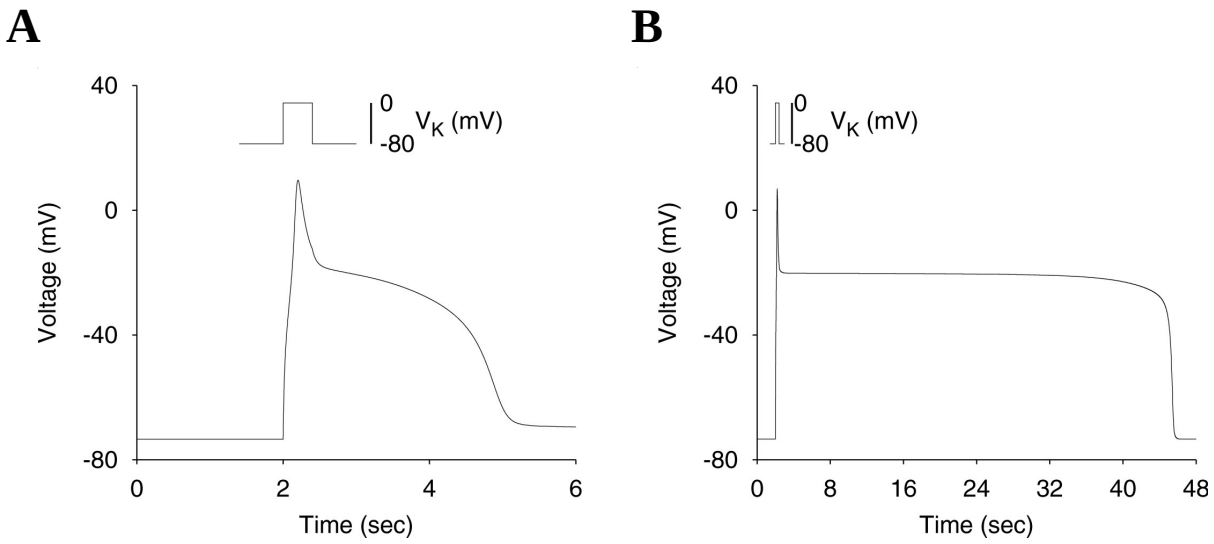

Figure 7 Excitation of the NRK fibroblast single-cell model by a potassium pulse with strontium in the external medium for two buffering conditions (A,B). The pulse was simulated by changing the potassium equilibrium potential from -80 mV to 0 mV during 400 msec under two different buffering conditions. Buffer parameters were: Left panel **A)** T_B=20 µM; k_{on}=320 $(mMsec)^{-1}$ and k_{off}=0.06 sec^{-1} and right panel **B)** T_B=0 µM.

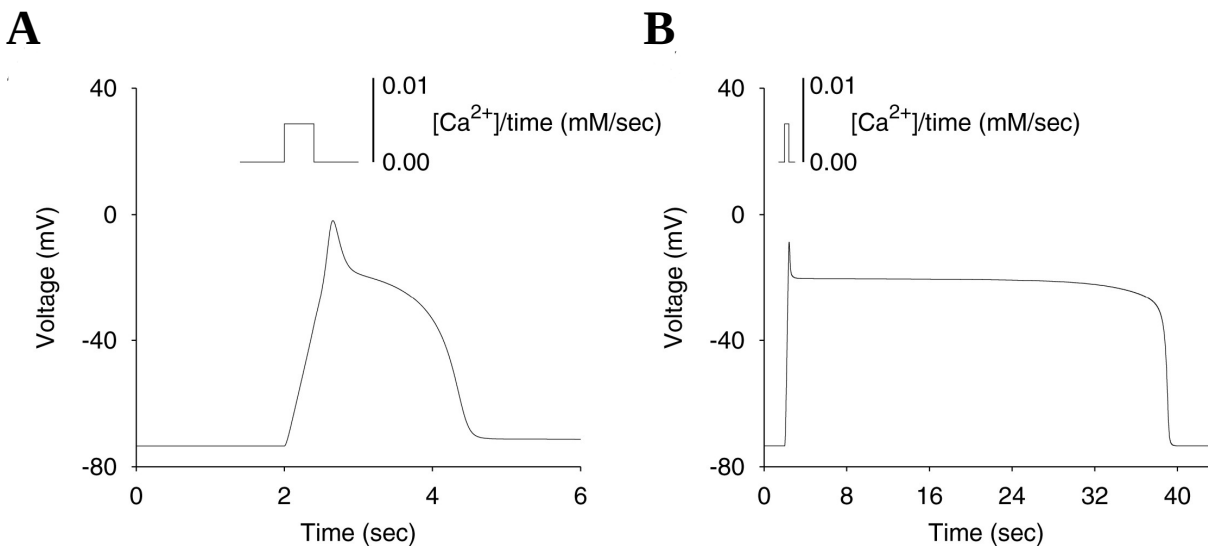

Figure 8 Excitation of the NRK fibroblast single-cell model by an intracellular calcium pulse with strontium in the external medium for two buffering conditions (A,B). The calcium pulse was simulated by increasing the intracellular calcium concentration with 5 μMsec^{-1} during 400 msec under two different buffering conditions. Buffer parameters were: Left panel **A)** T_B=20 μM; k_{on}=320 (mMsec)$^{-1}$ and k_{off}=0.06 sec^{-1} and right panel **B)** T_B=0 μM.

Excitability of small cell clusters

We have also performed several current-clamp simulation experiments in the presence of external calcium on small cell-clusters consisting of 7 model cells[2] coupled via gap junctions with conductance G_{gj}, since small clusters of real NRK fibroblasts appeared to be excitable (cf. Harks et al., 2003c). These simulations were also useful as a preparation for the more time consuming simulations on large monolayers. Fig. 9 and 10 show our main results. In Fig. 9 we applied increasing current steps in the cell in the center of such a 7-cell cluster, while the electrical conductance between the cells was G_{gj}=6 nS. This resulted in a physiological coupling conductance between the center cell and the surrounding ring of ~36 nS (Harks et al., 2001). The figure shows that an action potential (AP) was evoked in the cluster for current steps above 32 pA. In addition, we observed almost complete synchrony between the membrane potential change in the center and that in the neighboring cells due to the high electrical conductance of the gap junctions. As a consequence, to evoke an action potential it was necessary to apply much larger current steps in the cluster than in a single cell (cf. Fig. 4). In Fig. 10 we show the ability of the model to produce action potential propagation in a small cluster of model cells. Using the same current step in all experiments (I_{step}=32 pA), we observe that depending on the strength of the gap junctional electrical conductance, the action potential generated in the center of the cluster was able to propagate to the neighboring cells. A relatively small G_{gj} (~0.3 nS) was already sufficient for AP propagation in these high resistance NRK cells (R_m>1 GΩ). The figure also shows that the delay between action potential firing in the center cell and in a neighboring cell was smaller when G_{gj} was

[2] One cell in the center of the cluster and six neighboring cells

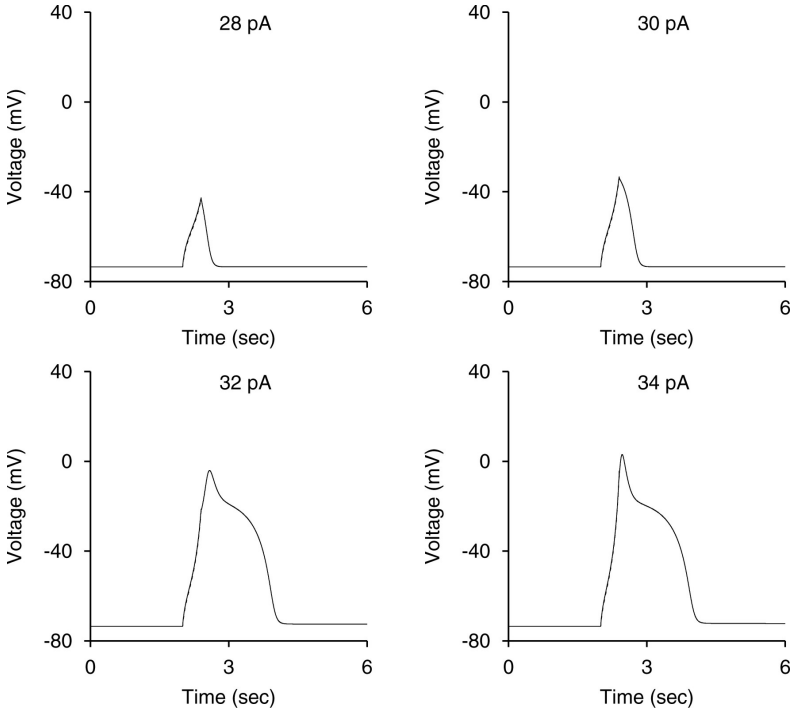

Figure 9 Current-clamp experiments in a cluster of 7 NRK fibroblast model cells. Current steps of various strengths have been applied to the center cell which is coupled with the surrounding 6 cells by gap junctions of strength 6 nS. Each panel represents two superimposed responses, one is recorded in the center cell of the cluster (solid line) and the other is one of the surrounding cells (dashed line, hardly visible at this coupling strength). The 4 different current steps are indicated in pA. Buffer parameters were: T_B=20 μM; k_{on}=320 (mMsec)$^{-1}$ and k_{off}=0.06 sec^{-1} for all cells in the cluster. Other parameter values as defined in the Appendix.

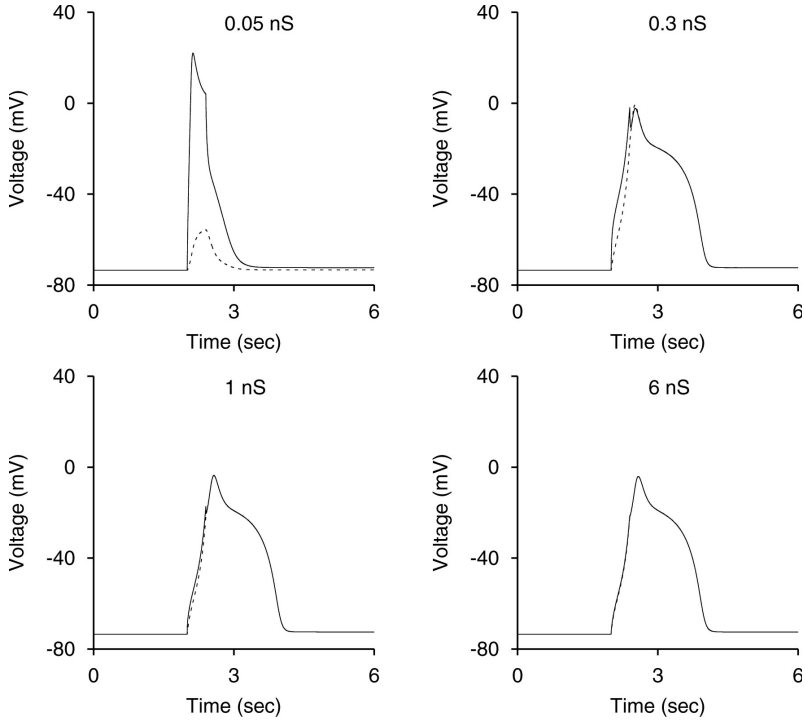

Figure 10 Current-clamp experiments in a cluster of 7 NRK fibroblast model cells. A current step of 32 pA and 400 msec duration was applied to the center cell, which is coupled with the surrounding 6 cells by gap junctions. Each panel represents the evoked action potential recorded in both the center cell of the cluster (solid line) and in one of the surrounding cells (dashed line), for 4 different values of the gap junctional strength indicated. Buffer parameters were: T_B=20 μM; k_{on}=320 (mMsec)$^{-1}$ and k_{off}=0.06 sec^{-1} for all cells in the cluster. Other parameters as defined in the Appendix.

increased, consistent with an increased propagation velocity of the action potential for increased values of G_{gj}.

Excitability and wave propagation in a monolayer of NRK fibroblasts

Finally, we simulated AP generation in a quiescent NRK monolayer with strontium in the extracellular medium. We used a 7 x 7 network with hexagonal geometry (*see* Fig. 1B), and applied a potassium stimulus to a cluster of 19 cells in the center of such a network, because stimulations of smaller central areas did not work. As we explained before, this is equivalent to changing the V_K from -80 mV to 0 mV in all these 19 cells and leaving the rest of the cells in the network unaltered. Buffering was left out (T_B=0) in order to look at the effect of coupling in a monolayer for the most simple AP

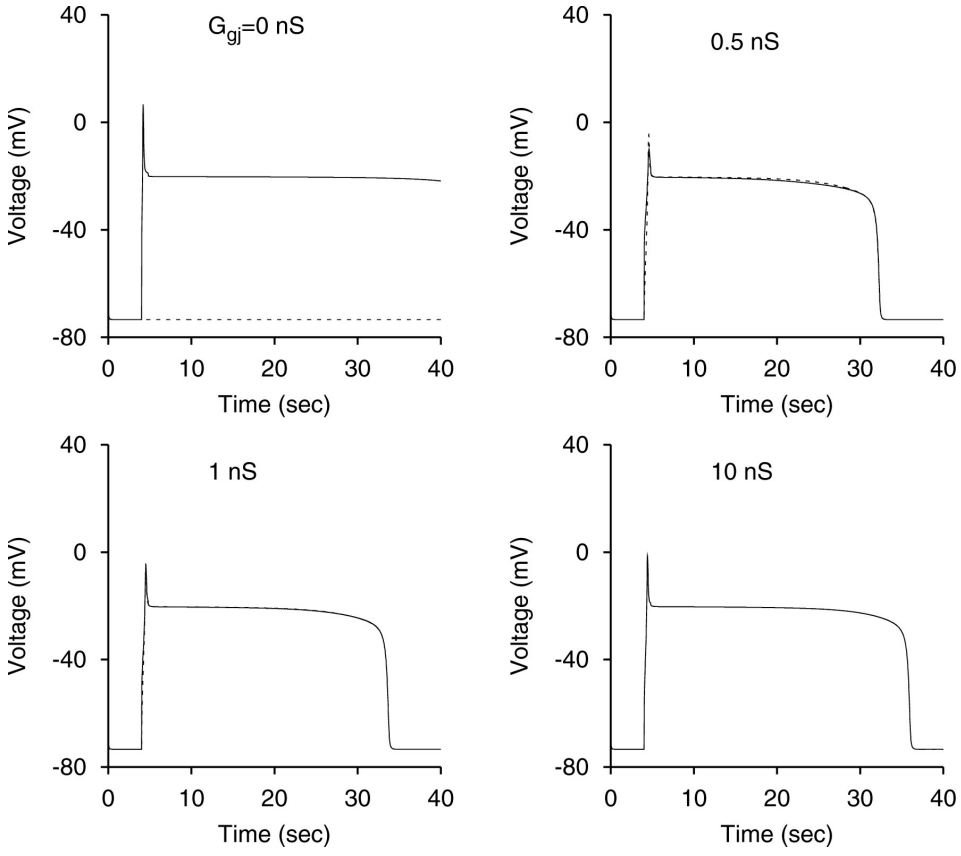

Figure 11 Excitability of the NRK fibroblast monolayer (of 7 x 7 cells) by a potassium pulse with strontium in the external medium for increasing gap junctional coupling. The pulse was simulated by changing the potassium equilibrium potential from -80 mV to 0 mV in the center region (consisting of 19 cells) of the monolayer during 800 msec. Each panel represents the synchronization of the electrical responses between the cell in the center of the monolayer (solid line) and the cell at the border of the monolayer (dashed line) for four different gap junctional conductances indicated. Intracellular calcium buffering was absent (T_B=0 μM).

mechanism. Fig. 11 illustrates the main results. The figure shows the electrical responses generated in two cells of the network, one in the center of the network and therefore in the stimulation area, and the other at the border outside the stimulation area. The figure shows AP generation and propagation through the network for different gap junctional strengths. Two main conclusions arise from the figure. First, the delay between the action potential of the cell in the center and that of a cell at the border decreases with increasing G_{gj}. At G_{gj}=0.5 nS it is 220 msec, while it is 7 msec at G_{gj}=10 nS. That means that the velocity of wave propagation from the center to the borders of the networks also increases with G_{gj}. Second, the height of the initial peak and the duration of the AP clearly depend on electrical coupling. AP-peak and duration decrease upon the establishment of coupling by G_{gj}=0.5 nS, but subsequently increase again upon a further increase in G_{gj}. The fact that AP-peak and duration change in the same direction indicates that AP-duration changes are caused by changes in the size of the inward calcium current causing changes in duration of the intracellular calcium pulse and associated $G_{Cl(Ca)}$ activation. These effects can be interpreted in terms of coupling dependent changes in loading of the central excited cells by the surrounding non-stimulated cells. At weak coupling (0.5 nS) the AP-delays in subsequent cell excitations are relatively long (~50 msec) compared to the used time constant of inactivation (~250 msec in the range of activation) causing partial inactivation of the calcium conductance during the depolarization phase of the AP. At stronger coupling loading and partial inactivation diminish again when the APs become almost synchronized. Whatever the mechanism of the coupling dependent AP-peak amplitude and duration, these simulation results show how the excitability of a larger ensemble of excitable cells such as an NRK-cell monolayer can depend on the strength of electrical coupling between the cells.

By a direct comparison with similar kinds of experiments reported in Harks et al. (2003) we can see the good agreement of our simulated AP generation in a monolayer with AP generation in real NRK monolayers in the quiescent state. The model is able to reproduce both the shape of the AP and the size of the long-duration plateaus (about 30 sec in this experiment). This could mean that intracellular calcium buffering in the cells of an NRK cell monolayer is not strong, but another possibility is that intracellular calcium release, not included here, lengthens the calcium transient in NRK cells. Finally, Fig. 12 shows a series of snapshots reflecting the propagation of the AP over a network of 9 x 9 cells (with speed v~1.5 mm/sec or equivalently ~90 cells/sec) where black color represents the lowest voltage regions (~resting membrane potential) and white color the highest voltage regions (action potential peak). The small size of the network and the particular network geometry produce some border effects in this simulation. These effects could be avoided by increasing the network size. Thus, with component properties in the physiological range, we could obtain excitability and action potential propagation in a relatively small model monolayer. The speed of propagation was in the order of mm/sec, near that in NRK monolayer cultures (*see* discussion).

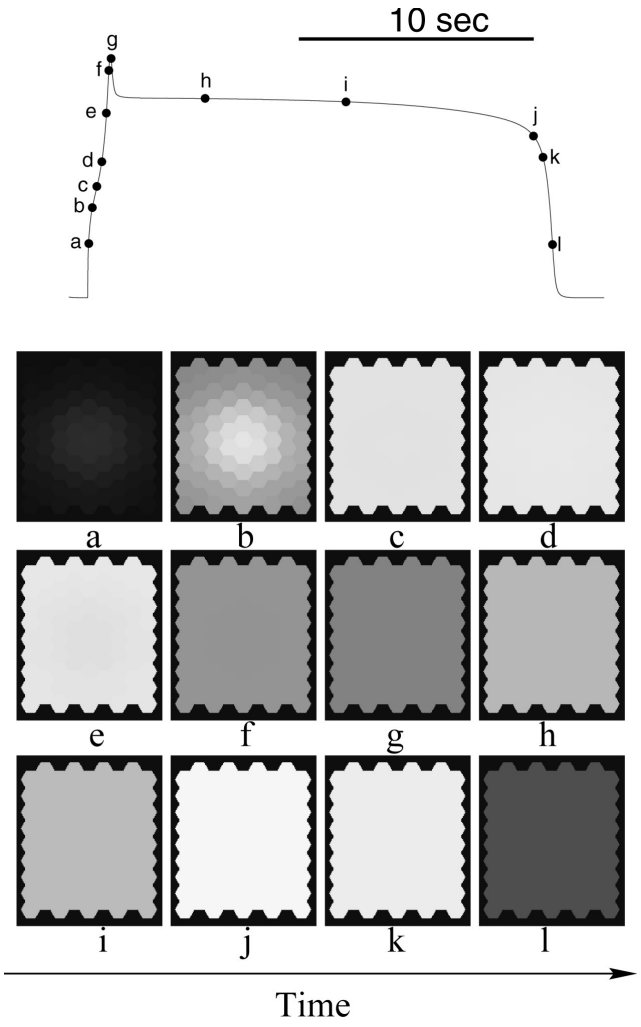

Figure 12 Consecutive snapshots (from left to right and from top to bottom) in a monolayer (of 9 x 9 cells) stimulated as in Fig. 11 showing wave propagation from the center to the border of the monolayer after stimulation with a potassium pulse in the center of the network. The time intervals between different snapshots were variable and the pictures were taken on the time points indicated by the dots over the AP of the center cell represented in the top panel. The gap junctional coupling among cells was G_{gj}=6 nS. Buffer conditions were: T_B=9 μM, k_{on}=320 (mMsec)$^{-1}$ and k_{off}=0.06 sec^{-1}. Other conditions the same as in Fig. 11. The black-to-white scale goes from negative to positive membrane potential.

Discussion

The NRK fibroblast cell-model presented in this paper is the first one describing the main features for AP generation and propagation in NRK fibroblasts. The model gives insights into the mechanism of AP generation in single cells and AP propagation in small cell clusters and monolayers of electrically coupled NRK cells. The model well reproduces the typical shape of the NRK cell AP with its initial spike and long duration plateau as well as calcium buffering effects on the shape of the AP. In short, G_{CaL} is responsible for the initial spike and $G_{Cl(Ca)}$ for the plateau of the AP. G_{Kir} is important for the resting membrane potential. Action potentials could be evoked by electrical stimulation with positive current pulses, by external potassium pulses and by intracellular calcium pulses, all acting by depolarization. In the first two cases the intracellular calcium transient follows excitation, in the third case it causes the excitation, as in experiments (De Roos et al., 1997d).

The present model is a minimal model, that is a model of minimal complexity, but containing the essential components to produce the qualitative electrical behavior of quiescent NRK cells in isolation

and in groups of electrically coupled cells. Apparently, the components of the model and their estimated properties were sufficient to reproduce that qualitative behavior. The model results (cf. Fig. 4B) illustrate that the role of the inward rectifier channels in NRK-cells is multiple. First, they serve to establish, together with a small leak conductance, a resting membrane potential at a high membrane resistance (R_m>1 GΩ) so that the resting condition does not require much energy expenditure. Second, G_{Kir} channels serve to contribute to excitability upon depolarizing events by way of their depolarization induced deactivation. The collapse of G_{Kir} may already occur below the potential of G_{CaL} activation (cf. Fig. 4B), and therefore, cause a membrane potential threshold for excitation below the activation potential of G_{CaL}. Third, the closure of G_{Kir} channels during the AP-plateau supports the maintenance of that plateau, while at the same time causing minimal energy expenditure for maintaining the ion concentration gradients across the fibroblast membrane. Finally, regenerative activation of G_{Kir} channels upon repolarization (Fig. 4B) due to $G_{Cl(Ca)}$ deactivation (following intracellular calcium clearance) contributes to this AP-repolarization. These important roles of G_{Kir} channels justify future studies for a further characterization and molecular identification of these channels and on regulation mechanisms of G_{Kir} channel modulation and expression.

The role of the intracellular calcium dynamics for the control of the long AP-duration is unique in comparison with that in nerve and muscle excitability. The fibroblast AP probably belongs to the longest-duration APs (~30 sec) in vertebrate excitable cells. Without buffering, the AP-duration in the model is very long (>30 sec) and only depends on calcium extrusion. With very strong buffering a very short AP occurs (<2 sec) with minimal or no contribution of $I_{Cl(Ca)}$. Similar differences in AP-duration with and without strong buffering have been found in patch-clamp experiments on NRK-cells (Harks et al., 2003c). However, in real NRK-cells calcium release from intracellular calcium stores may contribute to intracellular calcium dynamics, as suggested by experiments of (De Roos et al., 1997a). Since this calcium release is absent in our model, our model results primarily serve to illustrate the functional importance of intracellular calcium dynamics. Obviously, the relative contribution of calcium buffering and extrusion to AP-shaping may be different in real cells if calcium release is present. The model already shows that this internal calcium release is able to cause membrane excitation from within the cell (Fig. 6 and 8).

Another simplification of intracellular calcium dynamics may be the absence of intracellular compartmentalization. For example, the presence of a cytoplasmic shell just beneath the plasma membrane separated by a diffusion barrier from the deeper cytoplasm with calcium release stores would give a different calcium dynamics compared with that of our model with instantaneous single-compartment filling of the cytoplasmic space with calcium entering only via L-type calcium channels. Such a compartmentalization would affect the way calcium entry would feed back on L-type channels by calcium-induced inactivation and on the time course of inducing calcium release from calcium release stores deeper in the cell.

Considering these questions it is clear that a realistic modeling of fibroblastic intracellular calcium dynamics requires a detailed experimental characterization of the calcium in pathways (L-type channels with voltage and calcium-dependent inactivation, leak of calcium through the membrane, contribution of store-operated calcium channels), intracellular calcium buffering, intracellular calcium release and reuptake and calcium extrusion from the cells. Modeling the translation of calcium dynamics to $G_{Cl(Ca)}$ activation would require the experimental characterization of the calcium-dependent chloride channels. This would include possible voltage-dependent properties (Ho et al., 2001; Kidd and Thorn, 2001), which have been neglected in the present model.

The model results suggest that the degree of gap junctional coupling between an NRK-cell and its surrounding cells, where G_{gj}>60 nS (Harks et al., 2001), is much better than just required for intercellular AP-conduction (cf. Fig. 10 and 11). On the other hand, coupling seems too strong for AP-generation in single cells or small areas of cells embedded in the monolayer (Fig. 12). This indicates that fibroblast excitability in culture tends to be a collective property of the cells requiring, in case of local stimulation, a sufficient fraction of the whole cell culture to obtain a response of the culture as a whole. The same may hold for the *in vivo* excitability of the fibroblastic tissue component of an organ, where paracrine mechanisms are responsible for fibroblast activation in maintaining organ integrity, e.g. during wound healing (Bennett and Schultz, 1993).

The model properties are also of interest for the question of the relative importance of electrical conduction of excitation for the propagation of calcium waves in a tissue of cells coupled by gap junctions. Local stimulation signals (e.g. bradykinin) may cause local intracellular calcium transients as well as action potentials in a monolayer of NRK cells, which are then propagated over the monolayer (De Roos et al., 1997a; De Roos et al., 1997d). If the single or spontaneously repeating calcium wave has an intracellular origin, calcium diffusion through gap junctions causing calcium-induced calcium release in neighbor cells might be one mechanism for calcium wave propagation (Hofer, 1999). However, calcium buffering and removal have been recently shown to preclude the action of calcium as a purely diffusive gap junctional messenger over many cells, and also to limit strongly the velocity of calcium wave propagation from cell to cell (Hofer et al., 2001). In accordance with these theoretical predictions, intercellular calcium waves have been reported to propagate at ~5-50 μm/sec in the rat liver and the blow salivary gland (Robb-Gaspers and Thomas, 1995; Zimmermann and Walz, 1999), whereas in NRK fibroblasts locally-induced calcium action potentials propagate throughout the monolayer at a velocity as high as ~6 mm/sec (De Roos et al., 1997d). In the present study, we have shown that these much faster calcium waves can be achieved according to a mechanism in which the calcium influx through L-type calcium channels in one cell triggers an intracellular calcium rise in its neighbor cell. In our model, it is the fast electrotonically propagating calcium action potential that precedes the fast calcium-wave propagation in monolayers of these cells. The gap junctional conductances required for the fast propagation of calcium action potentials in the

model fall within the range of experimentally determined values for these conductances in NRK fibroblasts.

Although a propagating AP can be simulated with the present model, it was not possible to obtain spontaneous repetitive AP firing as observed in density-arrested NRK cells (De Roos et al., 1997c). So, the model predicts that this spontaneous firing does not result from altered expression levels of ion conducting channels in density-arrested NRK cultures but may involve more complex intracellular calcium dynamics. The present model can easily be extended by introducing more realistic assumptions in the calcium dynamics given in Eq. 10. For example, by including calcium-activated calcium release from endoplasmic reticulum, calcium pumping via SERCA pumps between cytosol and calcium stores, leak of calcium through the cell membrane, and calcium in via calcium release-activated calcium channels (CRAC) (Putney, 1986); (Torres et al., 2001). Current research is aimed at resolving the possible role and interplay of intracellular calcium stores in providing the cells a timing mechanism for spontaneous periodic electrical activity. In recent years it has become clear that cells may possess different types of calcium stores, and that these stores are able to interchange calcium ions in an oscillating manner (reviewed by e.g. Patel et al., 2001). It has been shown that in addition to the classical IP_3-sensitive calcium stores, cells may also contain cADPR-(cyclic adenosine diphosphate ribose) and NAADP (nicotinic acid adenine dinucleotide phosphate)-sensitive calcium stores (reviewed by Lee, 2000). Data that will become available will be used to expand the present minimal model with an intracellular calcium oscillator in order to simulate excitability of density-arrested NRK cultures. In this way, we will be able to study the conditions for generation, synchronization and propagation of calcium action potentials in cultured NRK monolayers. The coordination of action potentials in this system may serve to further understand how periodic, stochastic and chaotic generation of action potentials in other biological systems, such as the beating heart and neural networks, is modulated in a communicating network system.

Acknowledgments.

J.J.T. acknowledges support from the Spanish "Ministerio de Ciencia y Tecnología" and FEDER ("Ramón y Cajal" contract and project no BFM2001-2841), and partial support from University of Granada ("Plan Propio de Investigación") and the Dutch Foundation for Neural Networks (SNN). We thank Prof. Gielen (Medical Physics and Biophysics, KUN, Nijmegen, NL) for stimulating discussions and support in the preparation of the manuscript. D.L.Y. is supported by the Foundation Nijmegen University Found (SNUF).

Appendix: Mathematical Description of the Ionic Currents

Hodgkin-Huxley like currents

Table 1: Generalized Hodgkin-Huxley like currents: $I_i = \overline{G}_i m_i^p h_i^q (V_m - V_i)$

Current I_i	V_i (mV)	$\overline{G}_i$ (nS)	m_i	h_i	p	q
I_{Kir}	-80	2.2	$\Im(V_m)$	1	1	1
I_{CaL}	50	0.5	m	h	1	1
$I_{Cl(Ca)}$	-20	10	$\frac{[Ca^{2+}]}{[Ca^{2+}] + K_{Cl(Ca)}}$	1	1	1
I_{leak}	0	0.05	1	1	1	1

Table 2: Gating variables of I_{CaL}

Gating variable x	x_∞	τ_x (sec)
m	$\frac{1}{1 + e^{-(V_m+10)/6.24}}$	$\frac{m_\infty \cdot 0.01(1 - e^{-(V_m+10)/5.9})}{0.035(V_m + 10)}$
h	$\frac{1}{1 + e^{(V_m+45.06)/8.6}} + \frac{0.8}{1 + e^{0.05(50-V_m)}}$	$\frac{0.01}{0.02 + 0.0197 e^{-[0.0337(V_m+10)]^2}}$

Other parameters and functions in the model:

$\Im(V_m) = 0.0045 \cdot \exp(-1.489 \cdot V_m \cdot F / RT) / \{1 + 0.0045 \cdot \exp(-1.489 \cdot V_m \cdot F / RT)\}$

$K_d = 0.2 \mu M$

$V_{pump}^{\max} = 1.27 \times 10^{-3} mM \sec^{-1}$

$K_{Cl(Ca)} = 35 \mu M$

$F = 96480 C / mol$

$C_m = 20 pF$

$F / RT = 0.0396 (mV)^{-1}$

$z_{Ca} = +2$

$V_{cell} = 2.1 \times 10^{-12} l$

CHAPTER 5

Besides affecting intracellular calcium signaling, 2-APB reversibly blocks gap junctional coupling in confluent monolayers thereby allowing measurement of single-cell membrane currents in undissociated cells

E.G.A. Harks, J.P. Camiña, P.H.J. Peters, D.L. Ypey, W.J.J.M. Scheenen, E.J.J. van Zoelen and A.P.R. Theuvenet

Abstract. 2-Aminoethoxydiphenyl borate (2-APB) has been widely used as a blocker of the IP_3 receptor and TRP channels including store-operated calcium channels. We now show in monolayers of normal rat kidney cells (NRK/49F) that 2-APB completely and reversibly blocks gap junctional intercellular communication at concentrations similar to that required for inhibition of PGF2α-induced increases in intracellular calcium. Gap junctional conductances between NRK cells were estimated with single-electrode patch-clamp measurements and were fully blocked by 2-APB (50 μM), when applied extracellularly but not via the patch pipette. Half maximal inhibition (IC_{50}) of electrical coupling in NRK cells was achieved at 5.7 μM. Similar results were obtained for human embryonic kidney epithelial cells (HEK293/tsA201) with an IC_{50} of 10.3 μM. Using 2-APB as an electrical uncoupler of monolayer cells we could thus measure inward rectifier potassium, L-type calcium and calcium-dependent chloride membrane currents in confluent NRK monolayers, with properties similar to those in dissociated NRK cells in the absence of 2-APB. The electrical uncoupling action described here is a new 2-APB property that promises to provide a powerful pharmacological tool to study single-cell properties in cultured confluent monolayers and intact tissues by electrical and chemical uncoupling of the cells without the need of prior dissociation.

Introduction

In our studies, we use normal rat kidney (NRK) fibroblasts as a model system for investigating control mechanisms of cell growth and alterations during oncogenesis (De Roos et al., 1997c; Lahaye et al., 1999a; Van Zoelen, 1991). Prostaglandin F2α (PGF2α) has been shown to contribute to the phenotypic transformation of these cells (Lahaye et al., 1999b) and here we investigated the early effects of this stimulus on confluent monolayers of quiescent NRK cells. PGF2α is the natural ligand for the FP subtype of prostanoid receptors and activation of this G-protein coupled receptor induces phospho-inositide turnover and subsequent calcium release from IP_3 sensitive calcium stores (Narumiya et al., 1999). NRK fibroblasts have been shown to express receptors for this phospo-inositide mobilizing agent (Afink et al., 1994) such that PGF2α not only increased levels of inositol phosphates and intracellular calcium in these cells (Lahaye et al., 1999b), but also depolarized the membrane by the opening of calcium-dependent chloride channels (De Roos et al., 1997a). In this study we aimed to use 2-aminoethoxydiphenyl borate (2-APB) to investigate PGF2α-induced intracellular calcium rises and membrane depolarizations, but soon we discovered that 2-APB is able to block gap junctional channels.

2-APB (*see* chemical structure in Fig. 4) was first described by Maruyama *et al.* (1997) as a membrane permeable blocker of IP_3-induced calcium release in rat cerebellar microsomes by specific blocking of the IP_3 receptor (Maruyama et al., 1997). Since then, 2-APB has been shown to inhibit agonist- and IP_3-induced calcium signaling in a variety of cell types (Ma et al., 2000; Ma et al., 2001; Wu et al., 2000), without having an effect on thapsigargin-induced calcium release (Gregory et al., 2001; Ma et al., 2000). Although 2-APB has been used for assessing the role of IP_3 receptors in the activation of plasma membrane store-operated calcium (SOC) and TRPC3 channels (Ma et al., 2000; Ma et al., 2002; Van Rossum et al., 2000) it also seemed to block SOC and TRPC3 channels directly (Braun et al., 2001; Dobrydneva and Blackmore, 2001; Ma et al., 2001). So far, the action of 2-APB seemed to be restricted to the IP_3 receptor and TRP channels including SOCs.

In the present study, we report that in addition to its effects on intracellular calcium signaling 2-APB also completely and reversibly blocks electrical coupling of the cells. This uncoupling was achieved at concentrations that were similar to those required for blocking PGF2α-induced intracellular calcium increases. Using this observation, we were able to employ 2-APB to measure single-cell membrane currents in confluent monolayers by voltage-clamping electrically uncoupled NRK cells. Therefore, 2-APB appears to be a promising tool for studying single-cell properties of otherwise electrically and chemically coupled cells in cultured monolayers and intact tissues without the need of mechanically separating the cells.

Results

Effect of 2-APB on the PGF2α-induced intracellular calcium and membrane potential response in NRK fibroblasts

In order to investigate the efficiency of 2-APB to block PGF2α-induced increases in intracellular calcium in NRK cells, dynamic video imaging was performed on monolayers of NRK cells loaded with the fluorescent probe fura-2 to monitor the cytosolic free calcium concentration in a large number of cells. PGF2α induced intracellular calcium oscillations in individual cells in the monolayer (Fig. 1A), which were not synchronized in spite of the fact that these cells are known to be electrically coupled (Harks et al., 2001). Fig. 1B shows the average response of 39 cells within the monolayer. In every cell that was measured 75 μM 2-APB almost instantaneously blocked the PGF2α-induced calcium oscillations (n=158 cells from 4 independent monolayers) whereas in 78% of the cells the oscillations restarted after washout of 2-APB. These results clearly demonstrate that 2-APB rapidly and reversibly blocked the PGF2α-induced calcium increase in NRK cells.

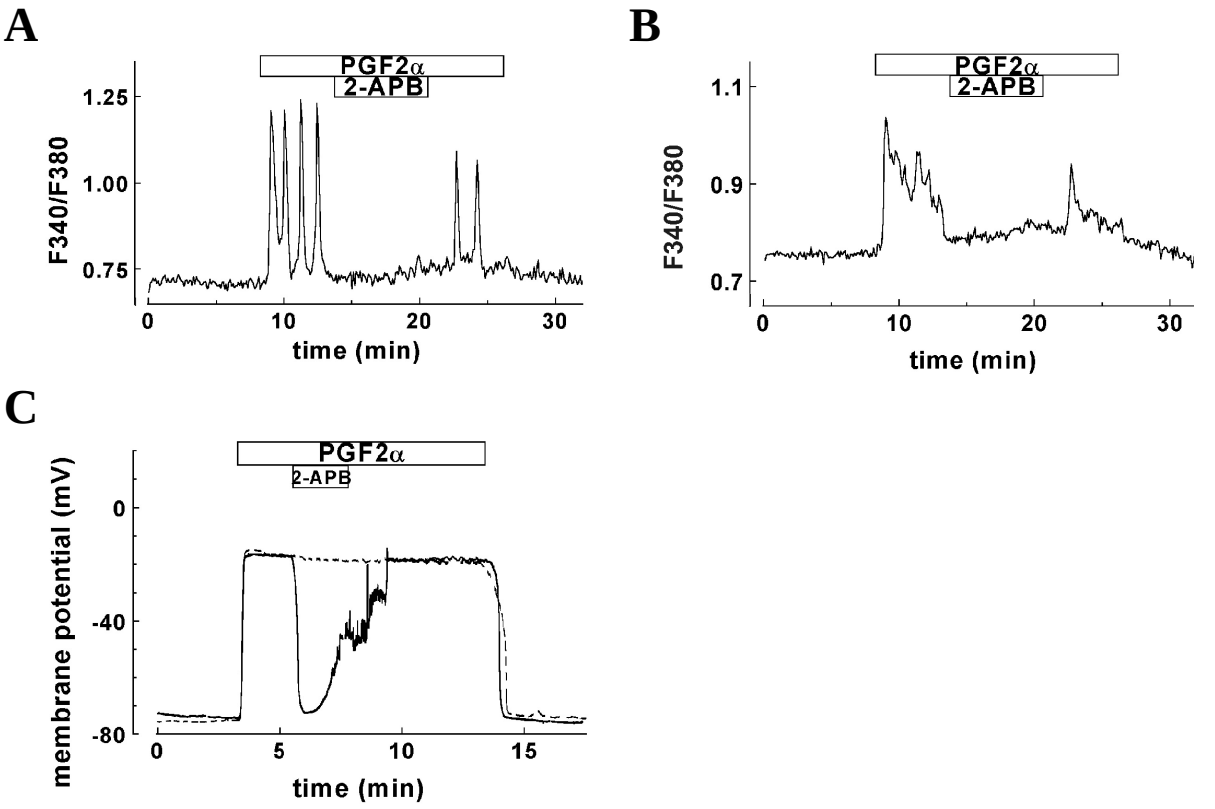

Figure 1 2-APB blocks the PGF2α response in confluent monolayers of NRK fibroblasts. **A)** The effect of PGF2α (100 nM) on the intracellular calcium level of an individual cell from a panel of 39 cells in the monolayer. The PGF2α-induced intracellular calcium oscillation was blocked by 2-APB (75 μM). **B)** The average response of 39 cells from the same monolayer. C) Effect of 2-APB (75 μM) on the PGF2α (50 nM)–induced depolarization of the membrane of an NRK-cell monolayer. The dashed line represents the effect on the membrane potential of PGF2α (50 nM) alone in the same monolayer, determined after the 2-APB experiment.

Based on this observation, we investigated whether 2-APB could also block the calcium-dependent depolarization of NRK cells induced by PGF2α. Quiescent monolayer NRK fibroblasts have a stable resting membrane potential around -70 mV (De Roos et al., 1997a) and PGF2α (50 nM) rapidly depolarized the membrane to around -20 mV (dashed line, Fig. 1C). This depolarization was blocked by 2-APB (75 μM) and the membrane rapidly repolarized towards the resting potential (n=3). However, still in the presence of 2-APB the membrane started to depolarize again but now the depolarization was accompanied by increased fluctuations of the membrane potential. In some experiments this response was even measured before the membrane had completely repolarized (n=4) or before the repolarization had started at all (n=2). The depolarization associated fluctuations have previously also been measured in single NRK cells in isolation (De Roos, 1997) and monolayers of NRK cells that had been electrically uncoupled by fenamates (Harks et al., 2001). Upon washout of 2-APB, but still in the presence of PGF2α, the fluctuations disappeared and the membrane potential recovered to the initial depolarized value. These data can best be explained if 2-APB, in addition to blocking the PGF2α-induced calcium-dependent depolarization of monolayer NRK cells, also electrically uncouples the cells. The depolarization with uncoupling would then result from a (fluctuating) depolarized membrane potential of the patched cell under the existing whole-cell conditions (pipette solution, seal resistance). The results also show that the PGF2α-induced unsynchronized intracellular calcium oscillations of the individual cells cause a steady average depolarization of the monolayer as a whole, obviously by electrical coupling.

2-APB blocks gap junctional electrical coupling in confluent monolayer cultures

To study directly whether 2-APB inhibited gap junctional intercellular communication in monolayers of NRK fibroblasts we applied voltage-clamp steps and measured the effect of 2-APB on the corresponding capacitive current transients, which are known to be a reflection of the state of electrical coupling between the cells in a monolayer. From these transients the monolayer input conductance (G01x) can be calculated (*see* Methods) as an approximation of the gap junctional conductance (G01) (Harks et al., 2001).

2-APB (50 μM) depolarized monolayers of NRK cells from -71.2 ± 0.5 mV to -48.2 ± 3.1 mV (n=12) with concomitant increased fluctuations of the membrane potential. Upon washout of 2-APB the membrane repolarized to resting potentials (Fig. 2A). In order to evoke capacitive current transients, membrane potential recordings were shortly interrupted for voltage-clamp steps (from –70 to -60 mV) at the indicated time points in Fig. 2A. Before addition of 2-APB (*a*, Fig. 2B) the capacitive current transient was characteristic for an electrically coupled monolayer, reflected by a slow and multi-exponential decay and a subsequent prolonged steady-state current (Harks et al., 2001). The steady-state current was already partially reduced within 0.5 min after addition of 2-APB

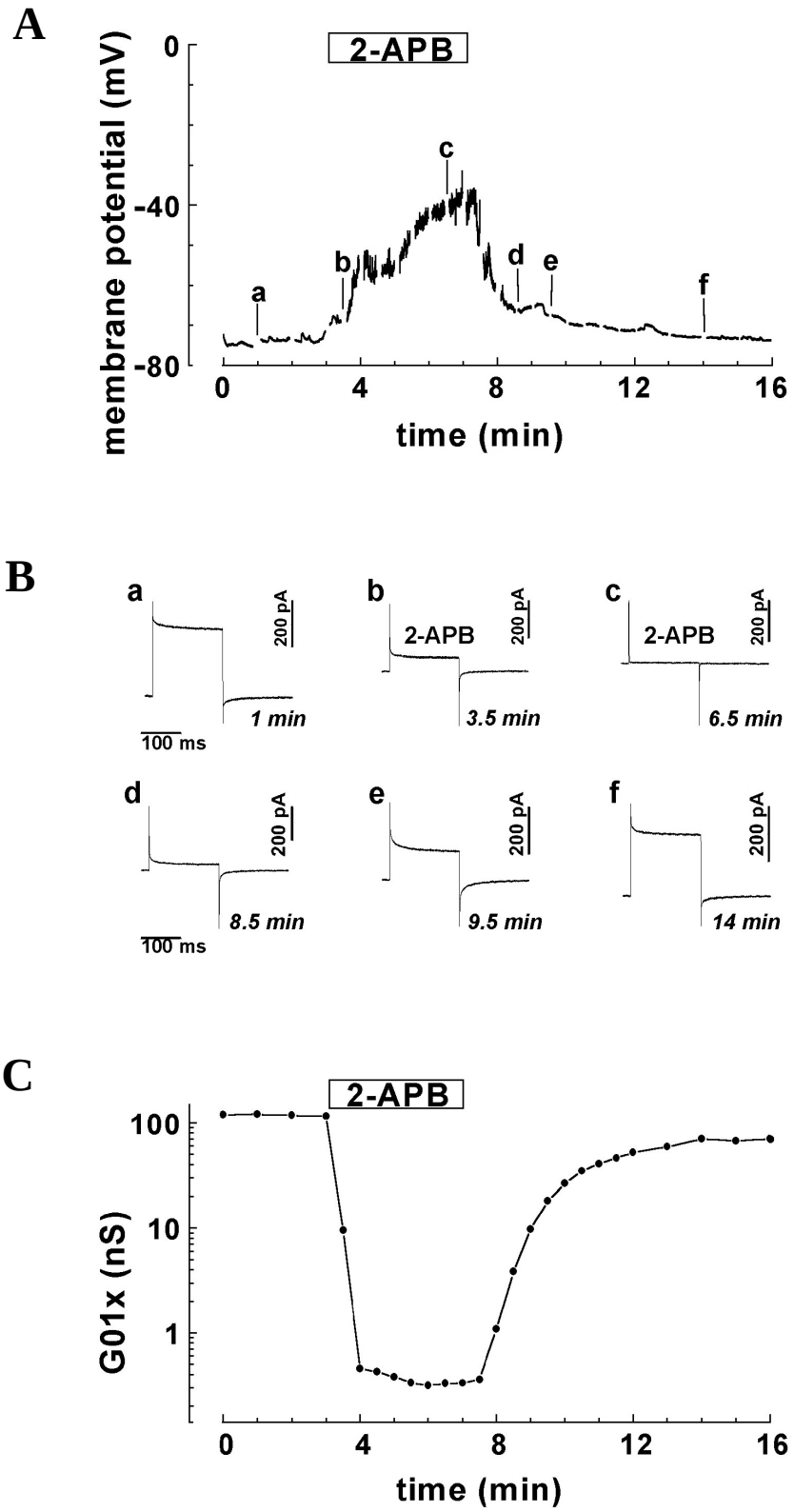

Figure 2 Effect of 2-APB on the membrane potential and electrical coupling of a confluent monolayer of NRK fibroblasts**. A)** Membrane potential was measured and recording was interrupted at the indicated time points (a-f) to switch to the voltage-clamp mode in order to evoke capacitive current transients. **B)** Capacitive current transients evoked by voltage steps of +10 mV (duration 180 ms) from a holding potential of -70 mV at the indicated time points. **C)** Corresponding time course of the estimated gap junctional conductance (G01x) calculated from the capacitive current transients. Perfusion with 2-APB (50 µM) is indicated by the bars.

reflecting partial electrical uncoupling of the cells (*b*, Fig. 2B), a condition under which the membrane potential had not yet changed very much (*b*, Fig. 2A). Finally, the capacitive current transient was changed to one which is typical for a single cell in isolation (*c*, Fig. 2B), with a rapid single-exponential decay (τ<0.5ms, Cm~20pF) and a strongly reduced level of the steady-state current (De Roos et al., 1996; Harks et al., 2001), corresponding to Rm>1GΩ. After washout of 2-APB the capacitive current transient gradually restored to its original form, indicating the recoupling of the cells (*d-f*, Fig. 2B). The time course of uncoupling was determined by calculating G01x (*see* Methods) from each capacitive current transient (Fig. 2C). In general, 2-APB (50 μM) reduced electrical coupling (G01x) in NRK monolayers from above 151.2 ± 12.7 nS in coupled monolayers to below 0.41 ± 0.06 nS (n=12) after complete uncoupling. This was achieved within 2.4 ± 0.2 min and electrical coupling was generally restored within 5 min after washout of 2-APB. These results demonstrate that NRK fibroblasts in monolayer culture are electrically well-coupled and that 2-APB rapidly and reversibly blocks gap junctions, which results in the electrical isolation of individual cells within the monolayer.

To study whether inhibition of gap junctional coupling by 2-APB was not a cell type specific phenomenon, we investigated its effect also on electrical coupling of human embryonic kidney (HEK) cells, which have an epithelial origin (Wilson et al., 2002). Monolayer HEK cells were also electrically well-coupled (G01x=63.2 ± 3.9 nS; Vm=-36.8 ± 1.8 mV; n=24) and upon application of ≥50 μM 2-APB electrical coupling could be completely blocked (G01x<1nS, n=6) while the cells depolarized to -19.3 mV, also with concomitant fluctuations of the membrane potential. Similar to NRK fibroblasts the electrical coupling was restored (to 50-70%) upon washout of 2-APB. This shows that the ability of 2-APB to inhibit electrical coupling is not restricted to NRK cells.

Dose-dependence of electrical uncoupling by 2-APB in NRK and HEK monolayers

The potency of 2-APB to inhibit electrical coupling in NRK and HEK monolayers was determined by measuring its effect on G01x at different concentrations. G01x was calculated at 20 min after addition of 2-APB under conditions that the capacitive current transients had reached a steady-state or before that time if the transient had already changed to a single-cell transient. Under conditions of partial uncoupling at low 2-APB concentrations, electrical coupling could be completely blocked by subsequent addition of 100 μM 2-APB (in NRK cells) or by the addition of 500 μM 1-octanol (in HEK cells). The dose-response curves show that 50 μM 2-APB completely blocked electrical coupling in NRK and HEK cells, with IC_{50} of 5.7 μM and 10.3 μM in NRK and HEK cells, respectively (Fig. 3). These results demonstrate that 2-APB blocks electrical coupling in NRK and HEK cells at similar concentrations.

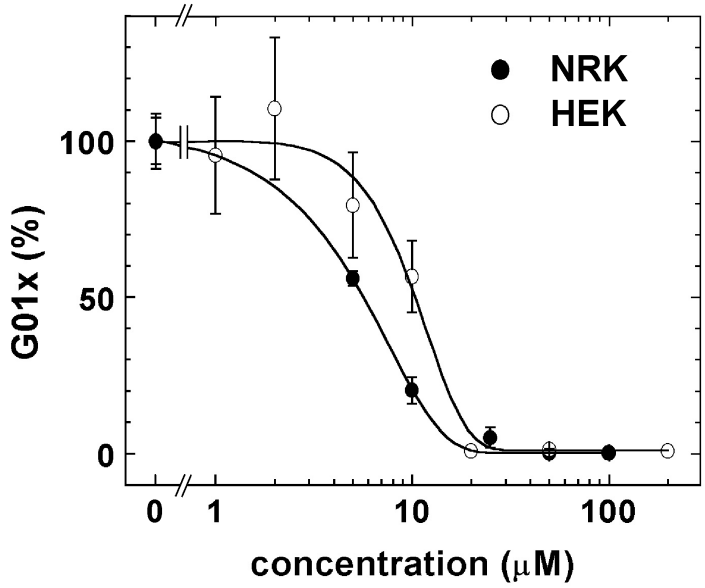

Figure 3 Dose-response curves for inhibition of the electrical coupling by 2-APB in NRK (-•-) and HEK (-o-) monolayers. Gap junctional conductance was estimated (G01x) from capacitive current transients that had reached a steady state (maximally after 20 min) and was normalized (mean ± S.E.M., n=4 and 3 for NRK and HEK respectively) to the maximal conductance values of the whole population. These 100% values were 130.4 nS (n=27) in NRK and 63.3 nS (n=24) in HEK cells. The variability in the HEK cultures was larger than in the NRK cultures.

Voltage-clamping NRK monolayer cells in the presence of 2-APB

Because of the ability of 2-APB to electrically isolate individual cells in the monolayer we investigated whether 2-APB could be used as a pharmacological tool to study membrane conductances of individual cells in intact monolayers. In electrically coupled monolayers it is not possible to determine membrane conductances in a reliable manner due to the large contribution of current flowing to neighboring cells through the gap junctions, as exemplified in Fig. 4A. However, when gap junctional channels in monolayers of NRK cells were blocked by 2-APB, the gap junctions constituted a background conductance of <~0.3 nS (*see* Fig. 2C), thus creating ideal biophysical conditions for single-cell voltage-clamp experiments. Three distinct membrane currents could be detected in the electrically isolated monolayer cell (n=6; Fig. 4B) with similar properties as the three currents recently described and characterized for enzymatically dissociated NRK cells (Harks et al., 2003c). First, an *inward rectifier potassium* current. Activation of this current is clearly visible at hyperpolarizing voltage steps to -120 and -100 mV. The mean peak current (measured after the capacitive current and leak-current corrected) at -120 mV was 87.0 ± 18.1 pA (n=9), which is similar to that in dissociated cells (67.7 ± 15.4 pA; n=9). The inward rectifier current often showed some (variable) decline under maintained hyperpolarization (Fig 4B,D). This inactivation was assessed as the ratio of the inward current at t=500 ms and the peak current and was 0.83±0.04 (n=9), while it was 0.88±0.02 (n=9) for dissociated cells. In addition, the *L-type calcium* current described elsewehere (Harks et al., 2003c)

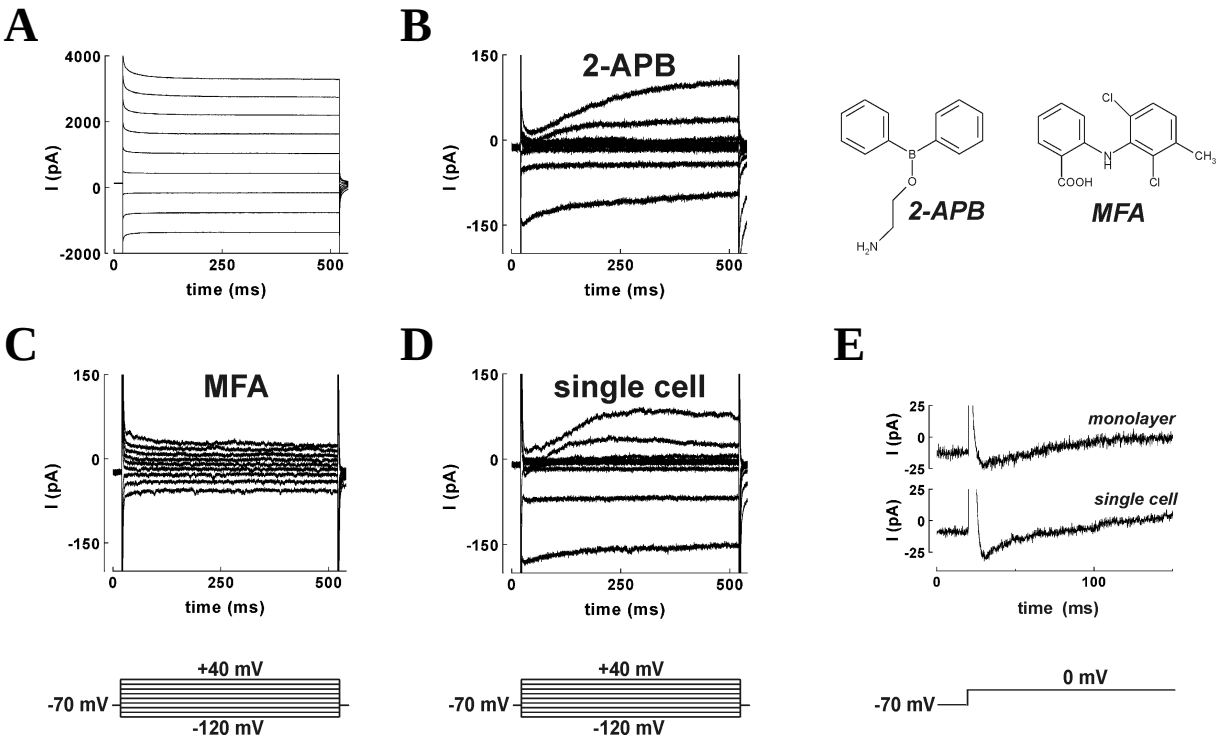

Figure 4 Membrane currents recorded in NRK cells by applying the voltage-clamp step protocols as illustrated. **A)** Membrane currents measured in a monolayer of electrically coupled cells and **B)** under conditions that gap junctions were completely blocked by 50 µM 2-APB and **C)** by 100 µM meclofenamic acid (MFA). **D)** Membrane currents measured in a single NRK cell that had been dissociated from a confluent monolayer by trypsinization. **E)** The inward L-type calcium currents at voltage steps to 0 mV are replotted from panel B (monolayer) and D (single cell) for better resolution. The inset shows the chemical structures of 2-APB and MFA.

was also detected. It was relatively small and variable and had its maximal inward current (34.9 ± 7.3 pA; n=9) at voltage steps to 0 mV, similar to that in dissociated cells (52.0 ± 17.6 pA; n=9). Calcium entry through these calcium channels activated, as described elsewhere (Harks et al., 2003c) for dissociated cells, a *calcium-dependent chloride current*, resulting in an outward current at voltage steps to +20 and +40 mV. These currents showed a large variability in size, probably because of variability in calcium current and intracellular buffering (Harks et al., 2003c), and had a peak amplitude at +40 mV of 169.4 ± 56.4 pA (n=9), while peak currents in dissociated cells were 351.3 ± 109.7 pA (n=9). In all cases, the differences in the above mentioned parameters of three currents (peak currents and inward rectifier inactivation) between 2-APB uncoupled cells and dissociated cells were not statistically significant (P>0.25 for the peak currents; P>0.10 for the inactivation). Thus, 2-APB did not affect the gross properties of the normally expressed ion channels in NRK cells. In contrast, NRK monolayers electrically uncoupled by 100 µM meclofenamic acid (Harks et al., 2001) did not show these distinct membrane currents (n=4; Fig. 4C). Fig. 4D shows for comparison the typical membrane current recordings from a single cell that had been dissociated from a monolayer (n=8). Since the small L-type calcium currents were hardly visible in these whole-cell current recordings,

they are replotted in Fig. 4E for voltage steps to 0 mV in the uncoupled monolayer (Fig. 4B) and dissociated single cell (Fig. 4D). In conclusion, 2-APB allows us to measure cell membrane currents through specific ion channels from individual cells in intact monolayers under conditions that gap junctional channels are completely blocked.

Dose-dependence of inhibition of PGF2α-induced calcium oscillations by 2-APB

In order to compare the effect of 2-APB on electrical coupling with its ability to inhibit agonist-induced calcium rises, we measured the potency of 2-APB to prevent PGF2α-induced intracellular calcium oscillations in NRK fibroblasts by making dose-response curves. First we stimulated monolayers in the presence of different extracellular 2-APB concentrations with supramaximal (1 μM) PGF2α concentrations and recorded the intracellular calcium response in >40 individual cells in the monolayer for 30 min (Fig. 5A). With increasing 2-APB concentrations the average frequency of calcium oscillations diminished (Fig. 5B). Moreover, the number of cells that gave a calcium response to PGF2α stimulation was also reduced at higher 2-APB concentrations (Fig. 5C). The IC_{50} of 2-APB was 5.5 μM when it was based on the average frequency of the oscillations whereas it was 30 μM when it was determined from the number of responding cells. These results show that 2-APB blocks agonist-induced calcium rises only at concentrations that also affect electrical coupling.

2-APB blocks electrical coupling from the extracellular side

Since gap junctional communication can be regulated by several mechanisms (Hossain and Boynton, 2000; Lampe and Lau, 2000), we investigated whether 2-APB blocked gap junctional coupling by acting from the intracellular or extracellular side. Therefore we included 2-APB at concentrations up to 500 μM in the solution of the patch-pipette and evoked capacitive current transients in both cell clusters (2-12 cells) and confluent monolayers. Fig. 6A shows the typical capacitive current transient evoked in a cluster of 8 cells patched for 10 min with a pipette containing 500 μM 2-APB. This single exponential transient is characteristic for electrically well-coupled clusters (De Roos et al., 1996). Upon subsequent addition of external 2-APB (50 μM) the relatively slow capacitive current transient is rapidly changed via a double-exponential transient (Fig. 6B) to a fast transient characteristic for a single cell in isolation (Fig. 6C). After washout of external 2-APB, but still in the presence of intracellular 2-APB, electrical coupling was almost completely restored (Fig. 6D). In general, incubation with 2-APB concentrations up to 500 μM within the patch-pipette did not affect electrical coupling in cell clusters (7.4 ± 1.0 cells, n=14) and monolayers of NRK cells (n=4). In addition, similar administration of relatively high intracellular 2-APB concentrations (100 μM) to monolayers of HEK cells did not affect electrical coupling (n=6). Therefore we conclude that 2-APB blocks gap junctions from the extracellular side.

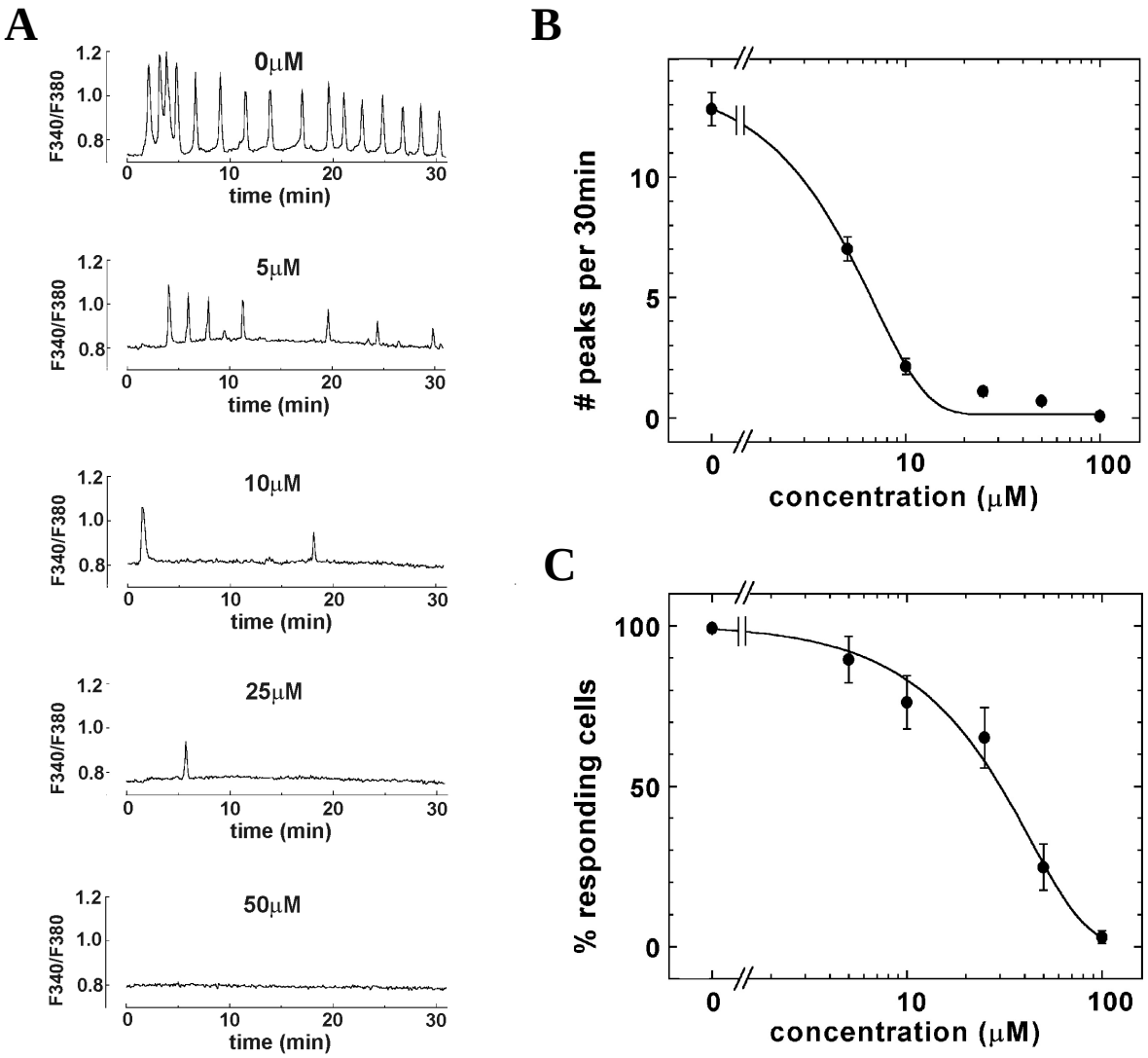

Figure 5 Inhibition of PGF2α-induced calcium transients by 2-APB. **A)** Typical calcium responses in an individual monolayer cell induced by PGF2α (1 μM) in the presence of different 2-APB concentrations. PGF2α was added at t=1 min after preincubation with 2-APB for 5 min. Traces shown are representative out of a panel of more than 40 cells in the monolayer. **B)** Corresponding dose-response curve showing the average number of calcium transients in individual cells during 30 min stimulation with PGF2α (1 μM). **C)** Dose-response curve showing the percentage of individual cells in the monolayer that responded to PGF2α (1 μM) stimulation with at least one calcium transient. Percentages were determined in a panel of 36-52 cells in the monolayer (n=3).

Discussion

In the present study, we describe a new property of 2-APB. In addition to inhibiting agonist-induced intracellular calcium increases, 2-APB fully blocked cell-to-cell coupling in confluent monolayers of NRK fibroblasts and HEK epithelial cells. Because 2-APB did not significantly affect the amplitudes of three membrane currents normally present in dissociated NRK cells (inward rectifier potassium, L-type calcium and calcium-dependent chloride currents), it allowed single-cell voltage-clamp

recording of these currents in the mechanically intact tissue. Because electrical uncoupling was reversible and without detectable effect on cell morphology 2-APB is a promising tool to measure single-cell membrane conductances in electrically highly coupled tissues such as epithelia and cardiomyocytes. The effects of 2-APB on monolayers of NRK fibroblasts are summarized in the conceptual model of Fig 7.

So far, 2-APB has been used to study the role of the IP_3 receptor, SOCs and TRP channels in cellular signaling in several systems (Ma et al., 2000; Maruyama et al., 1997; Wu et al., 2002) and appeared to be a reliable blocker of store-operated calcium entry but an inconsistent inhibitor of IP_3-induced calcium release (Bootman et al., 2002). Here we show that 2-APB can indeed block PGF2α-induced transient increases in intracellular calcium levels in NRK fibroblasts. With increasing 2-APB concentrations, the number of cells in the monolayer that gave a calcium response upon PGF2α stimulation decreased, whereas the response itself also changed to fewer calcium transients at higher 2-APB concentrations. In our study, the IC_{50} for inhibition of PGF2α-induced intracellular calcium oscillations by 2-APB was lower (5.5 μM) based on the average frequency of the oscillations than based on the number of responding cells (30 μM). Hypothetically, the initial calcium transient following PGF2α stimulation resulted from calcium release from IP_3 dependent calcium stores and

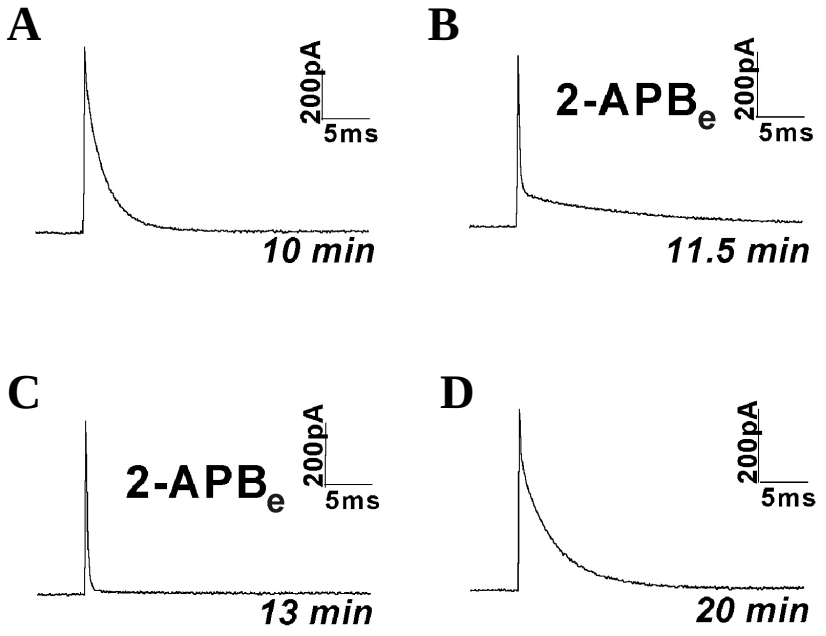

Figure 6 2-APB affects electrical coupling in a cluster of NRK cells only from the extracellular side. All capacitive current transients were evoked in the same cluster of 8 cells (patched cell surrounded by 7 cells) under conditions that 2-APB (500 μM) was included in the internal pipette solution (2-APB_i). **A)** Current transient evoked after 10 min incubation with 2-APB_i. Then, 2-APB (50 μM) was added to external medium (2-APB_e) and the capacitive current transient is shown after **B)** 1.5 min and **C)** 3 min perfusion with 2-APB_e. **(D)** Capacitive current transient after washout of 2-APB_e, but still in the presence of 2-APB_i.

was blocked at higher 2-APB concentrations (IC_{50}=42 μM; (Maruyama et al., 1997), whereas store-operated calcium entry is essential for the subsequent calcium transients and was blocked at lower concentrations (IC_{50}=10 μM; (Gregory et al., 2001). The dependence of the following calcium transients on calcium influx was confirmed by the observation that PGF2α induced only a single calcium transient in external calcium-free (3 mM EGTA) solution that probably resulted from calcium release from IP_3 sensitive calcium stores (data not shown). In addition, PGF2α has previously been reported to induce intracellular calcium oscillations in myometrial cells. In those cells calcium mobilization from IP_3 sensitive stores was also followed by repetitive calcium transients mediated by the store-operated calcium entry pathway (Fu et al., 2000).

Interestingly, 2-APB completely and reversibly blocked gap junctional communication at concentrations that were required to inhibit PGF2α-induced calcium rises. Moreover, the concentrations used in our studies were similar to those used by others to inhibit the IP_3 receptor, SOCs and TRP channels (Dobrydneva and Blackmore, 2001; Maruyama et al., 1997; Van Rossum et al., 2000). Therefore, the involvement of the IP_3 receptor, SOCs and TRPs in intercellular calcium signaling in electrically coupled systems cannot be studied using 2-APB without concomitant effects on intercellular communication (cf. Fig. 7). For example, Fig. 1C shows that 2-APB blocks the PGF2α-induced calcium-dependent depolarization, but after the repolarization the membrane starts to depolarize again. This would suggest that intracellular calcium levels are rising again, but we now know that this latter depolarization results from electrical uncoupling by 2-APB. Moreover, the uncoupling activity of 2-APB may explain unexpected effects of this compound on contraction of smooth muscle cells (Imai et al., 2002), which are functionally coupled by gap junctions comprising connexin43 (Neuhaus et al., 2002a; Neuhaus et al., 2002b).

Gap junctional intercellular communication is of paramount importance in regulating a variety of biological processes such as embryogenesis, cell proliferation, cardiac function, and propagation of calcium waves (Bruzzone et al., 1996; Kumar and Gilula, 1996). Gap junctions not only allow the transfer of small signaling molecules and metabolites between neighboring cells (Goldberg et al., 1999), but also establish electrical coupling between cells. Electrical coupling underlies synchronous electrical activity between excitable cells and is essential in the propagation of the cardiac action potential (Gros and Jongsma, 1996). The permeability of gap junction channels can be regulated by a variety of processes that result in the modification of these channels. Several growth factors have been described to initiate complex signaling pathways that eventually result in activation of kinases and phosphatases that modify the cytoplasmic C-terminal region of Cx43 (Giepmans et al., 2001; Hossain and Boynton, 2000). This Cx43-CT domain itself is not directly involved in the formation of junctional channels but appears to play a regulatory role in the permeability of the channels by the so called "ball-and chain" model (Zhou et al., 1999). In addition, several chemicals can block gap

junctions mostly by altering the lipid environment and cell membrane fluidity (Niggli et al., 1989; Takens-Kwak et al., 1992), but this pharmacological inhibition is not very specific and is accompanied by non-specific effects on ionic plasma membrane channels. For example, fenamates have been shown to block gap junctions (Harks et al., 2001) but have also been reported to modulate a diversity of ion channels (Li et al., 1998a), as we confirm here (*see* Fig. 4C).

In contrast, 2-APB seems to be a more specific gap junction blocker since it did not block membrane conductances in NRK cells. Also in other studies it has been reported not to block voltage-operated calcium and potassium conductances, nor calcium-dependent chloride conductances (Maruyama et al., 1997; Wu et al., 2000). Therefore, inhibition of gap junctional communication by 2-APB is probably not caused by a non-specific effect on plasma membrane properties. Moreover, 2-APB did not inhibit gap junctional communication from the intracellular side when it was applied via the pipette solution. Prolonged administration of high intracellular 2-APB concentrations via the patch pipette, even 10-fold higher than required to achieve full block when applied from the

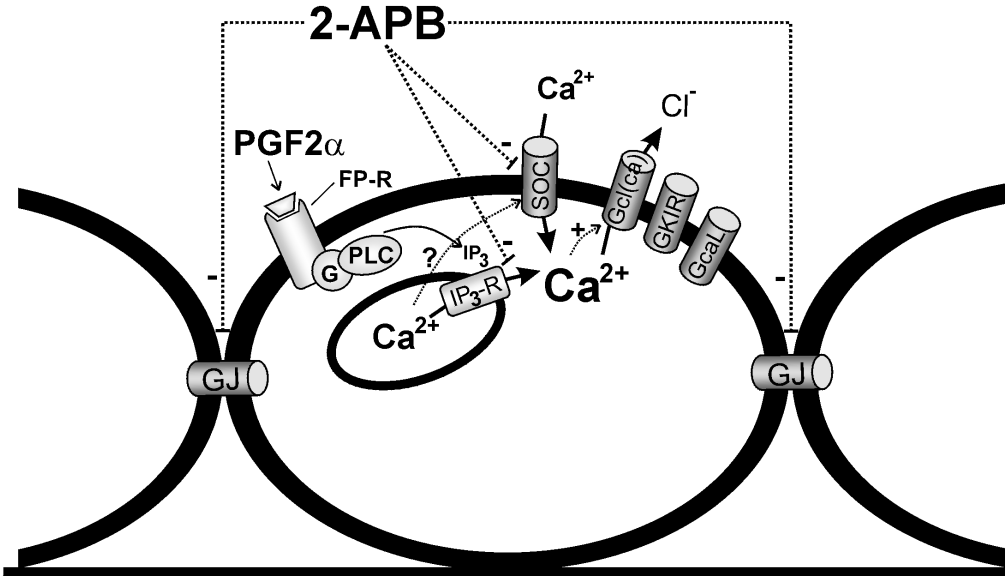

Figure 7 Schematic representation of the PGF2α response in NRK monolayers and the effect of 2-APB on this response. PGF2α binds to the FP-receptor resulting in an activation of phospholipase C (PLC), which liberates IP_3 from membrane phospho-inositides. IP_3 then binds to its receptor (IP_3-R) on the endoplasmic reticulum, thereby inducing a release of stored calcium. The decrease of the calcium content in the stores on its turn activates calcium entry through store-operated calcium channels (SOC) by a still unknown mechanism. The increase of the intracellular calcium concentration causes the opening of calcium-dependent chloride channels (Gcl(ca)), which results in membrane depolarization from a resting membrane potential, determined by inward rectifier K^+ channels (GKIR, cf. Fig. 4B,C). 2-APB inhibits both the IP_3 and SOC-mediated increase in the intracellular calcium concentration thereby repolarizing the membrane, while the action of 2-APB on SOCs is probably from the outside (Kukkonen et al., 2001). However, 2-APB also blocks gap junctional channels (GJ), resulting in uncoupling and fluctuating membrane depolarization. The L-type calcium channels in the diagram (GcaL, cf. Fig. 4E) determine fibroblast excitability, which is not considered here.

extracellular side, did not affect electrical coupling at all, while lower concentrations applied extracellularly apparently are able to reach the intracellularly located IP_3 receptor (*see* Fig. 5). Taken together, we suggest that 2-APB blocks gap junctions by a direct extracellular action on connexins. These connexins, mainly connexin43 in NRK fibroblasts (Li et al., 1996), constitute gap junctional hemi-channels (connexons) and gap junctions are formed by the extracellular docking of these connexons in apposing cells. This would imply that 2-APB has to penetrate the narrow extracellular gaps of the gap junctions before exerting effects. It also would explain that this extracellular action of 2-APB is not necessarily faster than the intracellular action on the IP_3 receptor, because 2-APB easily crosses the plasma membrane due to its lipophylic properties. 2-APB may block gap junctional communication by interfering with this docking interaction. In this respect it is interesting to mention that 2-APB has also been suggested to inhibit the conformational coupling between the IP_3 receptor and SOCs, thereby preventing store-operated calcium influx (Ma et al., 2000). Possibly, similar protein-protein interactions are involved in the conformational coupling of the IP_3 receptor with SOCs as in the docking of two gap junctional hemi-channels.

In several cellular systems such as epithelial cells and cardiomyocytes, cell-to-cell contacts are a prerequisite for their specific function and therefore studying these cells under conditions that they have grown in culture to confluence offers considerable experimental advantages compared to single cells that have been dissociated from these monolayer. However, studying excitability of electrically coupled systems is restricted to membrane potential recordings, since measurements of membrane conductances in voltage-clamp experiments cannot be performed on electrically coupled monolayers due to the considerable amount of current that is flowing through the gap junctions to neighboring cells. Electrical uncoupling of monolayer cells with gap junction blockers would circumvent this problem. However, other chemicals that are used to block electrical coupling such as halothane, n-alcohols and 18-β-glycyrrethinic acid, have been described to affect several membrane conductances (Bohmer et al., 2001; Buljubasic et al., 1992; Niggli et al., 1989). In the present study we show that after complete electrical uncoupling of NRK monolayers by meclofenamic acid membrane conductances were also blocked. In contrast to these gap junction blockers, 2-APB appears to be a useful tool for studying membrane conductances not only in NRK monolayers but also in other coupled cellular systems. In HEK cells and other expression systems, 2-APB would be useful to study heterologously expressed ion-channels with a low expression efficiency in cells in the intact monolayer, if the expressing cells can be recognized by a fluorescent label. In the present study we show that membrane conductances could be measured after complete electrical uncoupling of NRK monolayers by 2-APB. These conductances have been identified as an L-type calcium conductance, an inwardly rectifying potassium conductance and a calcium-dependent chloride conductance (Harks et al., 2003c) in single NRK cells that had been dissociated from the intact monolayer. Although more detailed studies are required to specify the 2-APB effects for the various types of connexins and to exclude effects of 2-APB on the properties of a larger variety of membrane conductances in various

tissues, the results in this study already clearly show that uncoupling of monolayer cells by 2-APB can create ideal biophysical conditions for single-cell voltage-clamp experiments on undissociated cells of a tissue. The reversibility of the electrical uncoupling by 2-APB is an important advantage when compared to enzymatic or mechanic dispersion, which create damage and irreversible uncoupling. In this respect, 2-APB may be a useful drug to monitor physiological changes in ion channel activity of cells in electrically coupled tissues in cultures, e.g. during their growth and oncogenic transformation. 2-APB may be used as well to study ion channel properties in single epithelial cells in their intact tissues, thus with maintained polarized cell morphology. Another important application of the present results may be the separation of intra- from intercellular signaling processes by chemically uncoupling cells with 2-APB. The 2-APB effect on gap junctions may even serve as a lead in developing more selective gap junctional blockers from 2-APB, both for basic research and for medical application.

Acknowledgements.

We thank G.Th.H Van Kempen for assistance in preparing HEK293/tsA201 cultures, Dr. W.P.M. Van Meerwijk for statistical advice and Dr. E. Pierson (General Instrumentation) for expert technical assistance with the digital imaging experiments. DLY is supported by the Foundation Nijmegen University Fund (SNUF).

Materials and Methods

Cell culturing: Normal rat kidney fibroblasts (NRK clone 49F) were cultured in bicarbonate buffered Dulbecco's modified Eagle's medium (DMEM; Life Technologies, Paisly, UK) supplemented with 10% newborn calf serum (HyClone Laboratories, Logan, UT, US). Confluent cultures were made quiescent by a subsequent one to three days incubation in serum-free DF medium (DMEM/Ham's F12, 1:1; Gibco; Life Technologies, Paisly, UK) supplemented with 30 nM Na_2SeO_3 and 10 µg/ml human transferrin. Single cells and small clusters (2-15 cells) were dissociated from quiescent monolayer cells by trypsinization and subsequently seeded in serum-free DF medium. Patch-clamp experiments on these cells were performed 2-4 hours after trypsinization.

Human embryonic kidney cells (HEK293 clone tsA201) were cultured in DMEM supplemented with 10% FCS (Gibco BRL, Paisley, UK). After 3-5 days monolayer cells forming large islands of >1000 cells were obtained and used for experiments.

Electrophysiology: Whole-cell current-clamp and voltage-clamp experiments on NRK cells were performed at room temperature as previously described (De Roos et al., 1996). Briefly, voltage pulses of +10 mV (duration 180 ms) from a holding potential of -70 mV were applied in order to evoke capacitive current transients for electrical coupling measurements. Voltage-activated membrane currents were measured by applying voltage-clamp steps from a holding potential (Vh) of -70 mV to test potentials of -120 mV up to +40 mV with increments of +20 mV and step intervals of 2 s. For patch-clamp experiments NRK cells were perfused with serum-free DF medium containing (in mM) 120 NaCl, 4.2 KCl, 1.1 $CaCl_2$, 0.3 $MgCl_2$, 0.4 $MgSO_4$, 44 $NaHCO_3$ and 1.0 NaH_2PO_4 and equilibrated with 7.5% CO_2 to pH 7.4. Intracellular pipette solution contained (in mM) 25 NaCl, 120 KCl, 1 $CaCl_2$, 1 $MgCl_2$, 3.5 EGTA, 10 HEPES/KOH (pH 7.4), while $CaCl_2$ was omitted and 100 µM EGTA was used when specific membrane currents were studied. Data were obtained with an EPC-7 patch-clamp amplifier (List Electronic, Darmstadt, Germany) in conjunction with Pulse/Pulsefit software (HEKA Elektronik, Lambrecht, Germany).

For patch-clamp experiments on HEK cells an EPC-7 patch-clamp amplifier was used in conjunction with pClamp7/Clampex software (Axon Instruments, Foster City, CA, US). HEK cells were studied at room temperature with extracellular medium, containing (in mM) 140 NaCl, 5 KCl, 1 $CaCl_2$, 1 $MgCl_2$ (pH 7.2), while the intracellular pipette solution contained 14 NaCl, 110 KCl, 1 $MgCl_2$, 10 EGTA, 10 HEPES/KOH (pH 7.2). Borosilicate patch pipettes (GC150-15; Clark, Reading, UK) with resistances of 4-6 MΩ (NRK cells) or 2-3 MΩ (HEK cells) were used. Series resistance (<15 MΩ) errors in the clamped voltage in the NRK whole-cell experiments on 2-APB and MFA uncoupled cells were <1.5 mV (*see* Fig. 4)

Intracellular calcium measurements: Coverslips with monolayers of NRK fibroblasts were placed in a Leiden cell chamber and loaded for 30 min at room temperature with 1.5 µM fura-2/AM (Molecular Probes, Eugene, OR, US) in PBS medium (in mM: 137 NaCl, 3 KCl, 1 $CaCl_2$, 0.5 $MgCl_2$, 6.5 Na_2HPO_4, 0.88 KH_2PO_4, pH 7.4) containing 0.025% Pluronic F127 and 3% FCS. After loading, the cells were washed for 30 min with PBS at room temperature. Dynamic video imaging was performed as elsewhere described (Cornelisse et al., 2002). Excitation wavelengths were 340 nm and 380 nm (band width 8-15 nm) and fura-2 fluorescence emission was monitored above 440 nm, using a 440 nm DCLP dichroic mirror in front of the camera. Image acquisition, using a camera pixel binning of 4, and computation of ratio images (F340/F380) was every 6 s and was operated through Metafluor v.4.6 (Universal Imaging Corporation, Downingtown, PA, US). Camera acquisition time was 100 ms per excitation wavelength.

Data analysis: Gap junctional conductance G01 (=1/R01) between the patched cell (#0), with normally Rm0>>R01, and the surrounding cell ring (#1) was approximated by the measurement of the input conductance G01x (=1/R01x) of the monolayer through the patched cell, as explained in (Harks et al., 2001). G01x is an underestimation of G01, because R01x=R01+Rx, with Rx the exit resistance from cell ring 1 through the monolayer to ground. The monolayer input resistance R01x is simply determined by subtracting the routinely measured series resistance Rser (between pipette and cell) from the total input resistance Rss in the steady state (between pipette and ground). The latter is the voltage step divided by the steady-state current. We consider changes of G01x (1/R01x) upon 2-APB application to reflect G01 changes rather than Gm changes, because of the gradual dissociation of the voltage step response into an initial single-cell capacitive current transient and a subsequent decreasing slow current transient (cf. 19). Dose-response curves were obtained by fitting a Gaussian curve through the data points using Origin 6.0 (Microcal, Northampton, MA, US) and frequency plots of the calcium dynamics studies were obtained using the "pick peak" algorithm of Origin. The amplitudes of specific membrane currents measured in 2-APB uncoupled monolayers and enzymatically dissociated cells were compared using a multivariate t test (T^2), while inactivation of the inward rectifier potassium current was compared with a Mann-Whitney U test. Numerical data are represented as mean ± S.E.M. throughout this article, with n for the number of cells tested.

Chemicals: 2-APB was from Tocris (Ballwin, MO, US) and all other chemicals were from Sigma (St. Louis, MO, US).

CHAPTER 6

Prostaglandin F2α induces unsynchronized intracellular calcium oscillations in monolayers of gap junctionally coupled NRK fibroblasts

E.G.A. Harks, W.J.J.M Scheenen, P.H.J. Peters, E.J.J. van Zoelen and A.P.R. Theuvenet

Abstract. We have investigated the intracellular calcium oscillations that are induced by prostaglandin F2α (PGF2α) in individual cells of confluent monolayers of normal rat kidney (NRK) fibroblasts, which are known to be coupled by gap junctions. PGF2α (1000 nM) induced oscillations in more than 90% of the cells in the monolayer, but the frequency of these oscillations was highly variable between individual cells and ranged from 0.2-1.4 min^{-1}. We show that the initial calcium peak results from calcium release from IP_3-sensitive stores, while subsequent calcium transients are mediated by an interplay between both IP_3-sensitive calcium stores and calcium influx. The oscillation frequency was increased by sensitizing the IP_3 receptor with thimerosal (10 μM) and was dependent on the extacellular calcium concentration. Thapsigargin (5 nM), which inhibits reuptake of calcium into the stores, only seemed to reduce the amplitude of the oscillation. Patch-clamp experiments revealed that PGF2α did not inhibit electrical coupling of the NRK cells in the monolayer. So, gap junctional permeability of NRK cells appears to be sufficient to allow electric coupling resulting in a uniform membrane potential throughout the entire monolayer, but insufficient to synchronize the intracellular calcium oscillations upon PGF2α stimulation.

Introduction

NRK fibroblasts have been widely used as an *in vitro* model system for studying the mechanisms of density-dependent growth regulation and oncogenic transformation of cells (Lahaye et al., 1998; Lahaye et al., 1999b; Van Zoelen, 1991). Previous studies have shown that the arachidonic acid metabolite prostaglandin F2α (PGF2α), which activates the FP subtype of prostanoid receptors (Narumiya et al., 1999), induces phospho-inositide turnover in NRK fibroblasts thereby increasing the intracellular calcium concentration in these cells (Lahaye et al., 1999b). This was accompanied by a depolarization of the membrane of confluent monolayers of NRK cells, which resulted from the opening of calcium-activated chloride channels (De Roos et al., 1997a) and thus reflects the increase in the intracellular calcium concentration upon stimulation with PGF2α.

So far, synchronized calcium signaling has been described in several cellular systems, whereby gap junctional communication regulates the coordinated activity of a large number of cells. For example, synchronized calcium oscillations or intercellular calcium waves have been reported after stimulation of epithelial cells (Sanderson, 1995), hepatocytes (Rink and Hallam, 1989), and astrocytes (Hofer et al., 2002). In all these systems, synchronization seems to be dependent primarily on the diffusion of IP_3 through gap junctions (Clair et al., 2001; Hofer et al., 2002), although diffusion of calcium may also contribute to synchronization (Giaume and Venance, 1998; Hofer, 1999). Moreover, synchronized calcium oscillations in pancreatic β-cells measured in the presence of glucose have been shown to result from a coordinated electrical bursting activity, which is mediated by gap junctions (Santos et al., 1991). Previously, we showed that confluent monolayers of NRK fibroblasts are also coupled by gap junctions thereby providing extensive electrical coupling of these cells (Harks et al., 2001). Therefore it was surprising that in a recent study unsynchronized intracellular calcium oscillations were measured upon stimulation of these monolayers with PGF2α (Harks et al., 2003a). However, agonists of G-protein coupled receptors have been shown to inhibit gap junctional coupling (Postma et al., 1998) and it was not obvious that NRK cells were still coupled after stimulation with PGF2α.

Agonist-induced cytosolic calcium oscillations have been observed in many different cell types (Berridge, 1993; Petersen et al., 1991; Thomas et al., 1996) and are generally based on the mobilization of calcium from the endoplasmic or sarcoplasmic reticulum. This liberation of stored calcium is mediated by calcium release channels known as the IP_3 and ryanodine receptor (Berridge, 1993; Clapham, 1995). The IP_3 receptor seems to play a pivotal role in many of the oscillations induced by IP_3-generating agonists, because cytosolic calcium both facilitates and inhibits the opening of this calcium release channel (Mak et al., 1998). First, binding of IP_3 and calcium to a primary activation site triggers calcium release (Marchant and Taylor, 1997), whereas a slower inhibitory process, which involves the binding of calcium to another site, terminates calcium liberation and leads to a refractory state from which the IP_3 receptor must recover before subsequent calcium release can

be triggered (Parker and Ivorra, 1990). This feedback mechanism of cytosolic calcium on the IP_3 receptor provides the basis for successive cycles of calcium-induced calcium release. Next to this model, several other mechanisms have been proposed to play a role in IP_3-dependent calcium oscillations, including calcium-dependent activation of phospholipase C (Meyer and Stryer, 1991), calcium-independent inactivation of the IP_3 receptor (Ilyin and Parker, 1994) and production of 1,3,4,5-tetrakisphosphate (Zhu et al., 2000a). Moreover, also IP_3-independent intracellular calcium oscillations have been reported (Cseresnyes et al., 1999; Szalai et al., 2000; Usachev and Thayer, 1999), which seem to result from the periodic release of stored calcium mediated by ryanodine receptors, which have been shown to share structural and functional properties with the IP_3 receptor (Pozzan et al., 1994), including the bell-shaped activation curve as a function the cytosolic calcium concentration (Fill and Copello, 2002). The role of calcium influx in intracellular calcium oscillations remains controversial. Although the presumed principal function for calcium influx during oscillations is to recharge intracellular stores and to replenish the intracellular calcium lost during oscillations (Berridge, 1993; Rink and Hallam, 1989), calcium entry has also been proposed to be the trigger required for repetitive calcium release (Martin and Shuttleworth, 1994; Shuttleworth and Thompson, 1996).

In NRK fibroblasts, PGF2α has been shown to activate phosphoinositide turnover (Lahaye et al., 1999b), indicating that the IP_3 receptor is involved in the intracellular calcium oscillations induced by this agonist (Harks et al., 2003a). We now demonstrate that these oscillations are mediated by the periodic release of calcium from IP_3-sensitive calcium stores and require influx of extracellular calcium to persist. Moreover, the lack of synchronization of the oscillations is not caused by an inhibition of gap junctional coupling since PGF2α did not affect electrical coupling. These results are discussed in terms of efficiency of electrical and metabolic coupling in NRK cells.

Results

Effect of PGF2α on the intracellular calcium concentration of individual cells in the monolayer

In order to measure the effect of PGF2α on the intracellular calcium concentration of individual NRK cells in confluent monolayers we performed dynamic video imaging of these cells loaded with the fluorescent probe fura-2.

The calcium response induced by PGF2α (1000 nM) differed between individual cells within the same monolayer and we could discriminate three typical responses after analyzing 367 cells in 8 independent monolayers. In 5.4% of the cells only one or two calcium transients were measured during administration of PGF2α (Fig. 1A). In most NRK cells (91.8%) the initial large calcium transient was followed by repetitive oscillations that appeared as large sharp transients (Fig. 1B-1D).

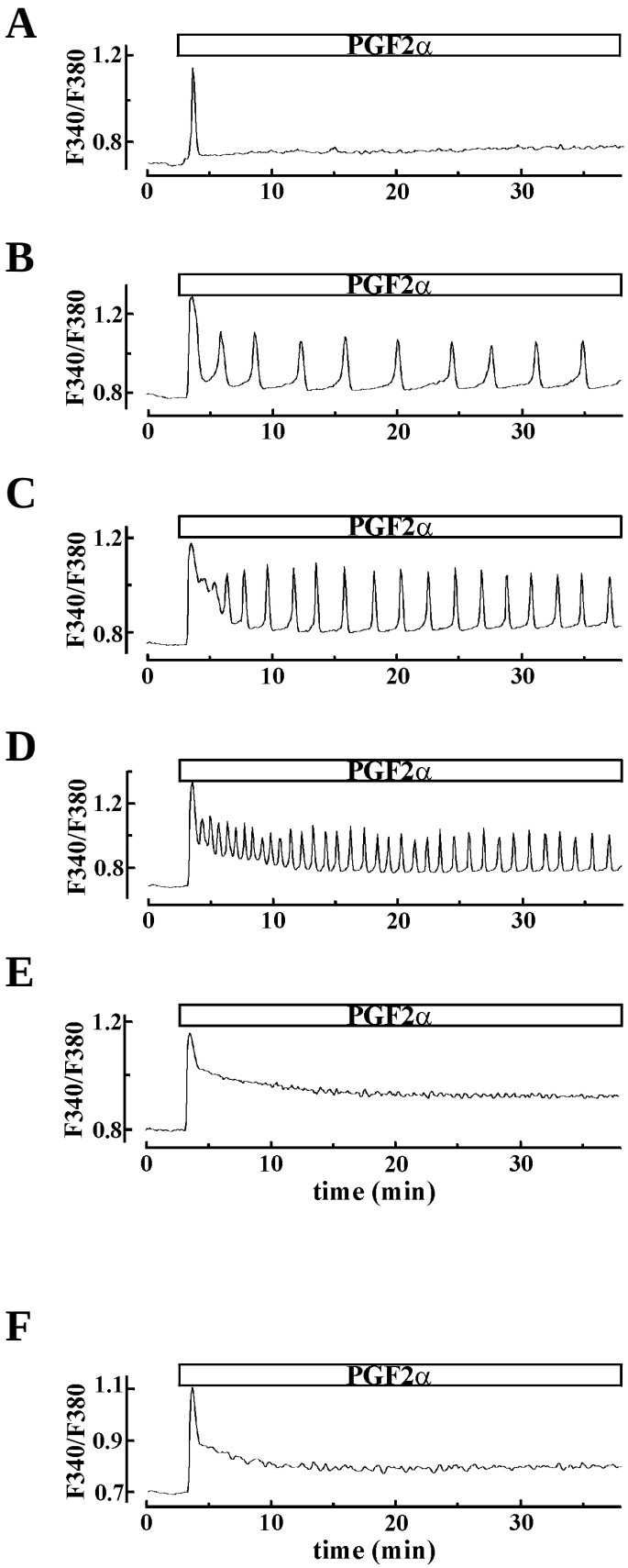

Figure 1 Effect of PGF2α on the intracellular calcium concentration of NRK fibroblasts. **A-E)** Typical calcium responses induced by PGF2α (1000 nM) in individual cells selected from a panel of 43 cells within one monolayer. **F)** Averaged response of these 43 cells. Addition of PGF2α is indicated by the bars.

Table 1: Overview of the calcium responses induced in individual cells of NRK monolayers by different PGF2α concentrations. Responses are divided into three categories and characterized by either 1-2 transients, repetitive oscillations or a peak and plateau phase. The average frequency of the oscillations was calculated after stimulation with PGF2α for 30 min.

[PGF2α] (nM)	#cells	1-2 transients (%)	oscillations (%)	oscillations (min^{-1}) *	peak+plateau (%)
1	45	6.7	-	-	-
10	40	15	65	0.38 ± 0.04	-
100	54	3.7	96.3	0.49 ± 0.03	-
1000	43	7	90.7	0.60 ± 0.05	2.3

* frequency of oscillations (mean ± S.E.M)

Each transient was preceded by slower elevations of the cytoplasmic calcium concentration and the frequency of the oscillations ranged from 0.2-1.4 min^{-1} (*see* examples). Although the calcium oscillations were not synchronized over the entire monolayer, small clusters of about 3-4 neighboring cells exhibited sometimes calcium oscillations with similar frequency, indicating that the oscillations in individual cells were not always completely autonomous. In 2.7% of the cells the initial rapid rise of cytosolic calcium was followed by an elevated plateau phase (Fig. 1E). When averaging the calcium response of individual cells an initial peak and a sustained plateau phase was observed (Fig. 1F).

Taken together, in spite of the fact that NRK cells are coupled by gap junctions the PGF2α-induced intracellular calcium oscillations are not synchronized. However, this does not necessarily rule out that there is no influence of neigboring cells at all on the oscillations.

Effect of the agonist concentration on the intracellular calcium response

In many cell types the level of external stimulation regulates the frequency of cytosolic calcium oscillations (Jacob et al., 1988; Visegrady et al., 2001; Wakui et al., 1989). So we next investigated whether this way of frequency regulation could also be observed in NRK fibroblasts when stimulated with different PGF2α concentrations.

The data (summarized in Table 1) show that at low PGF2α concentrations (1 or 10 nM) a calcium response is induced in only a fraction of the cells measured, whereas at higher concentrations (≥100 nM) a calcium response was measured in every cell. Moreover, the calcium response itself was also dependent on the agonist concentration. At 1 nM, PGF2α could only induce 1-2 calcium transients. At higher concentrations PGF2α predominantly triggered repetitive oscillations, while the average frequency of these oscillations increased with higher agonist concentrations. The typical effect of a step-wise increase of the PGF2α concentration on the calcium response is further shown in Fig. 2. At low concentration (1 nM) PGF2α could not induce calcium changes in this cell but the intracellular calcium concentration started to oscillate after elevating the PGF2α concentration to 10 nM. The

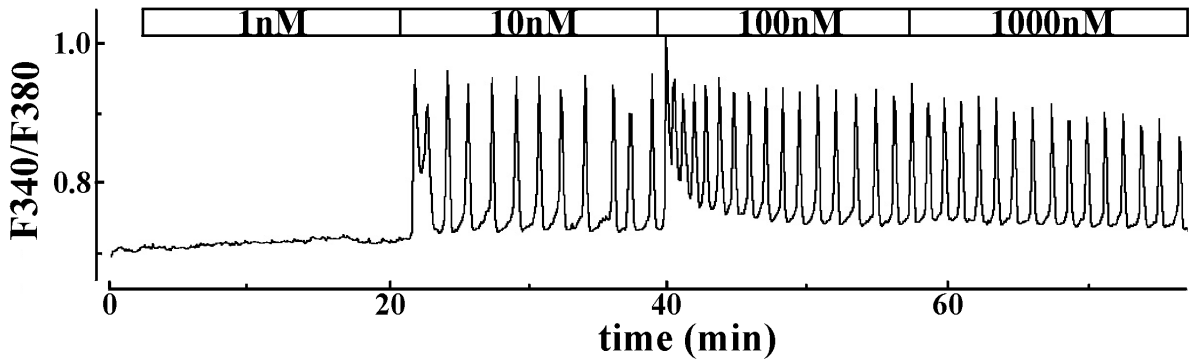

Figure 2 Effect of an increasing PGF2α concentration on the intracellular calcium response. The response of an individual cell within a monolayer is shown during a step-wise increase of the PGF2α concentration from 1 to 1000 nM. Addition of the different concentrations is indicated by the bars.

frequency of this oscillation increased upon changing the agonist concentration to 100 nM, while an additional increase to 1000 nM did not further affect the oscillation frequency.

In general, an increased stimulation of NRK cells by a higher PGF2α concentration results in an increased oscillation frequency.

Role of IP_3-sensitive calcium stores in the calcium oscillations

To further characterize the PGF2α-induced calcium oscillations in NRK fibroblasts, we examined the role of internal calcium stores by using an agonist of IP_3-sensitive calcium release channels and by inhibiting reuptake of calcium into the stores.

First we investigated whether IP_3-sensitive calcium stores were involved in the calcium oscillations. Therefore we used thimerosal, which has been shown to sensitize the IP_3 receptor without affecting IP_3 production (Bootman et al., 1992), resulting in altered calcium oscillation patterns e.g. in pancreatic acinar cells (Thorn et al., 1992; Wu et al., 1996). Fig. 3A shows that in NRK monolayers preincubated for 15 min with 10 μM thimerosal, PGF2α (1000 nM) did no longer trigger intracellular calcium oscillations in individual cells, but induced a calcium peak followed by a plateau phase. Such a response had also been measured in a small fraction of cells when stimulated by PGF2α in the absence of thimerosal (*see* Table 1). Moreover, when thimerosal was added to PGF2α-treated cells, it immediately increased the amplitude and frequency of PGF2α-induced intracellular calcium oscillations until the intracellular calcium level had reached a similar plateau phase (Fig. 3B). These results demonstrate that thimerosal amplifies the PGF2α-induced calcium response in NRK cells, consistent with the involvement of IP_3 receptors.

Next, we determined whether the oscillation frequency and/or amplitude was dependent on the rate of refilling of the calcium stores. For this reason, we inhibited calcium reuptake by blocking SERCA pumps using a low concentration of thapsigargin (5 nM). Fig. 3C shows that thapsigargin

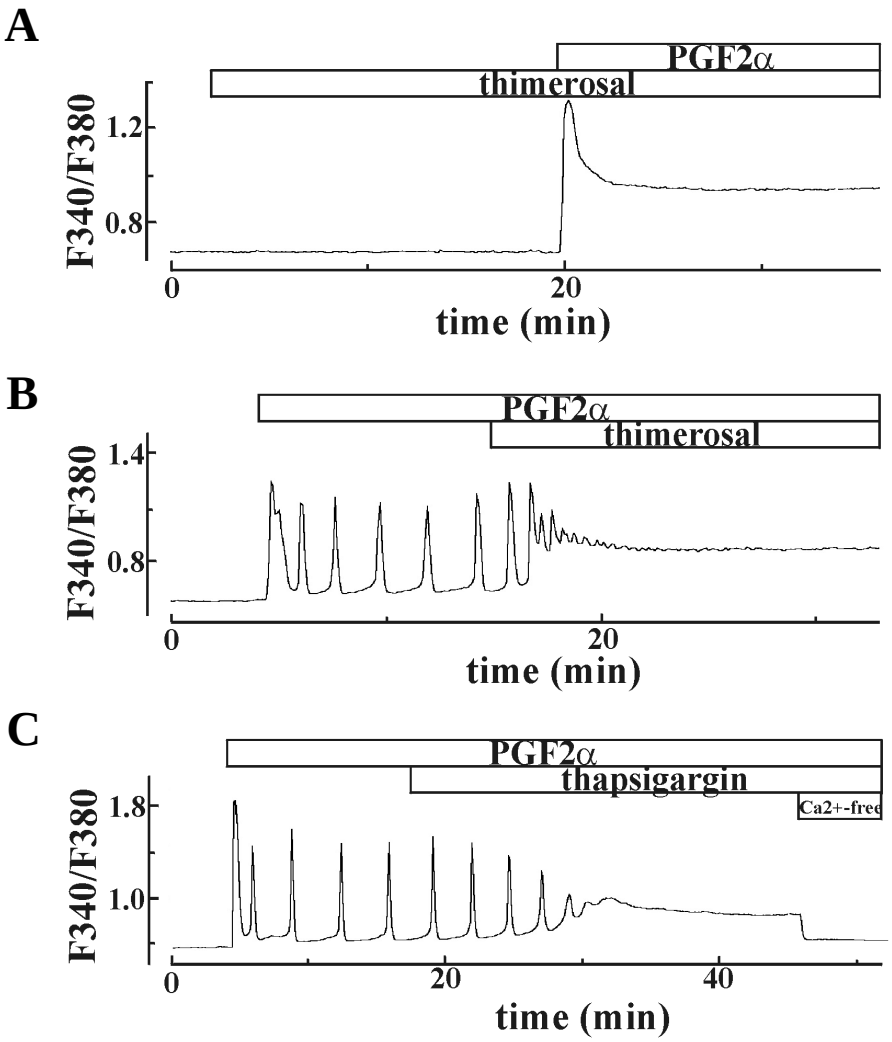

Figure 3 Role of internal calcium stores in the PGF2α-induced intracellular calcium response. **A)** Typical calcium response induced by PGF2α (1000 nM) after 15 min preincubation with thimerosal (10 μM). **B)** Effect of thimerosal (10 μM) and **C)** thapsigargin (5 nM) on intracellular calcium oscillations induced by 1000 nM PGF2α. Addition of each compound and the exchange of normal calcium containing medium by calcium-free (3.5 mM EGTA) medium is indicated by the bars.

gradually reduced the amplitude of the PGF2α-induced calcium oscillations. Under these conditions the frequency of the oscillations was hardly affected until the oscillatory pattern was changed to a sustained plateau phase. This plateau returned to basal levels upon removal of external calcium and was most likely caused by a constitutive activation of store-operated calcium influx when internal calcium stores were depleted. In general, the oscillation amplitude was reduced by thapsigargin (5 nM) from 1.19 ± 0.03 to 0.95 ± 0.01, while the plateau was reached within 7.0 ± 0.5 min after addition of the SERCA-pump inhibitor (mean ± S.E.M; n=34). When a higher thapsigargin concentration was applied (100 nM), this plateau was reached within 2 min (n=42).

These results show that the PGF2α-induced calcium oscillations are based on IP_3 receptor-mediated periodic release of stored calcium and that the rate of store refilling sets the oscillation amplitude.

Role of calcium influx in the calcium oscillations

Since cytoplasmic calcium can be derived from influx from the external medium, we next investigated the role of calcium influx in the PGF2α-induced intracellular calcium oscillations. Therefore we varied the extracellular calcium concentration and blocked plasma membrane calcium channels.

The data presented so far were measured in the presence of 1 mM external calcium. The results presented in Fig. 4 show that oscillations were not measured when NRK cells were stimulated with

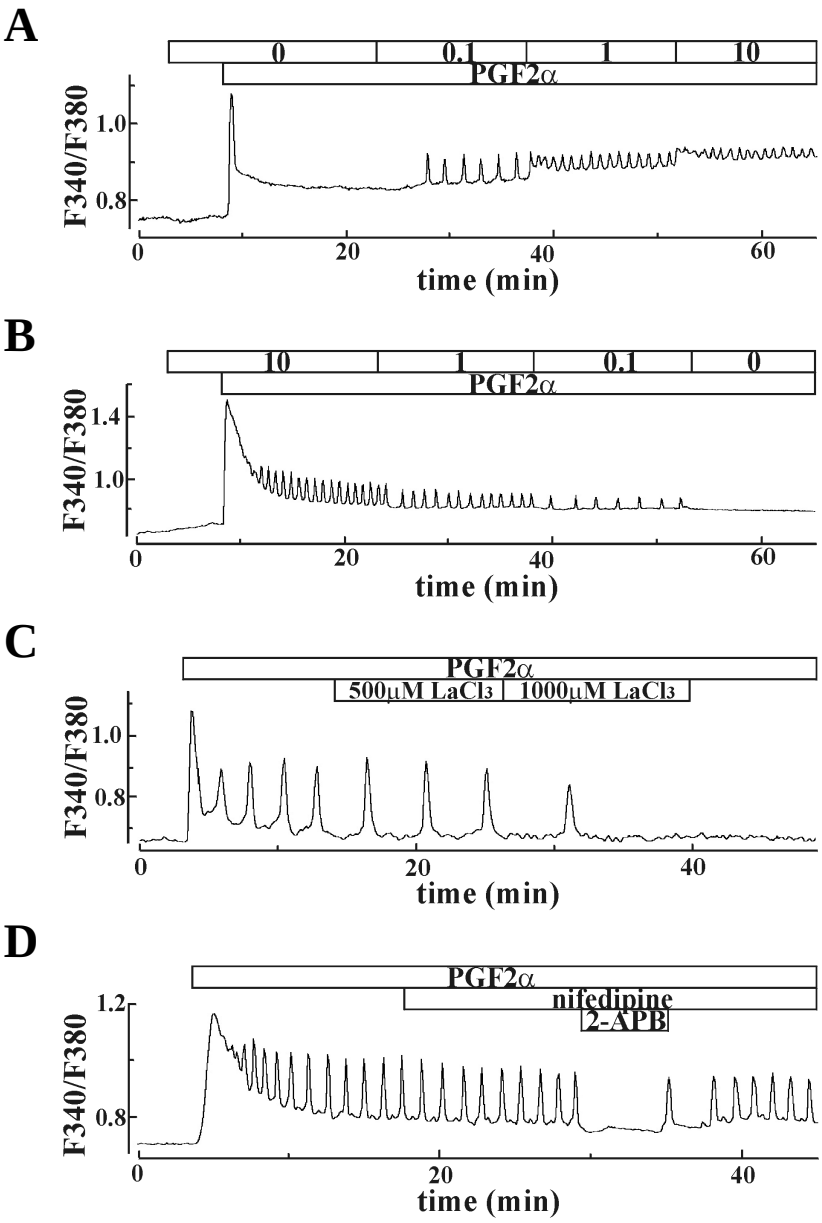

Figure 4 Contribution of calcium influx to the PGF2α-induced intracellular calcium oscillations. **A)** The external calcium concentration was step-wise increased from calcium-free (3.5 mM EGTA) to 10 mM and **B)** decreased from 10 mM to calcium-free (3.5 mM EGTA), while NRK cells were stimulated with PGF2α (1000 nM). **C)** Effect of $LaCl_3$ (500 and 1000 μM) and **D)** nifedipine (1 μM) and 2-APB (75 μM) on the PGF2α-induced intracellular calcium oscillations. Addition of each compound is indicated by the bars.

PGF2α (1000 nM) in the absence of external calcium (3 mM EGTA). Under these conditions only one or two calcium transients were observed. Step-wise increases (Fig. 4A) or decreases (Fig. 4B) of the extracellular calcium concentration strongly affected the oscillation frequency. Note that the initial transient was much larger and broader when cells were stimulated in the presence of a high external calcium medium concentration (10 mM).

Next, the rate of calcium influx was reduced by $LaCl_3$, which is a general blocker of calcium entry channels. Fig. 4C shows that the frequency of the intracellular calcium oscillations decreased upon addition of 500 μM $LaCl_3$ while the oscillations were completely blocked by 1000 μM $LaCl_3$. We have previously shown that NRK fibroblasts express L-type calcium channels (De Roos et al., 1997c), but inhibition of these voltage-activated channels by 1 μM nifedipine did not affect the PGF2α-induced calcium oscillations (Fig. 4D). In contrast, the oscillations disappeared immediately and reversibly upon subsequent addition of 75 μM 2-APB, which has been shown to block store-operated calcium channels (Bootman et al., 2002) and the IP_3 receptor (Maruyama et al., 1997), as well as to inhibit gap junctional communication between cells (Harks et al., 2003a).

Taken together, the results above clearly demonstrate that the initial calcium peak is mediated by calcium release from internal stores and that the following oscillations require calcium influx for continuation, such that the rate of calcium influx affects the oscillation frequency.

Effect of PGF2α on the membrane potential and gap junctional coupling of confluent monolayers of NRK fibroblasts

Because we previously measured that NRK cells in confluent monolayers are coupled by gap junctions (Harks et al., 2001), we investigated whether the lack of synchronization of the calcium oscillations in these monolayers was caused by an inhibition of gap junctions by PGF2α. Therefore, we performed patch-clamp experiments and applied voltage-clamp steps in order to evoke capacitive current transients. From these transients we could calculate the estimated gap junctional coupling between the patched cell and it surrounding cells (G01x) before and during stimulation with PGF2α (Harks et al., 2001).

Confluent monolayers of serum-deprived NRK fibroblasts exhibit a stable resting membrane potential around -70 mV and PGF2α (>10 nM) caused a sustained depolarization of the membrane towards around -20 mV (n=19; Fig. 5A), which has been shown to result from the opening of calcium-activated chloride channels (De Roos et al., 1997a). The capacitive current transient that was evoked before addition of PGF2α (1000 nM) was characterized by a slow multi-exponential decay and a large steady-state current (Fig. 5B, 1). Such a transient is typical for an electrically coupled monolayer (Harks et al., 2001). The transient was not changed even after prolonged (~25 min) stimulation with PGF2α (Fig. 5B, 2) indicating that gap junctional coupling was not affected by this agonist (n=4). In

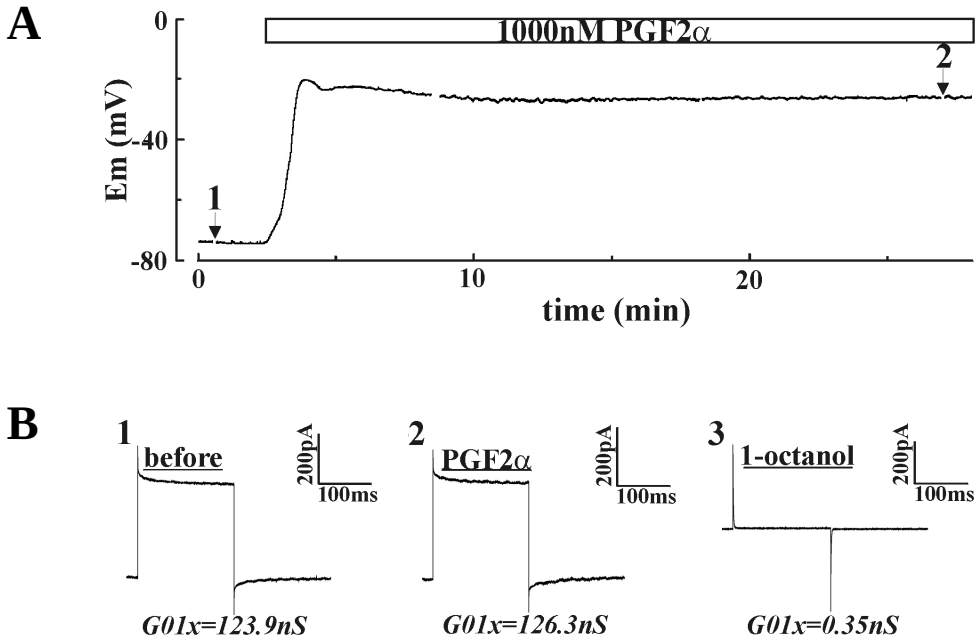

Figure 5 Effect of PGF2α on the membrane potential and electrical coupling of NRK fibroblasts. **A)** Effect of 1000 nM PGF2α on the membrane potential of a confluent monolayer of NRK cells. The recording was interrupted at the indicated time-points in order to evoke capacitive current transients. **B)** Corresponding capacitive current transients before (1; *see* timepoint in A) and during (2; *see* timepoint in A) PGF2α stimulation and after subsequent electrical uncoupling by 1 mM 1-octanol (3). Estimated gap junctional conductances (G01x) were calculated as described in Methods and addition of PGF2α is indicated by the bar.

contrast, addition of the gap junction blocker 1-octanol (1 mM) changed the capacitive current transient to a single-exponential (τ<0.5 ms) with a reduced steady-state current (Fig 5B, 3), which is characteristic for an electrically uncoupled monolayer cell (Harks et al., 2001), resulting in a value of G01x <1 nS (n=4).

These results show that the NRK cells in a confluent monolayers are electrically coupled and that PGF2α did not affect electrical coupling, resulting in a uniform membrane potential response throughout the monolayer.

Discussion

In the present study we show that PGF2α induces intracellular calcium oscillations in individual NRK fibroblasts cultured in monolayers and that these oscillations are not synchronized in spite of the fact that the cells remain electrically coupled. The lack of synchronization of the intracellular calcium oscillations is remarkable because gap junctions are generally known to transduce second messengers such as IP_3 and calcium (Giaume and Venance, 1998), thereby allowing cells to act in an organized organ-like way rather than a collection of isolated cells. For example, it has previously been reported

that proper intercellular diffusion of IP_3 is crucial for the coordination and synchronization of calcium waves and oscillations in astrocytes and hepatocytes (Clair et al., 2001; Hofer et al., 2002). We suggest that the oscillations in NRK monolayers are not synchronized because gap junctional permeability for IP_3 and/or calcium between NRK cells is insufficient to overcome intrinsic differences between individual cells. These differences may include variations in IP_3 levels and in expression and/or localization of the FP and IP_3 receptor. This proposed heterogeneity also explains why only a fraction of cells responds to PGF2α stimulation at low concentrations. The question remains whether the number of gap junctions, or the permeability of each gap junction per se, is insufficient for synchronization and although the oscillations are not completely synchronized they may still be influenced by their neighboring cells.

Remarkably, confluent monolayers of NRK cells show extensive electrical coupling (Harks et al., 2001) but poor dye-coupling (Van Zoelen and Tertoolen, 1991), while both are mediated by gap junctions. Obviously, gap junctional permeability is sufficient to allow the membrane potential to respond as a whole upon PGF2α stimulation by electrical coupling, but insufficient to synchronize the intracellular calcium oscillations most likely due to a restricted diffusion of IP_3 and/or calcium. Recently, a similar discrepancy between electrical coupling and dye-coupling has been shown for pancreatic islet cells, which also exhibit extensive electrical coupling but poor dye-coupling, although in these cells synchronized calcium oscillations were observed that were triggered by the electrical membrane activity (Quesada et al., 2003). Previously, several G-protein coupled receptor agonists such as lysophosphatidic acid (LPA), endothelin and thrombin have been shown to inhibit gap junctional communication in cells expressing connexin43 (Postma et al., 1998). This inhibition seemed to result from a Src-mediated tyrosine phosphorylation of this connexin. Although NRK fibroblasts also mainly express connexin43 (Li et al., 1996), cell to cell communication was not affected upon activation of the FP-receptor by PGF2α in these cells. So, inhibition of gap junctional communication is not a common response to activation of all types of G-protein coupled receptors.

The PGF2α-induced calcium response in individual NRK cells in the monolayer was characterized by an initial sharp calcium peak mediated by calcium release from IP_3-sensitive stores, which was in almost all cells followed by repetitive calcium oscillations. Literature data (Berridge, 1993; Liu et al., 1995; Shuttleworth and Thompson, 1996) have shown that the frequency of calcium oscillations is either dependent on the rate of refilling of the intracellular calcium stores such as the ER, or on the time that is required to reach a threshold cytosolic calcium concentration for calcium-induced calcium release. In our study the oscillation frequency of the PGF2α-induced calcium oscillations in NRK cells appears not to relay on the rate of store-refilling, because inhibition of SERCA pumps with a low concentration of thapsigargin gradually reduced the amplitude of the oscillation under conditions that the oscillation frequency hardly changed. We therefore conclude that the initiation of each oscillatory spike is independent of the relative filling state of the stores.

Most likely, the frequency of the calcium oscillations in NRK cells is determined by the time required for cytosolic calcium to reach a threshold for global calcium-induced calcium release. Each sharp calcium transient was preceded by a slower elevation of cytosolic calcium. Previously, it has already been shown that global intracellular calcium signals can be preceded by a so-called pacemaker phase that arises from the summation and coordination of subcellular elementary release events (Bootman et al., 1997). Our studies with different [PGF2α], thimerosal and various extracellular [Ca^{2+}] demonstrate that the duration of this pacemaker phase is determined by the number of IP_3 receptors that is recruted and by the rate of calcium influx over the plasma membrane.

First, upon increasing PGF2α concentrations the average oscillation frequency increased, presumably because more IP_3 receptors are recruted at those higher IP_3 levels. In this way, more calcium is released from IP_3-sensitive stores during the pacemaker phase thereby reducing the time to reach the threshold calcium concentration for global release. The second indication from our study that argues for a critical role of IP_3-sensitive calcium release in the oscillation frequency, comes from the effect of sensitizing the IP_3 receptor with thimerosal. Although thimerosal has also been shown to effect proteins whose activity is sensitive to redox state (Donoso et al., 2000; Evans and Bielefeldt, 2000; Marengo et al., 1998), this was only found at relatively high concentrations (≥100 μM). Therefore, the effect of thimerosal on the calcium oscillations in our study (at 10 μM), can be attributed to its effect on the IP_3 receptor. Thimerosal initially increased the oscillation frequency, until a plateau phase was reached. Such a plateau indicates that calcium sequestration and/or extrusion mechanisms are insufficient to deal with the large increase of calcium recruted in the cytoplasm. So, when more calcium was liberated from IP_3-sensitive calcium stores, the time between two subsequent calcium transients was reduced.

Finally, the oscillation frequency is also determined by the rate of calcium influx. When this rate was reduced by decreasing the external calcium concentration or by partial inhibition of calcium entry channels upon addition of 500 μM $LaCl_3$, the oscillation frequency was also decreased. The regulatory role of calcium influx on the frequency does not result from the recharging of internal calcium stores, since inhibition of reuptake of calcium into the stores hardly affected the oscillation frequency. Instead we propose that calcium influx indirectly affects the calcium oscillations by interfering with the kinetic properties of the IP_3 receptor, which is regulated by intracellular calcium. So, the time to reach the threshold calcium concentration for global calcium-induced calcium release from this calcium release channel is reduced when the rate of calcium influx is increased. The calcium influx in our study is most likely mediated by store-operated calcium channels, which are generally known to be activated upon depletion of calcium stores (Putney, 1986). Lanthanum, which has been shown to block these channels at various concentrations depending on the cellular system (Halaszovich et al., 2000; Krause et al., 1996), completely blocked the PGF2α-induced calcium oscillations. Morevover, the oscillations immediately stopped upon addition of 2-APB, which has been recently been described as

an effective blocker of store-operated calcium channels (Bootman et al., 2002). However, 2-APB also acts as an antagonist of the IP_3 receptor (Maruyama et al., 1997) and a blocker of gap junctional coupling (Harks et al., 2003a) and therefore the inhibitory action of 2-APB on the oscillations cannot solely be ascribed to inhibition of store-operated calcium channels. Although NRK cells have been shown to express L-type calcium channels, these voltage-activated channels did not contribute to the PGF2α-induced calcium oscillations in quiescent NRK monolayers since nifedipine did not affect the oscillations. This contrasts the repetitive calcium oscillations that accompanied spontaneous calcium action potentials in density-arrested NRK monolayers that were completely blocked by nifedipine (De Roos et al., 1997c).

Taken together, we suggest that cytoplasmic calcium that is rising between two subsequent calcium transients of the oscillation must reach a threshold concentration to trigger global calcium-induced calcium release from internal stores. Although both calcium release from IP_3-sensitive calcium stores and calcium influx from the extracellular medium determine the duration of this interspike interval, we conclude that the frequency of the calcium oscillations is primarily determined by the calcium release kinetics of the IP_3 receptor. Calcium influx may modulate the oscillation frequency by interfering with the calcium-dependent properties of this calcium release channel and is required for the continuation of the oscillations. The decline of calcium after each of the transients during the oscillations probably involves reuptake into the stores and the extrusion to the extracellular solution by plasma membrane calcium ATP-ases. The involvement of plasma membrane calcium ATP-ases arises from the observation that the oscillations stopped in the absence of external calcium, indicating that calcium influx is required to replenish for calcium that is transported to the extracellular space by these pumps. In addition, because the calcium oscillations are not synchronized and cells are coupled by gap junctions diffusion of calcium to the neighboring cells may also contribute to the decline of calcium after the calcium transient.

Previously, we have shown that NRK monolayers that had been cultured to density-arrest (contact inhibition) repetitively fire slow calcium action potentials that are accompanied by cytosolic calcium transients (De Roos et al., 1997c). The underlying mechanism that determines the periodicity of this spontaneous firing is still elusive but seems to include more parameters than just the membrane conductances. Strikingly, the frequency of these spontaneous action potentials is very similar to the frequency of the intracellular calcium oscillations measured in the present study. As density-arrested and quiescent NRK cells are the same cells in different growth states, it will be interesting to determine the possible role of the IP_3-dependent calcium oscillatory mechanism in the generation of repetitive action potentials and calcium oscillations in density-arrested NRK cells.

Acknowledgements.

We thank Dr. E. Pierson (General Instrumentation) for expert technical assistance with the digital imaging experiments.

Materials and Methods

Cell culturing: Normal rat kidney fibroblasts (NRK clone 49F) were cultured in bicarbonate-buffered Dulbecco's-modified Eagle's medium (DMEM; Life Technologies, Paisly, UK) supplemented with 10% newborn calf serum (HyClone Laboratories, Logan, UT, US). Confluent cultures were made quiescent by subsequent incubation for one to three days in serum-free DF medium (DMEM/Ham's F12, 1:1; Gibco; Life Technologies, Paisly, UK) supplemented with 30 nM Na_2SeO_3 and 10 µg/ml human transferrin.

Intracellular calcium measurements: Coverslips with monolayers of NRK fibroblasts were placed in a Leiden cell chamber and loaded for 30 min at room temperature with 2 µM fura-2/AM (Molecular Probes, Eugene, OR, US) in Hanks' medium containing (in mM) 137 NaCl, 5.4 KCl, 1.0 $CaCl_2$, 0.50 $MgCl_2$, 0.40 $MgSO_4$, 4.2 $NaHCO_3$, 0.34 NaH_2PO_4, 0.35 KH_2PO_4 and 5.6 glucose (pH 7.4), supplemented with 0.025% Pluronic F127 and 3% FCS. After loading, the cells were washed for 30 min with Hanks' medium at room temperature. In order to maintain osmolarity of the medium, equiosmolar NaCl was exchanged for $CaCl_2$ when the extracellular calcium concentration was varied. Calcium-free solutions were obtained by omitting $CaCl_2$ from the medium and adding 3.5 mM EGTA. To avoid precipitations when using $LaCl_3$, an external medium was used in those experiments that contained (in mM) 142 NaCl, 5.4 KCl, 1.0 $CaCl_2$, 0.90 $MgCl_2$, 5.6 glucose and 10 HEPES (pH 7.4). Dynamic video imaging was performed as described elsewhere (Cornelisse et al., 2002). Excitation wavelengths of 340 nm and 380 nm (band width 8-15 nm) were provided by a 150 W Xenon lamp (Ushio UXL S150 MO, Ushio, Tokio, Japan) and fura-2 fluorescence emission was monitored at wavelengths above 440 nm, using a 440 nm DCLP dichroic mirror in front of a Coolsnap fx monochrome digital camera (Roper Scientific, Tucson, US). Image acquisition, using a camera pixel binning of 4, and computation of ratio images (F340/F380) was every 6 s and was operated through Metafluor v.4.6 (Universal Imaging Corporation, Downingtown, PA, US). Camera acquisition time was 100 ms per excitation wavelength.

Electrophysiology: Whole-cell current-clamp and voltage-clamp experiments on NRK cells were performed as described previously (De Roos et al., 1996; Harks et al., 2001). In order to evoke capacitive current transients, voltage pulses of +10 mV (duration 180 ms) were applied from a holding potential of -70 mV. For patch-clamp experiments NRK cells were perfused at room temperature with serum-free DF medium containing (in mM) 120 NaCl, 4.2 KCl, 1.1 $CaCl_2$, 0.3 $MgCl_2$, 0.4 $MgSO_4$, 44 $NaHCO_3$ and 1.0 NaH_2PO_4 and equilibrated with 7.5% CO_2 to pH 7.4. Intracellular pipette solution contained (in mM) 25 NaCl, 120 KCl, 1.0 $CaCl_2$, 1.0 $MgCl_2$, 3.5 EGTA, 10 HEPES/KOH (pH 7.4). Data were obtained with an EPC-7 patch-clamp amplifier (List Electronic, Darmstadt, Germany) in conjunction with Pulse/Pulsefit v.8.40 software (HEKA Elektronik, Lambrecht, Germany). Borosilicate patch pipettes (GC150-15; Clark, Reading, UK) with resistances of 4-6 MΩ were used.

Data analysis: Gap junctional conductance between the patched cell and the surrounding ring of cells was approximated by measuring the input conductance of the monolayer through the patched cell (Harks et al., 2001). Frequencies of calcium oscillations were determined by counting the peaks using the "pick peak" algorithm of Origin 6.0 (Microcal, Northampton, MA, US), using a minimal peak height of 10% of the total signal as selection criteria.

Numerical data are represented as mean ± S.E.M. throughout this article.

CHAPTER 7

Phenotypic transformation of NRK fibroblasts is accompanied by a depolarization of the membrane due to the secretion of prostaglandin F2α

E.G.A. Harks, P.H.J. Peters, J.L. van Dongen, E.J.J. van Zoelen, A.P.R. Theuvenet

Abstract. Tumor cells are generally characterized by a depolarized membrane potential but the relationship between oncogenesis and the cellular membrane potentials is not clear yet. We have used normal rat kidney (NRK) fibroblasts as an *in vitro* model system to study cellular alterations upon transformation, and show here that phenotypically transformed NRK cells are strongly depolarized compared to their non-transformed counterparts. The depolarization of their membrane appeared to result from the presence of a biologically active compound in their culture medium, which enhanced intracellular calcium levels resulting in the opening of calcium-activated chloride channels. Blockers of the cyclooxygenase (COX) pathway prevented the production of this compound and the depolarization of the membrane, suggesting the involvement of COX products. ESI mass-spectrometry revealed that the active compound was prostaglandin F2α (PGF2α). The active PGF2α concentration in the culture medium of phenotypically transformed NRK cells as determined by a PGF2α-specific enzyme immunoassay was 20.5 nM, and to be at least 10-fold higher than released by non-transformed NRK cells. Thus phenotypic transformation of NRK cells results in the secretion of PGF2α, which depolarizes their membrane in an autocrine and possibly paracrine manner.

Introduction

During tumorigenesis, cells undergo numerous alterations that eventually lead to uncontrolled proliferation. These changes include up- and downregulation of enzyme activities and gene expression, phosphorylation and dephosporylation of proteins as well as morphological changes. Also, the membrane potential of cells can drastically change and many transformed cells are strongly depolarized compared to their normal counterparts (reviewed by Marino et al., 1994). However, the mechanism that causes this depolarization is not always clear.

Normal rat kidney (NRK) fibroblasts provide an attractive model system for studying density-dependent growth inhibition and cellular alterations upon transformation (De Roos et al., 1997c; Jinno et al., 2001; Lahaye et al., 1998; Lahaye et al., 1999a; Van Zoelen, 1991). Proliferation of these immortalized cells is strictly dependent on externally added growth factors and when cultured in the presence of epidermal growth factor (EGF) as the only growth-stimulating hormone, these cells exhibit a normal phenotype including the ability to undergo density-dependent growth inhibition. However, in the additional presence of transforming growth factor β (TGFβ) or retinoic acid (RA) these cells become phenotypically transformed (Assoian, 1985; Roberts et al., 1984). Phenotypically transformed NRK cells exhibit an enhanced gap junctional intercellular communication as measured by dye-coupling (Van Zoelen and Tertoolen, 1991), and are characterized by the ability to proliferate under anchorage-independent conditions (Lahaye et al., 1999a), which is known to be the best *in vitro* correlate of tumorigenic behavior of cells *in vivo* (Cifone and Fidler, 1980; Shin et al., 1975).

Most likely, the EGF receptor plays a prominent role in density-dependent growth inhibition and phenotypic transformation of NRK cells. Previously, it has been shown that the number of EGF receptors decreases in these cells at high cell densities (Rizzino et al., 1988). Moreover, phenotypic transformation by TGFβ and RA was accompanied by an upregulation of expression levels of the EGF receptor and these transforming agents could only induce phenotypic transformation in the additional presence of EGF (Assoian et al., 1984; Van Zoelen et al., 1986; Van Zoelen et al., 1988). The crucial role of the EGF receptor in the transformation of NRK cells has also been shown in NRK mutants, which had a defect in EGF receptor expression and failed to transform by EGF and TGFβ (Kizaka-Kondoh et al., 2000) However, when the EGF receptor was overexpressed in these mutants, EGF could induce transformation in the absence of TGFβ. Besides the EGF receptor, several other regulators have been shown to be involved in growth regulation of NRK cells including fibronectin, phosphatases, connective tissue growth factor, inositol polyphosphate 5-phosphatase, and cyclin A (Guadagno et al., 1993; Ignotz and Massague, 1986; Kothapalli et al., 1997; Rijksen et al., 1993; Speed et al., 1996).

In previous studies, we showed that the membrane potential and intracellular calcium concentration play an important role in growth regulation of NRK cells. Whereas quiescent monolayers of NRK fibroblasts have a stable membrane potential of around -70 mV which is

primarily determined by potassium conductances (Harks et al., 2003c), density-arrested monolayers spontaneously fire repetitive action potentials as a result of the sequential opening of L-type calcium, calcium-dependent chloride and inward rectifier potassium channels (De Roos et al., 1997c; Harks et al., 2003c). These action potentials are accompanied by transient rises of the intracellular calcium concentration (De Roos et al., 1997c).

In the present study, we show that the membrane potential of phenotypically transformed NRK fibroblasts is constitutively around ~-20 mV, and therefore strongly depolarized compared to that of the non-transformed cells. Analysis of the conditioned medium of these transformed cells showed that this depolarization is caused by an active compound secreted in their culture medium, which also depolarizes non-transformed NRK cells by the opening of calcium-activated chloride channels. This compound was purified from the conditioned medium and identified with ESI mass spectroscopy and enzyme immunoassay as prostaglandin F2α (PGF2α). In contrast, non-transformed NRK cells did not produce detectable amounts of PGF2α. These results are discussed in the light of the role of COX enzymes in cell transformation.

Results

Growth state-dependent membrane potential of NRK cells

Tumorigenic transformation of many different cell types is often accompanied by a membrane depolarization (Marino et al., 1994). Since NRK fibroblasts can reversibly be transformed by the addition of specific combinations of growth factors, these cells form an attractive *in vitro* model system to study the mechanisms of transformation (Van Zoelen, 1991), and we investigated whether the membrane potential of NRK cells was also changed upon transformation.

Depending on the combination of growth factors added, three different growth states of cultured NRK fibroblasts can be discriminated. First, confluent NRK monolayers can be made *quiescent* by serum deprivation. Under these conditions all cells in the monolayer are in the resting phase of the cell cycle but are still responsive to growth factor stimulation. These quiescent monolayers exhibit a stable resting membrane potential around -70 mV (Fig. 1A), which is not significantly different from confluent monolayers of exponentially growing cells (data not shown). Upon addition of EGF (5 ng/ml) as the only growth factor in combination with insulin (5 μg/ml), quiescent NRK cells can be triggered to restart their proliferation until the monolayer has reached a critical cell density and become *density-arrested* (Van Zoelen, 1991). Remarkably, density-arrested NRK cells spontaneously fire slow calcium action potentials in a repetitive manner (Fig. 1B) with a frequency ranging from 0.2-2 min^{-1}. Previous studies have shown that this firing of action potentials by NRK fibroblasts involves a sequential opening of L-type calcium, calcium-activated chloride and inwardly rectifying potassium

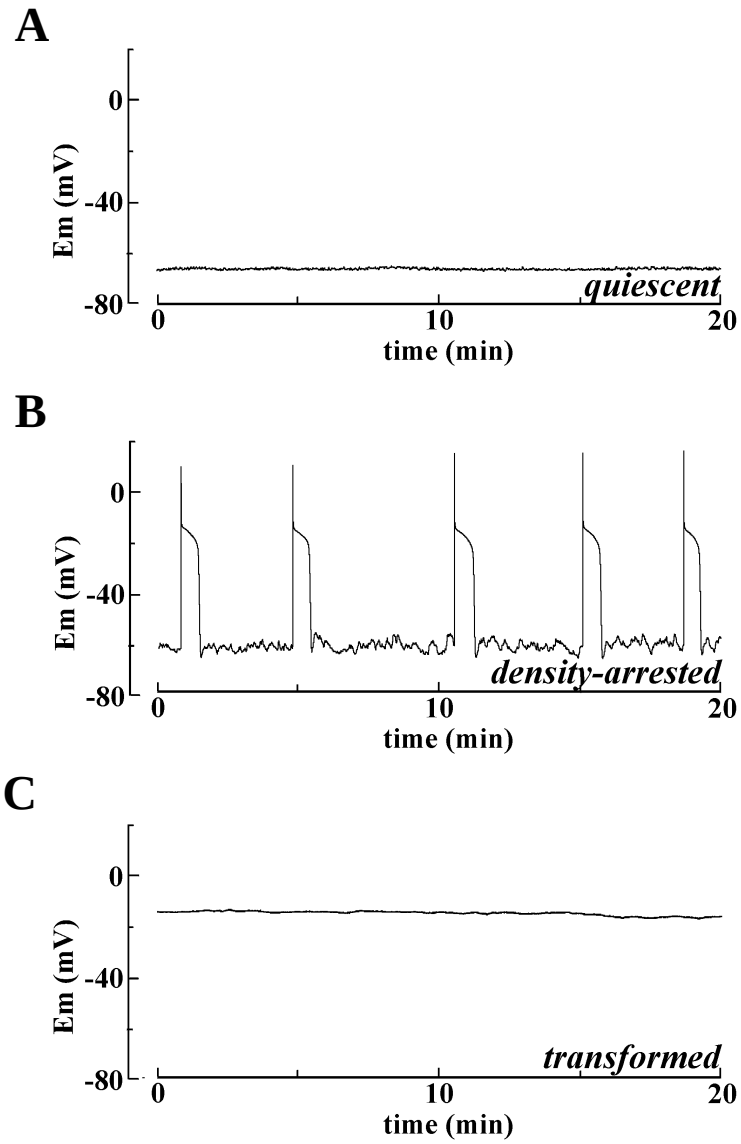

Figure 1 Membrane potential of NRK fibroblasts cultured at different growth states. A) Membrane potential of a confluent monolayer of quiescent NRK fibroblasts after 2 days serum-deprivation. B) Membrane potential of a confluent monolayer of density-arrested NRK fibroblasts measured 2 days after applying 5 ng/ml EGF and 5 µg/ml insulin to quiescent NRK monolayers. C) Membrane potential of a multilayer of phenotypically transformed NRK fibroblasts measured 4 days after applying of 50 ng/ml RA, 5 ng/ml EGF and 5 µg/ml insulin to density-arrested NRK monolayers.

channels (Harks et al., 2003c), but the underlying mechanism that determines the periodicity of this spontaneous firing activity is still elusive.

Density-dependent growth inhibition is one of the main differences that discriminates normal cells from tumor cells and prevents excessive cell growth. However, this protection mechanism can be overcome in NRK cells upon additional treatment with RA (50 ng/ml), resulting in a transformed phenotype after 2-4 days (Van Zoelen et al., 1988). In contrast to quiescent and density-arrested NRK monolayers, phenotypically transformed NRK cells grew in cellular multilayers. The membrane potential of these transformed NRK cells was -20 ± 3 mV (n=9) (Fig. 1C). Also, NRK cells

transformed upon addition of transforming growth factor β (TGFβ; 2 ng/ml) or lysophosphatidic acid (LPA; 100μM) were depolarized to -20 mV (data not shown).

These data show that transformation of NRK fibroblasts also clearly results in a depolarization of the cells.

Phenotypically transformed NRK cells secrete a compound that depolarizes their membrane

When monitoring the membrane potential of phenotypically transformed NRK cells over a longer period (>15 min), we found that under continuous perfusion with fresh serum-free medium, the membrane slowly started to repolarize. (Fig. 2A). Within 30 min, the cells started to fire repetitive action potentials that were similar to those observed in density-arrested monolayers (*see* Fig. 1B), indicating that the low membrane potential resulted from a secreted compound in the conditioned medium.

To investigate whether this compound also exhibits autocrine and paracrine effects, we harvested the culture medium of NRK cells that had been grown for 2-4 days in the additional presence of RA, and tested this conditioned medium of transformed NRK cells for its effects on quiescent NRK

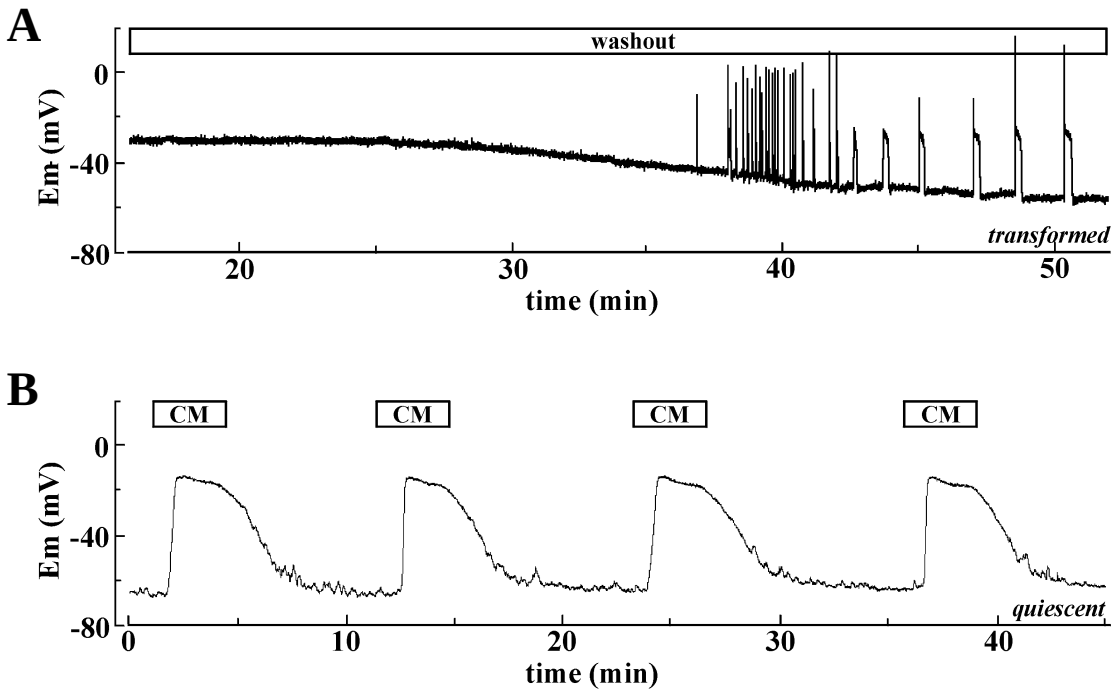

Figure 2 Phenotypically transformed NRK fibroblasts secrete a compound in their culture medium with depolarizing activity. **A)** Membrane potential of transformed NRK cells measured 4 days after applying 50 ng/ml RA, 5 ng/ml EGF and 5 μg/ml insulin to density-arrested NRK monolayers, under continuous perfusion with fresh serum-free DF medium (washout). **B)** Effect of repetitive addition and removal of the conditioned medium of phenotypically transformed NRK cells (CM) on the membrane potential of quiescent NRK monolayers. Washout and addition of culture medium is indicated by the bars.

monolayers. Exposure of such monolayers to this conditioned medium (CM) resulted in a reversible depolarization of the cells from about -70 mV to -20 mV (n=30), without any sign of homologous desensitization (Fig. 2B). The depolarization was caused by the opening of calcium-activated chloride channels, which are known to be present in NRK fibroblasts (De Roos et al., 1997a; Harks et al., 2003c). Under conditions that intracellular calcium was buffered with 50 μM BAPTA-AM the depolarization was prevented (n=4), whereas blocking of calcium-dependent chloride channels by 250 μM flufenamic acid (White and Aylwin, 1990) relieved the depolarization almost instantly (n=3). Of note, RA, EGF and insulin themselves or in combination did not affect the membrane potential of the quiescent cells in short term incubations with the concentrations that were used to induce phenotypic transformation, indicating that the depolarizing activity of CM is caused by a compound that is released by transformed NRK cells. Similar results were obtained with media conditioned by NRK cells that had been transformed with either TGFβ (n=6) or LPA (n=3).

These results demonstrate that phenotypically transformed NRK cells secrete a compound in their culture medium that depolarizes their membrane by the opening of calcium-activated chloride channels.

Role of COX activity in the production of the active compound

Because various types of both human and animal cancer cells have been shown to release prostaglandins (Bishop-Bailey et al., 2002), we investigated the possibility that the active compound secreted by phenotypically transformed NRK fibroblasts would be a prostaglandin.

The production of prostaglandins is mediated by the cyclooxygenase (COX) enzyme pathway and we investigated whether inhibiting COX activity would prevent the production of the active compound by transformed NRK cells.

Therefore, we applied a cocktail of COX inhibitors (indomethacin, flurbiprofen and ibuprofen; all 5 μM) before and after transformation of NRK cells and measured whether the conditioned medium could still depolarize quiescent NRK monolayers (Fig. 3). Media conditioned by NRK cells that had been transformed in the absence of COX inhibitors could reversibly depolarize the cells. However, when the cocktail of COX inhibitors was applied 1 h before addition of the growth factors and the conditioned medium was harvested 2 days later, depolarizing activity was absent.

Next, we investigated whether transformed NRK cells continued producing this depolarizing factor after removal of transforming factors from the medium. For that purpose, phenotypically transformed NRK cells were incubated in fresh serum-free DF medium, and after ~8 h the conditioned medium was applied to quiescent NRK monolayers. Fig. 3B shows that this resulted in a depolarization of these cells, showing that NRK cells continue to produce this active compound once they have obtained a transformed phenotype, also in the absence of externally added growth factors. In order to establish the involvement of COX activity in the production of the active compound by

transformed cells, we also incubated transformed NRK cells in fresh serum-free DF medium in the additional presence of the COX inhibitors. These inhibitors were applied 1 h prior to replacement of the culture medium by the fresh medium. Indeed, under conditions that COX activity was blocked, the conditioned medium did no longer contain depolarizing activity after subsequent incubation for 8 h.

These results show directly that the COX pathway is involved in the production of the active compound and suggest that it is a prostaglandin.

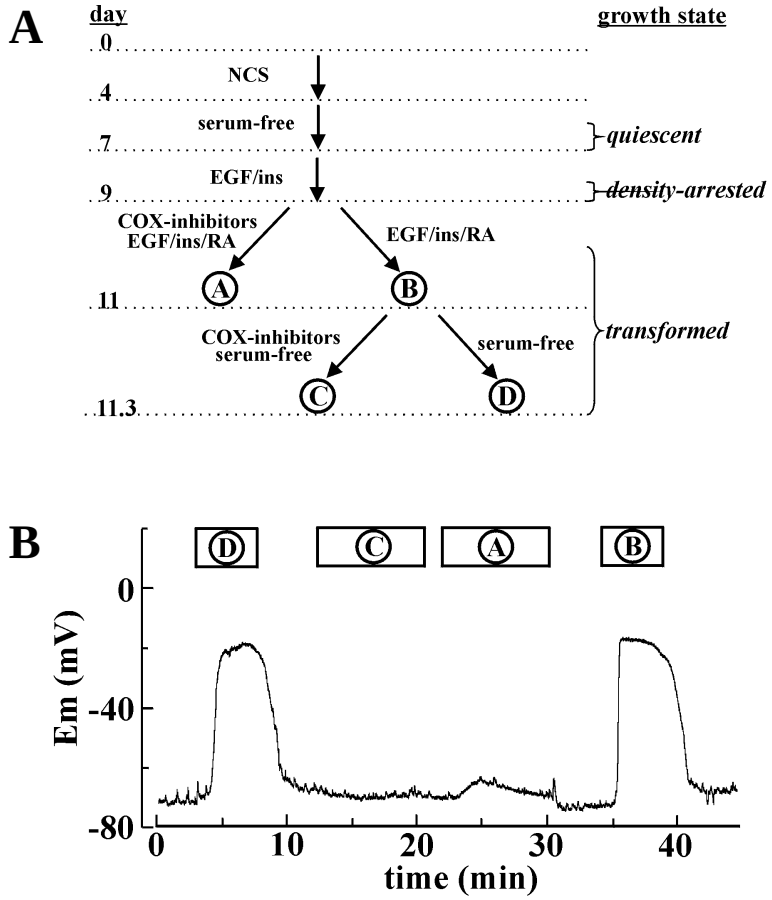

Figure 3 Contribution of the COX enzyme in the production of the active compound. **A)** Schematic overview showing how phenotypically transformed NRK fibroblasts were obtained. First, NRK cells grew in the presence of serum (newborn calf serum; NCS) to a confluent monolayer (day 4), after which all growth factors were removed from the culture medium and NRK cells became quiescent. Then, upon addition of 5 ng/ml EGF and 5 µg/ml insulin (day 7) NRK cells restarted to proliferate until they became density-arrested (day 9). Finally, by applying 50 ng/ml RA, 5 ng/ml EGF and 5 µg/ml to density-arrested NRK monolayers, NRK cells obtained a transformed phenotype (day 11). NRK cells were also cultured in the presence of a mixture of COX inhibitors (1 hr preincubation) containing indomethacin, flurbiprofen and ibuprofen (all 5 µM). The conditioned medium of NRK cells cultured in both the absence and presence of COX inhibitors was harvested (respectively A and B). In addition, transformed NRK cells were incubated in fresh serum-free DF medium and this medium was harvested after ~8 h (day 11.3) incubation in both the absence and presence of COX inhibitors (respectively C and D). **B)** The four different culture media as described in A were added to a monolayer of quiescent NRK cells and their effect on the membrane potential of these monolayers was measured. Addition of the each culture medium is indicated by the bars.

Identification of the active compound with mass-spectrometry

In order to unravel the chemical structure of the active compound, we purified it from the conditioned medium of phenotypically transformed NRK cells by a combination of reversed-phase chromatography and gel permeation chromatography, as described in the Materials and Methods section. After each separation step, the collected fractions were tested for their ability to depolarize quiescent monolayers of NRK cells. The active major fraction from the final HPLC separation, provisionally referred to as TransX, was subsequently analyzed by mass-spectrometry, using electrospray injection (ESI) in combination with time-of-flight (ToF) detection.

Fig. 4A shows the positive ion mass spectrum (ESI-MS) of the purified active fraction. Although several other peaks were measured in this fraction, we focussed on the major peak at m/z 377.3 and analyzed it by positive ion ESI-MS/MS (Fig. 4B). The fragmentation pattern showed peaks at m/z 377.3, m/z 359.3, m/z 341.3 and m/z 315.3. Fig. 4C and D shows the isotope peaks corresponding to respectively m/z 377.3 and m/z 359.3. Because the previous experiments with COX inhibitors indicated that the active compound is most likely a prostaglandin, we also measured the mass spectrum of prostaglandins with known calcium mobilizing activity (Woodward and Lawrence, 1994). Commercial PGE2 (Mw=352.5 g/mol), PGD2 (Mw=352.5 g/mol) and PGF2α (Mw=354.5 g/mol) were injected (all 1000 pmol; Cayman Chemicals, Ann Arbor, MI US), and while prominent peaks were measured at m/z 375.3 when testing PGE2 and PGD2, no peaks were measured at m/z 377.3. In contrast, Fig. 4E shows that PGF2α (*see* inset for structure) was measured as a sodium adduct at m/z 377.3 and when this peak was further analyzed with ESI-MS/MS the same fragmentation pattern was observed as for TransX (Fig. 4F), with similar isotope peaks (Fig. 4G and H). The fragmentation peaks resulted from the sequential losses of water (m/z 377.3 to 359.3 to 341.3) and both water and carboxyl (m/z 377.3 to 315.3) from the parent compound.

These results demonstrate that the purified active fraction from the culture medium of phenotypically transformed NRK fibroblasts (i.e. TransX) contains PGF2α as the predominant COX product released by the cells.

PGF2α concentration in conditioned medium of NRK cells cultured under different conditions

In order to confirm that PGF2α is present at elevated concentrations in the conditioned medium of phenotypically transformed NRK fibroblasts we used a PGF2α-specific enzyme immunoassay.

The PGF2α concentration was determined in the conditioned medium of NRK cells cultured under different conditions (*see* Table 1). Quiescent NRK monolayers did not secrete detectable amounts of PGF2α, while density-arrested NRK cells secreted PGF2α at a very low concentration in their medium (1.5 nM). In contrast, the PGF2α concentration in the conditioned medium of transformed NRK cells was at least 10 times higher (20.5 nM). In addition, after removal of the culture

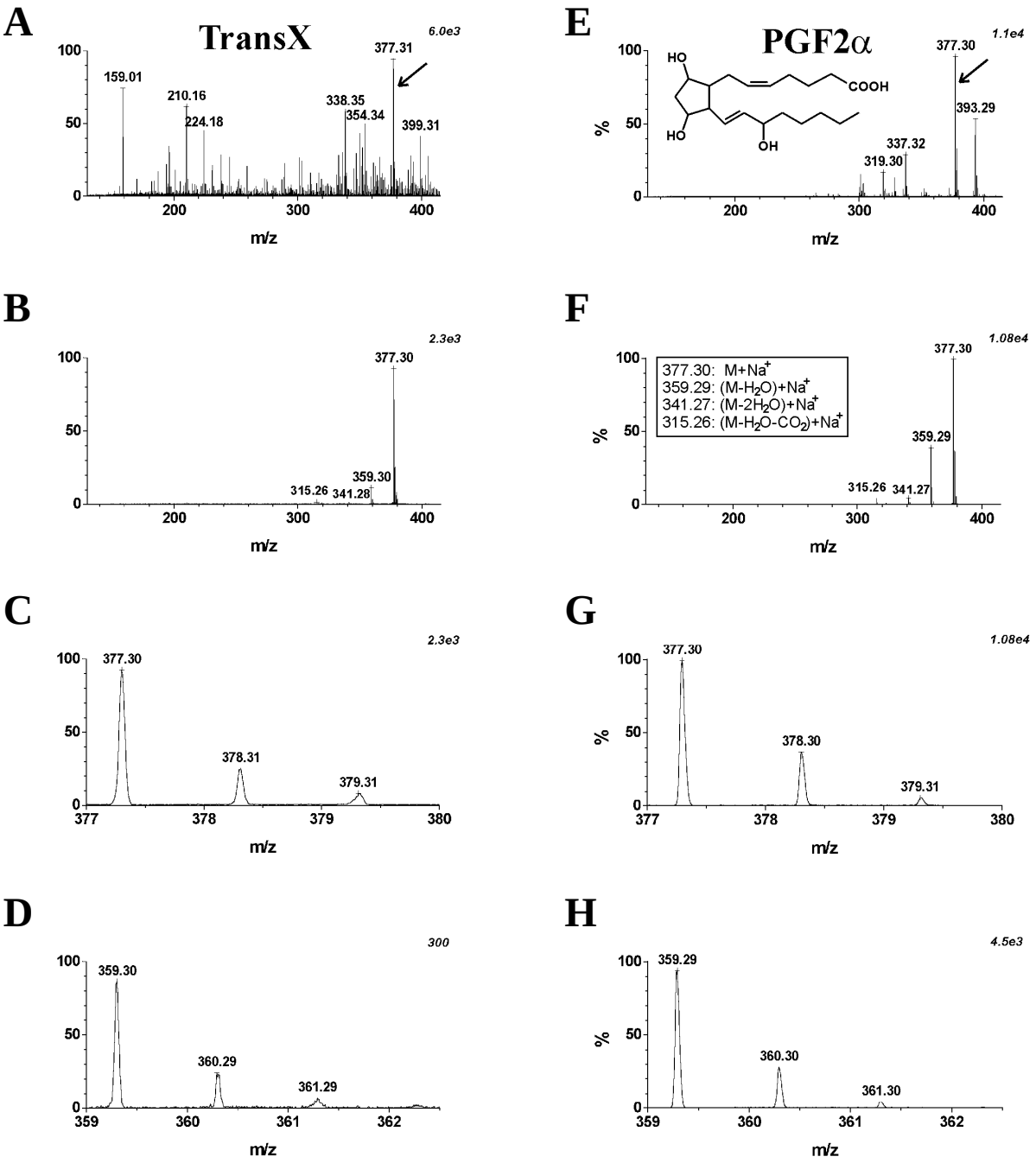

Figure 4 Electrospay ionization-mass spectra of the purified active fraction (TransX) and commercial PGF2α. **A)** ESI-MS spectrum of the purified fraction. **B)** ESI-MS/MS spectrum of m/z 377.3 in this fraction (indicated by the arrow in panel A) and amplifications of the isotope peaks **C)** m/z 377.3 and **D)** 359.3 in this spectrum. **E)** ESI-MS spectrum of commercial PGF2α (1μl; 1mM) with the inset showing the chemical structure of PGF2α. **F)** ESI-MS/MS spectrum of m/z 377.3 in the PGF2α sample and amplifications of the isotope peaks **G)** m/z 377.3 and **H)** 359.3 of this spectrum. In all experiments positive ions were detected.

Table 1: PGF2α concentration determined by immunoassay in the conditioned medium of NRK fibroblasts cultured under different conditions.

growth state	COX-inh.[#]	concentration (nM)
quiescent	-	<1
density arrested	-	1.5[a]
density arrested	+	<1[a]
transformed	-	20.5[b]
transformed	+	<1[b]
transformed	-	3.6[c]
transformed	+	<1[c]

[#]NRK cells were cultured either in the presence (+) or absence (-) of COX-inhibitors (cocktail of indomethacin/flurbiprofen/ibuprofen; all 5 μM).

[a] determined 2 days after addition of EGF/insulin to quiescent monolayers

[b] determined 2 days after addition of EGF/insulin/RA to density arrested monolayers

[c] determined 8 h after addition of fresh culture medium to transformed NRK cells

medium from phenotypically transformed NRK cells and a subsequent incubation in fresh serum-free medium, these cells continued with the release of PGF2α and the concentration after 8 h of incubation was 3.6 nM. In agreement with the previous observation that no depolarizing activity was measured in media conditioned by NRK cells cultured in the presence of COX inhibitors (Fig.3), PGF2α could not be detected in such conditioned media by the enzyme immunoassay.

Clearly, these results show that phenotypically transformed NRK cells exhibit an enhanced production and release of PGF2α as the depolarizing activity in their culture medium.

Effect of TransX on the intracellular calcium concentration of quiescent NRK cells

We have recently shown that PGF2α induces unsynchronized intracellular calcium oscillations in NRK cells cultured in quiescent monolayers (Harks et al., 2003b), and by performing dynamic video imaging measurements on fura-2 loaded quiescent NRK cells we investigated whether TransX had similar effects on intracellular calcium levels.

Fig. 5A shows the typical calcium response of an individual NRK cell in the monolayer upon exposure to TransX. In the presence of external calcium (1 mM) TransX induced an oscillatory calcium response in most cells (74%), while in the remainder of the cells the initial peak was followed by a plateau phase (n=34). The frequency of the oscillations was highly variable ranging from 0.6 to 1.2 min^{-1}. When calcium was removed from the external medium (1 mM EGTA), only one or two calcium transients were measured. The average response of 37 cells in the same monolayer is shown in Fig. 5B.

So, TransX increases the intracellular calcium concentration in NRK cells by both release from internal stores and calcium influx over the plasma membrane, with properties similar to PGF2α, which further confirms that specifically this prostaglandin is released by the phenotypically transformed NRK cells.

Discussion

In the present study we show that phenotypically transformed NRK fibroblasts exhibit a depolarized membrane compared to their non-transformed counterparts, resulting from a constitutive activation of calcium-dependent chloride channels. The increase of the intracellular calcium concentration responsible for the opening of these channels is caused by PGF2α which is released at strongly elevated concentrations upon transformation of the cells.

Previous studies have shown that NRK fibroblasts serve as an excellent *in vitro* model system for studying density-dependent growth and cellular alterations during transformation (Van Zoelen, 1991). Phenotypic transformation of NRK cells resulting from TGFβ or RA is accompanied by the loss of density-dependent growth inhibition and the ability to proliferate under anchorage-independent

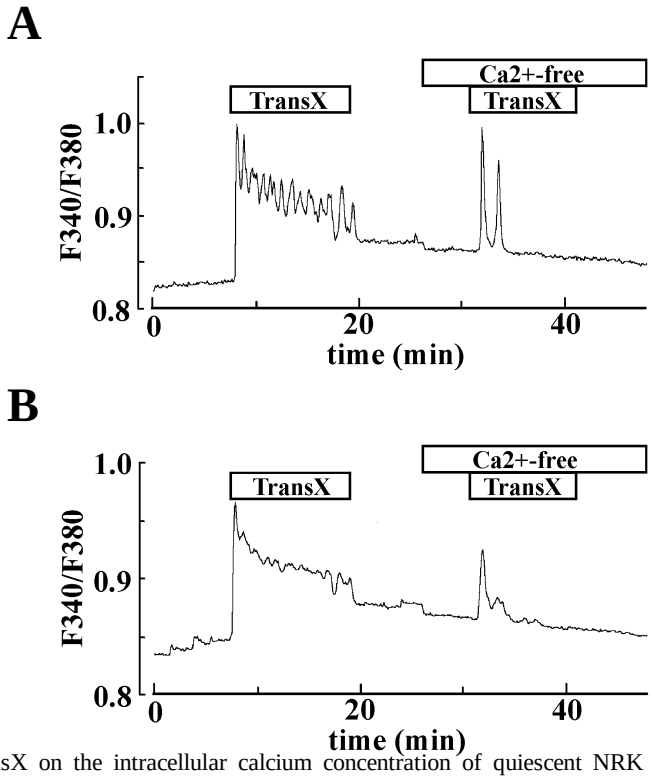

Figure 5 Effect of TransX on the intracellular calcium concentration of quiescent NRK fibroblasts. **A)** Typical calcium response induced by TransX in an individual cells selected from a panel of 37 cells within one monolayer. The response was measured in the presence and absence external calcium **B)** Averaged response of these 37 cells. Addition of the purified fraction (TransX) and calcium-free (1 mM EGTA) solution is indicated by the bars.

conditions (Lahaye et al., 1999a; Van Zoelen et al., 1988), which is the best *in vitro* correlate to tumorigenic behavior of cells *in vivo* (Cifone and Fidler, 1980; Shin et al., 1975). We now show for the first time that phenotypically transformed NRK fibroblasts share two other typical properties with tumor cells. First, phenotypically transformed NRK cells are depolarized compared to their non-transformed counterparts, which is a characteristic for many tumor cells (Marino et al., 1994). Second, in parallel with the enhanced COX activity observed in various types of both human and animal cancer cells (Marnett, 1992), transformed NRK fibroblasts secrete PGF2α in their culture medium at concentrations which are at least 10-fold higher than released by non-transformed NRK cells.

Although, in many cell types tumorigenic transformation results in a reduction or inhibition of gap junctional intercellular communication (Binggeli and Weinstein, 1986; Holder et al., 1993; Loewenstein, 1979), dye-coupling experiments have previously shown that phenotypic transformation of NRK fibroblasts is accompanied by an increase in gap junctional intercellular communication (Van Zoelen and Tertoolen, 1991). In agreement with this, transformed NRK cells seemed to be electrically well coupled as determined by single-electrode patch-clamp experiments (Peters et al., unpublished observation), and thus unlike other cells transformation of NRK cells does not result in a reduction of gap junctional coupling.

The identification of PGF2α as autocrine factor was based on mass spectrometry and confirmed by an enzyme immunoassay. The major peak in the mass spectrum of the purified active fraction was measured at m/z 377.3 and corresponded to PGF2α. The ESI-MS/MS spectrum of this peak, which serves as a fingerprint of the full size molecule, was the same as for commercial PGF2α within an accuracy of ~0.01 m/z. The PGF2α concentration in the conditioned medium of transformed NRK cells as determined by enzyme immunoassay was ~20 nM. Since we previously found that the minimal PGF2α concentration required to constitutively depolarize monolayers of quiescent NRK cells was about 10 nM (Harks et al., 2003b), the concentration present in the conditioned medium of transformed NRK cells is sufficient to explain the depolarizing activity of this medium. This depolarization is caused by the activation of calcium-dependent chloride channels as a result of an increase in the intracellular calcium concentration (De Roos et al., 1997a).

PGF2α enhances the cytoplasmic calcium concentration by activation of the FP-receptor, which is a G-protein coupled receptor (Narumiya et al., 1999). Activation of this receptor is accompanied by an increase in IP_3 and intracellular calcium levels and we have recently shown that in spite of the electrical coupling PGF2α induces unsynchronized intracellular calcium oscillations in NRK cells cultured in quiescent monolayers, which result from an intricate interplay between calcium release from internal stores and calcium influx over the plasma membrane (Harks et al., 2003b). We showed that similar oscillations were measured when TransX was applied to such monolayers, which confirms that PGF2α is the compound that is responsible for the activity of the conditioned medium of phenotypically transformed NRK cells. Both TransX and commercial PGF2α also increased the

intracellular calcium concentration in Swiss 3T3 cells, which have been shown to express the FP-receptor (Woodward and Lawrence, 1994), resulting in these cells in a hyperpolarization of the membrane as a result of the activation of the available calcium-dependent potassium channels (Kusano and Gainer, 1991) (Harks et al., unpublished observation). The membrane potential response of NRK monolayers upon addition of the conditioned medium of transformed NRK cells and TransX showed no homologous desensitization, which is in agreement with the finding that the PGF2α only partially desensitizes its receptor (Fujino et al., 2000), and confirms that the depolarizing activity of this medium is caused by the presence of PGF2α. We have found that PGE2 and PGD2 can mimic the effect of PGF2α on the membrane potential of quiescent NRK monolayers, although only at elevated concentrations (Harks et al., unpublished), which most likely reflects the ability of these prostaglandins to activate the FP-receptor with low affinity (Narumiya et al., 1999). Although it cannot be excluded that apart from PGF2α, phenotypically transformed NRK fibroblasts also secrete low concentrations of other prostaglandins, including PGE2 and PGD2, these prostaglandins were not found in the mass spectrum of the purified active fraction of the conditioned medium.

In recent years, many studies have been performed to elucidate the role of the cyclooxygenase enzyme (COX) and the production of prostaglandins in relation to cancer. (Bishop-Bailey et al., 2002; Prescott and Fitzpatrick, 2000; Singh-Ranger and Mokbel, 2002). While COX-1 is constitutively expressed in most tissues and involved in cellular physiological functions (DeWitt and Smith, 1995; Smith et al., 1994), COX-2 is inducible by growth factors, cytokines and tumor promoters, including EGF, TGFβ and LPA (Bradbury et al., 2002; Ershov and Bazan, 1999; Sato et al., 1997). Overexpression of COX-2 has been found to be play a key role in various stages of tumorigenesis (Singh and Lucci, 2002). While in most tumors particularly PGE2 seems to play a key role in tumor promotion (Sheng et al., 2001; Zweifel et al., 2002), COX-2-derived PGF2α has been identified as an endogenous tumor promoter in the mouse skin model of multistage carcinogenesis (Furstenberger et al., 1989) and seems to be involved in tumor promotion in the kidney (Iqbal et al., 1997). Nonsteroidal anti-inflammatory drugs (NSAIDs), such as aspirin, indomethacin, ibuprofen and flurbiprofen interrupt prostaglandin synthesis by inhibiting the COX reaction and both *in vitro* and animal models have shown that these drugs have promising properties for potential antitumor therapies (Bishop-Bailey et al., 2002). However, NSAIDs block both the "house-keeping" COX-1 and the "inflammatory" COX-2 enzyme which are both important for the regulation of angiogenesis, and as a result gastrointestinal side effects have been reported in patients using NSAIDs (Jones et al., 1999; Tanaka et al., 2002). For this reason increasing efforts are ongoing to develop inhibitors that specifically block COX-2 (Davies et al., 2002; Kalgutkar et al., 2000), and NRK fibroblasts may serve as a model system for studying the role of regulation of COX activity in cellular transformation.

Since the depolarizing activity was found in the conditioned medium of NRK fibroblasts, irrespectively whether they had been transformed with either RA, TGFβ or LPA, the production of

PGF2α seems to be a general property of transformed NRK cells and independent of way their transformation was achieved. The production of PGF2α by phenotypically transformed NRK cells was prevented by a cocktail of COX inhibitors. Moreover, the transformation of density-arrested NRK cells appears to be prevented or at least retarded in the presence of COX inhibitors, since after 2-4 days the cells still had the appearance of a normal monolayer culture while the control cells (stimulated in the absence of COX inhibitors) grew in cellular multilayers (Peters et al., unpublished observation). This indicates that the secreted PGF2α may be directly involved in the transformation process. We now propose two mechanisms by which PGF2α may contribute to the transformation of NRK fibroblasts. The first mechanism involves a critical role for the EGF receptor. Previously, it has been shown that phenotypic transformation of NRK fibroblasts is accompanied by an upregulation of the EGF receptor expression (Assoian et al., 1984; Van Zoelen et al., 1986), which explains that transformation can only be measured under conditions that the polypeptide growth factor EGF is present. Notably, PGF2α has been reported as one of the transforming agents that could transform NRK monolayers in the presence of EGF (Lahaye et al., 1999b), and pretreatment of quiescent NRK cells with PGF2α enhanced the subsequent EGF-induced proliferation (Lahaye et al., 1998). Therefore, we hypothesize that secreted PGF2α mediates the transformation of NRK cells by an upregulation of the expression of EGF receptors, thereby accelerating their proliferation in the presence of EGF. In this way, PGF2α may even induce phenotypic transformation in surrounding non-transformed cells by a paracrine action. The second pathway by which secreted PGF2α may contribute to transformation is via intracellular calcium, which regulates a great diversity of cellular processes (Berridge et al., 1998). The precursor of prostaglandins, arachidonic acid, is liberated from membrane phospholipids by phospholipase A2 (PLA2) and the activity of this enzyme is enhanced by increased calcium concentrations (Kramer and Sharp, 1997). So, by increasing the cytoplasmic calcium concentration PGF2α may stimulate arachidonic acid release and enhance its own production, such that the transformation process could be potentiated. Previously, it has been shown that NRK cells exhibit a transformed phenotype when the 43 kDa inositol polyphosphate 5-phosphatase is underexpressed and as a result have an increased basal intracellular calcium concentration (Speed et al., 1996). Based upon our present findings, we suggest that the elevated calcium concentration in these cells was paralleled by an enhanced PLA2 activity and the release of PGF2α, which may have contributed to the transformation of these transfected NRK cells.

Taken together, the results in the present study show that phenotypic transformation of NRK fibroblasts is accompanied by the secretion of PGF2α, presumably due to enhanced COX activity, thereby depolarizing the membrane of these cells. These effects may contribute to the transformation of cultured NRK cells and inhibiting the production of PGF2α with COX-inhibitors may counteract this process.

Acknowlegdements.

We thank Dr. E. Pierson (General Instrumentation, KUN-FNWI) for expert technical assistance with the digital imaging experiments and Hans Damen (SMO-Eindhoven) for technical assistance with HPLC experiments.

Materials and Methods

Cell culturing: Normal rat kidney fibroblasts (NRK clone 49F) and Swiss 3T3 fibroblasts (clone C7C2) were cultured in bicarbonate-buffered Dulbecco's modified Eagle's medium (DMEM; Life Technologies, Paisly, UK) supplemented with 10% newborn calf serum (HyClone Laboratories, Logan, UT, US). Confluent cultures were made quiescent by a subsequent one to three days incubation in serum-free DF medium (DMEM/Ham's F12, 1:1; Gibco; Life Technologies, Paisly, UK) supplemented with 30 nM Na_2SeO_3 and 10 μg/ml human transferrin. By the subsequent incubation for 48 h with 5 ng/ml EGF (Collaborative Biomedical Products, Bedford, US) in combination with 5 μg/ml insulin (Sigma, St. Louis, MO, US), density-arrested monolayers were obtained. Phenotypically transformed NRK cells were obtained by the addition of 50 ng/ml RA in combination with 5 ng/ml EGF and 5 μg/ml insulin to density-arrested monolayers. For the collection of conditioned media NRK cells were cultured in flasks (175 cm^2) in the presence of 50 ml culture medium.

Electrophysiology: Whole-cell current-clamp experiments were performed on NRK cells that were perfused at room temperature with serum-free DF medium equilibrated with 7.5% CO_2 to pH 7.4. Intracellular pipette solution contained (in mM) 25 NaCl, 120 KCl, 1.0 $CaCl_2$, 1.0 $MgCl_2$, 3.5 EGTA, 10 HEPES/KOH (pH 7.4). Data were obtained with an EPC-7 patch-clamp amplifier (List Electronic, Darmstadt, Germany) in conjunction with Pulse/Pulsefit software (HEKA Elektronik, Lambrecht, Germany). Borosilicate patch pipettes (GC150-15; Clark, Reading, UK) with resistances of 4-6 MΩ were used.

Intracellular calcium measurements: Coverslips with monolayers of NRK fibroblasts were placed in a Leiden cell chamber and loaded for 30 min at room temperature with 2 μM fura-2/AM (Molecular Probes, Eugene, OR, US) in Hanks' medium containing (in mM) 137 NaCl, 5.4 KCl, 1.0 $CaCl_2$, 0.50 $MgCl_2$, 0.40 $MgSO_4$, 4.2 $NaHCO_3$, 0.34 NaH_2PO_4, 0.35 KH_2PO_4 and 5.6 glucose (pH 7.4) supplemented with 0.025% Pluronic F127 and 3% FCS. Dynamic video imaging was performed as described elsewhere (Cornelisse et al., 2002). Excitation wavelengths of 340 nm and 380 nm (band width 8-15 nm) were provided by a 150 W Xenon lamp (Ushio UXL S150 MO, Ushio, Tokio, Japan) and fura-2 fluorescence emission was monitored, using a 440 nm cut off DCLP dichroic mirror in front of a Coolsnap fx monochrome digital camera (Roper Scientific, Tucson, US). Image acquisition, using a camera pixel binning of 4, and computation of ratio images (F340/F380) was every 6 s and was operated through Metafluor v.4.6 (Universal Imaging Corporation, Downingtown, PA, US). Camera acquisition time was 100 ms per excitation wavelength.

Purification procedure: The biologically active compound secreted by transformed NRK fibroblasts was purified from the culture medium by applying several separation steps. First, solid phase extraction (Sep-Pak C18; Waters, Milford MA, US) was performed and the activity eluted with in 0.1% acetic acid in ethanol. Aliquots of the active fraction were dried under N_2, resuspended in 10% acetonitrile with 0.1% TFA and subsequently loaded on a Ultrasphere ODS 5u (ID=4.6mm; L=25cm) reversed-phase HPLC column (Beckman, San Ramon CA, US). A linear gradient was applied from 0-90% acetonitrile in 0.1% TFA at a flow rate of 1 ml/min. The active HPLC fraction was loaded on a Superdex Peptide HR 10/30 gel permeation column (Pharmacia, Peapack NJ, US) and eluted with 27% acetonitrile in 0.1% TFA at a flow rate of 0.1 ml/min. The purified fraction was loaded on a second reversed-phase HPLC (100 μl direct loop injection) at a flow rate of 0.1 ml/min using a Alltima C18 5u (ID=2.1 mm; L=150 mm) column (Alltech, Deerfield IL, US). A linear gradient was applied from 0-90% acetonitrile in 0.1% TFA. Active fractions were analyzed along the purification procedure by testing it for the ability to depolarize confluent monolayers of quiescent NRK cells in patch-clamp experiments (*see* subhead electrophysiology).

ESI-TOF mass spectrometry:

The HPLC-purified active fraction (provisionally referred to as "TransX") and prostaglandins were analyzed with a Micromass Q-ToF Ultima Global (Micromass Ltd., Manchester, UK) equipped with an electrospray ionization (ESI) probe. The Flow Injection Analysis (FIA) mode was used at a flow rate of 50 µl/min (50% acetonitrile in 0.1% acetic acid). The instrument was operated in the positive mode, mass spectra were acquired using Time of Flight (ToF) mass separation and were collected over the mass-to-charge (m/z) range 150-2000.

Enzyme immunoassay:

The PGF2α concentration was determined in the conditioned media of NRK cells cultured under different growth conditions using an enzyme immunoassay kit (Cayman Chemicals; Ann Arbor, MI) according to the manufacturer's protocol.

CHAPTER 8

General Discussion

Normal rat kidney (NRK) fibroblasts have previously been described as an excellent cellular model system for studying the mechanisms of density-dependent growth inhibition and alterations upon phenotypic transformation (Van Zoelen, 1991). Since fibroblasts are considered as classical examples of non-excitable cells, it was rather surprising that NRK fibroblasts repetitively fired calcium action potentials when they were cultured to density-arrest (De Roos et al., 1997c). The present study was aimed to elucidate the underlying mechanisms that determine the excitability and periodicity in firing of NRK cells. We have demonstrated how an L-type calcium conductance (G_{CaL}), a calcium-activated chloride conductance ($G_{Cl(Ca)}$), an inwardly rectifying potassium conductance (G_{Kir}), and gap junctional intercellular communication (GJIC) contribute to action potential firing and propagation in NRK cells. Moreover, we have shown that the cytosolic calcium concentration can oscillate in these cells by an intricate interplay between internal calcium stores and plasma membrane ion channels. Such intracellular calcium oscillations provide NRK cells with a timing mechanism, and we will argue that they may underlie periodic action potential firing. During our studies we discovered a novel property of fenamates and 2-aminoethoxydiphenyl borate (2-APB), namely their ability to block gap junctions. The uncoupling action of 2-APB is unique, since 2-APB appears to be the first gap junction blocker that does not affect plasma membrane channels. Thus, it can be used to study ion channel properties in single cells in undissociated tissues. Finally, we have shown that NRK cells become depolarized and secrete a biologically active prostaglandin upon phenotypic transformation, which are both typical consequences of tumorigenic transformation. Although many tumor cells have been shown to secrete prostaglandin E2 (PGE2), transformed NRK fibroblasts secrete particularly prostaglandin F2α (PGF2α), which increases the intracellular calcium concentration and depolarizes non-transformed NRK cells.

It has been established by others that the expression level of the epidermal growth factor (EGF) receptor plays a key role in growth regulation of NRK cells (Lahaye et al., 1998; Rizzino et al., 1990; Van Zoelen, 1991). In our studies we have focused on the biophysical aspects of NRK cells including membrane potential, intracellular calcium dynamics and GJIC, in relation to their growth regulation.

Membrane potential and growth regulation

Confluent monolayers of quiescent NRK cells exhibit a resting membrane potential of around -70 mV, which is primarily determined by potassium conductances. Upon stimulation of these monolayers with bradykinin (BK), PGF2α or endothelin-1 (ET-1), all agonists of G-protein coupled receptors that have

been shown to modulate the proliferation of NRK cells (Lahaye et al., 1998; Lahaye et al., 1999b), the membrane depolarizes towards -20 mV by the opening of calcium-activated chloride channels (De Roos et al., 1997a). This depolarization by itself does not seem to be a mitogenic signal for these cells since bradykinin and ET-1 have no significant growth stimulatory activity on quiescent NRK cells, while PGF2α is only slightly mitogenic (Lahaye et al., 1999b). Moreover, monolayers of serum-grown proliferating NRK cells exhibited a similar resting membrane potential as quiescent monolayers (Harks et al., unpublished), indicating that proliferating NRK cells are not necessarily depolarized compared to their non-proliferating counterparts, which is in contrast to several other cell types (Binggeli and Weinstein, 1986).

The previous finding that density-arrested monolayers of NRK cells repetitively fire calcium action potentials, raised the question whether these action potentials mediate growth inhibition of NRK cells (De Roos et al., 1997c). It is unlikely however that they act as a growth-inhibiting signal since similar action potential firing was measured in NRK cells that had been transformed from quiescent monolayers, under conditions that density-dependent growth inhibition was prevented (Harks et al., unpublished; *see* chapter 1, Fig. 1 for growth conditions). Therefore, spontaneous action potential firing in NRK cells seems to be related to cell density, but not to regulation of density-dependent growth inhibition. After about 3-4 days of culturing quiescent NRK cells in the presence of transforming agents, the cells became constitutively depolarized around -20 mV, similarly as for NRK cells that had been transformed from density-arrested monolayers without development of action potentials. Such depolarization is in agreement with previous reports showing that tumorigenic transformation is often accompanied by a depolarization of the cells (Marino et al., 1994).

In chapter 3, we have characterized the membrane conductances that are present in quiescent NRK cells, and preliminary voltage-clamp experiments showed that the same conductances are also present in phenotypically transformed NRK cells (Harks et al., unpublished). Therefore, the depolarized membrane potential of phenotypically transformed NRK cells does not result from the expression of additional membrane conductances in transformed cells. Instead, it is caused by the constitutive opening of calcium-activated chloride channels and we have shown that this at least results in part from the autocrine secretion of a substance, PGF2α, in the culture medium of these cells, since we observed membrane repolarization upon washout with fresh medium (chapter 7). So, the PGF2α present in the culture medium of phenotypically transformed NRK cells increases the intracellular calcium concentration in these cells, thereby depolarizing them by the activation of calcium-dependent chloride channels. Although it would be interesting to establish the role of the membrane potential in the transformation of NRK cells, this cannot be achieved by a simple block of the PGF2α production, because PGF2α has more effects on NRK cells that may play a role in the transformation process. These include the elevation of the intracellular calcium concentration (chapter 6), and the enhancement of the EGF receptor expression (Lahaye et al., 1999b).

Inhibition of K^+ and Cl^- channels has been shown to block cell cycle progression in several cell types (Wonderlin and Strobl, 1996; Zheng et al., 2003). Therefore, it would be interesting to assess the role of G_{Kir} and $G_{Cl(Ca)}$ in the transformation of NRK cells, for example by culturing them in the additional presence of specific ion channel blockers. It should be realized, however, that prolonged treatment with these agents may be toxic to the cells. To circumvent this problem, specific knock-down of genes encoding for such ion channels in NRK fibroblasts by RNA interference (RNAi) may be useful. This relatively new technique is based on a sequence-specific degradation of messenger RNA (mRNA) by small interfering RNA (siRNA), thereby effectively silencing the expression of a given gene (for review *see* e.g. Brantl, 2002). Since inward rectifier potassium channels are essential for establishing the resting membrane potential in NRK cells around -70 mV (chapter 3), it would be interesting to test whether a knock-down of these channels in NRK cells with siRNA results in a depolarized membrane potential around -20 mV and uncontrolled proliferation as in transformed NRK cells.

Taken together, the membrane potential as such does not seem to play a major regulatory role in the proliferation of NRK cells, although it is related to cell density.

Intracellular calcium and growth regulation

Calcium is a universal second messenger that regulates a vast diversity of cellular events, including cell proliferation (Berridge, 1995a; Berridge et al., 1998). In most cells a rise in intracellular calcium is associated with oscillatory changes in the free calcium concentration and recent studies have revealed that the amplitude, duration and frequency of calcium signals affect the efficiency and specificity of gene expression (Berridge, 1997; Dolmetsch et al., 1998; Li et al., 1998b).

Several growth modulating agonists of NRK cells have been shown to elevate intracellular calcium levels in a transient manner (Afink et al., 1994; De Roos et al., 1997a; Lahaye et al., 1999b). Although ET-1, lysophosphatidic acid (LPA), BK and PGF2α all increase the intracellular calcium concentration in monolayers of NRK fibroblasts, these four agonists have different effects on the proliferation of NRK cells. LPA is mitogenic by itself by activation of a G_i-coupled receptor (Van Corven et al., 1989), while the three other agonists require the additional presence of EGF to induce proliferation of NRK cells (Lahaye et al., 1999b). Moreover, ET-1 and LPA rapidly induce phenotypic transformation whereas BK initially inhibits transformation of NRK cells (Afink et al., 1994; Lahaye et al., 1994). These results show that an increase in the intracellular calcium concentration is insufficient to trigger cell growth and indicate that activation of additional pathways is required for growth regulation.

The spontaneous action potentials in density-arrested NRK monolayers were accompanied by synchronized calcium transients (De Roos et al., 1997c), but similar action potentials have sometimes been observed in phenotypically transformed NRK cells (Harks et al., unpublished). It is therefore unlikely that these calcium transients mediate density-dependent growth inhibition. In addition, the calcium transients resulted from the regenerative opening of L-type calcium channels and it has

previously been shown that calcium influx through L-type calcium channels in PC12 cells leads to EGF receptor phosphorylation, MAPK activation and *c-fos* tanscription, thus stimulating growth factor receptor signaling (Rosen and Greenberg, 1996; Zwick et al., 1997; Zwick et al., 1999). These results suggest that if the calcium transients affect the proliferation of NRK cells, they most likely stimulate rather than inhibit cell growth.

Although we have not measured the intracellular calcium concentration in phenotypically transformed NRK cells, we expect that the average concentration is elevated compared to non-transformed NRK cells. First, transformed cells are constitutively depolarized due to the opening of chloride channels, which are dependent on the binding of intracellular calcium for their activation. In addition, transformed NRK cells secrete PGF2α, which induces unsynchronized calcium oscillations in monolayers of quiescent NRK cells (chapter 7). In fact, Speed and coworkers have measured spontaneous calcium oscillations in NRK cells that had been transformed by the underexpression the 43 kDa inositol polyphosphate 5-phosphatase, which was achieved by antisense transfection with the cDNA encoding this enzyme (Speed et al., 1999). These oscillations were measured in 14% of the cells and varied in frequency and intensity. We found that the secretion of PGF2α by transformed NRK cells is independent of the pathway of transformation (chapter 7), and therefore we expect that the oscillations measured in the NRK cells underexpressing the 43 kDa inositol polyphosphate 5-phosphatase were also caused by secreted PGF2α. However, it remains unclear whether such unsynchronized calcium oscillations may contribute in any way to the transformation of NRK cells.

Previously, it has been shown that cell growth can be correlated to the calcium content in internal stores, such that growth-inhibited cells have a reduced calcium pool load (Legrand et al., 2001; Short et al., 1993). Although we have not quantified the calcium content in internal stores of NRK cells at different growth conditions, it is unlikely that this parameter plays a regulatory role in the proliferation of NRK cells. First, calcium stores in density-arrested NRK cells were still filled, since BK could mobilize internal calcium in these cells, and therefore density-dependent growth inhibition of NRK cells does not result from a depletion of internal calcium stores (De Roos et al., 1997c). Moreover, NRK cells with decreased 43 kDa polyphosphate 5-phosphatase activity obtained a transformed phenotype under conditions that internal calcium stores were partially (40%) emptied (Speed et al., 1999), indicating that NRK cells are still able to proliferate under conditions that the calcium content in their stores is significantly reduced.

Gap junctional coupling and growth regulation

Gap junctional intercellular communication (GJIC) has an important function in maintaining tissue homeostasis and the role of GJIC in cell growth regulation has been widely studied. Previously, it has been postulated that an increase in GJIC at higher cell densities plays a role in growth arrest (Loewenstein, 1981), and it has been shown that GJIC is necessary for growth inhibition of 3T3 fibroblasts (Ruch et al., 1995). However, density-dependent growth inhibition of NRK cells is not

caused by an enhanced GJIC. Although NRK cells in density-arrested monolayers are electrically well-coupled (Harks et al., unpublished), these cells are also well-coupled when cultured in quiescent monolayers (chapter 2,5,6). In spite of this good electrical coupling, dye-coupling experiments have revealed that NRK cells in both density-arrested and quiescent monolayers show only limited GJIC (Van Zoelen and Tertoolen, 1991). In most tumor cells, GJIC is reduced or absent (Binggeli and Weinstein, 1986; Holder et al., 1993; Loewenstein, 1979), whereas reversion of the transformed phenotype could be achieved by the restoration of GJIC (Mesnil, 2002). This indicates that GJIC plays an important role in carcinogenesis, and chemopreventive strategies have been designed to prevent down regulation of GJIC by tumor promoters and to restore GJIC in neoplastic cells (Trosko and Ruch, 2002). On the other hand, phenotypically transformed NRK cells show enhanced dye-coupling compared to their non-transformed counterparts (Van Zoelen and Tertoolen, 1991). In agreement with this, capacitance measurements have revealed that also transformed NRK cells are electrically well-coupled (Harks et al., unpublished). So, transformation of NRK cells does not require a reduction of GJIC. In support of this, it has been shown that other transformed cells also exhibit high levels of intercellular communication (Enomoto and Yamasaki, 1984).

Ion channel composition for excitability of NRK fibroblasts

Although fibroblasts are generally considered as non-excitable cells, previous studies have already shown that NRK fibroblasts have excitable properties under certain growth conditions and are able to generate spontaneous or evoked action potentials, which are propagated by electrical conduction through gap junctions between cells in a confluent monolayer (De Roos et al., 1997c; De Roos et al., 1997d). We have investigated the ionic basis for this excitability and determined values for coupling and ion channel conductances by performing voltage-clamp experiments (chapters 2 and 3). The major plasma membrane ion conductances that constitute the components for excitability of NRK fibroblasts were assessed in voltage-clamp experiments on single NRK cells and small clusters of NRK cells that had been dissociated from quiescent monolayers. NRK cells are electrically well-coupled (De Roos et al., 1996), and therefore we could measure membrane currents under acceptable voltage-clamp conditions in small clusters (chapter 3). The advantage of experiments on clusters is that the membrane currents are measured under more physiological conditions than in single cells, due to the reduced effect of washout by the pipette solution. In fact, voltage-clamping cell clusters is comparable to measurements in the perforated patch-clamp mode, thereby considering gap junctional channels between the patched cell and its surrounding cells as the access to an NRK "super cell," formed by the cell ring around this centered cell. Another advantage of measuring on clusters is that current amplitudes are increased and that differences between individual cells are averaged. Especially the L-type current, which is sometimes hardly detectable in single cells, can easily be measured in this way. It should be realized, however, that for acceptable voltage-clamp recordings the gap junctional

series resistance to the surrounding cells must be small enough (e.g. <10 MΩ) to avoid significant voltage drop across this resistance at the measured currents.

We have shown that action potentials in NRK cells result from the sequential activation of three types of membrane conductances. First, the initiation of the action potential is caused by the activation of an L-type calcium conductance (G_{CaL}) as a result of a depolarizing step beyond the threshold value for activation of this conductance of around -40 mV (chapter 3). Calcium or strontium entry through L-type calcium channels results in the subsequent activation of a calcium-activated chloride conductance ($G_{Cl(Ca)}$). As a consequence and due to inactivation of the G_{CaL} (*see* chapter 3, Fig. 3), the initial spike of the action potential in NRK monolayers repolarizes towards -20 mV, which is the equilibrium potential for chloride in these monolayers (De Roos et al., 1997a). The following long lasting plateau phase (~30 s) is paralleled by a transient increase in the intracellular calcium concentration, resulting from calcium influx through G_{CaL} and probably supported by release from internal calcium stores. Upon removal of intracellular calcium, presumably by uptake into internal calcium stores and extrusion by plasma membrane ATP-ases, $G_{Cl(Ca)}$ becomes inactivated which makes NRK cells subject to repolarization by the activity of an inwardly rectifying potassium conductance (G_{Kir}). For the propagation of action potentials throughout confluent monolayers intercellular coupling by a gap junctional conductance (G_{gj}) is required. The mathematical model developed provided insight into the contribution of each membrane conductance in the excitability of NRK fibroblasts (chapter 4, Fig 4B). It will be interesting to determine with this model what the minimal and maximal values of each conductance are that are required for excitability.

The action potential can be triggered in single cells and clusters by current injection, and in monolayers by a local stimulation with a high $[K^+]$ or calcium mobilizing agent. The presence of G_{CaL} in NRK cells has previously been reported (De Roos et al., 1997c), while Western blot analysis revealed that NRK fibroblasts express the cardiac subtype of L-type calcium channels (De Kock, 1999). The characterization of the kinetic properties of G_{CaL} in voltage-clamp experiments showed that a small voltage window exists between -40 and -10 mV at which the G_{CaL} current is activated, but does not completely inactivate (chapter 3). This finding not only explains that the threshold for action potential firing is around -40 mV, but also predicts that under conditions that the action potential does not completely repolarize towards the resting membrane potential (e.g. due to insufficient G_{Kir}), NRK cells exhibit a relatively instable membrane potential which makes them competent to fire additional action potentials in a spontaneous manner. In fact, we found that quiescent monolayers of NRK cells started to fire membrane potential spikes from around -40 mV (-36.3 ± 2.8 mV; mean ± S.E.M., n=4) with a relatively high frequency (0.45 ± 0.03 s^{-1}; mean ± S.E.M., n=4), when inwardly rectifying potassium conductances (G_{Kir}) were blocked by Ba^{2+} under conditions that activation of $G_{Cl(Ca)}$ was prevented by BAPTA-AM (Harks et al., unpublished). This indicates that under specific conditions NRK monolayers can exhibit a relatively unstable membrane potential, which is different from the three more stable membrane potential states described so far (chapter 7, Fig. 1).

The mathematical model showed that a residual L-type calcium current is still present during the plateau of the action potential (*see* chapter 4, Fig 4), which is in agreement with our finding that G_{CaL} does not become completely inactivated at -20 mV (*see* chapter 3, Fig. 3), and which indicates that there is still calcium inflow during the plateau phase of the action potential. This calcium entry through the L-type channels may be amplified by calcium-induced calcium release (CICR) from internal stores but this was not considered in the mathematical model. However, L-type calcium channels are known to be functionally linked to ryanodine-sensitive calcium stores in muscle cells (Protasi, 2002), and therefore it would be interesting to test whether calcium release from these stores contributes to the prolongation of the plateau phase of the action potential in NRK cells. Preliminary experiments already revealed the existence of ryanodine-sensitive calcium stores in NRK fibroblasts (*see* below) and inhibition of ryanodine receptors by a high ryanodine concentration (50 μM) should reduce the duration of the plateau of evoked calcium action potentials. The role of intracellular calcium in the prolongation of the action potential became apparent when the plateau of the action potential disappeared under conditions that intracellular calcium was buffered by BAPTA-AM (chapter 3, Fig 6). The contribution of calcium removal mechanisms to the length of the plateau phase could be established by a partial block of SERCA pumps and plasma membrane ATP-ases.

Calcium-activated chloride channels are expressed in many cell types including non-excitable cells, such as epithelial, endothelial and blood cells. They are also found in excitable cells, such as neurones, cardiac and smooth muscle cells. The presence of $G_{Cl(Ca)}$ in NRK fibroblasts has previously been shown in current-clamp experiments (De Roos et al., 1997a) and has been confirmed in voltage-clamp experiments (chapter 3). The features of $G_{Cl(Ca)}$ are generally very similar in the various cell types, such that they are activated in a voltage-dependent manner as a result of an increase in the cytosolic calcium concentration (Nilius and Droogmans, 2003). They exhibit outward rectification and their activation at positive potentials is slow. These typical features of calcium-activated chloride channels became only in part evident in our voltage-clamp experiments on NRK cells, because its activation was caused by a dynamic change in the intracellular calcium concentration upon calcium entry through G_{CaL}. In order to fully characterize $G_{Cl(Ca)}$ in NRK cells it is necessary to isolate this conductance by blocking the others and measure its voltage-dependent activation at various clamped intracellular calcium concentrations. Molecular identification of the NRK-$G_{Cl(Ca)}$ would require cloning and sequencing of the channel gene and comparing it with published sequencies (cf. Gruber et al., 1998).

The presence of the inward rectifier has not been shown before in NRK fibroblasts, although it has previously been identified in other fibroblastic cells (Bakhramov et al., 1995; Estacion, 1991). The role of G_{Kir} is multiple. First, it serves to establish the resting membrane potential around -70 mV as indicated by the observation that inhibition by Cs^+ or Ba^{2+} resulted in a depolarization (chapter 3). Second, G_{Kir} channels serve to contribute to the initiation of the action potential because they deactivate upon depolarization, thereby lowering the threshold for excitability (chapter 4, Fig 4B).

Finally, regenerative activation of G_{Kir} is crucial for the repolarization of the action potential since this repolarization was prevented under conditions that G_{Kir} was blocked (*see* chapter 3, Fig. 6). Activation of G_{Kir} during the repolarization is also indicated in the mathematical model (*see* chapter 4, Fig.4B), while it has previously been shown to contribute to the repolarization of the cardiac action potential from -20 to -60 mV (Ishihara et al., 2002). So far, at least seven major subfamilies of inward rectifier potassium channels have been reported, while these subfamilies contain several subtypes (Abraham et al., 1999). Based on the voltage-clamp properties, G_{Kir} in NRK fibroblasts seems to share functional properties with Kir2.1, which is a strong inward rectifier that is essential for the cardiac repolarization and maintenance of the cardiac resting membrane potential (Miake et al., 2003). However, the identity of this subtype in NRK cells should be confirmed by cloning and sequencing (cf. Kubo et al., 1993).

Action potentials could be evoked in a significant fraction (~25%) of single cells by current injection (chapter 3). These results demonstrate that excitability is an intrinsic property of NRK cells and not restricted to cell clusters and monolayers in which cells are coupled by gap junctions. However, for the propagation of action potentials throughout confluent monolayers of cells, GJIC is required and capacitance measurements revealed that quiescent monolayers of NRK cells are electrically well-coupled (chapters 2, 5, 6). The results of the model suggest that the degree of gap junctional coupling between an NRK cell and its surrounding cells is much better than just required for intercellular action potential conduction (chapter 4, Fig. 10, 11). The propagation velocity of the action potential evoked in a network of 9 x 9 model cells was ~1.5 mm/s (chapter 4, Fig. 12), and thus of the same order of magnitude as for the locally induced propagating action potential in NRK monolayers, which propagated at a velocity of ~6 mm/s (De Roos et al., 1997d). Due to the extensive electrical coupling it was not possible, however, to evoke monolayer action potentials by stimulating single cells or small areas of cells embedded in the monolayer (chapter 4, Fig. 12).

In spite of the extensive electrical coupling of NRK cells, dye-coupling experiments have previously shown that these monolayers exhibit only poor diffusion-coupling (Van Zoelen and Tertoolen, 1991). A similar discrepancy between electrical coupling and dye-coupling has also been shown in pancreatic islet cells (Quesada et al., 2003), and may explain why the membrane potential of NRK monolayers responds as a whole upon PGF2α stimulation, whereas intracellular calcium oscillations are unsynchronized (chapter 6).

Unique for the action potential firing in NRK fibroblasts is the bifunctional role that cytosolic calcium plays in the excitability mechanism. First, as mentioned before, action potential firing is accompanied by an increase in cytosolic calcium concentration resulting from calcium influx through L-type calcium channels and probably supported by release from internal stores. However, intracellular calcium itself can also be the trigger for the initiation of an action potential, since $G_{Cl(Ca)}$ is activated at elevated intracellular calcium concentrations, e.g. by agonist-induced release from IP_3-sensitive calcium stores, thereby depolarizing NRK cells beyond the threshold for activation of G_{CaL}.

So, calcium dynamics and membrane potential signaling in NRK cells are linked by calcium-activated chloride channels.

Proposed mechanism for repetitive action potential firing in density-arrested monolayers

Although a propagating action potential could be simulated with the mathematical model on the basis of the membrane conductances present in quiescent NRK cells, it was not possible to describe repetitive action potential firing as observed in density-arrested monolayers (chapter 4). Thus, the model is unable to predict spontaneous firing as a result of altered expression levels of ion conducting channels in density-arrested NRK cultures as previously suggested for a density-dependent modulation of L-type calcium channels (De Roos et al., 1997c). In addition, NRK cells are capable to fire a subsequent action potential within 1 s after repolarization of the preceding action potential (chapter 3, Fig. 5B), indicating that the interspike interval in repetitively firing density-arrested NRK monolayers (~30-300 s) is not caused by a refractory period of the action potential due to inactivation of the calcium channels. In cardiac action potentials, delayed rectifying potassium conductances play an important role in pacemaking (Hille, 2001), and therefore the expression of this candidate conductance may render density-arrested NRK cells competent for repetitive firing. However, delayed rectifying potassium currents or other additional types of current were not found by preliminary voltage-clamp experiments in single NRK cells or small clusters of these cells when dissociated from density-arrested monolayers. Moreover, action potential firing in density-arrested monolayers remained unaffected in the presence of 10 mM TEA^+ (Harks, et al.; unpublished), indicating that a delayed rectifying potassium conductance is not involved in the firing mechanism (Hille, 2001). We have, therefore, no evidence that spontaneous action potential firing in density-arrested NRK monolayers requires the expression of an additional membrane conductance in these cells.

Three conceptual models can be postulated in which the regenerative action potential firing in density-arrested NRK monolayers results either from synchronized behavior (Fig. 1A) or propagation (Fig. 1B and 1C). In the first model, all NRK cells in the density-arrested monolayer are identical and exhibit synchronized intracellular calcium oscillations which repetitively trigger action potentials by a depolarization of the cells beyond the threshold for activation of G_{CaL} around -40 mV, following a calcium-dependent activation of $G_{Cl(Ca)}$. This is in agreement with the observation that density-arrested monolayers of NRK cells exhibit apparently synchronous intracellular calcium oscillations (De Roos et al., 1997c). Remarkably, the frequency of the IP_3-sensitive calcium oscillations measured upon stimulation of quiescent NRK cells with PGF2α (chapter 6) was of the same order of magnitude as the frequency of the synchronized calcium transients in density-arrested monolayers (De Roos et al., 1997c), both ranging from ~0.2-1.5 min^{-1}. Therefore such IP_3-sensitive calcium oscillation may perhaps also be the basis of the repetitive action potential firing in density-arrested NRK monolayers. However, in contrast to the IP_3-sensitive calcium oscillations in quiescent monolayers which remained

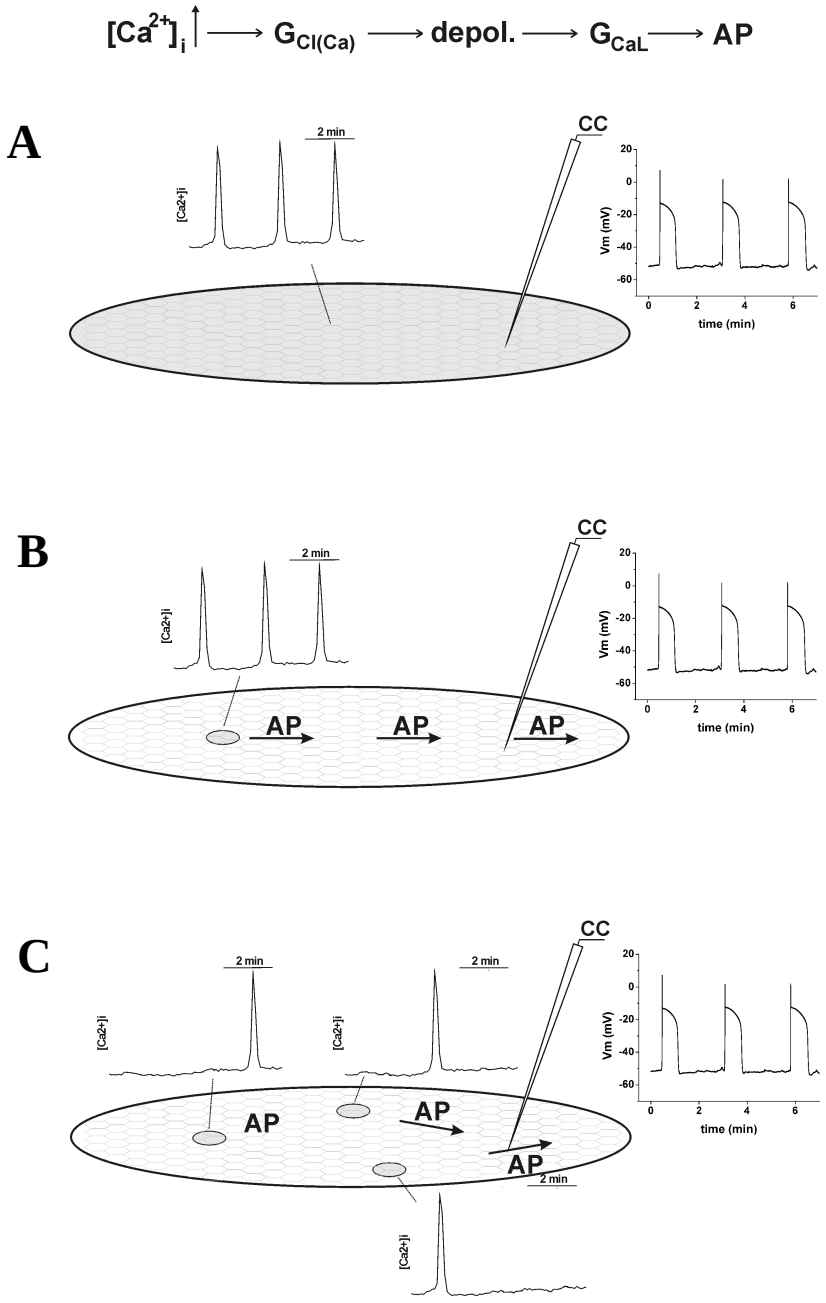

Figure 1 Proposed mechanisms for repetitive action potential firing in monolayers of NRK fibroblasts with the pacemaker mechanism localized in an intracellular calcium oscillation mechanism. An increase in the intracellular calcium concentration ($[Ca^{2+}]_i$), results in the activation of a calcium-dependent chloride conductance (G_{ClCa}), thereby depolarizing the membrane towards the equilibrium potential for chloride around -20 mV. Hence, the membrane potential passes the threshold for activation of the L-type calcium conductance (G_{caL}) around -40 mV, such that action potentials (AP) are triggered. In this schematic representation of a confluent monolayer of density-arrested NRK cells, the areas colored light-gray represent pacemaking cells which exhibit intracellular calcium oscillations that trigger the action potentials, whereas the white cells are the follower cells which only transduce these evoked action potentials. The membrane potential is recorded via the patch-electrode as indicated. Three conceptual models are depicted in order to explain the repetitive action potential firing in these monolayers in which **A)** all monolayer cells exhibit intracellular calcium oscillations that trigger action potentials, **B)** propagating action potentials are triggered from a pacemaker region at a constant position in the monolayer, **C)** or from pacemaker regions at alternating positions.

unaffected by dihydropyridines (chapter 6, Fig. 4D), the spontaneous action potentials and concomitant calcium transients in density-arrested NRK monolayers were inhibited when G_{CaL} was blocked (De Roos et al., 1997c). Furthermore, there is no external trigger to induce intracellular calcium oscillations and the resting membrane potential is hyperpolarized and not close to the threshold for opening of G_{CaL}.

In the two other conceptual models, the calcium action potentials in density-arrested NRK monolayers are induced by localized pacemaker regions (i.e. hotspots) and subsequently propagate through the monolayer. Although it has not been possible to visualize this putative propagation due to the high propagation velocity of action potentials in NRK monolayers in combination with the limited time resolution in dynamic video imaging experiments (De Roos et al., 1997c), it is possible that the apparent synchronization of the intracellular calcium oscillations in density-arrested NRK monolayers is caused by rapidly propagating calcium action potentials. In contrast to the first conceptual model where all cells behave identically, two different cell types are required to obtain spontaneously propagating action potentials, namely pacemakers and followers. The pacemaker cells trigger action potentials in their neighboring cells (i.e. followers) as a result of dynamic changes in their intracellular calcium concentration. This is achieved by a calcium-dependent activation of $G_{Cl(Ca)}$, and a subsequent depolarization beyond the threshold for activation of G_{CaL}. The pacemaker region should consist of a sufficient number of cells, because due to the extensive electrical coupling of NRK cells it is not possible to evoke action potentials by depolarizing only one or a few cells (chapter 4, Fig. 12). On the other hand, the follower cells only transduce the action potentials whereby the cytosolic calcium concentration in these cells also increases as a result of calcium influx through L-type calcium channels. The presence of cells with different properties (i.e. pacemakers vs. followers) in a monolayer of cells derived from the same clone (NRK 49F) may appear contradictory, but we have previously already shown that individual NRK cells can have different properties even when they are cultured under the same conditions. For example, the maximal values of the plasma membrane conductances were highly variable between individual cells (chapter 3), and individual cells of the same monolayer showed different calcium responses when stimulated by an agonist (chapter 6). The observation that the spontaneous action potentials and calcium oscillations in density-arrested monolayers were blocked by dihydropyridines is in agreement with a propagation mechanism, because activation of G_{CaL} is essential for the initiation of the action potentials (chapter 3). Under these conditions the intracellular calcium changes in the pacemaker regions should continue, but this has not been investigated. The propagation of action potentials in density-arrested NRK monolayers is supported by the finding that the action disappeared after blocking the gap junctions by octanol (De Roos et al., 1997c).

In case of propagation, the action potentials can either be induced by the same hotspot at a constant position in the monolayer (Fig. 1B), or by hotspots at alternating positions (Fig. 1C). When the repetitive action potential firing is triggered by an intracellular calcium oscillation in only one

pacemaker region, the firing frequency should be constant (cf. Fig. 1, chapter 6) and exactly correlate with the frequency of the calcium oscillation which drives the action potentials (Fig. 1B). Alternatively, when the action potentials are triggered in turn by calcium transients at different locations in the monolayer (Fig. 1C), they should appear in a more stochastic manner. In general, the frequency of the action potential firing in density-arrested NRK monolayers was rather constant (cf. Fig. 1B chapter 7), but irregular action potential firing has sometimes also been measured (De Roos et al., 1997c).

In each of the conceptual models action potentials result from dynamic changes in the intracellular calcium concentration. It has however previously been shown that action potential firing continued after buffering intracellular calcium with BAPTA, while the plateau phase of the action potentials disappeared (De Roos et al., 1997c). It is realized that this finding seems to argue against a role for intracellular calcium in driving the action potential firing. However, the inability of BAPTA to prevent the pulsatory firing of action potentials can be explained if localized periodic calcium transients in close proximity of the plasma membrane are not buffered by BAPTA and therefore still proceed. This may apply to the cytoplasmic regions where the surface of the intracellular calcium stores extends closely to the plasma membrane, thus creating a thin subcellular cytoplasmic compartment in which calcium buffering by BAPTA may be less efficient than in the remainder bulk of the cytoplasm.

By measuring the membrane potential at two distant positions in the monolayer using two patch-clamp electrodes, the three possible mechanisms that determine the spontaneous action potential firing in density-arrested monolayers of NRK cells may be discriminated. In case of synchrony, the action potentials recorded with both electrodes should appear simultaneously, while they should appear with a delay in case of propagation. Moreover, using this experimental set-up it would also be possible to establish whether propagating action potentials result from unifocal pacemaking (Fig. 1B) or multifocal pacemaking (Fig. 1C) by mapping the time delays between multiple electrode positions. In addition, by dividing the density-arrested monolayer in two partitions by making a scratch, the firing frequency should either remain unaffected in both partitions (Fig. 1A), remain unaffected in one partition while firing stops in the other (Fig. 1B), or decrease in both partitions (Fig. 1C). The possible role of an IP_3-sensitive calcium oscillation in driving the action potential firing can be investigated by varying the external calcium concentration, sensitizing the IP_3 receptor by thimerosal or partially inhibiting calcium reuptake by thapsigargin, and to establish whether these actions have the same effects on the oscillation frequency of the spontaneously firing action potentials in density-arrested monolayers, as on the frequency of the PGF2α-induced calcium oscillations in quiescent monolayers (chapter 6). If both responses are correlated, the frequency of the spontaneous action potentials in density-arrested NRK monolayers is most likely determined by the properties of the IP_3 receptor (*see* chapter 6). Moreover, if an IP_3-sensitive mechanism determines the periodicity, knock-down of the IP_3 receptor with siRNA should prevent the action potential firing.

Based on the current experimental findings we propose here that density-arrested NRK monolayers exhibit propagating action potentials, which can originate from either one or more hotspots (Fig. 1B and 1C). Moreover, we postulate that the pacemaker regions consist of NRK cells which have obtained a transformed phenotype and that the intracellular calcium changes in these pacemaker regions are induced by the local secretion of PGF2α by transformed NRK cells. In the pacemaker regions, this locally secreted PGF2α may activate an IP_3-sensitive intracellular calcium oscillator (Fig. 1B) or induce a single calcium transient (Fig. 1C), thus triggering propagating action potentials. The pacemaker cells may release PGF2α at a constant rate, or alternatively in a periodic manner such that a calcium transient is induced each time that PGF2α is released. Interestingly, if a calcium-dependent mechanism underlies the secretion of PGF2α, a positive feedback loop is created by which PGF2α induces its own secretion. Notably, the PGF2α concentration, as determined by enzyme immunoassay, was elevated in the conditioned medium of density-arrested monolayers (1.5 nM) compared to that of quiescent monolayers (below limit of detection; chapter 7). In order to establish the putative role of the secretion of PGF2α in the induction of action potentials in density-arrested monolayers, it would be interesting to investigate whether this firing is stopped by blocking its production with a COX-inhibitor, or by preventing its action with an inhibitor of the FP-receptor.

Physiological relevance of fibroblast excitability

Although we have elucidated the excitability mechanism of cultured NRK fibroblasts, we can only speculate on the *in vivo* function of this excitability. Since fibroblasts can form cellular communicating networks *in vivo* (Hashizume et al., 1992; Komuro, 1989; Komuro, 1990) which expand throughout entire organs, their excitability in combination with electrical coupling may provide them with an efficient tool for fast and long-distance signaling. In this way, agonist-induced depolarizations evoked in a few cells, for example by PGF2α (chapter 6), may be transduced to unstimulated neighboring cells, thereby recruting a larger population of cells to respond in unison to local stimuli. So, fibroblasts may serve as an excitable and conductive pathway by which signals generated on one side of a tissue or organ can be transduced to the other side.

Because fibroblasts can be coupled to other cell types including epithelial cells (Hunter and Pitts, 1981), myocytes (De Maziere et al., 1992) and cells from the immune system (Oliani et al., 1995), and because action potentials can be transduced via heterocellular gap junctions (De Roos, 1997), fibroblasts may also affect the physiological function of many cell types *in vivo*. However, this still has to be established experimentally. In addition, we have demonstrated the excitability of only one particular fibroblastic cell line, namely NRK clone 49F, but it is unknown whether excitability and action potential propagation is a more general feature of fibroblasts. In this respect, it is interesting to mention that voltage-activated ion channels have been reported in several other fibroblastic cell lines,

including Balb/c 3T3 fibroblasts (Lovisolo et al., 1988), NIH/3T3 fibroblasts (Chen et al., 1988), Swiss 3T3 fibroblasts (Peres et al., 1988), and HF fibroblasts (Baumgarten et al., 1992).

Periodicity in NRK fibroblasts derives from intracellular calcium oscillations

Agonist-induced cytosolic calcium oscillations have been observed in many different cell types (Berridge, 1993; Petersen et al., 1991; Thomas et al., 1996). We showed that the intracellular calcium concentration in quiescent NRK cells also oscillates after stimulation with PGF2α (chapter 6). In this respect, it would be interesting to test whether ET-1, BK, and LPA, which are other activators of G-protein coupled receptors that have been shown to increase the average intracellular calcium concentration in NRK monolayers (Lahaye et al., 1999b), also induce calcium oscillations in individual cells of these monolayers. Remarkably, the frequency of the PGF2α-induced oscillations was highly variable and the oscillations in individual cells of confluent monolayers were not synchronized in spite of their coupling by gap junctions. In our experiments, we have only measured the calcium response upon systemic addition of PGF2α to NRK cells, which were all embedded in confluent monolayers. We expect that PGF2α induces similar calcium oscillations in single NRK cells and clusters of cells (e.g. 2-100 cells) dissociated from these monolayers. However, it would be interesting to investigate whether the oscillations are synchronized in smaller clusters (e.g. 2 gap junctionally coupled cells or 1 cell surrounded by 1 cell ring), and become unsynchronized by increasing the number of cluster cells. In contrast to the apparent autonomous calcium oscillations in NRK monolayers, GJIC allowed the membrane potential of confluent NRK monolayers to respond as a whole upon stimulation with PGF2α due to electrical coupling. So, gap junctional permeability of NRK cells is sufficient to allow electrical coupling, but insufficient to synchronize the intracellular calcium oscillations upon PGF2α stimulation. Previously, it has been shown that individual hepatocytes can have very different intrinsic calcium oscillation frequencies when they are stimulated by noradrenalin, while the oscillations are synchronized when they are coupled by gap junctions (Tordjmann et al., 1997). Subsequent mathematical modeling revealed that gap junctional permeability required for synchronization of the oscillations primarily depended on the heterogeneity between individual cells, including differences in the effective volume of the ER, the cytoplasm and the total area of the plasma membrane (Hofer, 1999). These results suggest that the unsynchronized calcium oscillations in monolayers of NRK cells may become synchronized when gap junctional coupling would further increase, for example by overexpressing Cx43 in NRK cells. We will address this question in a mathematical model for the PGF2α-induced calcium oscillations in NRK cells, which is currently under construction.

We concluded that the frequency of the PGF2α-induced calcium oscillations in NRK fibroblasts is determined by the time required for cytosolic calcium to reach a threshold for global CICR, and that this time is primarily determined by the calcium release kinetics of the IP_3 receptor (chapter 6). In our

experiments we have only considered the global calcium response of individual cells of NRK monolayers upon stimulation with PGF2α, but it would be interesting to investigate whether the global calcium increases (i.e. the sharp calcium transients) are preceded by localized calcium puffs, as shown in Xenopus oocytes (Marchant and Parker, 2001). Such elementary calcium puffs may form loci from which calcium spreads throughout the cell by global CICR.

Although the PGF2α-induced calcium oscillations in NRK cells can be attributed to an interplay between calcium release from IP_3-sensitive calcium stores and calcium influx through plasma membrane calcium channels, it cannot be excluded that other calcium stores also contribute to the oscillatory mechanism. In fact, we found that by blocking ryanodine-sensitive (i.e. cADPR-sensitive) calcium stores with a high concentration of ryanodine (50 μM), the oscillations were completely and reversibly inhibited in a fraction of the cells (~30%). In ~40% of the cells, ryanodine only reduced the oscillation amplitude without an apparent effect on the frequency, whereas the calcium oscillation in the other cells remained unaffected by ryanodine. These results indicate that ryanodine-sensitive (i.e. cADPR-sensitive) calcium stores are sometimes involved in the PGF2α-induced calcium oscillations. This can best be explained when calcium release mediated by ryanodine receptors contributes only to the global CICR during the calcium transient. The large discrepancy in the effect of ryanodine on the calcium oscillations in individual NRK cells of the same origin (clone 49F) and in the same monolayers is indicative for the intercellular variation. Preliminary experiments revealed that NRK fibroblasts also possess NAADP-sensitive calcium stores, since externally added NAADP increased the intracellular calcium concentration in monolayers of permeabilized NRK fibroblasts. However, it is unlikely that these stores contribute to the PGF2α-induced intracellular calcium oscillations because they become desensitized after binding of NAADP to its receptor (Lee, 2000) and are insensitive to CICR (Chini and Dousa, 1996). Finally, mitochondrial calcium buffering has been shown to contribute to intracellular calcium signaling in several cell types (Vandecasteele et al., 2001). Future experiments should be performed to investigate whether mitochondria also contribute to calcium signaling in NRK fibroblasts, for example by simultaneously monitoring cytoplasmic and mitochondrial calcium concentrations using the calcium-sensitive dye Rhod-2 (Collins et al., 2001).

So, NRK cells possess a highly variable timing mechanism provided by intracellular calcium oscillations. The frequency of these oscillations is primarily dependent on the kinetic properties of IP_3 receptors, which can be modulated by interfering with its calcium-dependent properties e.g. increasing the rate of calcium influx by elevating external calcium concentration or its IP_3-dependent properties e.g. increasing the sensitivity for IP_3 by treatment with thimerosal.

Actions of gap junction blockers compared

So far, several classes of chemicals have been described as gap junction blockers. These include alcohols such as heptanol and octanol (Johnston et al., 1980), halothane (Burt and Spray, 1989), and

fatty acids such as oleamide (Lerner, 1997), arachidonamide (Boger et al., 1999), and anandamide (Venance et al., 1995). These chemicals primarily seem to block gap junctions by altering the lipid environment and cell membrane fluidity, but this pharmacological inhibition is not very specific, and accompanied by non-specific effects on ionic plasma membrane channels (Buljubasic et al., 1992; Niggli et al., 1989; Poling et al., 1996; Takens-Kwak et al., 1992).

We have found that fenamates also block GJIC (chapter 2), and similar to the above gap junction blockers, fenamates have been shown to modulate a diversity of ion channels (Farrugia et al., 1993; Gogelein et al., 1990; Grover et al., 1994; Lee and Wang, 1999; Li et al., 1998a; Ottolia and Toro, 1994; White and Aylwin, 1990). In agreement with this, we found that under conditions that meclofenamic acid had completely blocked gap junctional coupling of NRK cells, the membrane conductances in these cells ($G_{CaL,}$ G_{Kir} and $G_{Cl(Ca)}$) were also completely inhibited (chapter 5). In our studies, we showed that fenamates blocked Cx43-mediated GJIC in NRK cells and SKHep1 cells transfected with Cx43. Subsequently, it was shown in N2A neuroblastoma cells transfected with various connexins that flufenamic acid, which is one the fenamates that we identified as a gap junction blocker, blocks other connexin subtypes with similar potency as Cx43 (Srinivas and Spray, 2003). In this respect flufenamic acid differs from e.g. quinine and some synthetic oligopeptides which inhibit gap junction channel subtypes in a selective manner (Kwak and Jongsma, 1999; Srinivas et al., 2001).

In order to be able to monitor changes in ion channel activity in electrically coupled tissues, for example during growth or oncogenic transformation, gap junctions have to be blocked due to the considerable amount of current flowing through gap junctional channels, which impairs the detection of membrane currents in voltage-clamp experiments. However, the gap junction blockers described so far also affect membrane conductances. For this reason, membrane conductance properties of single cells could not be studied so far in intact tissues. For example, Bohmer and coworkers have employed 18-β-glycyrrethinic acid, which blocks gap junctions by dephosporylation of Cx43 (Guan et al., 1996), as an electrical uncoupler to perform voltage-clamp studies on confluent cultures of rat hepatocytes (Bohmer et al., 2001). Although this compound reduced cell-to-cell coupling, it also completely blocked the membrane Cl^- conductance in these cells.

We have shown here that 2-APB completely blocks electrical coupling under conditions that membrane conductances in NRK cells could still be measured, which were not significantly different from those measured in single cells that had been dissociated from these monolayers (chapter 5). This finding is in agreement with previous findings showing that 2-APB does not block voltage-operated calcium conductances, voltage-operated potassium conductances, and calcium-activated chloride conductances (Maruyama et al., 1997; Wu et al., 2000). Because 2-APB seems to lack nonspecific effects on other ion channels, this observation provides the unique possibility to solve the long-standing problem in cellular electrophysiology of measuring single-cell properties on cells in multicellular tissues. To our knowledge, we showed for the first time reliable voltage-clamped ion currents from individual cells in an intact culture after electrically isolating the measured cell from its

surrounding cells with the use of 2-APB as an uncoupler. This procedure may open new possibilities to perform voltage-clamp experiments on e.g. individual cardiac myocytes in the myocardium and thereby separate excitability properties of the cells from conductive properties of the tissue, as we explored in fibroblastic cultures. It may also allow studies of the electrical properties of polarized cells in intact epithelia. The procedure is reversible and does not cause damage to the cells as observed during enzymatic cell dissociation.

We showed that 2-APB does not block electrical coupling when applied intracellularly via the pipette solution, indicating that the inhibition of GJIC by 2-APB is not caused by the binding of this drug in the pore of the gap junction channel. Instead, we propose that 2-APB interferes with the docking of two apposing connexons of neighboring cells. Fenamates share some structural properties with 2-APB (*see* chapter 5, Fig. 4 for the chemical structure of 2-APB and meclofenamic acid), and similar to 2-APB intracellular application of flufenamic acid did neither affect gap junctional conductance (Srinivas and Spray, 2003). Single channel recordings showed that external application of this fenamate reduced the open probability of the gap junctional channel indicating that the effect of this drug on GJIC is not caused by an open-channel block (Srinivas and Spray, 2003). In contrast, the blocking of chloride channels by fenamates results from the binding of these drugs to the permeation pathway in a manner consistent with open-channel block (McCarty et al., 1993; McDonough et al., 1994). Structure-activity studies have shown that several structural elements are crucial for this open-channel block of chloride channels by fenamates (Walsh et al., 1999). One of these elements is a carboxy-group, which is present in fenamates but not in 2-APB. The absence of this functional group in 2-APB may explain the lack of effect on chloride currents by this drug. Although we did not conduct elaborate structure-activity studies, fenamates and 2-APB may serve as a lead to develop new and more selective gap junction blockers.

Possible mechanisms of phenotypic transformation of NRK cells

NRK fibroblasts have been described as an attractive *in vitro* cellular model system to study the mechanisms of density-dependent growth inhibition and phenotypic transformation (Van Zoelen, 1991). By the addition of specific combinations of growth factors, density-dependent growth inhibition of NRK cells is lost and phenotypically transformed NRK cells become able to grow under anchorage-independent conditions, which is considered to be the best *in vitro* correlate to tumorigenesis *in vivo* (Cifone and Fidler, 1980; Shin et al., 1975).

In recent years, it has been established that the cyclooxygenase (COX)-mediated production of prostaglandins from arachidonic acid plays a major role during various stages of tumorigenesis (Singh and Lucci, 2002). Moreover, inhibiting COX activity by non-steroidal anti-inflammatory drugs (NSAIDs) including aspirin has promising properties for anticancer therapies (Bishop-Bailey et al., 2002). We showed that NRK cells secrete a biologically active prostaglandin when they obtain a transformed phenotype (chapter 7). This prostaglandin was identified with mass spectrometry and

enzyme immunoassay as PGF2α. It has been established that PGF2α acts on a subfamily of G-protein coupled receptors, known as the FP prostanoid receptors (Coleman et al., 1994), and activation of this receptor stimulates the release of intracellular calcium (Narumiya et al., 1999), followed by capacitative calcium entry from the extracellular medium (Putney, 1986). In NRK cells, the increase in the intracellular calcium concentration upon systemic treatment with PGF2α is accompanied by a depolarization of the membrane due to the opening of calcium-activated chloride channels (De Roos et al., 1997a). Since relatively high concentrations of PGF2α are present in the conditioned medium of phenotypically transformed NRK cells, these cells are constitutively depolarized around -20 mV (chapter 7). Although many cancer cells are depolarized compared to their non-transformed counterparts (Marino et al., 1994), it is uncertain whether the depolarization in those cells is also mediated by prostagladins, and more particularly by PGF2α. In this respect, prostaglandins may also hyperpolarize cells as we measured upon stimulation of Swiss 3T3 fibroblasts with PGF2α. This hyperpolarization was caused by the opening of calcium-activated potassium channels at elevated intracellular calcium levels.

Besides PGF2α, phenotypically transformed NRK cells may also secrete other prostanoids, including PGD2 and PGE2. These two prostaglandins mimicked the effect of PGF2α on the membrane potential of quiescent NRK cells, presumably by the activation of the FP-receptor, although with much lower affinity than PGF2α (Narumiya et al., 1999). However, PGD2 and PGE2 were not found in the mass spectrum of the purified active fraction of the conditioned medium, indicating that the depolarizing activity of this medium was not caused by PGD2 or PGE2.

The production of PGF2α by NRK cells seems to be a crucial step in the transformation of these cells because this process is blocked, or at least retarded, when the production of PGF2α is prevented by COX-inhibitors. Although we used non-selective COX-inhibitors that blocked both isozymes, we expect that the synthesis of PGF2α by transformed NRK cells is mediated by the inducible COX-2 isozyme, which is overexpressed in many cancer cells (Ota et al., 2002; Singh and Lucci, 2002; Singh-Ranger and Mokbel, 2002). To address this issue it would be worthwhile to test whether transformed NRK cells continue their secretion of PGF2α when they are incubated in the presence of a specific COX-2 inhibitor, such as celecoxib (Howe et al., 2002). In order to confirm the putative role of PGF2α in the transformation of NRK cells, it would be important to perform growth assay experiments in the presence and absence of COX inhibitors.

Previously it has been shown that phenotypic transformation of NRK cells is accompanied by an upregulation of the EGF receptor expression (Assoian et al., 1984; Van Zoelen et al., 1986), and that PGF2α can transform NRK cells in the additional presence of EGF (Lahaye et al., 1999b). So, PGF2α may contribute to the transformation of NRK cells in the presence of EGF by increasing the number EGF receptors, thus triggering density-arrested NRK cells to restart their proliferation. In this way, PGF2α could affect "normal" density-arrested NRK cells in a paracrine fashion and coordinate the

transformation process. Moreover, activation of the EGF receptor may lead to induction of COX-2 expression resulting in the release of prostaglandins, as shown in human colon cancer cells which predominantly produce PGE2 and PGF2α (Coffey et al., 1997). Hence, the production of PGF2α by transformed NRK cells may be enhanced by this positive feedback loop, thereby accelerating the transformation process. Alternatively, PGF2α may stimulate its own production by increasing the intracellular calcium concentration since phosholipase A2 (PLA2), which liberates the prostaglandin precursor arachidonic acid from membrane phospholipids, is activated at elevated intracellular calcium concentrations (Kramer and Sharp, 1997).

So far, two splice variants of the FP-receptor have been identified, designated FP_A and FP_B, which both activate phosphoinositide turnover (Pierce et al., 1997). The FP_B isoform is basically the truncated version of the FP_A isoform, which lacks the last 46 amino acids of the intracellular carboxyl-terminal domain. Recently, it has been shown that this domain is critical for the resensitization, which explains the slower resensitization of the FP_B isoform (Fujino et al., 2000). In contrast to the FP_A prostanoid receptor, activation of the FP_B receptor by PGF2α has been shown to result in the activation of β-catenin/Tcf signaling and increased PI3K activity (Fujino and Regan, 2001; Fujino et al., 2002), which are both associated with the development of colon cancer (Petiot et al., 2000; Srivastava et al., 2001). In addition, activation of the FP_B receptor can stimulate COX-2 promotor activity and may therefore regulate the expression of COX-2, thus providing a positive feedback loop that would drive β-catenin signaling and could be involved in cancer (Fujino and Regan, 2003). It is currently unknown which isoform(s) of the FP-receptor is expressed by NRK fibroblasts. In order to assess the role of the FP-receptor activation in the transformation of NRK cells, it would be interesting to culture these cells in the presence of a specific antagonist of the FP-receptor, such as AL 8810 (Griffin et al., 1999). If the transformation of NRK cells is blocked by this inhibitor, this would indicate that activation of the FP-receptor by PGF2α is a crucial step in the transformation of NRK cells. Alternatively, the role of the FP-receptor in the transformation of NRK cells could be determined by preventing the expression of this receptor by siRNA.

CHAPTER 9

References

Aarhus, R., Dickey, D.M., Graeff, R.M., Gee, K.R., Walseth, T.F. and Lee, H.C. (1996) Activation and inactivation of Ca2+ release by NAADP+. *J Biol Chem*, **271**, 8513-8516.

Abraham, M.R., Jahangir, A., Alekseev, A.E. and Terzic, A. (1999) Channelopathies of inwardly rectifying potassium channels. *Faseb J*, **13**, 1901-1910.

Afink, G.B., Van Alewijk, D.C., De Roos, A.D. and Van Zoelen, E.J. (1994) Lysophosphatidic acid and bradykinin have opposite effects on phenotypic transformation of normal rat kidney cells. *J Cell Biochem*, **56**, 480-489.

Akasu, T., Nishimura, T. and Tokimasa, T. (1990) Calcium-dependent chloride current in neurones of the rabbit pelvic parasympathetic ganglia. *J Physiol*, **422**, 303-320.

Allen, G.J., Muir, S.R. and Sanders, D. (1995) Release of Ca2+ from individual plant vacuoles by both InsP3 and cyclic ADP-ribose. *Science*, **268**, 735-737.

Assoian, R.K. (1985) Biphasic effects of type beta transforming growth factor on epidermal growth factor receptors in NRK fibroblasts. Functional consequences for epidermal growth factor-stimulated mitosis. *J Biol Chem*, **260**, 9613-9617.

Assoian, R.K., Frolik, C.A., Roberts, A.B., Miller, D.M. and Sporn, M.B. (1984) Transforming growth factor-beta controls receptor levels for epidermal growth factor in NRK fibroblasts. *Cell*, **36**, 35-41.

Atwater, I., Rosario, L. and Rojas, E. (1983) Properties of the Ca-activated K+ channel in pancreatic beta-cells. *Cell Calcium*, **4**, 451-461.

Bak, J., White, P., Timar, G., Missiaen, L., Genazzani, A.A. and Galione, A. (1999) Nicotinic acid adenine dinucleotide phosphate triggers Ca2+ release from brain microsomes. *Curr Biol*, **9**, 751-754.

Bakhramov, A., Boriskin, Y.S., Booth, J.C. and Bolton, T.B. (1995) Activation and deactivation of membrane currents in human fibroblasts following infection with human cytomegalovirus. *Biochim Biophys Acta*, **1265**, 143-151.

Baumgarten, L.B., Toscas, K. and Villereal, M.L. (1992) Dihydropyridine-sensitive L-type Ca2+ channels in human foreskin fibroblast cells. Characterization of activation with the growth factor Lys-bradykinin. *J Biol Chem*, **267**, 10524-10530.

Bennett, M.V., Barrio, L.C., Bargiello, T.A., Spray, D.C., Hertzberg, E. and Saez, J.C. (1991) Gap junctions: new tools, new answers, new questions. *Neuron*, **6**, 305-320.

Bennett, N.T. and Schultz, G.S. (1993) Growth factors and wound healing: biochemical properties of growth factors and their receptors. *Am J Surg*, **165**, 728-737.

Beny, J.L. and Pacicca, C. (1994) Bidirectional electrical communication between smooth muscle and endothelial cells in the pig coronary artery. *Am J Physiol*, **266**, H1465-1472.

Berridge, G., Dickinson, G., Parrington, J., Galione, A. and Patel, S. (2002) Solubilization of receptors for the novel Ca2+-mobilizing messenger, nicotinic acid adenine dinucleotide phosphate. *J Biol Chem*, **277**, 43717-43723.

Berridge, M.J. (1993) Inositol trisphosphate and calcium signalling. *Nature*, **361**, 315-325.

Berridge, M.J. (1995a) Calcium signalling and cell proliferation. *Bioessays*, **17**, 491-500.

Berridge, M.J. (1995b) Capacitative calcium entry. *Biochem J*, **312**, 1-11.

Berridge, M.J. (1997) The AM and FM of calcium signalling. *Nature*, **386**, 759-760.

Berridge, M.J., Bootman, M.D. and Lipp, P. (1998) Calcium--a life and death signal. *Nature*, **395**, 645-648.

Bigiani, A. and Roper, S.D. (1995) Estimation of the junctional resistance between electrically coupled receptor cells in Necturus taste buds. *J Gen Physiol*, **106**, 705-725.

Binggeli, R. and Weinstein, R.C. (1986) Membrane potentials and sodium channels: hypotheses for growth regulation and cancer formation based on changes in sodium channels and gap junctions. *J Theor Biol*, **123**, 377-401.

Bishop-Bailey, D., Calatayud, S., Warner, T.D., Hla, T. and Mitchell, J.A. (2002) Prostaglandins and the regulation of tumor growth. *J Environ Pathol Toxicol Oncol*, **21**, 93-101.

Bocher, V., Pineda-Torra, I., Fruchart, J.C. and Staels, B. (2002) PPARs: transcription factors controlling lipid and lipoprotein metabolism. *Ann N Y Acad Sci*, **967**, 7-18.

Boger, D.L., Sato, H., Lerner, A.E., Guan, X. and Gilula, N.B. (1999) Arachidonic acid amide inhibitors of gap junction cell-cell communication. *Bioorg Med Chem Lett*, **9**, 1151-1154.

Bohmer, C., Kirschner, U. and Wehner, F. (2001) 18-beta-Glycyrrhetinic acid (BGA) as an electrical uncoupler for intracellular recordings in confluent monolayer cultures. *Pflügers Arch*, **442**, 688-692.

Boonstra, J., Mummery, C.L., Tertoolen, L.G., Van Der Saag, P.T. and De Laat, S.W. (1981) Cation transport and growth regulation in neuroblastoma cells. Modulations of K+ transport and electrical membrane properties during the cell cycle. *J Cell Physiol*, **107**, 75-83.

Bootman, M.D., Berridge, M.J. and Lipp, P. (1997) Cooking with calcium: the recipes for composing global signals from elementary events. *Cell*, **91**, 367-373.

Bootman, M.D., Collins, T.J., Mackenzie, L., Roderick, H.L., Berridge, M.J. and Peppiatt, C.M. (2002) 2-aminoethoxydiphenyl borate (2-APB) is a reliable blocker of store-operated Ca2+ entry but an inconsistent inhibitor of InsP3-induced Ca2+ release. *Faseb J*, **16**, 1145-1150.

Bootman, M.D., Taylor, C.W. and Berridge, M.J. (1992) The thiol reagent, thimerosal, evokes Ca2+ spikes in HeLa cells by sensitizing the inositol 1,4,5-trisphosphate receptor. *J Biol Chem*, **267**, 25113-25119.

Bradbury, D.A., Newton, R., Zhu, Y.M., Stocks, J., Corbett, L., Holland, E.D., Pang, L.H. and Knox, A.J. (2002) Effect of bradykinin, TGF-beta1, IL-1beta, and hypoxia on COX-2 expression in pulmonary artery smooth muscle cells. *Am J Physiol Lung Cell Mol Physiol*, **283**, L717-725.

Brantl, S. (2002) Antisense-RNA regulation and RNA interference. *Biochim Biophys Acta*, **1575**, 15-25.

Braun, A.P. and Schulman, H. (1996) Distinct voltage-dependent gating behaviours of a swelling-activated chloride current in human epithelial cells. *J Physiol*, **495**, 743-753.

Braun, F.J., Broad, L.M., Armstrong, D.L. and Putney, J.W., Jr. (2001) Stable activation of single Ca2+ release-activated Ca2+ channels in divalent cation-free solutions. *J Biol Chem*, **276**, 1063-1070.

Brogden, R.N. (1986) Non-steroidal anti-inflammatory analgesics other than salicylates. *Drugs*, **32 Suppl 4**, 27-45.

Bruzzone, R., White, T.W. and Paul, D.L. (1996) Connections with connexins: the molecular basis of direct intercellular signaling. *Eur J Biochem*, **238**, 1-27.

Bukauskas, F.F., Jordan, K., Bukauskiene, A., Bennett, M.V., Lampe, P.D., Laird, D.W. and Verselis, V.K. (2000) Clustering of connexin 43-enhanced green fluorescent protein gap junction channels and functional coupling in living cells. *Proc Natl Acad Sci U S A*, **97**, 2556-2561.

Buljubasic, N., Rusch, N.J., Marijic, J., Kampine, J.P. and Bosnjak, Z.J. (1992) Effects of halothane and isoflurane on calcium and potassium channel currents in canine coronary arterial cells. *Anesthesiology*, **76**, 990-998.

Burt, J.M. and Spray, D.C. (1989) Volatile anesthetics block intercellular communication between neonatal rat myocardial cells. *Circ Res*, **65**, 829-837.

Cancela, J.M., Churchill, G.C. and Galione, A. (1999) Coordination of agonist-induced Ca2+-signalling patterns by NAADP in pancreatic acinar cells. *Nature*, **398**, 74-76.

Cancela, J.M., Gerasimenko, O.V., Gerasimenko, J.V., Tepikin, A.V. and Petersen, O.H. (2000) Two different but converging messenger pathways to intracellular Ca(2+) release: the roles of nicotinic acid adenine dinucleotide phosphate, cyclic ADP-ribose and inositol trisphosphate. *Embo J*, **19**, 2549-2557.

Chen, C.F., Corbley, M.J., Roberts, T.M. and Hess, P. (1988) Voltage-sensitive calcium channels in normal and transformed 3T3 fibroblasts. *Science*, **239**, 1024-1026.

Chen, L., Wang, L., Zhu, L., Nie, S., Zhang, J., Zhong, P., Cai, B., Luo, H. and Jacob, T.J. (2002) Cell cycle-dependent expression of volume-activated chloride currents in nasopharyngeal carcinoma cells. *Am J Physiol Cell Physiol*, **283**, C1313-1323.

Chen, S.C., Pelletier, D.B., Ao, P. and Boynton, A.L. (1995) Connexin43 reverses the phenotype of transformed cells and alters their expression of cyclin/cyclin-dependent kinases. *Cell Growth Differ*, **6**, 681-690.

Chini, E.N. and Dousa, T.P. (1996) Nicotinate-adenine dinucleotide phosphate-induced Ca(2+)-release does not behave as a Ca(2+)-induced Ca(2+)-release system. *Biochem J*, **316**, 709-711.

Churchill, G.C. and Galione, A. (2001) Prolonged inactivation of nicotinic acid adenine dinucleotide phosphate-induced Ca2+ release mediates a spatiotemporal Ca2+ memory. *J Biol Chem*, **276**, 11223-11225.

Cifone, M.A. and Fidler, I.J. (1980) Correlation of patterns of anchorage-independent growth with in vivo behavior of cells from a murine fibrosarcoma. *Proc Natl Acad Sci U S A*, **77**, 1039-1043.

Clair, C., Chalumeau, C., Tordjmann, T., Poggioli, J., Erneux, C., Dupont, G. and Combettes, L. (2001) Investigation of the roles of Ca(2+) and InsP(3) diffusion in the coordination of Ca(2+) signals between connected hepatocytes. *J Cell Sci*, **114**, 1999-2007.

Clapham, D.E. (1995) Calcium signaling. *Cell*, **80**, 259-268.

Coffey, R.J., Hawkey, C.J., Damstrup, L., Graves-Deal, R., Daniel, V.C., Dempsey, P.J., Chinery, R., Kirkland, S.C., DuBois, R.N., Jetton, T.L. and Morrow, J.D. (1997) Epidermal growth factor receptor activation induces nuclear targeting of cyclooxygenase-2, basolateral release of prostaglandins, and mitogenesis in polarizing colon cancer cells. *Proc Natl Acad Sci U S A*, **94**, 657-662.

Coleman, R.A., Smith, W.L. and Narumiya, S. (1994) International Union of Pharmacology classification of prostanoid receptors: properties, distribution, and structure of the receptors and their subtypes. *Pharmacol Rev*, **46**, 205-229.

Collins, T.J., Lipp, P., Berridge, M.J. and Bootman, M.D. (2001) Mitochondrial Ca(2+) uptake depends on the spatial and temporal profile of cytosolic Ca(2+) signals. *J Biol Chem*, **276**, 26411-26420.

Cornelisse, L.N., Deumens, R., Coenen, J.J., Roubos, E.W., Gielen, C.C., Ypey, D.L., Jenks, B.G. and Scheenen, W.J. (2002) Sauvagine Regulates Ca2+ Oscillations and Electrical Membrane Activity of Melanotrope Cells of Xenopus laevis. *J Neuroendocrinol*, **14**, 778-787.

Cseresnyes, Z., Bustamante, A.I. and Schneider, M.F. (1999) Caffeine-induced [Ca2+] oscillations in neurones of frog sympathetic ganglia. *J Physiol*, **514**, 83-99.

Dalton, S.L., Marcantonio, E.E. and Assoian, R.K. (1992) Cell attachment controls fibronectin and alpha 5 beta 1 integrin levels in fibroblasts. Implications for anchorage-dependent and -independent growth. *J Biol Chem*, **267**, 8186-8191.

Da Silva, C.P. and Guse, A.H. (2000) Intracellular Ca(2+) release mechanisms: multiple pathways having multiple functions within the same cell type? *Biochim Biophys Acta*, **1498**, 122-133.

Davies, G., Martin, L.A., Sacks, N. and Dowsett, M. (2002) Cyclooxygenase-2 (COX-2), aromatase and breast cancer: a possible role for COX-2 inhibitors in breast cancer chemoprevention. *Ann Oncol*, **13**, 669-678.

De Kock, C.P.J. (1999) *An attempt to unravel the involvement of the alpha1C-subunit of the L-type calcium channel in the regulation of contact-inhibition in rat fibroblasts*. University of Nijmegen, Nijmegen, The Netherlands.

De Koninck, P. and Schulman, H. (1998) Sensitivity of CaM kinase II to the frequency of Ca2+ oscillations. *Science*, **279**, 227-230.

De Maziere, A.M., Van Ginneken, A.C., Wilders, R., Jongsma, H.J. and Bouman, L.N. (1992) Spatial and functional relationship between myocytes and fibroblasts in the rabbit sinoatrial node. *J Mol Cell Cardiol*, **24**, 567-578.

De Mello, W.C. (1994) Gap junctional communication in excitable tissues; the heart as a paradigma. *Prog Biophys Mol Biol*, **61**, 1-35.

De Roos, A.D. (1997) *Electrophysiological Aspects of Growth Factor Signaling in NRK Fibroblasts*. University of Nijmegen, Nijmegen, The Netherlands.

De Roos, A.D., Van Zoelen, E.J. and Theuvenet, A.P. (1996) Determination of gap junctional intercellular communication by capacitance measurements. *Pflűgers Arch*, **431**, 556-563.

De Roos, A.D., Van Zoelen, E.J. and Theuvenet, A.P. (1997a) Membrane depolarization in NRK fibroblasts by bradykinin is mediated by a calcium-dependent chloride conductance. *J Cell Physiol*, **170**, 166-173.

De Roos, A.D., Van Zoelen, E.J. and Theuvenet, A.P. (1997b) Molecular mechanisms of signalling and targeting. *NATO ASI series*, 113-126.

De Roos, A.D., Willems, P.H., Peters, P.H., Van Zoelen, E.J. and Theuvenet, A.P. (1997c) Synchronized calcium spiking resulting from spontaneous calcium action potentials in monolayers of NRK fibroblasts. *Cell Calcium*, **22**, 195-207.

De Roos, A.D., Willems, P.H., Van Zoelen, E.J. and Theuvenet, A.P. (1997d) Synchronized Ca2+ signaling by intercellular propagation of Ca2+ action potentials in NRK fibroblasts. *Am J Physiol*, **273**, C1900-1907.

De Mello, W.C. (1994) Gap junctional communication in excitable tissues; the heart as a paradigma. *Prog Biophys Mol Biol*, **61**, 1-35.

DeWitt, D. and Smith, W.L. (1995) Yes, but do they still get headaches? *Cell*, **83**, 345-348.

Dobrydneva, Y. and Blackmore, P. (2001) 2-Aminoethoxydiphenyl borate directly inhibits store-operated calcium entry channels in human platelets. *Mol Pharmacol*, **60**, 541-552.

Dolmetsch, R.E., Xu, K. and Lewis, R.S. (1998) Calcium oscillations increase the efficiency and specificity of gene expression. *Nature*, **392**, 933-936.

Donoso, P., Aracena, P. and Hidalgo, C. (2000) Sulfhydryl oxidation overrides Mg(2+) inhibition of calcium-induced calcium release in skeletal muscle triads. *Biophys J*, **79**, 279-286.

Doughty, J.M., Miller, A.L. and Langton, P.D. (1998) Non-specificity of chloride channel blockers in rat cerebral arteries: block of the L-type calcium channel. *J Physiol*, **507**, 433-439.

Empson, R.M. and Galione, A. (1997) Cyclic ADP-ribose enhances coupling between voltage-gated Ca2+ entry and intracellular Ca2+ release. *J Biol Chem*, **272**, 20967-20970.

Enomoto, T. and Yamasaki, H. (1984) Lack of intercellular communication between chemically transformed and surrounding nontransformed BALB/c 3T3 cells. *Cancer Res*, **44**, 5200-5203.

Ershov, A.V. and Bazan, N.G. (1999) Induction of cyclooxygenase-2 gene expression in retinal pigment epithelium cells by photoreceptor rod outer segment phagocytosis and growth factors. *J Neurosci Res*, **58**, 254-261.

Estacion, M. (1991) Characterization of ion channels seen in subconfluent human dermal fibroblasts. *J Physiol*, **436**, 579-601.

Evans, J.R. and Bielefeldt, K. (2000) Regulation of sodium currents through oxidation and reduction of thiol residues. *Neuroscience*, **101**, 229-236.

Farrugia, G., Rae, J.L., Sarr, M.G. and Szurszewski, J.H. (1993) Potassium current in circular smooth muscle of human jejunum activated by fenamates. *Am J Physiol*, **265**, G873-879.

Fill, M. and Copello, J.A. (2002) Ryanodine receptor calcium release channels. *Physiol Rev*, **82**, 893-922.

Fu, X., Favini, R., Kindahl, K. and Ulmsten, U. (2000) Prostaglandin F2alpha-induced Ca++ oscillations in human myometrial cells and the role of RU 486. *Am J Obstet Gynecol*, **182**, 582-588.

Fujino, H., Pierce, K.L., Srinivasan, D., Protzman, C.E., Krauss, A.H., Woodward, D.F. and Regan, J.W. (2000) Delayed reversal of shape change in cells expressing FP(B) prostanoid receptors. Possible role of receptor resensitization. *J Biol Chem*, **275**, 29907-29914.

Fujino, H. and Regan, J.W. (2001) FP prostanoid receptor activation of a T-cell factor/beta -catenin signaling pathway. *J Biol Chem*, **276**, 12489-12492.

Fujino, H. and Regan, J.W. (2003) Prostaglandin F(2alpha) stimulation of cyclooxygenase-2 promoter activity by the FP(B) prostanoid receptor. *Eur J Pharmacol*, **465**, 39-41.

Fujino, H., Srinivasan, D. and Regan, J.W. (2002) Cellular conditioning and activation of beta-catenin signaling by the FPB prostanoid receptor. *J Biol Chem*, **277**, 48786-48795.

Furstenberger, G., Gross, M. and Marks, F. (1989) Eicosanoids and multistage carcinogenesis in NMRI mouse skin: role of prostaglandins E and F in conversion (first stage of tumor promotion) and promotion (second stage of tumor promotion). *Carcinogenesis*, **10**, 91-96.

Genazzani, A.A. and Galione, A. (1996) Nicotinic acid-adenine dinucleotide phosphate mobilizes Ca2+ from a thapsigargin-insensitive pool. *Biochem J*, **315**, 721-725.

Genazzani, A.A., Mezna, M., Dickey, D.M., Michelangeli, F., Walseth, T.F. and Galione, A. (1997) Pharmacological properties of the Ca2+-release mechanism sensitive to NAADP in the sea urchin egg. *Br J Pharmacol*, **121**, 1489-1495.

Giaume, C. and Venance, L. (1998) Intercellular calcium signaling and gap junctional communication in astrocytes. *Glia*, **24**, 50-64.

Giepmans, B.N., Hengeveld, T., Postma, F.R. and Moolenaar, W.H. (2001) Interaction of c-Src with gap junction protein connexin-43. Role in the regulation of cell-cell communication. *J Biol Chem*, **276**, 8544-8549.

Gogelein, H., Dahlem, D., Englert, H.C. and Lang, H.J. (1990) Flufenamic acid, mefenamic acid and niflumic acid inhibit single nonselective cation channels in the rat exocrine pancreas. *FEBS Lett*, **268**, 79-82.

Goldberg, G.S., Lampe, P.D. and Nicholson, B.J. (1999) Selective transfer of endogenous metabolites through gap junctions composed of different connexins. *Nat Cell Biol*, **1**, 457-459.

Goldberg, G.S. and Lau, A.F. (1993) Dynamics of connexin43 phosphorylation in pp60v-src-transformed cells. *Biochem J*, **295**, 735-742.

Goodenough, D.A. and Revel, J.P. (1970) A fine structural analysis of intercellular junctions in the mouse liver. *J Cell Biol*, **45**, 272-290.

Graier, W.F., Simecek, S. and Sturek, M. (1995) Cytochrome P450 mono-oxygenase-regulated signalling of Ca2+ entry in human and bovine endothelial cells. *J Physiol*, **482**, 259-274.

Gregory, R.B., Rychkov, G. and Barritt, G.J. (2001) Evidence that 2-aminoethyl diphenylborate is a novel inhibitor of store-operated Ca2+ channels in liver cells, and acts through a mechanism which does not involve inositol trisphosphate receptors. *Biochem J*, **354**, 285-290.

Griffin, B.W., Klimko, P., Crider, J.Y. and Sharif, N.A. (1999) AL-8810: a novel prostaglandin F2 alpha analog with selective antagonist effects at the prostaglandin F2 alpha (FP) receptor. *J Pharmacol Exp Ther*, **290**, 1278-1284.

Gros, D.B. and Jongsma, H.J. (1996) Connexins in mammalian heart function. *Bioessays*, **18**, 719-730.

Grover, G.J., D'Alonzo, A.J., Sleph, P.G., Dzwonczyk, S., Hess, T.A. and Darbenzio, R.B. (1994) The cardioprotective and electrophysiological effects of cromakalim are attenuated by meclofenamate through a cyclooxygenase-independent mechanism. *J Pharmacol Exp Ther*, **269**, 536-540.

Gruber, A.D., Elble, R.C., Ji, H.L., Schreur, K.D. Fuller, C.M. and Pauli, B.U. (1998) Genomic cloning, molecular characterization, and functional analysis of human CLCA1, the first human member of the family of Ca2+-activated Cl- channel proteins. *Genomics* **54**, 200-14.

Guadagno, T.M., Ohtsubo, M., Roberts, J.M. and Assoian, R.K. (1993) A link between cyclin A expression and adhesion-dependent cell cycle progression. *Science*, **262**, 1572-1575.

Guan, X., Wilson, S., Schlender, K.K. and Ruch, R.J. (1996) Gap-junction disassembly and connexin 43 dephosphorylation induced by 18 beta-glycyrrhetinic acid. *Mol Carcinog*, **16**, 157-164.

Guo, X. and Becker, P.L. (1997) Cyclic ADP-ribose-gated Ca2+ release in sea urchin eggs requires an elevated. *J Biol Chem*, **272**, 16984-16989.

Halaszovich, C.R., Zitt, C., Jungling, E. and Luckhoff, A. (2000) Inhibition of TRP3 channels by lanthanides. Block from the cytosolic side of the plasma membrane. *J Biol Chem*, **275**, 37423-37428.

Haluska, P. and Adjei, A.A. (2001) Receptor tyrosine kinase inhibitors. *Curr Opin Investig Drugs*, **2**, 280-286.

Hamill, O.P., Marty, A., Neher, E., Sakmann, B. and Sigworth, F.J. (1981) Improved patch-clamp techniques for high-resolution current recording from cells and cell-free membrane patches. *Pflűgers Arch*, **391**, 85-100.

Harks, E.G., Camina, J.P., Peters, P.H., Ypey, D.L., Scheenen, W.J., Van Zoelen, E.J. and Theuvenet, A.P. (2003a) Besides affecting intracellular calcium signaling, 2-APB reversibly blocks gap junctional coupling in confluent monolayers, thereby allowing the measurement of single-cell membrane currents in undissociated cells. *Faseb J*, 10.1096/fj.02-0786fje.

Harks, E.G., De Roos, A.D., Peters, P.H., De Haan, L.H., Brouwer, A., Ypey, D.L., Van Zoelen, E.J. and Theuvenet, A.P. (2001) Fenamates: a novel class of reversible gap junction blockers. *J Pharmacol Exp Ther*, **298**, 1033-1041.

Harks, E.G., Scheenen, W.J., Peters, P.H., Van Zoelen, E.J. and Theuvenet, A.P. (2003b) PGF2a induces unsynchronized intracellular calcium oscillations in monolayers of gap junctionally coupled NRK fibroblasts. *Pflűgers Arch*, in press.

Harks, E.G., Torres, J.J., Cornelisse, L.N., Ypey, D.L. and Theuvenet, A.P. (2003c) Ionic basis for excitability of normal rat kidney (NRK) fibroblasts. *J Cell Physiol*, **196**, 493-503 (2003).

Hashii, M., Minabe, Y. and Higashida, H. (2000) cADP-ribose potentiates cytosolic Ca2+ elevation and Ca2+ entry via L-type voltage-activated Ca2+ channels in NG108-15 neuronal cells. *Biochem J*, **345**, 207-215.

Hashizume, T., Imayama, S. and Hori, Y. (1992) Scanning electron microscopic study on dendritic cells and fibroblasts in connective tissue. *J Electron Microsc (Tokyo)*, **41**, 434-437.

Hermans, M.M., Kortekaas, P., Jongsma, H.J. and Rook, M.B. (1995) pH sensitivity of the cardiac gap junction proteins, connexin 45 and 43. *Pflűgers Arch*, **431**, 138-140.

Hille, B. (2001) *Ion Channels of Excitable Membranes*. Sinauer Associates, Inc., Sunderland, Massachusetts, US.

Ho, M.W., Kaetzel, M.A., Armstrong, D.L. and Shears, S.B. (2001) Regulation of a human chloride channel. a paradigm for integrating input from calcium, type ii calmodulin-dependent protein kinase, and inositol 3,4,5,6-tetrakisphosphate. *J Biol Chem*, **276**, 18673-18680.

Hodgkin, A.L. and Huxley, A.F. (1952) A quantitative description of membrane current and its application to conduction and excitation in nerve. *J. Physiol. (Lond.)*, **117**, 500-544.

Hoenderop, J.G., Nilius, B. and Bindels, R.J. (2002) ECaC: the gatekeeper of transepithelial Ca2+ transport. *Biochim Biophys Acta*, **1600**, 6-11.

Hofer, T. (1999) Model of intercellular calcium oscillations in hepatocytes: synchronization of heterogeneous cells. *Biophys J*, **77**, 1244-1256.

Hofer, T., Politi, A. and Heinrich, R. (2001) Intercellular Ca2+ wave propagation through gap-junctional Ca2+ diffusion: a theoretical study. *Biophys J*, **80**, 75-87.

Hofer, T., Venance, L. and Giaume, C. (2002) Control and plasticity of intercellular calcium waves in astrocytes: a modeling approach. *J Neurosci*, **22**, 4850-4859.

Holder, J.W., Elmore, E. and Barrett, J.C. (1993) Gap junction function and cancer. *Cancer Res*, **53**, 3475-3485.

Hossain, M.Z. and Boynton, A.L. (2000) Regulation of Cx43 gap junctions: the gatekeeper and the password. *Sci STKE*, **2000**, E1.

Hotz-Wagenblatt, A. and Shalloway, D. (1993) Gap junctional communication and neoplastic transformation. *Crit Rev Oncog*, **4**, 541-558.

Howe, L.R., Subbaramaiah, K., Patel, J., Masferrer, J.L., Deora, A., Hudis, C., Thaler, H.T., Muller, W.J., Du, B., Brown, A.M. and Dannenberg, A.J. (2002) Celecoxib, a selective cyclooxygenase 2 inhibitor, protects against human epidermal growth factor receptor 2 (HER-2)/neu-induced breast cancer. *Cancer Res*, **62**, 5405-5407.

Hunter, G.K. and Pitts, J.D. (1981) Non-selective junctional communication between some different mammalian cell types in primary culture. *J Cell Sci*, **49**, 163-175.

Ignotz, R.A. and Massague, J. (1986) Transforming growth factor-beta stimulates the expression of fibronectin and collagen and their incorporation into the extracellular matrix. *J Biol Chem*, **261**, 4337-4345.

Ilyin, V. and Parker, I. (1994) Role of cytosolic Ca2+ in inhibition of InsP3-evoked Ca2+ release in Xenopus oocytes. *J Physiol*, **477**, 503-509.

Imai, T., Tanaka, Y., Okamoto, T., Horinouchi, T., Tanaka, H., Koike, K. and Shigenobu, K. (2002) 2-Aminoethoxydiphenyl borate causes dissociation between membrane electrical and mechanical activity in guinea-pig urinary bladder smooth muscle. *Naunyn Schmiedebergs Arch Pharmacol*, **366**, 282-285.

Iqbal, M., Giri, U., Giri, D.K. and Athar, M. (1997) Evidence that Fe-NTA-induced renal prostaglandin F2 alpha is responsible for hyperplastic response in kidney: implications for the role of cyclooxygenase-dependent arachidonic acid metabolism in renal tumor promotion. *Biochem Mol Biol Int*, **42**, 1115-1124.

Irvine, R.F. (1990) 'Quantal' Ca2+ release and the control of Ca2+ entry by inositol phosphates--a possible mechanism. *FEBS Lett*, **263**, 5-9.

Ishihara, K., Yan, D.H., Yamamoto, S. and Ehara, T. (2002) Inward rectifier K(+) current under physiological cytoplasmic conditions in guinea-pig cardiac ventricular cells. *J Physiol*, **540**, 831-841.

Jacob, R., Merritt, J.E., Hallam, T.J. and Rink, T.J. (1988) Repetitive spikes in cytoplasmic calcium evoked by histamine in human endothelial cells. *Nature*, **335**, 40-45.

Jinno, S., Lin, J., Yageta, M. and Okayama, H. (2001) Oncogenic cell cycle start control. *Mutat Res*, **477**, 23-29.

Johnston, M.F., Simon, S.A. and Ramon, F. (1980) Interaction of anaesthetics with electrical synapses. *Nature*, **286**, 498-500.

Jones, M.K., Wang, H., Peskar, B.M., Levin, E., Itani, R.M., Sarfeh, I.J. and Tarnawski, A.S. (1999) Inhibition of angiogenesis by nonsteroidal anti-inflammatory drugs: insight into mechanisms and implications for cancer growth and ulcer healing. *Nat Med*, **5**, 1418-1423.

Jongsma, H.J. and Wilders, R. (2000) Gap junctions in cardiovascular disease. *Circ Res*, **86**, 1193-1197.

Kalgutkar, A.S., Crews, B.C., Rowlinson, S.W., Marnett, A.B., Kozak, K.R., Remmel, R.P. and Marnett, L.J. (2000) Biochemically based design of cyclooxygenase-2 (COX-2) inhibitors: facile conversion of nonsteroidal antiinflammatory drugs to potent and highly selective COX-2 inhibitors. *Proc Natl Acad Sci U S A*, **97**, 925-930.

Kalimi, G.H. and Lo, C.W. (1988) Communication compartments in the gastrulating mouse embryo. *J Cell Biol*, **107**, 241-255.

Kanemitsu, M.Y. and Lau, A.F. (1993) Epidermal growth factor stimulates the disruption of gap junctional communication and connexin43 phosphorylation independent of 12-0-tetradecanoylphorbol 13-acetate-sensitive protein kinase C: the possible involvement of mitogen-activated protein kinase. *Mol Biol Cell*, **4**, 837-848.

Kidd, J.F. and Thorn, P. (2001) The properties of the secretagogue-evoked chloride current in mouse pancreatic acinar cells. *Pflűgers Arch*, **441**, 489-497.

Kim, H.R., Upadhyay, S., Li, G., Palmer, K.C. and Deuel, T.F. (1995) Platelet-derived growth factor induces apoptosis in growth-arrested murine fibroblasts. *Proc Natl Acad Sci U S A*, **92**, 9500-9504.

Kizaka-Kondoh, S., Akiyama, N. and Okayama, H. (2000) Role of TGF-beta in EGF-induced transformation of NRK cells is sustaining high-level EGF-signaling. *FEBS Lett*, **466**, 160-164.

Koch, C. (1999) *Biophysics of Computation: Information processing in single neurons.* Oxford University Press, New York, US.

Komuro, T. (1989) Three-dimensional observation of the fibroblast-like cells associated with the rat myenteric plexus, with special reference to the interstitial cells of Cajal. *Cell Tissue Res*, **255**, 343-351.

Komuro, T. (1990) Re-evaluation of fibroblasts and fibroblast-like cells. *Anat Embryol (Berl)*, **182**, 103-112.

Kothapalli, D., Frazier, K.S., Welply, A., Segarini, P.R. and Grotendorst, G.R. (1997) Transforming growth factor beta induces anchorage-independent growth of NRK fibroblasts via a connective tissue growth factor-dependent signaling pathway. *Cell Growth Differ*, **8**, 61-68.

Kramer, R.M. and Sharp, J.D. (1997) Structure, function and regulation of Ca2+-sensitive cytosolic phospholipase A2 (cPLA2). *FEBS Lett*, **410**, 49-53.

Krause, E., Pfeiffer, F., Schmid, A. and Schulz, I. (1996) Depletion of intracellular calcium stores activates a calcium conducting nonselective cation current in mouse pancreatic acinar cells. *J Biol Chem*, **271**, 32523-32528.

Kubo, Y., Baldwin T.J., Jan, Y.N., Jan, L.Y. (1993) Primary structure and functional expression of a mouse inward rectifier potassium channel. *Nature* **362**, 127-33.

Kukkonen, J.P., Lund, P.E. and Akerman, K.E. (2001) 2-aminoethoxydiphenyl borate reveals heterogeneity in receptor-activated Ca(2+) discharge and store-operated Ca(2+) influx. *Cell Calcium*, **30**, 117-129.

Kumar, N.M. and Gilula, N.B. (1996) The gap junction communication channel. *Cell*, **84**, 381-388.

Kusano, K. and Gainer, H. (1991) Bombesin-like peptides induce Ca2(+)-activated K+ conductance increases in mouse fibroblasts. *Am J Physiol*, **260**, C701-707.

Kwak, B.R. and Jongsma, H.J. (1999) Selective inhibition of gap junction channel activity by synthetic peptides. *J Physiol (Lond)*, **516**, 679-685.

Lahaye, D.H., Afink, G.B., Bleijs, D.A., Van Alewijk, D.C. and Van Zoelen, E.J. (1994) Effect of bradykinin on loss of density-dependent growth inhibition of normal rat kidney cells. *Cell Mol Biol (Noisy-le-grand)*, **40**, 717-721.

Lahaye, D.H., Camps, M.G., Erp, P.E., Peters, P.H. and Zoelen, E.J. (1998) Epidermal growth factor (EGF) receptor density controls mitogenic activation of normal rat kidney (NRK) cells by EGF. *J Cell Physiol*, **174**, 9-17.

Lahaye, D.H., Camps, M.G. and Van Zoelen, E.J. (1999a) Central role of epidermal growth factor (EGF) receptor density in anchorage-independent growth of normal rat kidney cells. *FEBS Lett*, **446**, 256-260.

Lahaye, D.H., Walboomers, F., Peters, P.H., Theuvenet, A.P. and Van Zoelen, E.J. (1999b) Phenotypic transformation of normal rat kidney fibroblasts by endothelin-1. Different mode of action from lysophosphatidic acid, bradykinin, and prostaglandin f2alpha. *Biochim Biophys Acta*, **1449**, 107-118.

Laird, D.W., Fistouris, P., Batist, G., Alpert, L., Huynh, H.T., Carystinos, G.D. and Alaoui-Jamali, M.A. (1999) Deficiency of connexin43 gap junctions is an independent marker for breast tumors. *Cancer Res*, **59**, 4104-4110.

Lampe, P.D. (1994) Analyzing phorbol ester effects on gap junctional communication: a dramatic inhibition of assembly. *J Cell Biol*, **127**, 1895-1905.

Lampe, P.D. and Lau, A.F. (2000) Regulation of gap junctions by phosphorylation of connexins. *Arch Biochem Biophys*, **384**, 205-215.

Lampe, P.D., TenBroek, E.M., Burt, J.M., Kurata, W.E., Johnson, R.G. and Lau, A.F. (2000) Phosphorylation of connexin43 on serine368 by protein kinase C regulates gap junctional communication. *J Cell Biol*, **149**, 1503-1512.

Lau, A.F., Kanemitsu, M.Y., Kurata, W.E., Danesh, S. and Boynton, A.L. (1992) Epidermal growth factor disrupts gap-junctional communication and induces phosphorylation of connexin43 on serine. *Mol Biol Cell*, **3**, 865-874.

Lau, A.F., Kurata, W.E., Kanemitsu, M.Y., Loo, L.W., Warn-Cramer, B.J., Eckhart, W. and Lampe, P.D. (1996) Regulation of connexin43 function by activated tyrosine protein kinases. *J Bioenerg Biomembr*, **28**, 359-368.

Lee, H.C. (1993) Potentiation of calcium- and caffeine-induced calcium release by cyclic ADP-ribose. *J Biol Chem*, **268**, 293-299.

Lee, H.C. (1997) Mechanisms of calcium signaling by cyclic ADP-ribose and NAADP. *Physiol Rev*, **77**, 1133-1164.

Lee, H.C. (2000) NAADP: An emerging calcium signaling molecule. *J Membr Biol*, **173**, 1-8.

Lee, H.C. and Aarhus, R. (1995) A derivative of NADP mobilizes calcium stores insensitive to inositol trisphosphate and cyclic ADP-ribose. *J Biol Chem*, **270**, 2152-2157.

Lee, H.C., Aarhus, R., Graeff, R., Gurnack, M.E. and Walseth, T.F. (1994) Cyclic ADP ribose activation of the ryanodine receptor is mediated by calmodulin. *Nature*, **370**, 307-309.

Lee, H.C., Walseth, T.F., Bratt, G.T., Hayes, R.N. and Clapper, D.L. (1989) Structural determination of a cyclic metabolite of NAD+ with intracellular Ca2+-mobilizing activity. *J Biol Chem*, **264**, 1608-1615.

Lee, Y.T. and Wang, Q. (1999) Inhibition of hKv2.1, a major human neuronal voltage-gated K+ channel, by meclofenamic acid. *Eur J Pharmacol*, **378**, 349-356.

Legrand, G., Humez, S., Slomianny, C., Dewailly, E., Vanden Abeele, F., Mariot, P., Wuytack, F. and Prevarskaya, N. (2001) Ca2+ pools and cell growth. Evidence for sarcoendoplasmic Ca2+-ATPases 2B involvement in human prostate cancer cell growth control. *J Biol Chem*, **276**, 47608-47614.

Lerner, R.A. (1997) A hypothesis about the endogenous analogue of general anesthesia. *Proc Natl Acad Sci U S A*, **94**, 13375-13377.

Li, H., Liu, T.F., Lazrak, A., Peracchia, C., Goldberg, G.S., Lampe, P.D. and Johnson, R.G. (1996) Properties and regulation of gap junctional hemichannels in the plasma membranes of cultured cells. *J Cell Biol*, **134**, 1019-1030.

Li, L., Vapaatalo, H., Vaali, K., Paakkari, I. and Kankaanranta, H. (1998a) Fenamates inhibit contraction of guinea-pig isolated bronchus in vitro independent of prostanoid synthesis inhibition. *Life Sci*, **62**, L289-294.

Li, W., Llopis, J., Whitney, M., Zlokarnik, G. and Tsien, R.Y. (1998b) Cell-permeant caged InsP3 ester shows that Ca2+ spike frequency can optimize gene expression. *Nature*, **392**, 936-941.

Liu, L.W., Thuneberg, L. and Huizinga, J.D. (1995) Cyclopiazonic acid, inhibiting the endoplasmic reticulum calcium pump, reduces the canine colonic pacemaker frequency. *J Pharmacol Exp Ther*, **275**, 1058-1068.

Loewenstein, W.R. (1979) Junctional intercellular communication and the control of growth. *Biochim Biophys Acta*, **560**, 1-65.

Loewenstein, W.R. (1981) Junctional intercellular communication: the cell-to-cell membrane channel. *Physiol Rev*, **61**, 829-913.

Lovisolo, D., Alloatti, G., Bonelli, G., Tessitore, L. and Baccino, F.M. (1988) Potassium and calcium currents and action potentials in mouse Balb/c 3T3 fibroblasts. *Pflűgers Arch*, **412**, 530-534.

Ma, H.T., Patterson, R.L., Van Rossum, D.B., Birnbaumer, L., Mikoshiba, K. and Gill, D.L. (2000) Requirement of the inositol trisphosphate receptor for activation of store-operated Ca2+ channels. *Science*, **287**, 1647-1651.

Ma, H.T., Venkatachalam, K., Li, H.S., Montell, C., Kurosaki, T., Patterson, R.L. and Gill, D.L. (2001) Assessment of the role of the inositol 1,4,5-trisphosphate receptor in the activation of transient receptor potential channels and store-operated Ca2+ entry channels. *J Biol Chem*, **276**, 18888-18896.

Ma, H.T., Venkatachalam, K., Parys, J.B. and Gill, D.L. (2002) Modification of store-operated channel coupling and inositol trisphosphate receptor function by 2-aminoethoxydiphenyl borate in DT40 lymphocytes. *J Biol Chem*, **277**, 6915-6922.

MacFarlane, S.N. and Sontheimer, H. (2000) Changes in ion channel expression accompany cell cycle progression of spinal cord astrocytes. *Glia*, **30**, 39-48.

Mak, D.O., McBride, S. and Foskett, J.K. (1998) Inositol 1,4,5-trisphosphate [correction of tris-phosphate] activation of inositol trisphosphate receptor Ca2+ channel by ligand tuning of Ca2+ inhibition. *Proc Natl Acad Sci U S A*, **95**, 15821-15825.

Maldonado, P.E., Rose, B. and Loewenstein, W.R. (1988) Growth factors modulate junctional cell-to-cell communication. *J Membr Biol*, **106**, 203-210.

Marchant, J.S. and Parker, I. (2001) Role of elementary Ca(2+) puffs in generating repetitive Ca(2+) oscillations. *Embo J*, **20**, 65-76.

Marchant, J.S. and Taylor, C.W. (1997) Cooperative activation of IP3 receptors by sequential binding of IP3 and Ca2+ safeguards against spontaneous activity. *Curr Biol*, **7**, 510-518.

Marengo, J.J., Hidalgo, C. and Bull, R. (1998) Sulfhydryl oxidation modifies the calcium dependence of ryanodine-sensitive calcium channels of excitable cells. *Biophys J*, **74**, 1263-1277.

Marino, A.A., Iliev, I.G., Schwalke, M.A., Gonzalez, E., Marler, K.C. and Flanagan, C.A. (1994) Association between cell membrane potential and breast cancer. *Tumour Biol*, **15**, 82-89.

Marnett, L.J. (1992) Aspirin and the potential role of prostaglandins in colon cancer. *Cancer Res*, **52**, 5575-5589.

Martin, S.C. and Shuttleworth, T.J. (1994) Ca2+ influx drives agonist-activated [Ca2+]i oscillations in an exocrine cell. *FEBS Lett*, **352**, 32-36.

Maruyama, T., Kanaji, T., Nakade, S., Kanno, T. and Mikoshiba, K. (1997) 2APB, 2-aminoethoxydiphenyl borate, a membrane-penetrable modulator of Ins(1,4,5)P3-induced Ca2+ release. *J Biochem (Tokyo)*, **122**, 498-505.

Masgrau, R., Churchill, G.C., Morgan, A.J., Ashcroft, S.J. and Galione, A. (2003) NAADP. A New Second Messenger for Glucose-Induced Ca(2+) Responses in Clonal Pancreatic beta Cells. *Curr Biol*, **13**, 247-251.

McCarty, N.A., McDonough, S., Cohen, B.N., Riordan, J.R., Davidson, N. and Lester, H.A. (1993) Voltage-dependent block of the cystic fibrosis transmembrane conductance regulator Cl- channel by two closely related arylaminobenzoates. *J Gen Physiol*, **102**, 1-23.

McDonough, S., Davidson, N., Lester, H.A. and McCarty, N.A. (1994) Novel pore-lining residues in CFTR that govern permeation and open-channel block. *Neuron*, **13**, 623-634.

McNutt, N.S. and Weinstein, R.S. (1970) The ultrastructure of the nexus. A correlated thin-section and freeze-cleave study. *J Cell Biol*, **47**, 666-688.

Mesnil, M. (2002) Connexins and cancer. *Biol Cell*, **94**, 493-500.

Meyer, T. and Stryer, L. (1991) Calcium spiking. *Annu Rev Biophys Biophys Chem*, **20**, 153-174.

Miake, J., Marban, E. and Nuss, H.B. (2003) Functional role of inward rectifier current in heart probed by Kir2.1 overexpression and dominant-negative suppression. *J Clin Invest*, **111**, 1529-1536.

Moreno, A.P., Laing, J.G., Beyer, E.C. and Spray, D.C. (1995) Properties of gap junction channels formed of connexin 45 endogenously expressed in human hepatoma (SKHep1) cells. *Am J Physiol*, **268**, C356-365.

Narumiya, S. (1994) Prostanoid receptors. Structure, function, and distribution. *Ann N Y Acad Sci*, **744**, 126-138.

Narumiya, S., Sugimoto, Y. and Ushikubi, F. (1999) Prostanoid receptors: structures, properties, and functions. *Physiol Rev*, **79**, 1193-1226.

Neuhaus, J., Weimann, A., Stolzenburg, J.U., Wolburg, H., Horn, L.C. and Dorschner, W. (2002a) Smooth muscle cells from human urinary bladder express connexin 43 in vivo and in vitro. *World J Urol*, **20**, 250-254.

Neuhaus, J., Wolburg, H., Hermsdorf, T., Stolzenburg, J.U. and Dorschner, W. (2002b) Detrusor smooth muscle cells of the guinea-pig are functionally coupled via gap junctions in situ and in cell culture. *Cell Tissue Res*, **309**, 301-311.

Neyton, J. and Trautmann, A. (1985) Single-channel currents of an intercellular junction. *Nature*, **317**, 331-335.

Niggli, E., Rudisuli, A., Maurer, P. and Weingart, R. (1989) Effects of general anesthetics on current flow across membranes in guinea pig myocytes. *Am J Physiol*, **256**, C273-281.

Nilius, B. and Droogmans, G. (2003) Amazing chloride channels: an overview. *Acta Physiol Scand*, **177**, 119-147.

Oliani, S.M., Girol, A.P. and Smith, R.L. (1995) Gap junctions between mast cells and fibroblasts in the developing avian eye. *Acta Anat (Basel)*, **154**, 267-271.

Ota, S., Bamba, H., Kato, A., Kawamoto, C., Yoshida, Y. and Fujiwara, K. (2002) Review article: COX-2, prostanoids and colon cancer. *Aliment Pharmacol Ther*, **16**, 102-106.

Ottolia, M. and Toro, L. (1994) Potentiation of large conductance KCa channels by niflumic, flufenamic, and mefenamic acids. *Biophys J*, **67**, 2272-2279.

Parker, I. and Ivorra, I. (1990) Inhibition by Ca2+ of inositol trisphosphate-mediated Ca2+ liberation: a possible mechanism for oscillatory release of Ca2+. *Proc Natl Acad Sci U S A*, **87**, 260-264.

Patel, S., Churchill, G.C. and Galione, A. (2000) Unique kinetics of nicotinic acid-adenine dinucleotide phosphate (NAADP) binding enhance the sensitivity of NAADP receptors for their ligand. *Biochem J*, **352**, 725-729.

Patel, S., Churchill, G.C. and Galione, A. (2001) Coordination of Ca2+ signalling by NAADP. *Trends Biochem Sci*, **26**, 482-489.

Patterson, R.L., Van Rossum, D.B. and Gill, D.L. (1999) Store-operated Ca2+ entry: evidence for a secretion-like coupling model. *Cell*, **98**, 487-499.

Pelletier, D.B. and Boynton, A.L. (1994) Dissociation of PDGF receptor tyrosine kinase activity from PDGF-mediated inhibition of gap junctional communication. *J Cell Physiol*, **158**, 427-434.

Peres, A., Sturani, E. and Zippel, R. (1988) Properties of the voltage-dependent calcium channel of mouse Swiss 3T3 fibroblasts. *J Physiol*, **401**, 639-655.

Petersen, C.C., Toescu, E.C. and Petersen, O.H. (1991) Different patterns of receptor-activated cytoplasmic Ca2+ oscillations in single pancreatic acinar cells: dependence on receptor type, agonist concentration and intracellular Ca2+ buffering. *Embo J*, **10**, 527-533.

Petersen, O.H. and Cancela, J.M. (1999) New Ca2+-releasing messengers: are they important in the nervous system? *Trends Neurosci*, **22**, 488-495.

Petiot, A., Ogier-Denis, E., Blommaart, E.F., Meijer, A.J. and Codogno, P. (2000) Distinct classes of phosphatidylinositol 3'-kinases are involved in signaling pathways that control macroautophagy in HT-29 cells. *J Biol Chem*, **275**, 992-998.

Pierce, K.L., Bailey, T.J., Hoyer, P.B., Gil, D.W., Woodward, D.F. and Regan, J.W. (1997) Cloning of a carboxyl-terminal isoform of the prostanoid FP receptor. *J Biol Chem*, **272**, 883-887.

Poling, J.S., Rogawski, M.A., Salem, N., Jr. and Vicini, S. (1996) Anandamide, an endogenous cannabinoid, inhibits Shaker-related voltage-gated K+ channels. *Neuropharmacology*, **35**, 983-991.

Postma, F.R., Hengeveld, T., Alblas, J., Giepmans, B.N., Zondag, G.C., Jalink, K. and Moolenaar, W.H. (1998) Acute loss of cell-cell communication caused by G protein-coupled receptors: a critical role for c-Src. *J Cell Biol*, **140**, 1199-1209.

Pozzan, T., Rizzuto, R., Volpe, P. and Meldolesi, J. (1994) Molecular and cellular physiology of intracellular calcium stores. *Physiol Rev*, **74**, 595-636.

Prescott, S.M. and Fitzpatrick, F.A. (2000) Cyclooxygenase-2 and carcinogenesis. *Biochim Biophys Acta*, **1470**, M69-78.

Protasi, F. (2002) Structural interaction between RYRs and DHPRs in calcium release units of cardiac and skeletal muscle cells. *Front Biosci*, **7**, d650-658.

Putney, J.W., Jr. (1986) A model for receptor-regulated calcium entry. *Cell Calcium*, **7**, 1-12.

Quesada, I., Fuentes, E., Andreu, E., Meda, P., Nadal, A. and Soria, B. (2003) On-line analysis of gap junctions reveals more efficient electrical than dye coupling between islet cells. *Am J Physiol Endocrinol Metab*, **7**, 7.

Randriamampita, C. and Tsien, R.Y. (1993) Emptying of intracellular Ca2+ stores releases a novel small messenger that stimulates Ca2+ influx. *Nature*, **364**, 809-814.

Rasmusson, R.L., Clark, J.W., Giles, W.R., Shibata, E.F. and Campbell, D.L. (1990) A mathematical model of a bullfrog cardiac pacemaker cell. *Am J Physiol*, **259**, H352-369.

Rich, J.B., Rasmusson, D.X., Folstein, M.F., Carson, K.A., Kawas, C. and Brandt, J. (1995) Nonsteroidal anti-inflammatory drugs in Alzheimer's disease. *Neurology*, **45**, 51-55.

Rijksen, G., Voller, M.C. and Van Zoelen, E.J. (1993) The role of protein tyrosine phosphatases in density-dependent growth control of normal rat kidney cells. *FEBS Lett*, **322**, 83-87.

Rink, T.J. and Hallam, T.J. (1989) Calcium signalling in non-excitable cells: notes on oscillations and store refilling. *Cell Calcium*, **10**, 385-395.

Rizzino, A., Kazakoff, P. and Nebelsick, J. (1990) Density-induced down regulation of epidermal growth factor receptors. *In Vitro Cell Dev Biol*, **26**, 537-542.

Rizzino, A., Kazakoff, P., Ruff, E., Kuszynski, C. and Nebelsick, J. (1988) Regulatory effects of cell density on the binding of transforming growth factor beta, epidermal growth factor, platelet-derived growth factor, and fibroblast growth factor. *Cancer Res*, **48**, 4266-4271.

Robb-Gaspers, L.D. and Thomas, A.P. (1995) Coordination of Ca2+ signaling by intercellular propagation of Ca2+ waves in the intact liver. *J Biol Chem*, **270**, 8102-8107.

Roberts, A.B., Anzano, M.A., Lamb, L.C., Smith, J.M. and Sporn, M.B. (1984) Antagonistic actions of retinoic acid and dexamethasone on anchorage-independent growth and epidermal growth factor binding of normal rat kidney cells. *Cancer Res*, **44**, 1635-1641.

Rosen, L.B. and Greenberg, M.E. (1996) Stimulation of growth factor receptor signal transduction by activation of voltage-sensitive calcium channels. *Proc Natl Acad Sci U S A*, **93**, 1113-1118.

Ruch, R.J., Guan, X. and Sigler, K. (1995) Inhibition of gap junctional intercellular communication and enhancement of growth in BALB/c 3T3 cells treated with connexin43 antisense oligonucleotides. *Mol Carcinog*, **14**, 269-274.

Rzigalinski, B.A., Willoughby, K.A., Hoffman, S.W., Falck, J.R. and Ellis, E.F. (1999) Calcium influx factor, further evidence it is 5, 6-epoxyeicosatrienoic acid. *J Biol Chem*, **274**, 175-182.

Sachs, H.G., Stambrook, P.J. and Ebert, J.D. (1974) Changes in membrane potential during the cell cycle. *Exp Cell Res*, **83**, 362-366.

Saez, J.C., Connor, J.A., Spray, D.C. and Bennett, M.V. (1989) Hepatocyte gap junctions are permeable to the second messenger, inositol 1,4,5-trisphosphate, and to calcium ions. *Proc Natl Acad Sci U S A*, **86**, 2708-2712.

Sanderson, M.J. (1995) Intercellular calcium waves mediated by inositol trisphosphate. *Ciba Found Symp*, **188**, 175-189; discussion 189-194.

Santos, R.M., Rosario, L.M., Nadal, A., Garcia-Sancho, J., Soria, B. and Valdeolmillos, M. (1991) Widespread synchronous [Ca2+]i oscillations due to bursting electrical activity in single pancreatic islets. *Pflűgers Arch*, **418**, 417-422.

Sato, T., Nakajima, H., Fujio, K. and Mori, Y. (1997) Enhancement of prostaglandin E2 production by epidermal growth factor requires the coordinate activation of cytosolic phospholipase A2 and cyclooxygenase 2 in human squamous carcinoma A431 cells. *Prostaglandins*, **53**, 355-369.

Sauviat, M.P., Frizelle, H.P., Descorps-Declere, A. and Mazoit, J.X. (2000) Effects of halothane on the membrane potential in skeletal muscle of the frog. *Br J Pharmacol*, **130**, 619-624.

Schoenmakers, T.J., Visser, G.J., Flik, G. and Theuvenet, A.P. (1992) CHELATOR: an improved method for computing metal ion concentrations in physiological solutions. *Biotechniques*, **12**, 870-874, 876-879.

Sheng, H., Shao, J., Kirkland, S.C., Isakson, P., Coffey, R.J., Morrow, J., Beauchamp, R.D. and DuBois, R.N. (1997) Inhibition of human colon cancer cell growth by selective inhibition of cyclooxygenase-2. *J Clin Invest*, **99**, 2254-2259.

Sheng, H., Shao, J., Washington, M.K. and DuBois, R.N. (2001) Prostaglandin E2 increases growth and motility of colorectal carcinoma cells. *J Biol Chem*, **276**, 18075-18081.

Sherman, A., Rinzel, J. and Keizer, J. (1988) Emergence of organized bursting in clusters of pancreatic beta-cells by channel sharing. *Biophys J*, **54**, 411-425.

Shin, S.I., Freedman, V.H., Risser, R. and Pollack, R. (1975) Tumorigenicity of virus-transformed cells in nude mice is correlated specifically with anchorage independent growth in vitro. *Proc Natl Acad Sci U S A*, **72**, 4435-4439.

Short, A.D., Bian, J., Ghosh, T.K., Waldron, R.T., Rybak, S.L. and Gill, D.L. (1993) Intracellular Ca2+ pool content is linked to control of cell growth. *Proc Natl Acad Sci U S A*, **90**, 4986-4990.

Shuttleworth, T.J. and Thompson, J.L. (1996) Ca2+ entry modulates oscillation frequency by triggering Ca2+ release. *Biochem J*, **313**, 815-819.

Siegenbeek van Heukelom, J., Denier van der Gon, J.J. and Prop, F.J.A. (1970) Epithelial monolayers: a study object for cell communication. *Biochim. Biophys. Acta*, **211**, 98-101.

Singh, B. and Lucci, A. (2002) Role of cyclooxygenase-2 in breast cancer. *J Surg Res*, **108**, 173-179.

Singh-Ranger, G. and Mokbel, K. (2002) The role of cyclooxygenase-2 (COX-2) in breast cancer, and implications of COX-2 inhibition. *Eur J Surg Oncol*, **28**, 729-737.

Smith, W.L., DeWitt, D.L. and Garavito, R.M. (2000) Cyclooxygenases: structural, cellular, and molecular biology. *Annu Rev Biochem*, **69**, 145-182.

Smith, W.L., Meade, E.A. and DeWitt, D.L. (1994) Interactions of PGH synthase isozymes-1 and -2 with NSAIDs. *Ann N Y Acad Sci*, **744**, 50-57.

Solbach, C., Roller, M., Ahr, A., Loibl, S., Nicoletti, M., Stegmueller, M., Kreysch, H.G., Knecht, R. and Kaufmann, M. (2002) Anti-epidermal growth factor receptor-antibody therapy for treatment of breast cancer. *Int J Cancer*, **101**, 390-394.

Speed, C.J., Little, P.J., Hayman, J.A. and Mitchell, C.A. (1996) Underexpression of the 43 kDa inositol polyphosphate 5-phosphatase is associated with cellular transformation. *Embo J*, **15**, 4852-4861.

Speed, C.J., Neylon, C.B., Little, P.J. and Mitchell, C.A. (1999) Underexpression of the 43 kDa inositol polyphosphate 5-phosphatase is associated with spontaneous calcium oscillations and enhanced calcium responses following endothelin-1 stimulation. *J Cell Sci*, **112**, 669-679.

Spray, D.C. and Bennett, M.V. (1985) Physiology and pharmacology of gap junctions. *Annu Rev Physiol*, **47**, 281-303.

Spray, D.C. and Burt, J.M. (1990) Structure-activity relations of the cardiac gap junction channel. *Am J Physiol*, **258**, C195-205.

Spray, D.C., Harris, A.L. and Bennett, M.V. (1981) Gap junctional conductance is a simple and sensitive function of intracellular pH. *Science*, **211**, 712-715.

Srinivas, M., Hopperstad, M.G. and Spray, D.C. (2001) Quinine blocks specific gap junction channel subtypes. *Proc Natl Acad Sci U S A*, **98**, 10942-10947.

Srinivas, M. and Spray, D.C. (2003) Closure of Gap Junction Channels by Arylaminobenzoates. *Mol Pharmacol*, **63**, 1389-1397.

Srivastava, S., Verma, M. and Henson, D.E. (2001) Biomarkers for early detection of colon cancer. *Clin Cancer Res*, **7**, 1118-1126.

Stauffer, P.L., Zhao, H., Luby-Phelps, K., Moss, R.L., Star, R.A. and Muallem, S. (1993) Gap junction communication modulates [Ca2+]i oscillations and enzyme secretion in pancreatic acini. *J Biol Chem*, **268**, 19769-19775.

Szalai, G., Csordas, G., Hantash, B.M., Thomas, A.P. and Hajnoczky, G. (2000) Calcium signal transmission between ryanodine receptors and mitochondria. *J Biol Chem*, **275**, 15305-15313.

Takens-Kwak, B.R., Jongsma, H.J., Rook, M.B. and Van Ginneken, A.C. (1992) Mechanism of heptanol-induced uncoupling of cardiac gap junctions: a perforated patch-clamp study. *Am J Physiol*, **262**, C1531-1538.

Tanaka, A., Hase, S., Miyazawa, T. and Takeuchi, K. (2002) Up-regulation of cyclooxygenase-2 by inhibition of cyclooxygenase-1: a key to nonsteroidal anti-inflammatory drug-induced intestinal damage. *J Pharmacol Exp Ther*, **300**, 754-761.

Thomas, A.P., Bird, G.S., Hajnoczky, G., Robb-Gaspers, L.D. and Putney, J.W., Jr. (1996) Spatial and temporal aspects of cellular calcium signaling. *Faseb J*, **10**, 1505-1517.

Thorn, P., Brady, P., Llopis, J., Gallacher, D.V. and Petersen, O.H. (1992) Cytosolic Ca2+ spikes evoked by the thiol reagent thimerosal in both intact and internally perfused single pancreatic acinar cells. *Pflűgers Arch*, **422**, 173-178.

Tordjmann, T., Berthon, B., Claret, M. and Combettes, L. (1997) Coordinated intercellular calcium waves induced by noradrenaline in rat hepatocytes: dual control by gap junction permeability and agonist. *Embo J*, **16**, 5398-5407.

Torres, J.J., Cornelisse, L.N., Harks, E.G., Theuvenet, A.P. and Ypey, D.L. (2003) Modeling Action Potential (AP) Generation and Propagation in Quiescent Fibroblastic (NRK) Cells. *Am J Physiol*, submitted.

Torres, J.J., Willems, P.H., Kappen, H.J. and Koopman, W.J. (2001) Hysteresis and bistability in a realistic model for IP3-driven Ca2+ oscillations. *Europhys. Lett.*, **55**, 746-752.

Trosko, J.E. and Ruch, R.J. (2002) Gap junctions as targets for cancer chemoprevention and chemotherapy. *Curr Drug Targets*, **3**, 465-482.

Usachev, Y.M. and Thayer, S.A. (1999) Ca2+ influx in resting rat sensory neurones that regulates and is regulated by ryanodine-sensitive Ca2+ stores. *J Physiol*, **519 Pt 1**, 115-130.

Van Corven, E.J., Groenink, A., Jalink, K., Eichholtz, T. and Moolenaar, W.H. (1989) Lysophosphatidate-induced cell proliferation: identification and dissection of signaling pathways mediated by G proteins. *Cell*, **59**, 45-54.

Vandecasteele, G., Szabadkai, G. and Rizzuto, R. (2001) Mitochondrial calcium homeostasis: mechanisms and molecules. *IUBMB Life*, **52**, 213-219.

Van Rossum, D.B., Patterson, R.L., Ma, H.T. and Gill, D.L. (2000) Ca2+ entry mediated by store depletion, S-nitrosylation, and TRP3 channels. Comparison of coupling and function. *J Biol Chem*, **275**, 28562-28568.

Van Zoelen, E.J. (1991) Phenotypic transformation of normal rat kidney cells: a model for studying cellular alterations in oncogenesis. *Crit Rev Oncog*, **2**, 311-333.

Van Zoelen, E.J., Peters, P.H., Afink, G.B., Van Genesen, S., De Roos, D.G., Van Rotterdam, W. and Theuvenet, A.P. (1994) Bradykinin-induced growth inhibition of normal rat kidney (NRK) cells is paralleled by a decrease in epidermal-growth-factor receptor expression. *Biochem J*, **298**, 335-340.

Van Zoelen, E.J. and Tertoolen, L.G. (1991) Transforming growth factor-beta enhances the extent of intercellular communication between normal rat kidney cells. *J Biol Chem*, **266**, 12075-12081.

Van Zoelen, E.J., Van Oostwaard, T.M. and De Laat, S.W. (1986) Transforming growth factor-beta and retinoic acid modulate phenotypic transformation of normal rat kidney cells induced by epidermal growth factor and platelet-derived growth factor. *J Biol Chem*, **261**, 5003-5009.

Van Zoelen, E.J., Van Oostwaard, T.M. and De Laat, S.W. (1988) The role of polypeptide growth factors in phenotypic transformation of normal rat kidney cells. *J Biol Chem*, **263**, 64-68.

Veenstra, R.D. (2001) Voltage clamp limitations of dual whole-cell gap junction current and voltage recordings. I. Conductance measurements. *Biophys J*, **80**, 2231-2247.

Venance, L., Piomelli, D., Glowinski, J. and Giaume, C. (1995) Inhibition by anandamide of gap junctions and intercellular calcium signalling in striatal astrocytes. *Nature*, **376**, 590-594.

Vikhamar, G., Rivedal, E., Mollerup, S. and Sanner, T. (1998) Role of Cx43 phosphorylation and MAP kinase activation in EGF induced enhancement of cell communication in human kidney epithelial cells. *Cell Adhes Commun*, **5**, 451-460.

Visegrady, A., Lakos, Z., Czimbalek, L. and Somogyi, B. (2001) Stimulus-dependent control of inositol 1,4,5-trisphosphate-induced Ca(2+) oscillation frequency by the endoplasmic reticulum Ca(2+)-ATPase. *Biophys J*, **81**, 1398-1405.

Voldborg, B.R., Damstrup, L., Spang-Thomsen, M. and Poulsen, H.S. (1997) Epidermal growth factor receptor (EGFR) and EGFR mutations, function and possible role in clinical trials. *Ann Oncol*, **8**, 1197-1206.

Wakui, M., Potter, B.V. and Petersen, O.H. (1989) Pulsatile intracellular calcium release does not depend on fluctuations in inositol trisphosphate concentration. *Nature*, **339**, 317-320.

Wallinga, W., Meijer, S.L., Alberink, M.J., Vliek, M., Wienk, E.D. and Ypey, D.L. (1999) Modelling action potentials and membrane currents of mammalian skeletal muscle fibres in coherence with potassium concentration changes in the T-tubular system. *Eur Biophys J*, **28**, 317-329.

Walsh, K.B., Long, K.J. and Shen, X. (1999) Structural and ionic determinants of 5-nitro-2-(3-phenylpropylamino)-benzoic acid block of the CFTR chloride channel. *Br J Pharmacol*, **127**, 369-376.

White, M.M. and Aylwin, M. (1990) Niflumic and flufenamic acids are potent reversible blockers of Ca2(+)-activated Cl- channels in Xenopus oocytes. *Mol Pharmacol*, **37**, 720-724.

Willecke, K., Eiberger, J., Degen, J., Eckardt, D., Romualdi, A., Guldenagel, M., Deutsch, U. and Sohl, G. (2002) Structural and functional diversity of connexin genes in the mouse and human genome. *Biol Chem*, **383**, 725-737.

Willson, T.M. and Wahli, W. (1997) Peroxisome proliferator-activated receptor agonists. *Curr Opin Chem Biol*, **1**, 235-241.

Wilson, H.L. and Galione, A. (1998) Differential regulation of nicotinic acid-adenine dinucleotide phosphate and cADP-ribose production by cAMP and cGMP. *Biochem J*, **331**, 837-843.

Wilson, H.L., Wilson, S.A., Surprenant, A. and North, R.A. (2002) Epithelial Membrane Proteins Induce Membrane Blebbing and Interact with the P2X7 Receptor C Terminus. *J Biol Chem*, **277**, 34017-34023.

Wonderlin, W.F. and Strobl, J.S. (1996) Potassium channels, proliferation and G1 progression. *J Membr Biol*, **154**, 91-107.

Woodward, D.F. and Lawrence, R.A. (1994) Identification of a single (FP) receptor associated with prostanoid-induced Ca2+ signals in Swiss 3T3 cells. *Biochem Pharmacol*, **47**, 1567-1574.

Wu, J., Kamimura, N., Takeo, T., Suga, S., Wakui, M., Maruyama, T. and Mikoshiba, K. (2000) 2-Aminoethoxydiphenyl borate modulates kinetics of intracellular Ca(2+) signals mediated by inositol 1,4,5-trisphosphate-sensitive Ca(2+) stores in single pancreatic acinar cells of mouse. *Mol Pharmacol*, **58**, 1368-1374.

Wu, J., Takeo, T., Kamimura, N., Wada, J., Suga, S., Hoshina, Y. and Wakui, M. (1996) Thimerosal modulates the agonist-specific cytosolic Ca2+ oscillatory patterns in single pancreatic acinar cells of mouse. *FEBS Lett*, **390**, 149-152.

Wu, X., Babnigg, G., Zagranichnaya, T. and Villereal, M.L. (2002) The role of endogenous human trp4 in regulating carbachol-induced calcium oscillations in HEK-293 cells. *J Biol Chem*, **5**, 5.

Xie, Q., Zhang, Y., Zhai, C. and Bonanno, J.A. (2002) Calcium influx factor from cytochrome P-450 metabolism and secretion-like coupling mechanisms for capacitative calcium entry in corneal endothelial cells. *J Biol Chem*, **277**, 16559-16566.

Yamasaki, H. and Naus, C.C. (1996) Role of connexin genes in growth control. *Carcinogenesis*, **17**, 1199-1213.

Yamasaki, H., Omori, Y., Krutovskikh, V., Zhu, W., Mironov, N., Yamakage, K. and Mesnil, M. (1999) Connexins in tumour suppression and cancer therapy. *Novartis Found Symp*, **219**, 241-254; discussion 254-260.

Yarden, Y. and Sliwkowski, M.X. (2001) Untangling the ErbB signalling network. *Nat Rev Mol Cell Biol*, **2**, 127-137.

Ypey, D.L. and DeFelice, L.J. (2000) The patch-clamp technique: *A theoretical and practical introduction using simple electrical equivalent circuits*, in Channels, Receptors & Transporters (DeFelice LJ ed.) volume of the Biophysics Textbook On Line (BTOL) of the Biophysical Society: *http://www.biophysics.org/biophys/society/btol/*.

Zhang, Z.Q., Zhang, W., Wang, N.Q., Bani-Yaghoub, M., Lin, Z.X. and Naus, C.C. (1998) Suppression of tumorigenicity of human lung carcinoma cells after transfection with connexin43. *Carcinogenesis*, **19**, 1889-1894.

Zheng, Y.J., Furukawa, T., Tajimi, K. and Inagaki, N. (2003) Cl- channel blockers inhibit transition of quiescent (G0) fibroblasts into the cell cycle. *J Cell Physiol*, **194**, 376-383.

Zhou, L., Kasperek, E.M. and Nicholson, B.J. (1999) Dissection of the molecular basis of pp60(v-src) induced gating of connexin 43 gap junction channels. *J Cell Biol*, **144**, 1033-1045.

Zhu, D.M., Tekle, E., Huang, C.Y. and Chock, P.B. (2000a) Inositol tetrakisphosphate as a frequency regulator in calcium oscillations in HeLa cells. *J Biol Chem*, **275**, 6063-6066.

Zhu, X., Ohtsubo, M., Bohmer, R.M., Roberts, J.M. and Assoian, R.K. (1996) Adhesion-dependent cell cycle progression linked to the expression of cyclin D1, activation of cyclin E-cdk2, and phosphorylation of the retinoblastoma protein. *J Cell Biol*, **133**, 391-403.

Zhu, X., Scharf, E. and Assoian, R.K. (2000b) Induction of anchorage-independent growth by transforming growth factor-beta linked to anchorage-independent expression of cyclin D1. *J Biol Chem*, **275**, 6703-6706.

Zimmermann, B. and Walz, B. (1999) The mechanism mediating regenerative intercellular Ca2+ waves in the blowfly salivary gland. *Embo J*, **18**, 3222-3231.

Zweifel, B.S., Davis, T.W., Ornberg, R.L. and Masferrer, J.L. (2002) Direct evidence for a role of cyclooxygenase 2-derived prostaglandin E2 in human head and neck xenograft tumors. *Cancer Res*, **62**, 6706-6711.

Zwick, E., Daub, H., Aoki, N., Yamaguchi-Aoki, Y., Tinhofer, I., Maly, K. and Ullrich, A. (1997) Critical role of calcium-dependent epidermal growth factor receptor transactivation in PC12 cell membrane depolarization and bradykinin signaling. *J Biol Chem*, **272**, 24767-24770.

Zwick, E., Wallasch, C., Daub, H. and Ullrich, A. (1999) Distinct calcium-dependent pathways of epidermal growth factor receptor transactivation and PYK2 tyrosine phosphorylation in PC12 cells. *J Biol Chem*, **274**, 20989-20996.

Summary

During development and also in the adult organism cellular growth is strictly regulated by various control mechanisms that ensure cells to start and stop dividing at the proper time and place. Dysfunction of these intricate regulatory mechanisms may result in uncontrolled proliferation of cells and can be the basis for a large diversity of pathogenic conditions including cancer. Therefore, insight into the elementary mechanisms that control normal cell growth is crucial for understanding pathogenic abnormalities.

Normal cells undergo density-dependent growth inhibition at high cell densities. By this protection mechanism, which is also known as contact-inhibition, excessive cell growth is prevented. In the present studies normal rat kidney (NRK) fibroblasts were used as a cellular model system to study the mechanisms underlying density-dependent growth control. These cells undergo density-dependent growth inhibition when they are cultured in the presence of epidermal growth factor (EGF) as the only growth stimulating factor present. Moreover, when NRK cells are cultured in the presence of additional growth modulating factors such as transforming growth factor β (TGFβ) or retinoic acid (RA) density-dependent growth inhibition is lost or prevented, which is accompanied by a phenotypic transformation. This transformation of NRK cells can be considered as an *in vitro* correlate to tumorigenesis.

Several studies have shown that the expression level of the EGF receptor plays a crucial role in the density-dependent growth regulation of NRK cells. More recently the biophysical properties of NRK fibroblasts have been investigated in relation to growth control and it has been shown that in confluent monolayer culture density-arrested NRK fibroblasts spontaneously fire repetitive calcium action potentials. The ability of NRK fibroblasts to fire action potentials seemed to contradict the classical view on fibroblasts as non-excitable cells.

In this thesis, the excitability mechanism of NRK cells was further examined in terms of ion channel activity and gap junctional intercellular communication. For this purpose quiescent NRK cells were used, which did not exhibit spontaneous action potential firing. In these electrically-silent cells a single propagating calcium action potential could be evoked by a local depolarization induced by a high $[K^+]$ or a calcium mobilizing agent such as bradykinin. For the propagation of action potentials through confluent monolayers intercellular coupling by gap junctions is required. Capacitive current transients evoked by single-electrode voltage-clamp steps showed that monolayers of NRK fibroblasts are electrically well-coupled. From these transients the estimated gap junctional conductance could be determined. The ionic membrane conductances were characterized and quantified in voltage-clamp experiments on single NRK cells and small cell clusters derived from the quiescent monolayers. In addition to the previously reported L-type calcium conductance and calcium-activated chloride conductance, it was discovered that NRK cells exhibit a prominent inwardly rectifying potassium

conductance. Excitability of NRK cells is not restricted to electrically coupled cells in monolayer culture, because a significant percentage of isolated single cells was already able to generate action potentials.

In order to gain insight into the excitability mechanism of NRK fibroblasts a Hodgkin-Huxley-like mathematical model was constructed including the cell membrane components that were measured in patch-clamp experiments. This minimal model, which only comprised simplified intracellular calcium dynamics, reproduced excitability of single NRK cells and cell clusters as well as intercellular action potential propagation in monolayers. The contribution of each membrane conductance to action potential firing in NRK fibroblasts became evident from patch-clamp experiments and mathematical modeling. The initiation of the action potential is caused by the activation of an L-type calcium conductance as a result of a depolarizing step beyond the threshold value for activation of this conductance of around -40 mV. Calcium or strontium entry through L-type calcium channels results in the subsequent activation of a calcium-activated chloride conductance which accounts for the long lasting plateau phase (~30 s) around -20 mV. Upon removal of intracellular calcium, this chloride conductance becomes inactivated which makes NRK cells subject to repolarization by the activity of an inwardly rectifying potassium conductance. This latter conductance is also responsible for the maintenance of the resting potential around -70 mV. Although a propagating action potential could be simulated with the mathematical model, it was not possible to reproduce the spontaneous repetitive action potential firing observed in density-arrested NRK monolayers.

Dynamic video imaging experiments revealed that prostaglandin F2α (PGF2α) induced intracellular calcium oscillations in individual cells of quiescent monolayers of NRK fibroblasts, which resulted from an interplay between both IP_3-sensitive calcium stores and calcium influx. The frequency of these oscillations was highly variable and seemed to be determined primarily by the kinetic properties of the IP_3 receptor. In spite of the observation that the cells were coupled by gap junctions, the PGF2α-induced intracellular calcium oscillations were not synchronized. In contrast, elecrical coupling mediated a uniform membrane depolarization upon stimulation of these monolayers with PGF2α. Apparently, NRK cells possess a timing mechanism via intracellular calcium oscillations. The frequency of the PGF2α-induced intracellular calcium oscillations was of the same order of magnitude as the frequency of the spontaneous action potentials in density-arrested monolayers. Therefore, such intracellular calcium oscillations may underlie the periodic action potential firing in density-arrested NRK fibroblasts. This expected correlation between intracellular calcium oscillations and repetitive action potential firing is subject of ongoing research.

During our studies we discovered a novel feature of fenamates and 2-aminoethoxydiphenyl borate (2-APB), namely that these drugs completely and reversibly block gap junctions. The uncoupling action of 2-APB was unique because plasma membrane ion currents in NRK cells were apparently

unaffected by this drug. Thus, by using 2-APB as an electrical uncoupler it was for the first time possible to measure plasma membrane ion currents in electrically uncoupled monolayers.

Phenotypically transformed NRK fibroblasts were strongly depolarized compared to their non-transformed counterparts. This depolarization was caused by the secretion of a biologically active compound in their culture medium, which enhanced intracellular calcium levels resulting in the opening of calcium-activated chloride channels. After several isolation steps this active compound was identified by mass spectrometry as PGF2α, while the presence of elevated levels of this prostaglandin in the medium conditioned by transformed NRK fibroblasts was confirmed by an enzyme immunoassay. The transformation of NRK cells was blocked, or at least retarded, when the production of PGF2α was inhibited by cyclooxygenase blockers. The exact mechanism by which the secretion of PGF2α contributes to the transformation of NRK fibroblasts is subject of further investigations.

The results described in this thesis will form the basis for future studies on the role of membrane potential, calcium oscillations and gap junctional intercellular communication in density-dependent growth control and transformation of NRK cells. In order to address these issues the use of new techniques, including the double patch-clamp, new imaging techniques and RNAi, is of paramount importance. Finally, due to its unique properties as a gap junction blocker 2-APB can become an important pharmacological tool to study single-cell electrophysiological properties of cells in multicellular tissues.

Samenvatting

Tijdens de ontwikkeling en ook in het volwassen organisme is cellulaire groei nauwkeurig gereguleerd door een groot aantal controlemechanismen die ervoor zorgen dat cellen zich op het juiste moment en op de juiste plaats vermenigvuldigen. Ontregeling van deze gecompliceerde mechanismen kan leiden tot ongeremde celgroei en daarmee de grondslag vormen voor een grote diversiteit aan ziektes waaronder kanker. Om inzicht te krijgen in deze ziektes is het daarom van wezenlijk belang om eerst de elementaire mechanismen die normale celgroei sturen te begrijpen.

Normale cellen worden bij hoge celdichtheden geremd in hun groei door contact-inhibitie. Door deze dichtheidsafhankelijke groeiremming wordt overmatige celgroei voorkomen. In het onderzoek dat beschreven staat in dit proefschrift zijn de onderliggende mechanismen van dichtheidsafhankelijke groeiregulatie van cellen bestudeerd door gebruik te maken van “normal rat kidney” (NRK) fibroblasten. Deze cellen ondergaan dichtheidsafhankelijke groeiremming in aanwezigheid van “epidermal growth factor” (EGF) als de enige groeistimulerende factor. Indien echter ook stoffen als “transforming growth factor β” (TGFβ) of “retinoic acid” (RA) aan het kweekmedium worden toegevoegd, wordt dichtheidsafhankelijke groeiremming voorkomen of opgeheven, wat gepaard gaat met een verandering van het fenotype van deze cellen. Het ondergaan van fenotypische transformatie bij NRK cellen kan vergeleken worden met tumorvorming in weefsels.

Verschillende onderzoeken hebben aangetoond dat het expressie-niveau van de EGF receptor een cruciale rol speelt in de dichtheidsafhankelijke groeiregulatie van NRK cellen. Onlangs zijn ook de biofysische aspecten van groeiregulatie in NRK fibroblasten bestudeerd. Daarbij is aangetoond dat contact-geïnhibeerde NRK fibroblasten spontaan periodieke calcium actiepotentialen vuren. Het vuren van actiepotentialen in NRK fibroblasten leek in strijd met de klassieke opvatting dat fibroblasten niet-exciteerbare cellen zijn.

In dit proefschrift is de exciteerbaarheid van NRK cellen verder onderzocht met de nadruk op ionkanaal-activiteiten en koppeling van cellen door gap junctions. Hiervoor zijn rustende NRK cellen gebruikt die in tegenstelling tot contact-geïnhibeerde NRK cellen geen spontane actiepotentialen vuren. Door een lokale stimulatie met een hoge kalium concentratie of een calcium mobilizerende factor zoals bradykinine, was het echter wel mogelijk om een enkele propagerende actiepotentiaal in dergelijke monolagen op te wekken. Voor de propagatie van actiepotentialen in confluente monolagen is intercellulaire koppeling door gap junctions vereist. Aan de hand van metingen waarbij capaciteitsstromen werden opgewekt door het opleggen van een spanningsstap, bleek dat NRK cellen in monolagen electrisch goed gekoppeld zijn. De geschatte koppelingsconductantie kon worden bepaald door de gemeten stromen te analyseren. De ionconductanties in het plasmamembraan werden gekarakteriseerd en gekwantificeerd in voltage-clamp experimenten in enkele cellen en kleine celklusters die waren gedissocieerd uit monolagen. Naast het eerder aangetoonde L-type calcium

kanaal en calcium-geactiveerde chloride kanaal bleken NRK cellen een prominent aanwezige inward rectifier te bezitten. Bovendien kon worden aangetoond dat exciteerbaarheid van NRK cellen niet beperkt is tot cellen in gekoppelde monolagen, aangezien een significant percentage van de geïsoleerde cellen actiepotentialen kon vuren.

Om meer inzicht te krijgen in de exciteerbaarheid van NRK cellen werd een wiskundig model gebouwd. Dit minimale model waarin de intracellulaire calcium dynamiek in vereenvoudigde vorm was opgenomen, was gebaseerd op het Hodgkin-Huxley model en bevatte de plasmamembraan conductanties die in de patch-clamp experimenten gemeten waren. Met het model kon de exciteerbaarheid van geïsoleerde NRK cellen en kleine celklusters worden gereproduceerd, evenals de propagatie van actiepotentialen in monolagen. Aan de hand van het model kon in combinatie met patch-clamp experimenten de bijdrage van de individuele conductanties aan het actiepotentiaalmechanisme in NRK cellen worden bepaald. De actiepotentiaal ontstaat door het openen van het L-type calcium kanaal als gevolg van een depolarizerende stap voorbij de drempelspanning voor activatie van deze conductantie. Deze drempelspanning ligt rond -40 mV. Door de instroom van calcium of strontium door L-type calcium kanalen worden vervolgens calcium-geactiveerde chloride kanalen geopend die verantwoordelijk zijn voor het ontstaan van een langdurige plateaufase (~30 s) rond de -20 mV. Deze chloride kanalen sluiten weer wanneer de intracellulaire calcium concentratie weer is gedaald, waarna NRK cellen repolarizeren door activatie van inwaards rectificerende kalium kanalen. Deze kalium conductantie is ook verantwoordelijk voor het handhaven van de rustmembraanpotentiaal rond de -70 mV. Hoewel met het wiskundinge model een propagerende actiepotentiaal kon worden gesimuleerd, was het niet mogelijk om het spontaan repetitieve vuren van actiepotentialen te reproduceren, zoals dat in contact-geïnhibeerde NRK cellen is gemeten.

Dynamic video imaging experimenten lieten zien dat prostaglandine F2α (PGF2α) intracellulaire calcium-oscillaties opwekte in individuele cellen van monolagen met rustende NRK fibroblasten. Deze calcium-oscillaties waren het gevolg van een samenspel tussen IP_3-gevoelige calcium-opslagplaatsen en calcium-instroom. De frequentie, die erg variabel was, bleek voornamelijk te worden bepaald door de kinetische eigenschappen van de IP_3 receptor. Ondanks het feit dat de cellen gekoppeld waren via gap junctions, waren de door PGF2α opgewekte intracellulaire calcium-oscillaties niet gesynchroniseerd. Daarentegen zorgde de electrische koppeling juist voor een gelijkmatige depolarizatie van het plasmamembraan na stimulatie met PGF2α. NRK cellen bleken dus in de vorm van intracellulaire calcium-oscillaties over een soort tijdsmechanisme te beschikken. Aangezien de frequentie van de door PGF2α opgewekte intracellulaire calcium-oscillaties van dezelfde ordegrootte was als de frequentie van de spontane actiepotentialen in contact-geïnhibeerde monolagen, is het goed mogelijk dat dergelijke calcium-oscillaties de drijvende kracht zijn voor het periodiek vuren van actiepotentialen in contact-geïnhibeerde monolagen. Dit veronderstelde verband

tussen intracellulaire calcium-oscillaties en periodieke actiepotentialen wordt momenteel nog onderzocht.

Tijdens ons onderzoek ontdekten we dat zowel fenamaten als 2-aminoethoxydiphenyl borate (2-APB) reversibel gap junctions blokkeren. Daarbij was de werking van 2-APB uniek omdat de ionstromen in het plasma membraan van NRK cellen ogenschijnlijk niet beinvloed werden door deze stof. Daardoor was het voor de eerste keer mogelijk om in een electrisch ontkoppelde monolaag de stromen door ionkanalen te meten.

Fenotypisch getransformeerde NRK fibroblasten bleken sterk gedepolarizeerd te zijn vergeleken met ongetransformeerde NRK fibroblasten. De depolarizatie werd veroorzaakt doordat ze een biologisch actieve stof uitscheidden in hun groeimedium. Deze actieve stof verhoogde de intracellulaire calcium concentratie waardoor calcium-geactiveerde chloride kanalen werden geopend. Na opzuivering uit het groeimedium kon deze stof met behulp van massaspectrometrie worden geïdentificeerd als PGF2α, terwijl met een immunoassay werd bevestigd dat dit prostglandine in verhoogde concentratie aanwezig was in het groeimedium van getransformeerde NRK cellen. De transformatie van NRK cellen werd geremd, of in ieder geval vertraagd, wanneer de productie van PGF2α was onderdrukt door remmers van het cyclo-oxygenase. Hoe PGF2α precies bijdraagt aan de transformatie van NRK fibroblasten moet nog verder worden bestudeerd.

De resultaten die beschreven staan in dit proefschrift zullen de basis vormen voor verder onderzoek naar dichtheidsafhankelijke groeiregulatie and transformatie van NRK fibroblasten en de rol die de membraanpotentiaal, calcium-oscillaties en koppeling van cellen door gap junctions in deze processen spelen. Hierbij zal het gebruik van nieuwe technieken zoals de dubbele patch-clamp, nieuwe imaging technieken en RNAi van groot belang zijn. Tenslotte kan 2-APB door zijn unieke eigenschappen als gap junction-blokker gebruikt gaan worden als een farmacologisch hulpmiddel om de electrofysiologische eigenschappen van individuele cellen te bestuderen in intacte weefsels. Daarmee is mogelijk een belangrijke doorbraak geleverd voor toekomstig cellulair electrofysiologisch onderzoek aan weefsels en organen.

Dankwoord

Dit proefschrift zou niet tot stand zijn gekomen zonder de steun van velen. Ten eerste gaat mijn dank gaat uit naar Lex Theuvenet en Joop van Zoelen voor de prettige samenwerking en de mogelijkheid die jullie me gaven om het onderzoek te verrichten dat in dit proefschrift beschreven staat. Ondanks een moeizame start en hier en daar wat tegenslagen heeft ons onderzoek een aantal mooie resultaten opgeleverd en ik hoop dat het de basis vormt voor succesvol vervolgonderzoek. Mijn speciale dank gaat uit naar Dick Ypey. Dick, door je uitgebreide kennis op het gebied van de electrofysiologie en je aanstekelijke enthousiasme was je inbreng essentieel voor het onderzoek. Peter Peters wil ik bedanken voor de technische ondersteuning en met name voor de opzuivering van stof X. Peter, het zal je vooral deugd doen dat we er uiteindelijk in zijn geslaagd om de structuur van deze voor lange tijd onbekende stof op te helderen. Dit laatste is mede te danken aan Joost van Dongen. Joost, ik ben blij dat je erin bleef geloven dat we met massaspectrometrie de structuur zouden kunnen ontrafelen en wil je bedanken voor het feit dat je bereid was om vaak tot in de late uren door te gaan om mijn fracties te testen. Van degenen met wie ik verder prettig heb samengewerkt wil ik met name Christiaan, Catelijn, Wim, Niels, Joaquin, Jesus, Wilbert, Marc, Martijn en Stan bedanken. Mijn familie en vrienden wil ik bedanken voor de interesse die zij getoond hebben in mijn onderzoek. Zonder steun van het thuisfront was het nooit gelukt. Mijn dank gaat vooral uit naar mijn ouders, Viola en natuurlijk naar Laura. Zonder dat je het wist was je mijn allergrootste motivatie.

Curriculum vitae

Erik Harks werd op 16 maart 1976 geboren te Veldhoven. Na het afronden van de VWO opleiding aan het Anton van Duinkerken College te Veldhoven werd in 1994 begonnen met de studie Scheikundige Technologie aan de Technische Universiteit Eindhoven. Deze studie werd in augustus 1998 *cum laude* afgerond met onder meer een stage op de afdeling Analytische Chemie aan de Comenius University te Bratislava (Slowakije) en een afstudeerproject bij het Bakken Research Center van Medtronic in Maastricht (Prof. Dr. F.M. Everaerts). In oktober 1998 begon de auteur van dit proefschrift als Assistent in Opleiding op de afdeling Celbiologie onder begeleiding van Dr. A.P.R. Theuvenet en Prof. Dr. E.J.J. Van Zoelen.

Publications

Harks E.G., De Roos A.D., Peters P.H., de Haan L.H., Brouwer A., Ypey D.L., Van Zoelen E.J., Theuvenet A.P. (2001) Fenamates: a novel class of reversible gap junction blockers. *J Pharmacol Exp Ther*, 298, 1033-1041.

Harks E.G., Camiña J.P. Peters P.H., Ypey D.L., Van Zoelen E.J., Theuvenet A.P. (2003) Besides affecting calcium signaling, 2-APB reversibly blocks gap junctional communication thereby allowing voltage-clamp measurements of ion currents in intact monolayers. *Faseb J*, 10.1096/fj.02-0786fje.

Harks E.G., Torres J.J., Cornelisse L.N., Ypey D.L., Theuvenet A.P. (2003) Ionic basis for excitability in normal rat kidney (NRK) fibroblasts. *J Cell Physiol*, 196, 493-503.

Harks E.G., Scheenen W.J., Peters P.H., Van Zoelen E.J., Theuvenet A.P. (2003) PGF2α induces unsynchronized intracellular calcium oscillations in monolayers of gap junctionally coupled NRK fibroblasts. *Pflűgers Archiv*, in press.

Harks E.G., Peters P.H., Van Dongen J.L., Van Zoelen E.J., Theuvenet A.P. Phenotypic transformation of NRK fibroblasts is accompanied by a depolarization of the membrane due to the secretion of prostaglandin F2α, to be submitted.

Camiña J.P., Diaz-Rodriguez E., **Harks E.G.**, Theuvenet A.P., Ypey D.L., Casanueva F.F. (2003) Lipid factor (bVLF) from bovine vitreous body evokes in EGFR-T17 cells a Ca2+-dependent K+ current associated with inositol 1,4,5-trisphosphate-independent Ca2+ mobilization. *J Cell Physiol* 195, 108-18.

Torres J.J., Cornelisse L.N., **Harks E.G.**, Theuvenet A.P., Ypey D.L. Modeling action potential generation and propagation in normal rat kidney fibroblasts, submitted.